Long Range Interactions

van der Waals' Equation

$p = nRT/V$

i.g. from kinetic theory of gasses
Atoms can pass through each other
No enthalpy of interaction
Totally entropic

Modify for excluded volume "*b*"

$p = nRT/(V\text{-}b)$

Which increases pressure

Modify for excluded volume "*b*"
and
Attractive enthalpic interaction "*a*"

$p = nRT/(V\text{-}b) - a(n/V)^2$

$-T\Delta S \quad + \quad \Delta H$

$n/V = \rho \sim \phi$ *or c*

Binary attractive interactions
(can form a liquid)

Which decreases pressure

Van der Waals' Equation

$p = nRT/(V\text{-}b) - a(n/V)^2$ Van der Waals Equation

Compressibility Factor $Z = pV_{molar}/RT = p/\rho RT = 1 + B_2\,\rho + \ldots$ Virial Expansion

B_2 has units of molar volume

Solve for B_2 using the van der Waals Equation

$B_2 = b - a/RT$ for molar volume or $B_2 = b - a/k_BT$ for molecular volume

Flory and Krigbaum knew they needed an energy for an expanded chain of the van der Waals form

Molar Energy $= pV_{molar} = RT\,(1 + B_2\,/\,V_{molar})$

Where: B_2 = Excluded Volume – Attractive Potential$/RT = b - a/RT$

Energy = Ideal + repulsive "*b*" and attractive "*a*"

When $T^* = a/Rb$, interactions disappear, $B_2 = 0$, and system becomes "ideal". This is a "critical point" just before phase separation.

Van der Waals' Equation

$p = nRT/(V\text{-}b) - a(n/V)^2$ Van der Waals Equation

Compressibility Factor $Z = pV_{molar}/RT = p/\rho RT = 1 + B_2\,\rho + \ldots$ Virial Expansion

B_2 has units of molar volume

$Z_{\mathrm{VdW}} = pV_{molar}/RT = V/(V\text{-}b) - a\rho = 1/(1\text{-}b\rho) - a\rho$

Geometric series $\Sigma ar^k = a/(1\text{-}r)$ sum from 0 to ∞

So, $1/(1\text{-}b\rho) = \Sigma ar^k = 1 + b\rho + (b\rho)^2 + \ldots$ and for $b\rho = b/V$ is very small

$Z_{\mathrm{VdW}} = 1/(1\text{-}b\rho) - a\rho = 1 + (b - a/RT)\,\rho + (b\rho)^2 + \ldots$

Compare with the virial expansion

$Z = pV_{molar}/RT = p/\rho RT = 1 + B_2\,\rho + B_3\,\rho^2 + \ldots$

$B_2 = b - a/RT$ and $B_3 = b^2$

Van der Waals' Equation

$p = nRT/(V\text{-}b) - a(n/V)^2 + c\,(n/V)^3$ Van der Waals Equation with repulsive ternary interactions

Compressibility Factor $Z = pV_{molar}/RT = p/\rho RT = 1 + B_2\,\rho + B_3\,\rho^2 + \ldots$ Virial Expansion

B_2 has units of molar volume

$Z_{\mathrm{VdW}} = pV_{molar}/RT = V/(V\text{-}b) - a\rho = 1/(1\text{-}b\rho) - a\rho + c\rho^2$

Geometric series $\Sigma ar^k = a/(1\text{-}r)$ sum from 0 to ∞

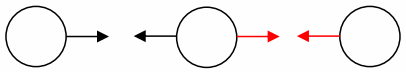

Red detracts from Black

So, $1/(1\text{-}b\rho) = \Sigma ar^k = 1 + b\rho + (b\rho)^2 + \ldots$ and for $b\rho = b/V$ is very small

$Z_{\mathrm{VdW}} = 1/(1\text{-}b\rho) - a\rho = 1 + (b - a/RT)\,\rho + (b^2 + c/\mathrm{RT})\,\rho^2 + \ldots$

Compare with the virial expansion

$Z = pV_{molar}/RT = p/\rho RT = 1 + B_2\,\rho + B_3\,\rho^2 + \ldots$

$B_2 = b - a/RT$ and $B_3 = b^2 + c/\mathrm{RT}$

For an immiscible system B_2 is negative or very small (low temperature)
B_3 can be positive leading to a discrete phase transition or negative leading to a continuous transition

The Secondary Structure for Synthetic Polymers
Long-Range Interactions

Boltzman Probability
For a Thermally Equilibrated System

$$P_B(R) = \exp\left(-\frac{E(R)}{kT}\right)$$

Gaussian Probability
For a Chain of End-to-End Distance R

$$P(R) = \left(\frac{3}{2\pi\sigma^2}\right)^{3/2} \exp\left(-\frac{3(R)^2}{2(\sigma)^2}\right)$$

By Comparison, The Energy to stretch a Thermally Equilibrated Chain Can be Written

$$E = kT\frac{3R^2}{2nl_K^2}$$

For a Chain with Long-Range Interactions There is and Additional Term

$$P_{Ex}(R) = \left(1 - V_c/R^3\right)^{n^2/2} = \exp\left(\frac{n^2 \ln\left(1 - V_c/R^3\right)}{2}\right) \sim \exp\left(-\frac{n^2 V_c}{2R^3}\right)$$

Number of pairs

$$\frac{n(n-1)}{2!}$$

$$exp(x) = 1 + x + \frac{x^2}{2} + \cdots$$

So,

$$E = kT\left(\frac{3R^2}{2nl_K^2} + \frac{n^2 V_c}{2R^3}\right)$$

Flory-Krigbaum Theory
Result is called a Self-Avoiding Walk

$$R^* \sim l_K\, n^{3/5}$$

$W_0(R)$ is the Gaussian probability $P(R,N)4\pi R^2 dR$ times the total number of chain conformations possible for chains of N steps, Z^N,

$$W_0(R)dR = Z^N 4\pi R^2 \left(\frac{2\pi}{3} Nb^2\right)^{-3/2} \exp\left[-\frac{3}{2}\left(\frac{R}{b\sqrt{N}}\right)^2\right] dR$$

of this number the fraction which follow self-avoidance is $p(R) = (1 - V_C/R^3)^{N(N-1)/2}$ where V_C is the volume of one segment of the chain so $(1- V_C/R^3)$ is the probability of the chain avoiding one segment, and this is raised to the total number of possible combinations of two segment pairs, N(N-1)/2!. This function for p(R) can be expressed as an exponential,

$$p(R) = \exp\left[\frac{1}{2} N(N-1)\ln\left(1-\frac{V_C}{R^3}\right)\right] = \exp\left(-\frac{N^2 V_C}{2R^3}\right)$$

where the second equality uses the fact that for small x, ln(1-x) = -x, and that for large N, (N-1)=>N. W(R)dR for the excluded volume chain can be estimated by $W_0(R)p(R)dR$ and since both are expressed as exponentials the powers sum leading to,

$$W(R)dR = W_0(R)p(R)dR = kR^2 \exp\left(-\frac{3R^2}{2Nb^2} - \frac{N^2 V_C}{2R^3}\right)$$

The derivative of $W_0(R)$ will equal 0 at $R^*_0 = (2Nb^2/3)^{1/2}$. This is proportional to $N^{1/2}b$ as expected. Setting the derivative of W(R) to 0 yields,

$$-\frac{3R^{*2}}{2Nb^2} + \frac{3N^2 V_C}{4R^{*3}} + 1 = 0$$

Rearranging and substituting R^*_0 yields,

$$\left(\frac{R^*}{R_0^*}\right)^5 - \left(\frac{R^*}{R_0^*}\right)^3 = \frac{9\sqrt{6}}{16}\frac{V_C}{b^3}\sqrt{N}$$

For large N the R ratio is large and the cubic term can be ignored with respect to the 5'th power term. This yields,

$$R^* \cong R_0^*\left(\frac{N^{1/2}V_C}{b^3}\right)^{1/5} = kN^{3/5}$$

This ***critical result*** was first noted by Flory and Krigbaum and its development is termed Flory-Krigbaum theory.

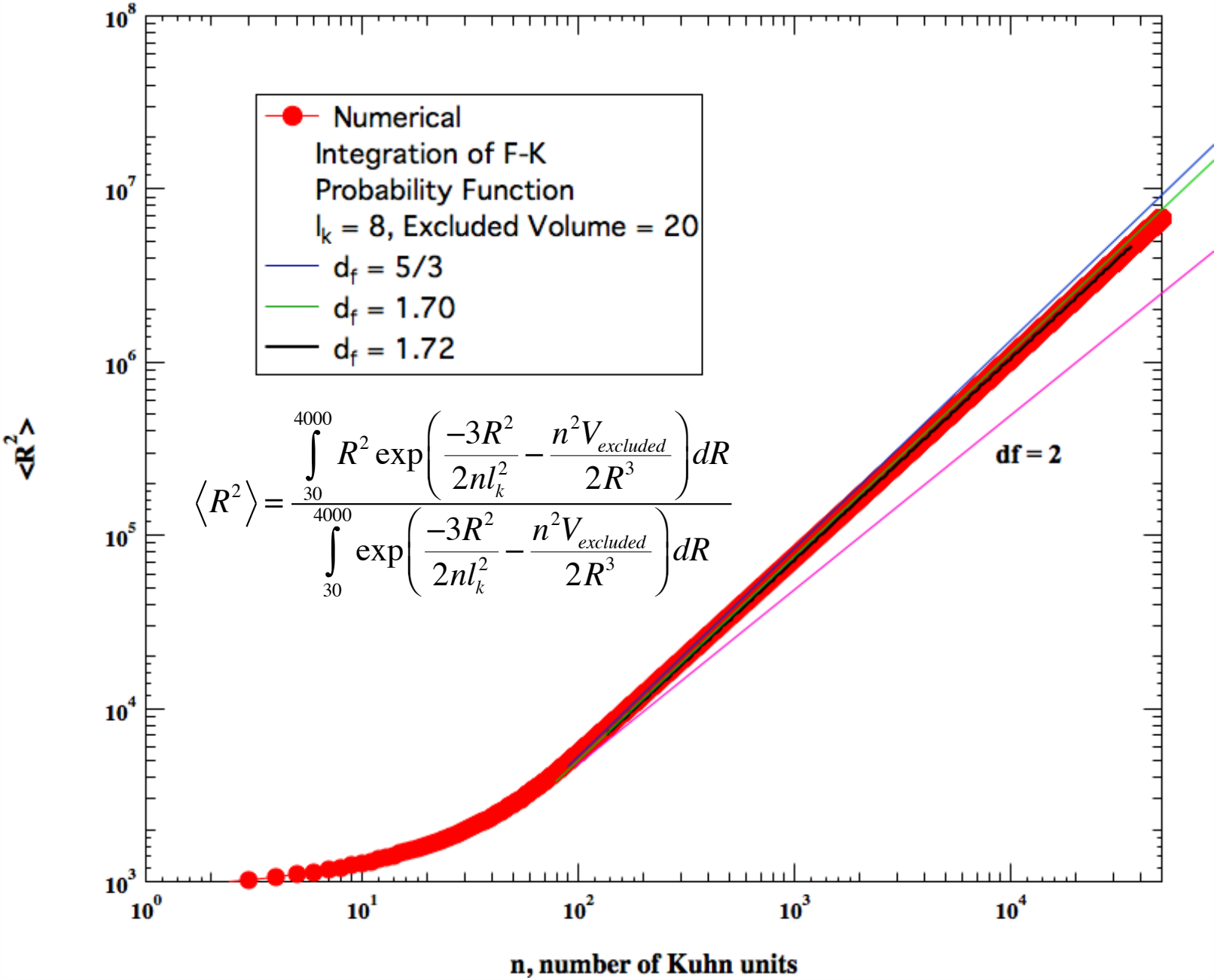

$$\langle R^2 \rangle = \frac{\int_{30}^{4000} R^2 \exp\left(\frac{-3R^2}{2nl_k^2} - \frac{n^2 V_{excluded}}{2R^3}\right) dR}{\int_{30}^{4000} \exp\left(\frac{-3R^2}{2nl_k^2} - \frac{n^2 V_{excluded}}{2R^3}\right) dR}$$

The Secondary Structure for Synthetic Polymers

Linear Polymer Chains have Two Possible Secondary Structure States:

Self-Avoiding Walk Good Solvent Expanded Coil (The Normal Condition in Solution)	Gaussian Chain Random Walk Theta-Condition Brownian Chain (The Normal Condition in the Melt/Solid)
$R^* \sim l_K\, n^{3/5}$	$\langle R^2 \rangle = Nl^2$
$d_f = 5/3 \approx 1.67$	$d_f = 2$

These are statistical features. That is, a single simulation of a SAW and a GC could look identical.

The Secondary Structure for Synthetic Polymers

Linear Polymer Chains have Two Possible Secondary Structure States:

Self-Avoiding Walk Good Solvent Expanded Coil (The Normal Condition in Solution)	Gaussian Chain Random Walk Theta-Condition Brownian Chain (The Normal Condition in the Melt/Solid)
$R^* \sim l_K\, n^{3/5}$	$\langle R^2 \rangle = Nl^2$
$d_f = 5/3 \approx 1.67$	$d_f = 2$

Concentration driven contraction

Consider going from dilute conditions, c < c*, to the melt by increasing concentration.
The transition in chain size is gradual not discrete.
Synthetic polymers at thermal equilibrium accommodate concentration changes through a scaling transition. Primary, Secondary, Tertiary Structures.

The Secondary Structure for Synthetic Polymers

Linear Polymer Chains have Two Possible Secondary Structure States:

Self-Avoiding Walk Good Solvent Expanded Coil (The Normal Condition in Solution)	Gaussian Chain Random Walk Theta-Condition Brownian Chain (The Normal Condition in the Melt/Solid)
$R^* \sim l_K\, n^{3/5}$	$\langle R^2 \rangle = Nl^2$
$d_f = 5/3 \approx 1.67$	$d_f = 2$

Thermally driven expansion

Consider going from *Theta Temperature*, $T = \theta$, to the expanded coil by increasing temperature.
The transition in chain size is gradual not discrete.
Synthetic polymers at thermal equilibrium accommodate thermal changes through a scaling transition. Primary, Secondary, Tertiary Structures.

Problem: The transition in chain size is gradual not discrete as predicted by FK theory.

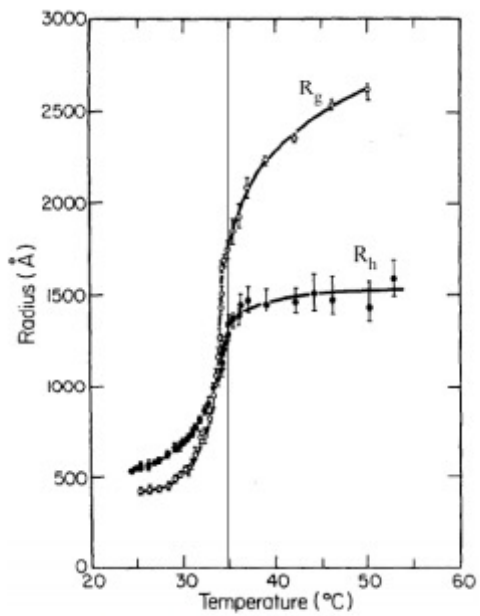

Figure 3. *Radius of gyration, R_g, and hydrodyamic radius R_h versus temperature for polystyrene in cyclohexane. Vertical line indicates the phase separation temperature. From Reference [21].*

We have considered an athermal hard core potential (excluded volume, 'b', from VdW equation)

$$E = kT\left(\frac{3R^2}{2nl_K^2} + \frac{n^2V_c}{2R^3}\right)$$

Excluded volume like "*b*"

VdW equation

$$p = nRT/(V\text{-}b) - a(n/V)^2$$

$$B_2 = b - a/RT$$

$$PV = RT + RT\,B_2/V \quad \text{(Virial Expansion)}$$

Energy = Ideal + repulsive "*b*" and attractive "*a*"

But V_c actually has an inverse temperature component associated with attractive enthalpic interactions between monomers and solvent molecules (attractive binary interactions, '*a*', from VdW equation)

The interaction (attractive) energy between a monomer and the polymer/solvent system is on average <E(R)> for a given end-to-end distance R (defining a conformational state). This modifies the probability of a chain having an end-to-end distance R by the Boltzmann probability,

$$P_{Boltzman}(R) = \exp\left(\frac{-\langle E(R)\rangle}{kT}\right)$$

<E(R)> is made up of pp, ps, ss interactions with an average change in attractive energy on solvation of a polymer $\Delta\varepsilon = (\varepsilon_{pp}+\varepsilon_{ss}-2\varepsilon_{ps})/2$

For a monomer with z sites of interaction we can define a unitless attractive energy parameter $\chi = z\Delta\varepsilon/kT$ that reflects the average enthalpy of attractive interaction per kT per monomer

For a monomer with z sites of interaction we can define a unitless energy parameter $\chi = z\Delta\varepsilon/kT$ that reflects the average enthalpy of attractive interaction per kT for a monomer

The volume fraction of monomers in the polymer coil with a conformational state of end-to-end distance R is nV_c/R^3
And there are n monomers in the chain, attractive chain energy "$n\chi$", so,

$$\frac{\langle E(R)\rangle}{kT} = \frac{n^2 V_c \chi}{R^3}$$

$$E = kT\left(\frac{3R^2}{2nl_K^2} + \frac{n^2 V_c}{2R^3}\right)$$

We can then write the energy of the chain as, *(remember $\chi \sim 1/T$)*

$$E(R) = kT\left(\frac{3R^2}{2nl^2} + \frac{n^2 V_c\left(\frac{1}{2} - \chi\right)}{R^3}\right)$$

$$PV = RT(1 + B_2/V)$$
$$B_2 = b - a/RT$$

When $T^* = a/Rb$ interactions disappear

This indicates that when $\chi = ½$ the coil acts as if it were an ideal chain, excluded volume disappears. This condition is called the theta-state and the temperature where $\chi = ½$ is called the theta-temperature. It is a critical point for the polymer coil in solution.

$$E(R) = kT\left(\frac{3R^2}{2nl^2} + \frac{n^2 V_c\left(\frac{1}{2} - \chi\right)}{R^3}\right)$$

$$E = kT\left(\frac{3R^2}{2nl_K^2} + \frac{n^2 V_c}{2R^3}\right)$$

The effective excluded volume is now $V_{ex} = V_0\,(1/2-\chi)$

The Flory-Krigbaum result for coil size is:

$$R^* \cong R_0^*\left(\frac{N^{1/2}V_C}{b^3}\right)^{1/5} = kN^{3/5}$$

Using this approximation for conditions of large molecular weight:

$$R^* = R_0^*\left(\frac{n^{1/2}V_0\left(1/2 - \chi\right)}{b^3}\right)^{1/5}$$

where $\chi = z\Delta\varepsilon/kT$

This Solves the Problem: The transition in chain size is gradual not discrete as predicted by FK theory.

$$R^* = R_0^* \left(\frac{n^{1/2} V_0 \left(1/2 - \chi\right)}{b^3} \right)^{1/5}$$

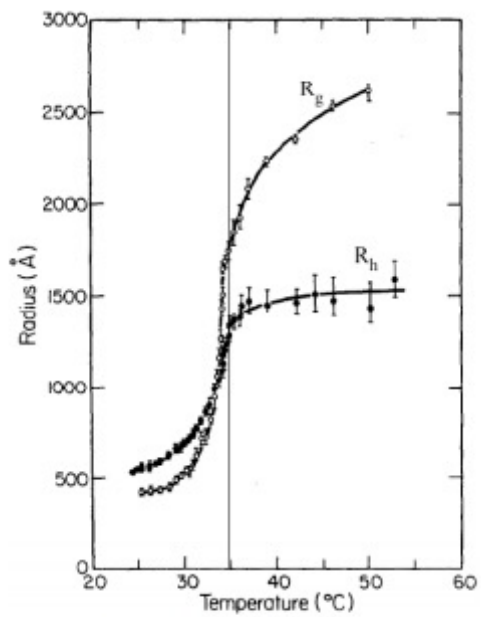

Figure 3. *Radius of gyration, R_g, and hydrodyamic radius R_h versus temperature for polystyrene in cyclohexane. Vertical line indicates the phase separation temperature. From Reference [21].*

$$R^* = R_0^* \left(\frac{n^{1/2} V_0 \left(1/2 - \chi\right)}{b^3} \right)^{1/5}$$

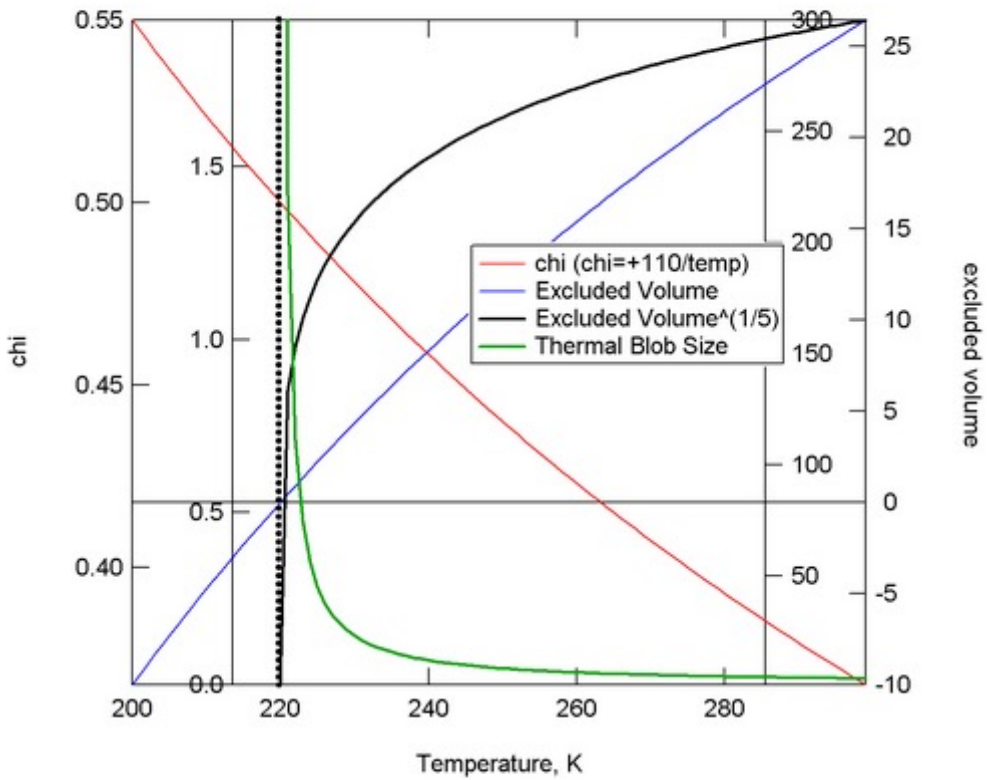

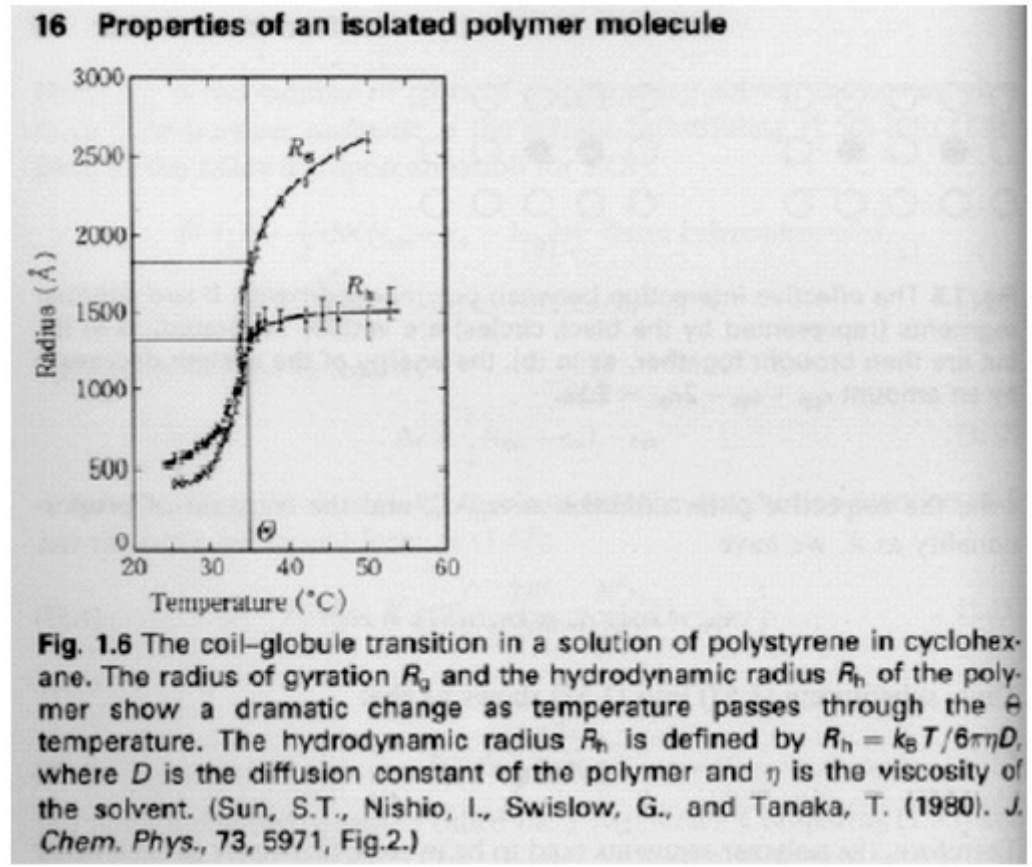

Fig. 1.6 The coil–globule transition in a solution of polystyrene in cyclohexane. The radius of gyration R_g and the hydrodynamic radius R_h of the polymer show a dramatic change as temperature passes through the Θ temperature. The hydrodynamic radius R_h is defined by $R_h = k_B T / 6\pi\eta D$, where D is the diffusion constant of the polymer and η is the viscosity of the solvent. (Sun, S.T., Nishio, I., Swislow, G., and Tanaka, T. (1980). *J. Chem. Phys.*, **73**, 5971, Fig.2.)

Flory Krigbaum prediction (left) and experimental measurement (right)

For a single polymer coil

$$\frac{\langle E(R)\rangle}{kT} = \frac{n^2 V_c \chi}{R^3}$$

Average attractive enthalpy of interaction

$\chi = z\Delta\varepsilon/kT$

$$E(R) = kT\left(\frac{3R^2}{2nl^2} + \frac{n^2 V_c\left(\frac{1}{2} - \chi\right)}{R^3}\right)$$

$PV = RT(1 + B_2/V)$

$B_2 = b - a/RT$

When $T^* = a/Rb$ interactions disappear

$B_2 = V_c/2 - V_c\,\chi$

$\chi = z\Delta\varepsilon/kT$

For a polymer mixture (polymer/polymer or polymer/solvent)

Flory-Huggins Equation

$$\frac{\Delta G}{kTN_{cells}} = \frac{\phi_A}{N_A}\ln\phi_A + \frac{\phi_B}{N_B}\ln\phi_B + \phi_A\phi_B\chi + \frac{PV}{kTN_{cells}}$$

$$E(R) = kT\left(\frac{3R^2}{2nl^2} + \frac{n^2 V_c\left(\frac{1}{2} - \chi\right)}{R^3}\right)$$

$$\frac{\Delta G}{kTN_{cells}} = \frac{\phi_A}{N_A}\ln\phi_A + \frac{\phi_B}{N_B}\ln\phi_B + \phi_A\phi_B\chi$$

$$\chi = \frac{z\Delta\varepsilon}{kT} = \frac{B}{T}$$

Lower-Critical Solution Temperature (LCST)

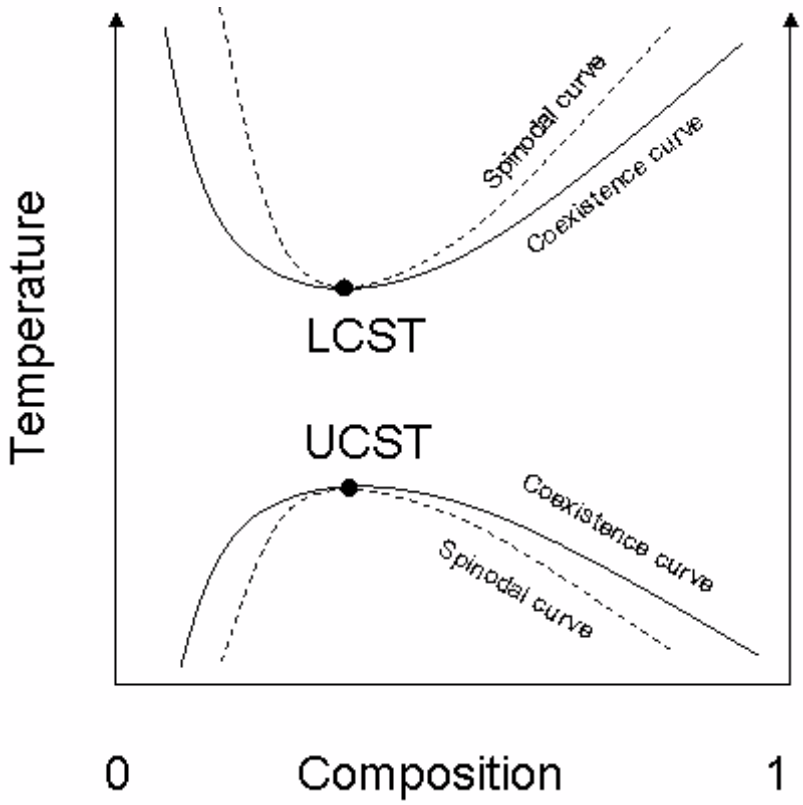

Polymers can order or disorder on mixing leading to a noncombinatorial entropy term, A in the interaction parameter.

$$\chi = A + \frac{B}{T}$$

If the polymer orders on mixing then A is positive and the energy is lowered.

If the polymer-solvent shows a specific interaction then B can be negative.

This Positive A and Negative B favors mixing at low temperature and demixing at high temperature, LCST behavior.

$$E(R) = kT\left(\frac{3R^2}{2nl^2} + \frac{n^2 V_c\left(\frac{1}{2} - \chi\right)}{R^3}\right)$$

$$\chi = \frac{z\Delta\varepsilon}{kT} = \frac{B}{T}$$

Lower-Critical Solution Temperature (LCST)

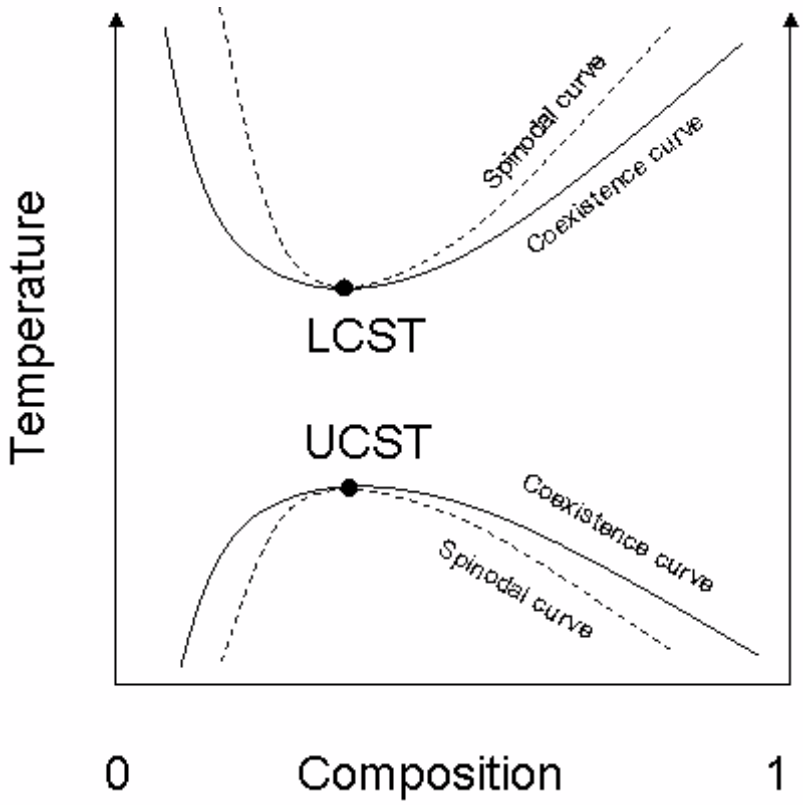

$$\chi = A + \frac{B}{T}$$

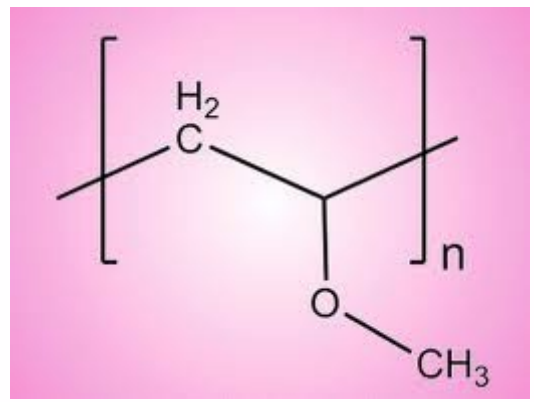

Poly vinyl methyl ether/Water
PVME/PS

Also see Poly(N-isopropylacrylamide)/Water

$$\Delta G_m = RT(x_A \ln(x_A) + x_B \ln(x_B)) + \Omega\, x_A x_B$$

$\frac{d\Delta G}{d\phi} = 0$ Miscibility Limit Binodal

$\frac{d^2\Delta G}{d\phi^2} = 0$ Spinodal

$\frac{d^3\Delta G}{d\phi^3} = 0$ Critical Point

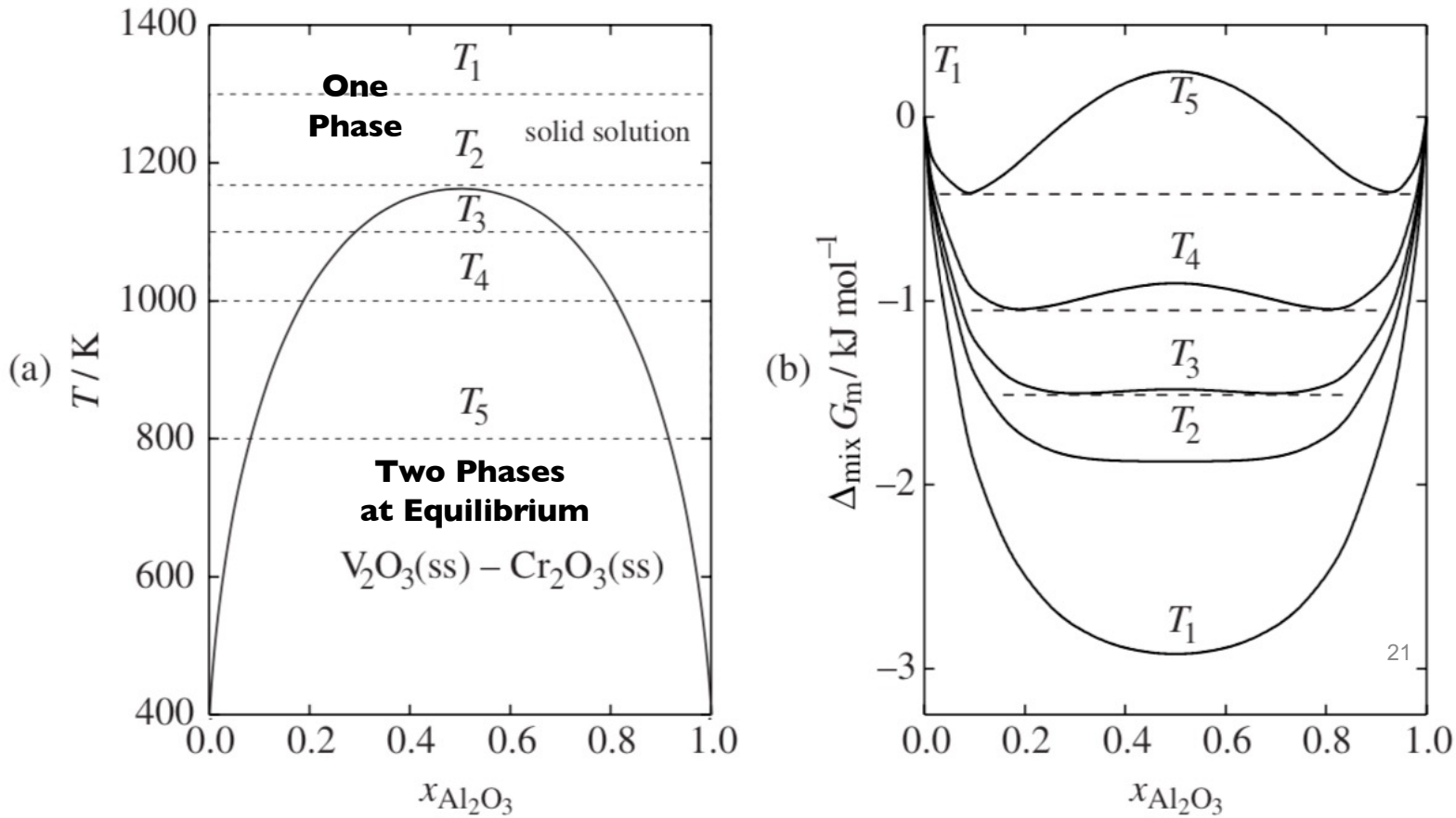

Figure 4.9 (a) Immiscibility gap of the binary solid solution V_2O_3–Cr_2O_3 as described by the regular solution model. (b) Gibbs energy of mixing curve of the solid solution at the temperatures marked in the phase diagram. Thermodynamic data are taken from reference [7].

Wilding, Müller, and Binder: Polymer–solvent critical point parameters
J. Chem. Phys., Vol. 105, No. 2, 8 July 1996

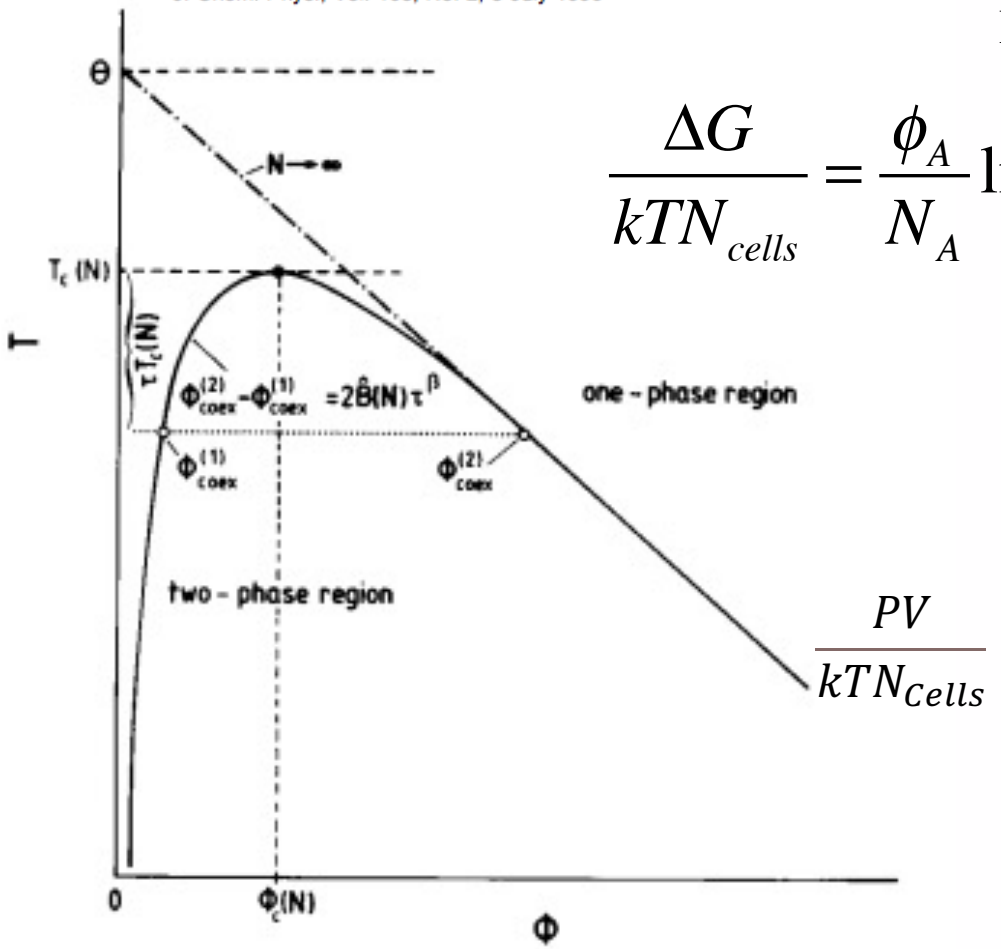

FIG. 1. Schematic phase diagram of a polymer solution in the space of the temperature T and the volume fraction ϕ. The coexistence curve separates a dilute solution of collapsed chains [at $\phi^{(1)}_{coex}$] from a semidilute solution of overlapping chains [at $\phi^{(2)}_{coex}$]. These two branches of the coexistence curve merge at a critical point $T_c(N)$, $\phi_c(N)$. For $N\to\infty$ the critical point merges with the Θ point of a dilute polymer solution [$T_c(N\to\infty)\to\Theta$, $\phi_c(N\to\infty)\to 0$] and the unmixing transition has a tricritical character. At $T=\Theta$, the chain con/Egurations are ideal Gaussian coils, while their structure at $T_c(N)$ is nontrivial.

Flory-Huggins Equation

$$\frac{\Delta G}{kTN_{cells}} = \frac{\phi_A}{N_A}\ln\phi_A + \frac{\phi_B}{N_B}\ln\phi_B + \phi_A\phi_B\chi + \frac{PV}{kTN_{cells}}$$

Hildebrandt Regular Solution Model

$$\Delta_{mix}G_m = RT[x_A \ln x_A + x_B \ln x_B] + \Omega_{AB}x_A x_B$$

$$\frac{PV}{kTN_{Cells}}$$

$$\frac{d\Delta G}{d\phi} = 0$$ Miscibility Limit
Binodal

$$\frac{d^2\Delta G}{d\phi^2} = 0$$ Spinodal

$$\frac{d^3\Delta G}{d\phi^3} = 0$$ Critical Point

All three equalities apply
At the critical point

http://rkt.chem.ox.ac.uk/lectures/liqsolns/regular_solutions.html

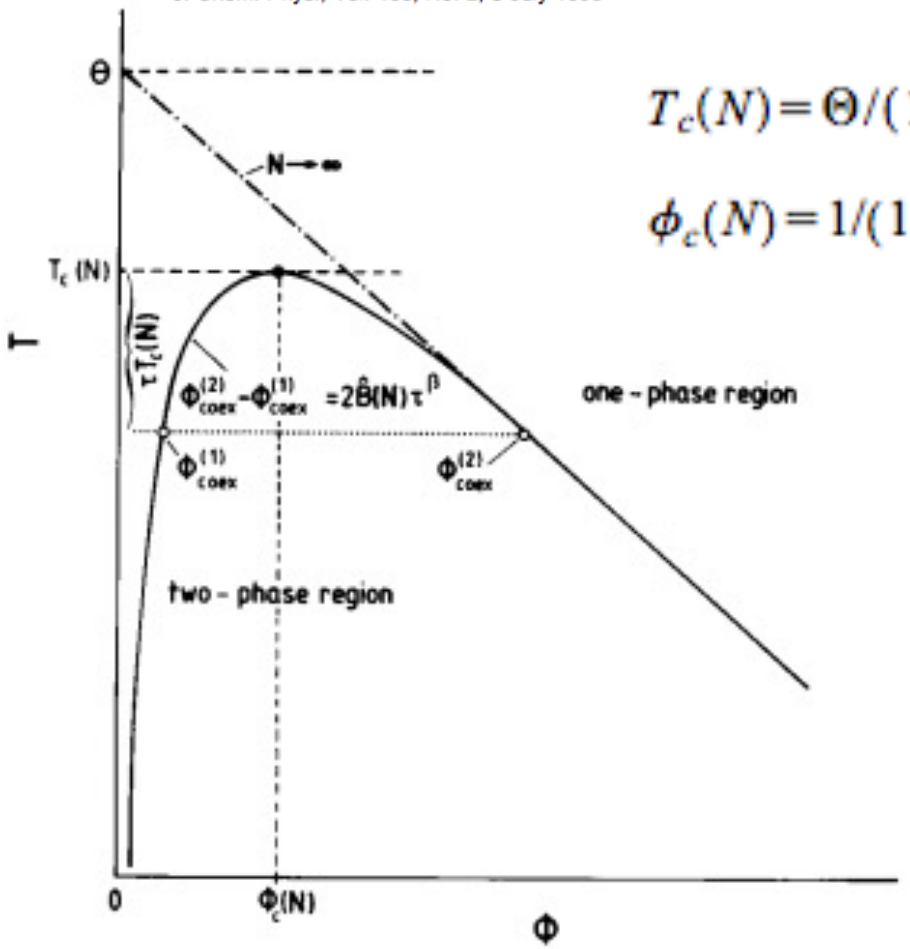

$$T_c(N)=\Theta/(1+1/\sqrt{N})^2\approx\Theta-2\Theta/\sqrt{N},\quad N\to\infty, \tag{1}$$

$$\phi_c(N)=1/(1+\sqrt{N})\approx 1/\sqrt{N},\quad N\to\infty. \tag{2}$$

FIG. 1. Schematic phase diagram of a polymer solution in the space of the temperature T and the volume fraction ϕ. The coexistence curve separates a dilute solution of collapsed chains [at $\phi^{(1)}_{coex}$] from a semidilute solution of overlapping chains [at $\phi^{(2)}_{coex}$]. These two branches of the coexistence curve merge at a critical point $T_c(N)$, $\phi_c(N)$. For $N\to\infty$ the critical point merges with the Θ point of a dilute polymer solution [$T_c(N\to\infty)\to\Theta$, $\phi_c(N\to\infty)\to 0$] and the unmixing transition has a tricritical character. At $T=\Theta$, the chain con/Egurations are ideal Gaussian coils, while their structure at $T_c(N)$ is nontrivial.

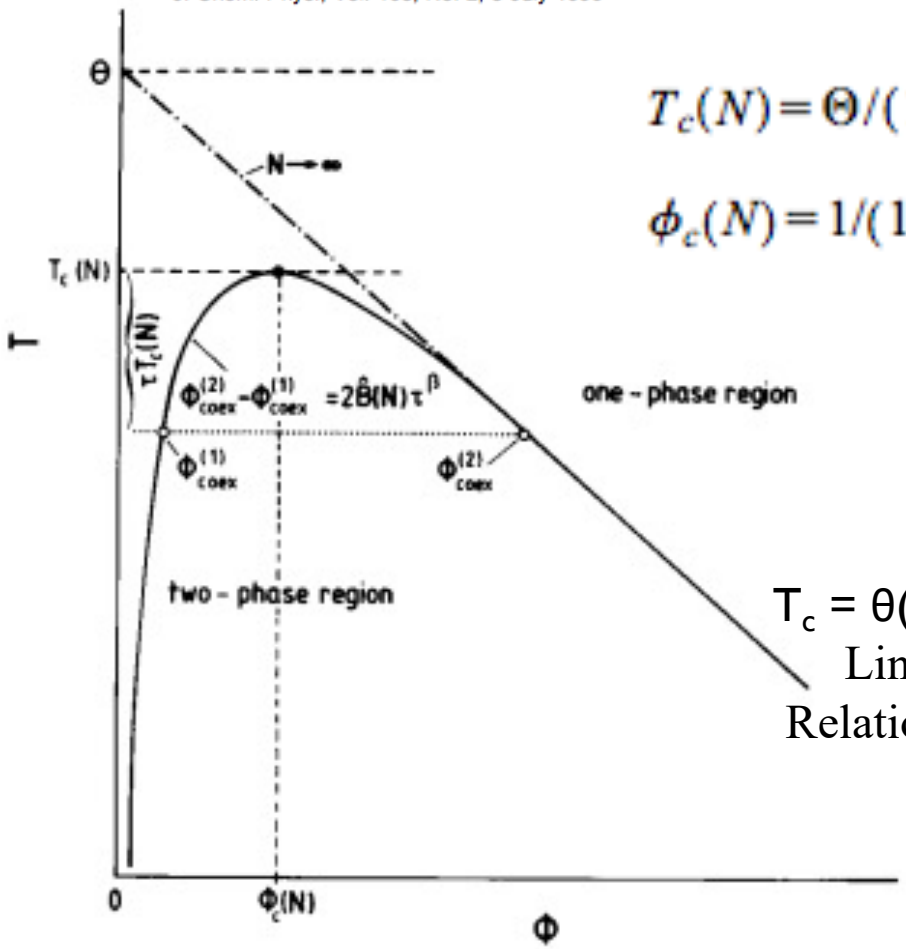

$$T_c(N) = \Theta/(1+1/\sqrt{N})^2 \approx \Theta - 2\Theta/\sqrt{N}, \quad N\to\infty, \tag{1}$$

$$\phi_c(N) = 1/(1+\sqrt{N}) \approx 1/\sqrt{N}, \quad N\to\infty. \tag{2}$$

$T_c = \theta(1-2\Phi_c)$
Linear
Relationship

FIG. 1. Schematic phase diagram of a polymer solution in the space of the temperature T and the volume fraction ϕ. The coexistence curve separates a dilute solution of collapsed chains [at $\phi^{(1)}_{coex}$] from a semidilute solution of overlapping chains [at $\phi^{(2)}_{coex}$]. These two branches of the coexistence curve merge at a critical point $T_c(N)$, $\phi_c(N)$. For $N\to\infty$ the critical point merges with the Θ point of a dilute polymer solution [$T_c(N\to\infty)\to\Theta$, $\phi_c(N\to\infty)\to 0$] and the unmixing transition has a tricritical character. At $T=\Theta$, the chain con/Egurations are ideal Gaussian coils, while their structure at $T_c(N)$ is nontrivial.

Wilding, Müller, and Binder: Polymer–solvent critical point parameters
J. Chem. Phys., Vol. 105, No. 2, 8 July 1996

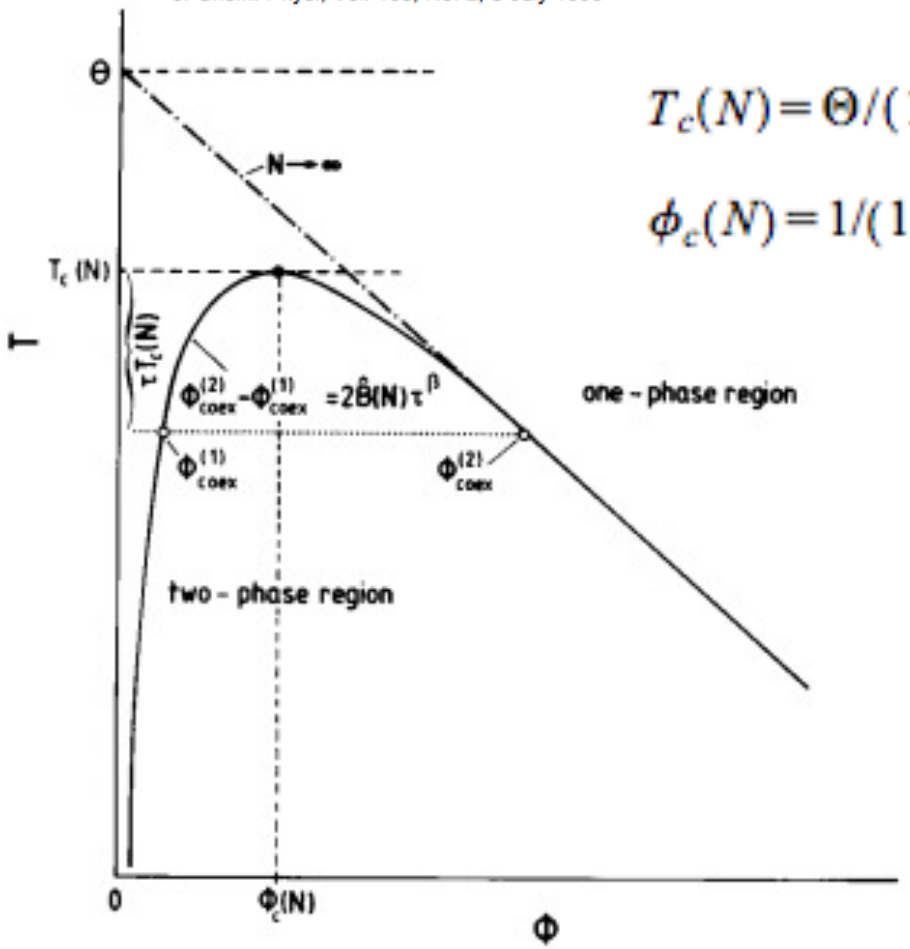

$$T_c(N) = \Theta/(1+1/\sqrt{N})^2 \approx \Theta - 2\Theta/\sqrt{N}, \quad N\to\infty, \qquad (1)$$

$$\phi_c(N) = 1/(1+\sqrt{N}) \approx 1/\sqrt{N}, \quad N\to\infty. \qquad (2)$$

FIG. 1. Schematic phase diagram of a polymer solution in the space of the temperature T and the volume fraction ϕ. The coexistence curve separates a dilute solution of collapsed chains [at $\phi^{(1)}_{coex}$] from a semidilute solution of overlapping chains [at $\phi^{(2)}_{coex}$]. These two branches of the coexistence curve merge at a critical point $T_c(N)$, $\phi_c(N)$. For $N\to\infty$ the critical point merges with the Θ point of a dilute polymer solution [$T_c(N\to\infty)\to\Theta$, $\phi_c(N\to\infty)\to 0$] and the unmixing transition has a tricritical character. At $T=\Theta$, the chain con/Egurations are ideal Gaussian coils, while their structure at $T_c(N)$ is nontrivial.

Overlap Composition

Consider also ϕ^* which is the coil composition, generally below the critical composition for normal n or N

$$\phi^* = \frac{n}{V} = \frac{n}{R^3}$$

$$\sim n^{-4/5} \text{ (for good solvents)}$$

$$\text{or} \sim n^{-1/2} \text{ (for theta solvents)}$$

Wilding, Müller, and Binder: Polymer–solvent critical point parameters
J. Chem. Phys., Vol. 105, No. 2, 8 July 1996

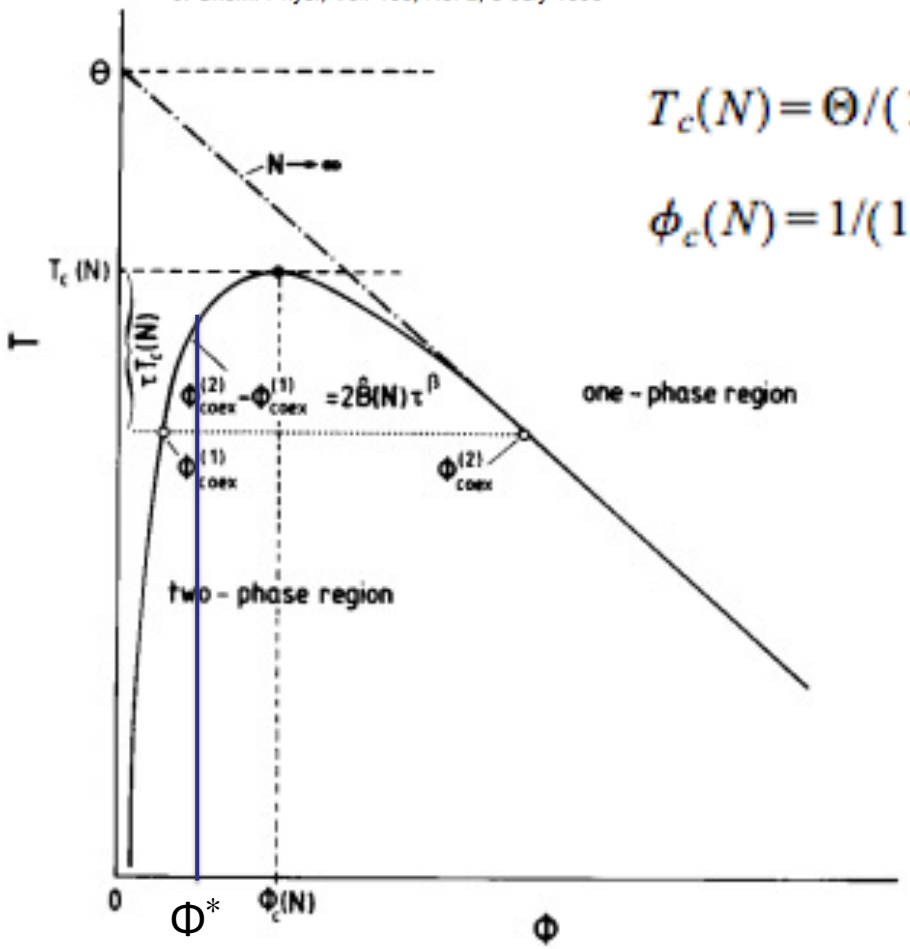

$$T_c(N)=\Theta/(1+1/\sqrt{N})^2 \approx \Theta-2\Theta/\sqrt{N}, \quad N\to\infty, \tag{1}$$

$$\phi_c(N)=1/(1+\sqrt{N}) \approx 1/\sqrt{N}, \quad N\to\infty. \tag{2}$$

FIG. 1. Schematic phase diagram of a polymer solution in the space of the temperature T and the volume fraction ϕ. The coexistence curve separates a dilute solution of collapsed chains [at $\phi^{(1)}_{coex}$] from a semidilute solution of overlapping chains [at $\phi^{(2)}_{coex}$]. These two branches of the coexistence curve merge at a critical point $T_c(N)$, $\phi_c(N)$. For $N\to\infty$ the critical point merges with the Θ point of a dilute polymer solution [$T_c(N\to\infty)\to\Theta$, $\phi_c(N\to\infty)\to 0$] and the unmixing transition has a tricritical character. At $T=\Theta$, the chain con/Egurations are ideal Gaussian coils, while their structure at $T_c(N)$ is nontrivial.

Overlap Composition

Both ϕ^* and ϕ_c depend on $1/\sqrt{N}$

Below ϕ^* the composition is fixed since the coil can not be diluted!

Wilding, Müller, and Binder: Polymer–solvent critical point parameters
J. Chem. Phys., Vol. 105, No. 2, 8 July 1996

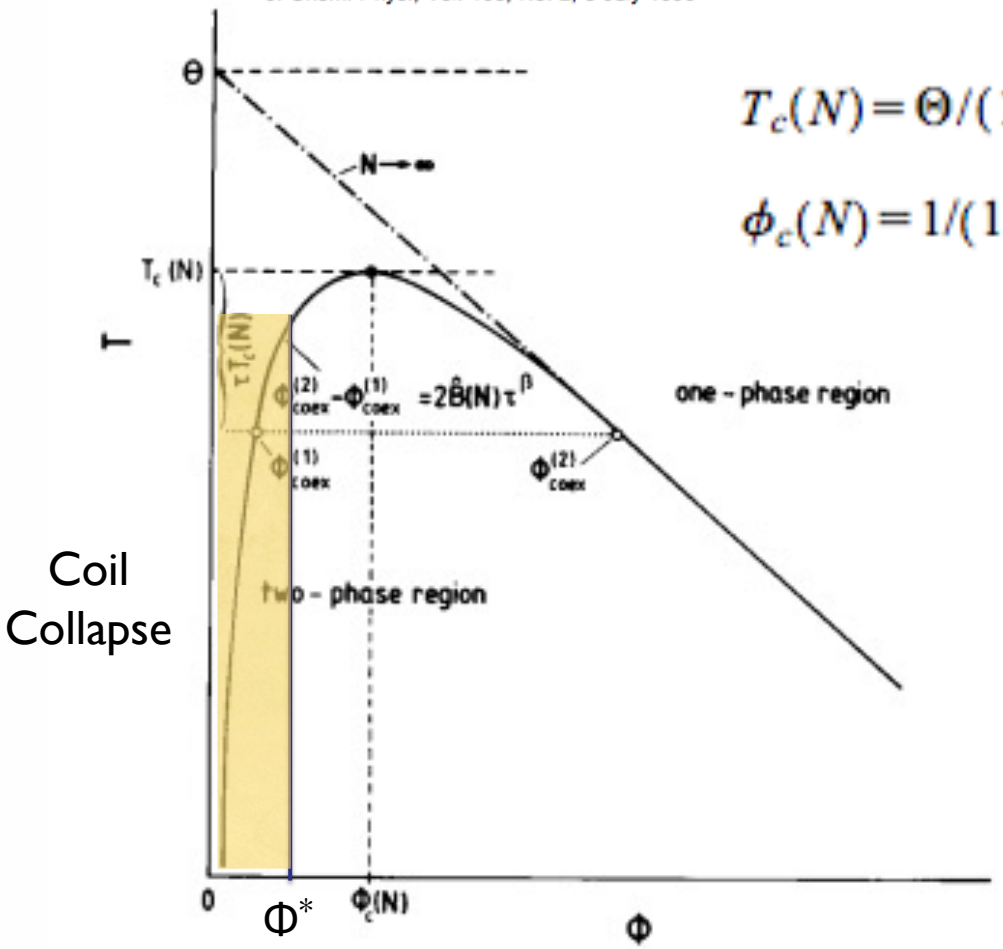

Coil Collapse

$$T_c(N) = \Theta/(1+1/\sqrt{N})^2 \approx \Theta - 2\Theta/\sqrt{N}, \quad N\to\infty, \qquad (1)$$

$$\phi_c(N) = 1/(1+\sqrt{N}) \approx 1/\sqrt{N}, \quad N\to\infty. \qquad (2)$$

FIG. 1. Schematic phase diagram of a polymer solution in the space of the temperature T and the volume fraction ϕ. The coexistence curve separates a dilute solution of collapsed chains [at $\phi^{(1)}_{coex}$] from a semidilute solution of overlapping chains [at $\phi^{(2)}_{coex}$]. These two branches of the coexistence curve merge at a critical point $T_c(N)$, $\phi_c(N)$. For $N\to\infty$ the critical point merges with the Θ point of a dilute polymer solution [$T_c(N\to\infty)\to\Theta$, $\phi_c(N\to\infty)\to 0$] and the unmixing transition has a tricritical character. At $T=\Theta$, the chain con/Egurations are ideal Gaussian coils, while their structure at $T_c(N)$ is nontrivial.

Overlap Composition

Both ϕ^* and ϕ_c depend on $1/\sqrt{N}$

Below ϕ^* the composition is fixed since the coil can not be diluted!

So, there is a region (yellow) of coil collapse below the binodal at ϕ^* in composition and temperature

Wilding, Müller, and Binder: Polymer–solvent critical point parameters
J. Chem. Phys., Vol. 105, No. 2, 8 July 1996

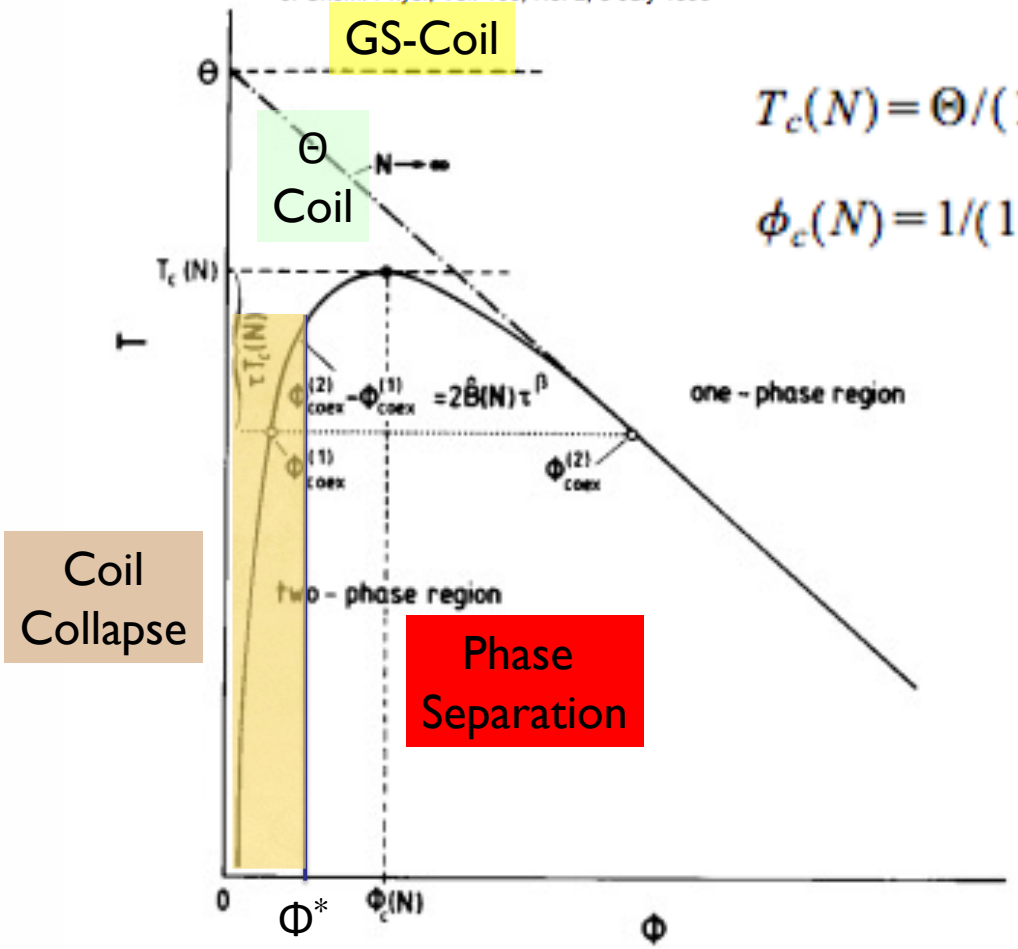

$$T_c(N) = \Theta/(1+1/\sqrt{N})^2 \approx \Theta - 2\Theta/\sqrt{N}, \quad N\to\infty, \qquad (1)$$

$$\phi_c(N) = 1/(1+\sqrt{N}) \approx 1/\sqrt{N}, \quad N\to\infty. \qquad (2)$$

FIG. 1. Schematic phase diagram of a polymer solution in the space of the temperature T and the volume fraction ϕ. The coexistence curve separates a dilute solution of collapsed chains [at $\phi^{(1)}_{coex}$] from a semidilute solution of overlapping chains [at $\phi^{(2)}_{coex}$]. These two branches of the coexistence curve merge at a critical point $T_c(N)$, $\phi_c(N)$. For $N\to\infty$ the critical point merges with the Θ point of a dilute polymer solution [$T_c(N\to\infty)\to\Theta$, $\phi_c(N\to\infty)\to 0$] and the unmixing transition has a tricritical character. At $T=\Theta$, the chain con/Egurations are ideal Gaussian coils, while their structure at $T_c(N)$ is nontrivial.

Overlap Composition

Both ϕ^* and ϕ_c depend on $1/\sqrt{N}$

Below ϕ^* the composition is fixed since the coil can not be diluted!

So, there is a regime of coil collapse below the binodal at ϕ^* in composition and temperature

For a polymer in solution there is an inherent concentration to the chain since the chain contains some solvent

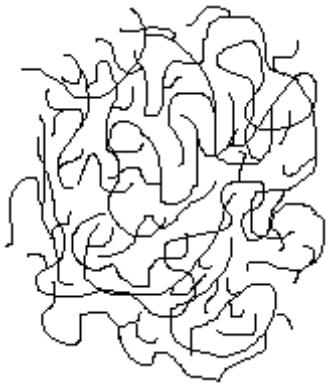

The polymer concentration is Mass/Volume, within a chain

$$c^* = \frac{Mass}{Volume} = \frac{Mass}{Size^3} = \frac{Size^{d_f}}{Size^3} \sim Size^{d_f - 3}$$

$$c^* \sim n^{\left(1 - 3/d_f\right)}$$

When the solution concentration matches c* the chains "overlap"
Then an individual chain is can not be resolved and the chains entangle
This is called semi-dilute since the solution is still of very low concentration.
The regime below c* is called dilute. Very high concentrations, θ-coil, are called concentrated.

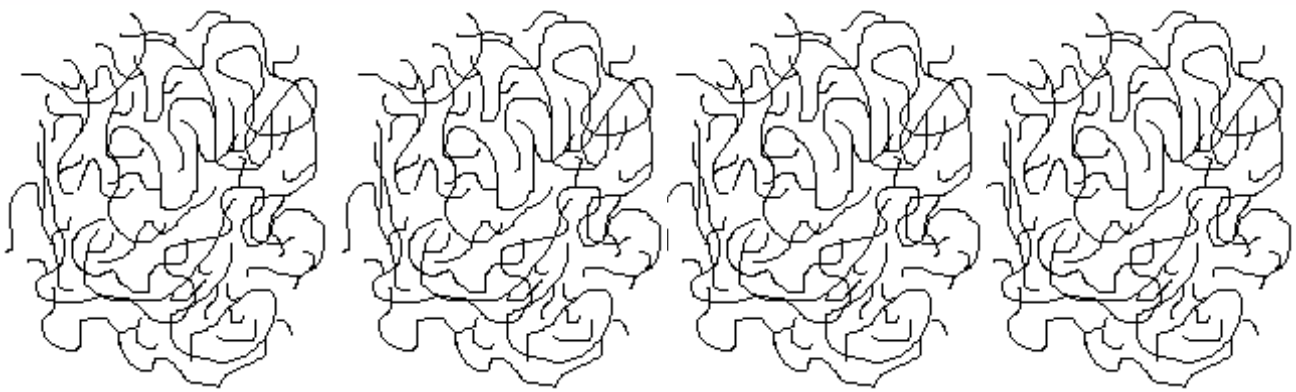

In concentrated solutions with chain overlap chain entanglements lead to a higher solution viscosity

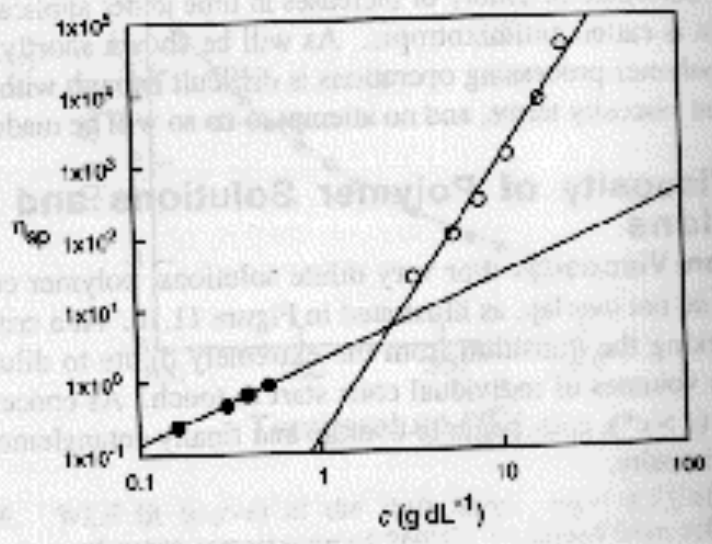

Figure 11.17. Concentration dependence of the specific viscosity of dilute and moderately concentrated solutions of cellulose acetate in dimethyl sulfoxide.[3] The intersection of straight lines that are drawn through the dilute-solution (●) and concentrated-solution (○) data marks the critical concentration, c^* (ca. 3.7 g dL^{-1} in this case).

J.R. Fried Introduction to Polymer Science

$$\eta \sim c^P$$

$$P = 1 \text{ for } c < c^*$$

Later called c_e, entanglement concentration

Structure and linear viscoelasticity of flexible polymer solutions: comparison of polyelectrolyte and neutral polymer solutions R. Colby, Rheo. Acta **49** 425-442 (2010)

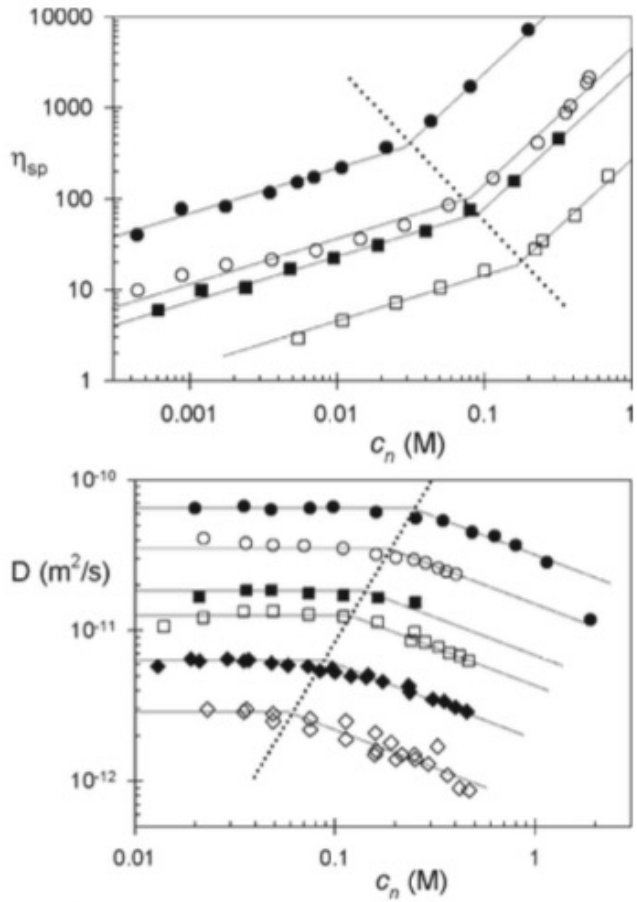

Fig. 15 Concentration dependences of specific viscosity and diffusion coefficient for polyelectrolyte solutions clearly showing the entanglement concentration. **a** Specific viscosity of sodium poly(2-acrylamido-2-methylpropane sulfonate) in water: *filled circles* $M = 1.7 \times 10^6$, *filled squares* $M = 9.5 \times 10^5$ (Krause et al. 1999) and sodium poly(styrene sulfonate) in water: *open circles* $M = 1.2 \times 10^6$ (Boris and Colby 1998), *open squares* $M = 3.0 \times 10^5$ (Fernandez Prini and Lagos 1964). *Solid lines* have the expected slopes of 1/2 and 3/2, *dotted line* has slope −1.76. **b** Diffusion coefficient of sodium poly(styrene sulfonate) in water: *filled circles* $M = 16{,}000$, *open circles* $M = 31000$, *filled squares* $M = 65000$, *open squares* $M = 88{,}000$, *filled diamonds* $M = 177{,}000$, *open diamonds* $M = 354{,}000$ (Oostwal et al. 1993). *Solid lines* have the expected slopes of 0 and −1/2, *dotted line* has slope 2.29

$$\eta = \eta_0 (1 + [\eta]c)$$

$$\eta_{sp} = (\eta - \eta_0)/\eta_0$$

$$[\eta] = \lim_{c=>0} (\eta_{sp}/c)$$

$$[\eta] = V_{coil}/m = 1/c^* = m^{3/df - 1}$$

Structure and linear viscoelasticity of flexible polymer solutions: comparison of polyelectrolyte and neutral polymer solutions R. Colby, Rheo. Acta **49** 425-442 (2010)

This can be explained if you consider that c* is on a chain size-scale while c_e is on a bulk size scale, that is c_e is for bulk network pathways while c* is for the coil pathway. c_e behaves the same in rigid rods and coils because both make a self-avoiding network on large size scales, c* is different because one chain is a rod the other a self-avoiding walk.

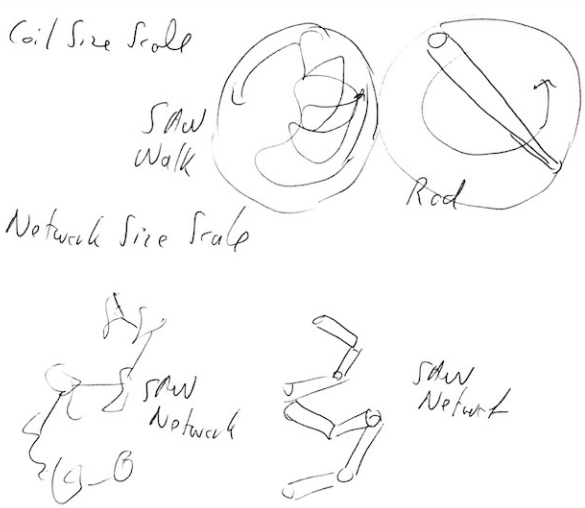

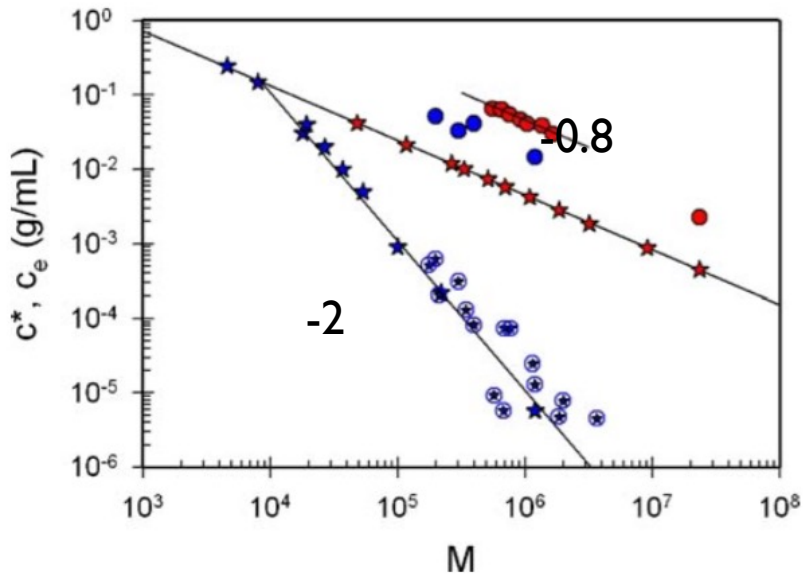

Fig. 2 Comparison of overlap concentrations and entanglement concentrations for neutral polymer solutions in good solvent; *red stars* overlap concentrations, c^*, of polystyrene in toluene (Kulicke and Kniewske 1984); *red circles* entanglement concentrations, c_e, of polystyrene in toluene (Onogi et al. 1966 viscosity data fit to power laws with slope 1.3 and 3.9, highest M point from Kulicke and Kniewske 1984) with polyelectrolyte solutions in water with no added salt; *blue stars* overlap concentrations, c^*, of sodium poly(styrene sulfonate) from SAXS (Kaji et al. 1988); *stars with blue circles* overlap concentrations, c^*, of sodium poly(styrene sulfonate) from viscosity (Boris and Colby 1998); *blue circles* entanglement concentrations of sodium poly(styrene sulfonate) from viscosity (Boris and Colby 1998). *Lowest line* has slope −2, expected for c^* of polyelectrolyte solutions with no salt; *middle line* is Mark–Houwink fit with slope −0.7356 (predicted slope is −0.76); *upper line* has same slope going through neutral c_e data

Red circles neutral good solvent c_e
Red stars neutral good solvent c*

Blue circles polyelectrolyte c_e
Blue stars polyelectrolyte c*

$$c^* \sim n^{\left(1-3/d_f\right)}$$

$d_f = 5/3$	-0.8
$d_f = 2$	-0.5
$d_f = 1.$	-2

Extensional Flow

Shadowgraph images from the capillary breakup of a 0.2 wt. % polyethylene oxide (PEO, Mw= 4 × 106 g/mol) in a 60/40 wt. % glycerol/water solution. Images are taken at t = −0.05, 0.25, 0.43, and 0.65 s (cf. Fig. 4). The size of the images is 0.55 × 1.1 mm. The horizontal lines in the second image indicate the region shown in Fig. 5. The last image shows the final instability of the viscoelastic thread when many small droplets are formed.

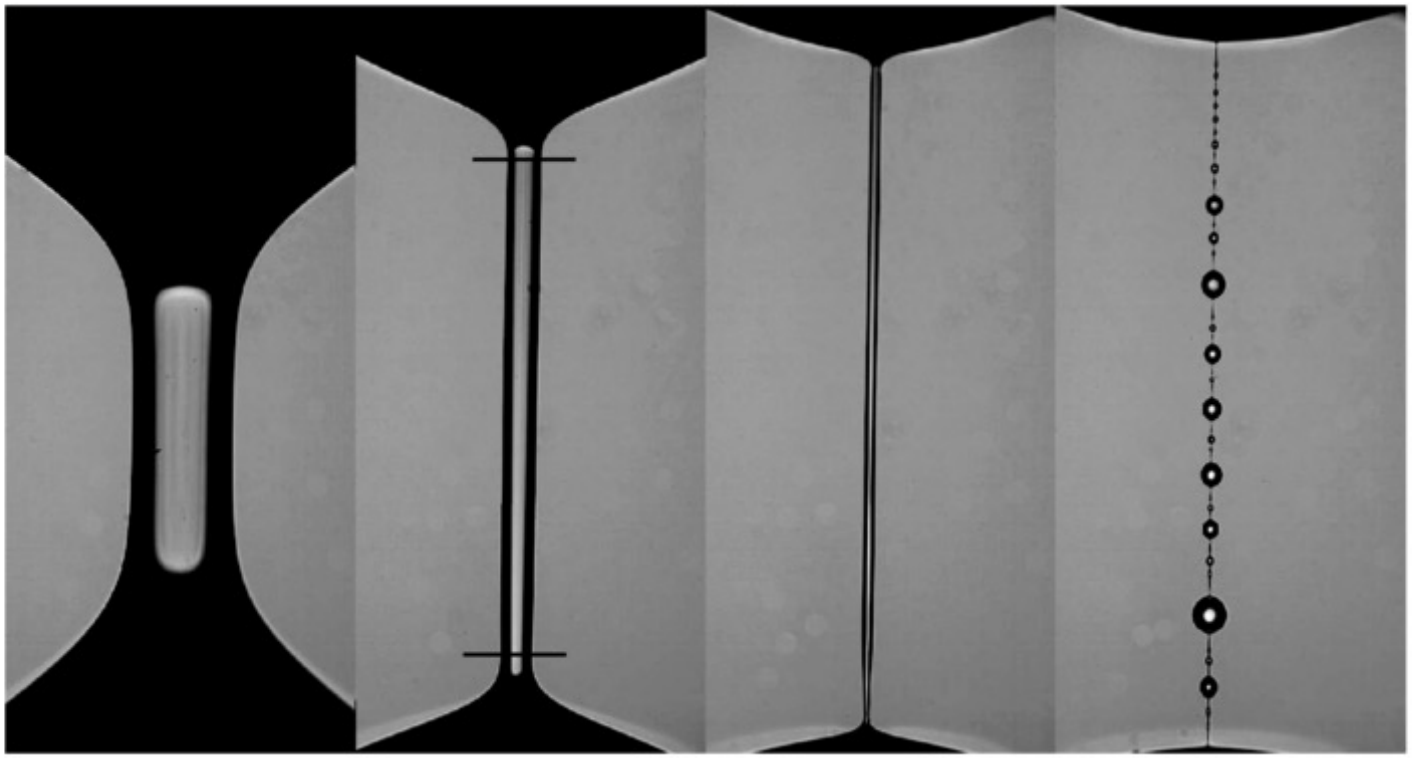

Visualization of the flow profile inside a thinning filament during capillary breakup of a polymer solution via particle image velocimetry and particle tracking velocimetry

Physics of Fluids 24, 053102 (2012); https://doi.org/10.1063/1.4718675

S. Gier *and* C. Wagner[a)]

Extensional Flow

$$\eta_e = \frac{\sigma_{zz} - \frac{1}{2}\sigma_{xx} - \frac{1}{2}\sigma_{yy}}{\dot{\varepsilon}}$$

$Tr = \eta_e / \eta$ **Trouton Viscosity = 3 Shear Viscosity for a Newtonian fluid**

For a constant extensional strain rate, $\gamma'_{zz} = dv_z/dz$ = constant

So, $v_z = dz/dt$ = constant z

dz/z = constant dt

$z = \exp(Kt)$

You need to stretch the fluid with exponentially increasing length.

That is hard to do in a lab.

How dilute are dilute solutions in extensional flows? C. Clasen, J. P. Plog,, W.-M. Kulicke, M. Owens, C. Macosko, L. E. Scriven, M. Verani and G. H. McKinley, J. Rheol. **50** 849-881 (2006);

Graessley (1980) provides a simple definition of c^* that is widely accepted for demarking the boundary separating the physical and rheological definition of dilute and semidilute polymer solutions

$$c^* = \frac{0.77}{[\eta]},$$

$$c^*_{R_G} = \frac{M_w}{\frac{4}{3}\pi\langle R_G^2\rangle^{3/2} N_A}$$

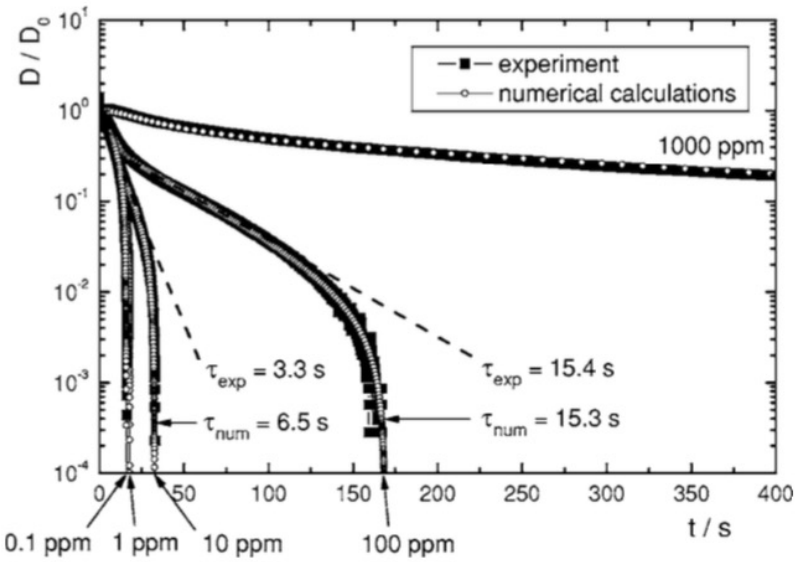

FIG. 1. Comparison of the numerically calculated evolution in the filament diameter (open symbols) with experimental data from capillary thinning experiments (closed symbols) for a dilution series of the Boger fluid from sample E (M_w=8.3×10^6 g/mol) for different concentrations spanning $0.1 \leq c \leq 1000$ ppm. In addition the relaxation times τ_{exp}, determined from fitting the elasto-capillary thinning regime [Eq. (22)] of the experiments, and τ_{num}, determined from fitting the numerical calculations [Eqs. (17)–(21)] to the experimental data, are given for selected concentrations.

Diameter from capillary thinning experiments

$$\frac{D(t)}{D_0} = \left(\frac{GD_0}{4\gamma}\right)^{1/3} \exp(-t/3\tau_0)$$

How dilute are dilute solutions in extensional flows? C. Clasen, J. P. Plog,, W.-M. Kulicke, M. Owens, C. Macosko, L. E. Scriven, M. Verani and G. H. McKinley, J. Rheol. **50** 849-881 (2006);

Shear Measurement

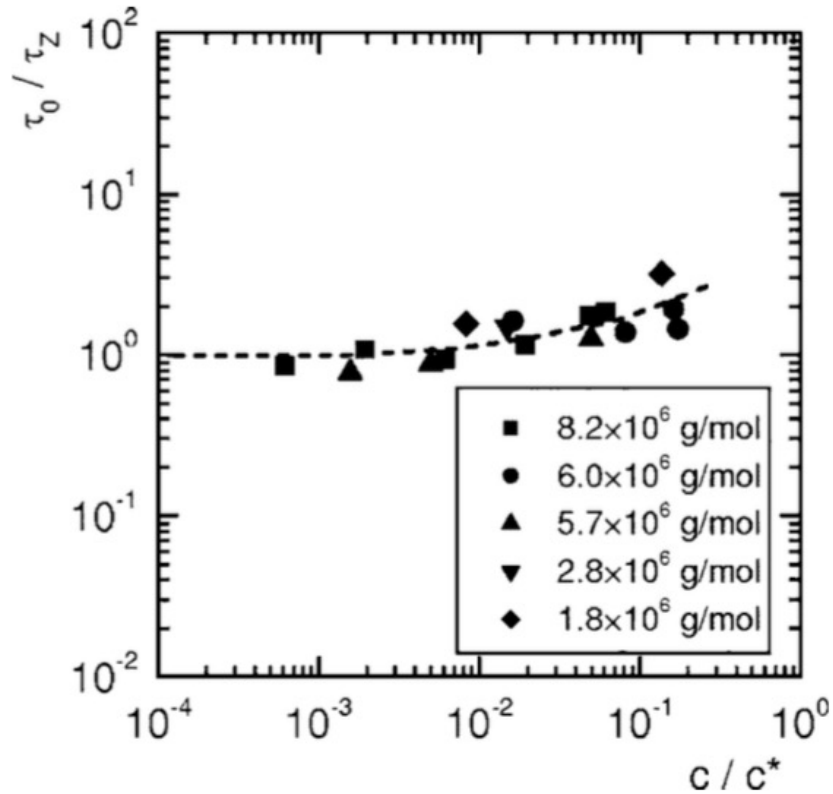

SAOS = small amplitude oscillatory shear

FIG. 5. Reduced relaxation time τ_0/τ_z as a function of the reduced concentration c/c^*, determined from SAOS experiments and fits of the moduli to Eqs. (2) and (3) for polystyrene of different molar masses dissolved in styrene oligomer.

Thurston relation, Eq. (5), giving a Zimm relaxation time τ_Z of

$$\tau_z = \frac{1}{\sum_i \frac{1}{i^{2+\tilde{\sigma}}}} \frac{[\eta]\eta_s M_w}{RT}. \qquad (31)$$

How dilute are dilute solutions in extensional flows? C. Clasen, J. P. Plog,, W.-M. Kulicke, M. Owens, C. Macosko, L. E. Scriven, M. Verani and G. H. McKinley, J. Rheol. **50** 849-881 (2006);

Extensional Measurement

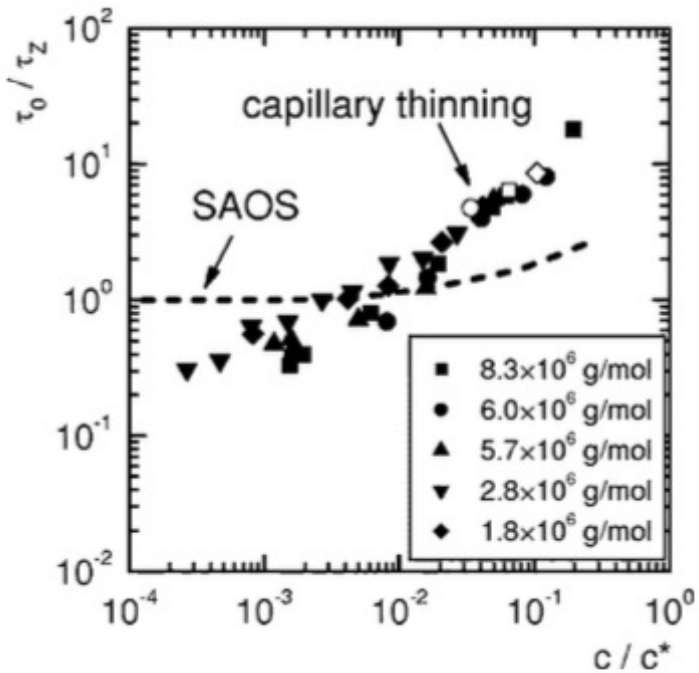

FIG. 6. Reduced relaxation time τ_0/τ_z as a function of the reduced concentration c/c^* for several dilution series of polystyrene Boger fluids determined from capillary break thinning experiments. In addition to the data obtained in this work, data points for the boger fluids SM1 (2×10^6 g/mol, ○), SM2 (6.5×10^6 g/mol, □), and SM3 (20×10^6 g/mol, ◇) are shown (taken from [7] and [20]). For comparison, also a mean square fit to the results from the SAOS experiments in Fig. 5 is shown.

Thurston relation, Eq. (5), giving a Zimm relaxation time τ_Z of

$$\tau_z = \frac{1}{\sum_i \frac{1}{i^{2+\tilde{\sigma}}}} \frac{[\eta]\eta_s M_w}{RT}. \qquad (31)$$

Structure and linear viscoelasticity of flexible polymer solutions: comparison of polyelectrolyte and neutral polymer solutions R. Colby, Rheo. Acta **49** 425-442 (2010)

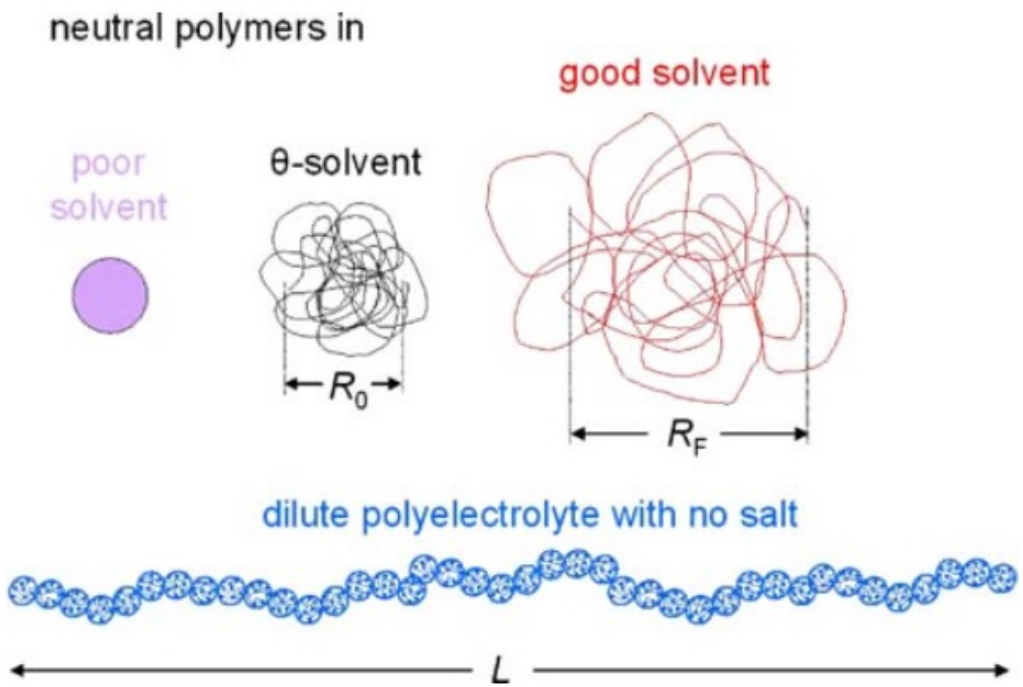

Fig. 1 Conformations of polymers in dilute solution. Neutral polymers in poor solvent collapse into dense coils with size $\approx bN^{1/3}$ (*purple*). Neutral polymers in θ-solvent are random walks with ideal end-to-end distance $R_0 = bN^{1/2}$ (*black*). Neutral polymers in good solvent are self-avoiding walks with Flory end-to-end distance $R_F = bN^{0.588}$ (*red*). Polyelectrolytes with no salt adopt the highly extended directed random walk conformation (*blue*) with length L proportional to N

Structure and linear viscoelasticity of flexible polymer solutions: comparison of polyelectrolyte and neutral polymer solutions R. Colby, Rheo. Acta **49** 425-442 (2010)

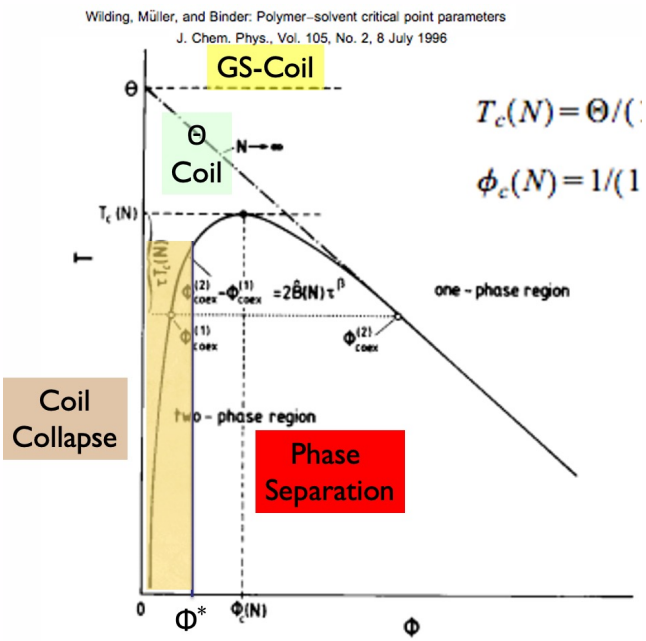

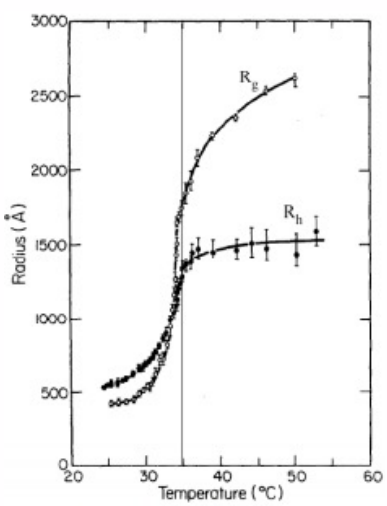

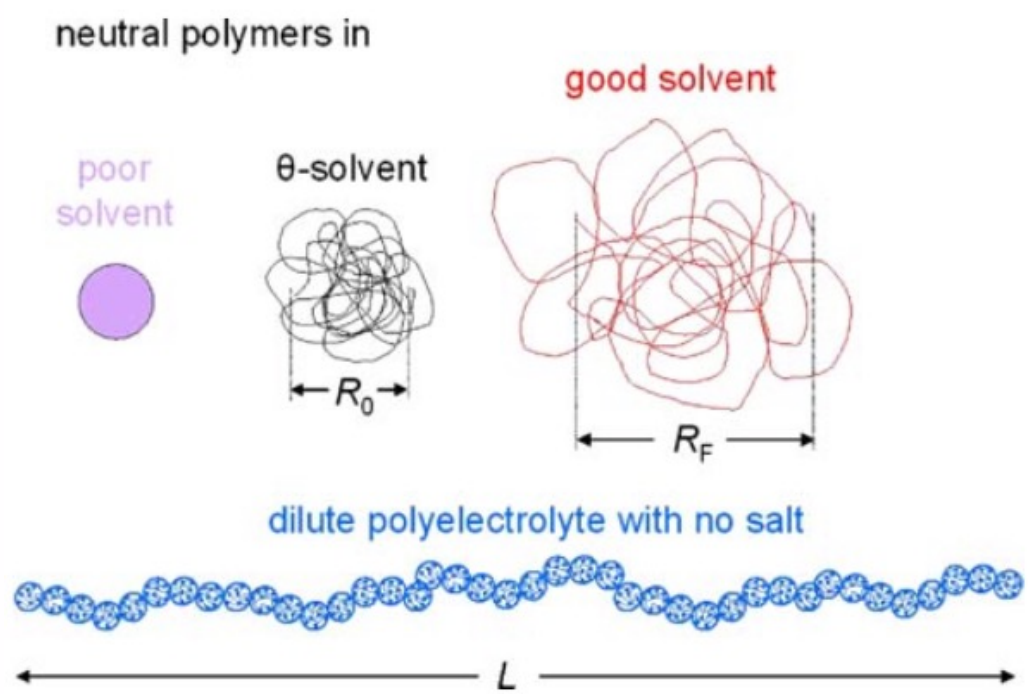

Fig. 1 Conformations of polymers in dilute solution. Neutral polymers in poor solvent collapse into dense coils with size $\approx bN^{1/3}$ (*purple*). Neutral polymers in θ-solvent are random walks with ideal end-to-end distance $R_0 = bN^{1/2}$ (*black*). Neutral polymers in good solvent are self-avoiding walks with Flory end-to-end distance $R_F = bN^{0.588}$ (*red*). Polyelectrolytes with no salt adopt the highly extended directed random walk conformation (*blue*) with length L proportional to N

Coil Collapse Following A. Y. Grosberg and A. R. Khokhlov "Giant Molecules"

What Happens to *the* left of the theta temperature?

Coil Expansion Factor α

Grosberg uses: $$\alpha^2 = \frac{R^2}{R_0^2}$$

Rather than the normal definition used by Flory: $$\alpha = \frac{R^2}{R_0^2}$$

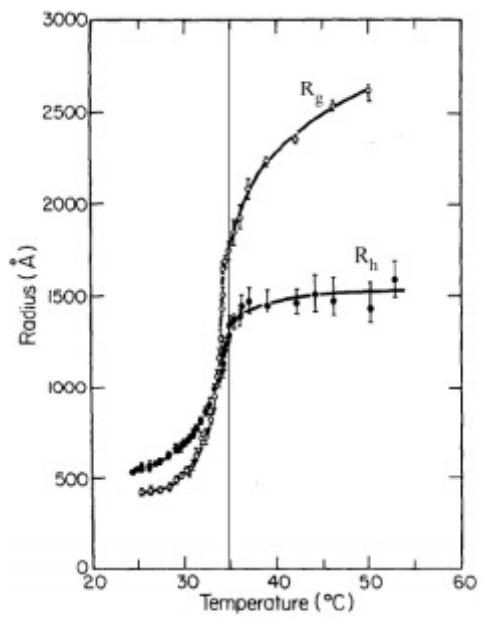

$$E(R) = kT\left(\frac{3R^2}{2nl^2} + \frac{n^2 V_c\left(\frac{1}{2} - \chi\right)}{R^3}\right)$$

Figure 3. *Radius of gyration, R_g, and hydrodyamic radius R_h versus temperature for polystyrene in cyclohexane. Vertical line indicates the phase separation temperature. From Reference [21].*

Coil Collapse Following A. Y. Grosberg and A. R. Khokhlov "Giant Molecules"

What Happens to *the* left of the theta temperature?

Grosberg uses: $\alpha^2 = \dfrac{R^2}{R_0^2}$ Rather than the normal definition used by Flory: $\alpha = \dfrac{R^2}{R_0^2}$

Short-Range Interactions

We had $C_\infty = R^2/R^2_0 = n_K l_K^2/n_0 l_0^2 = L l_K/L l_0 = l_K/l_0$

Long-Range Interactions

Flory $\alpha = R^2/R^2_0 = n^{6/5} l^2/n l^2 \sim n^{1/5}$

Grosberg

$\alpha^2 = R^2/R^2_0 \;\therefore\; \alpha \sim n^{1/10}$

Coil Collapse … ant Molecules”

ture?

Grosberg uses: … lory: $\alpha = \frac{R^2}{R_0^2}$

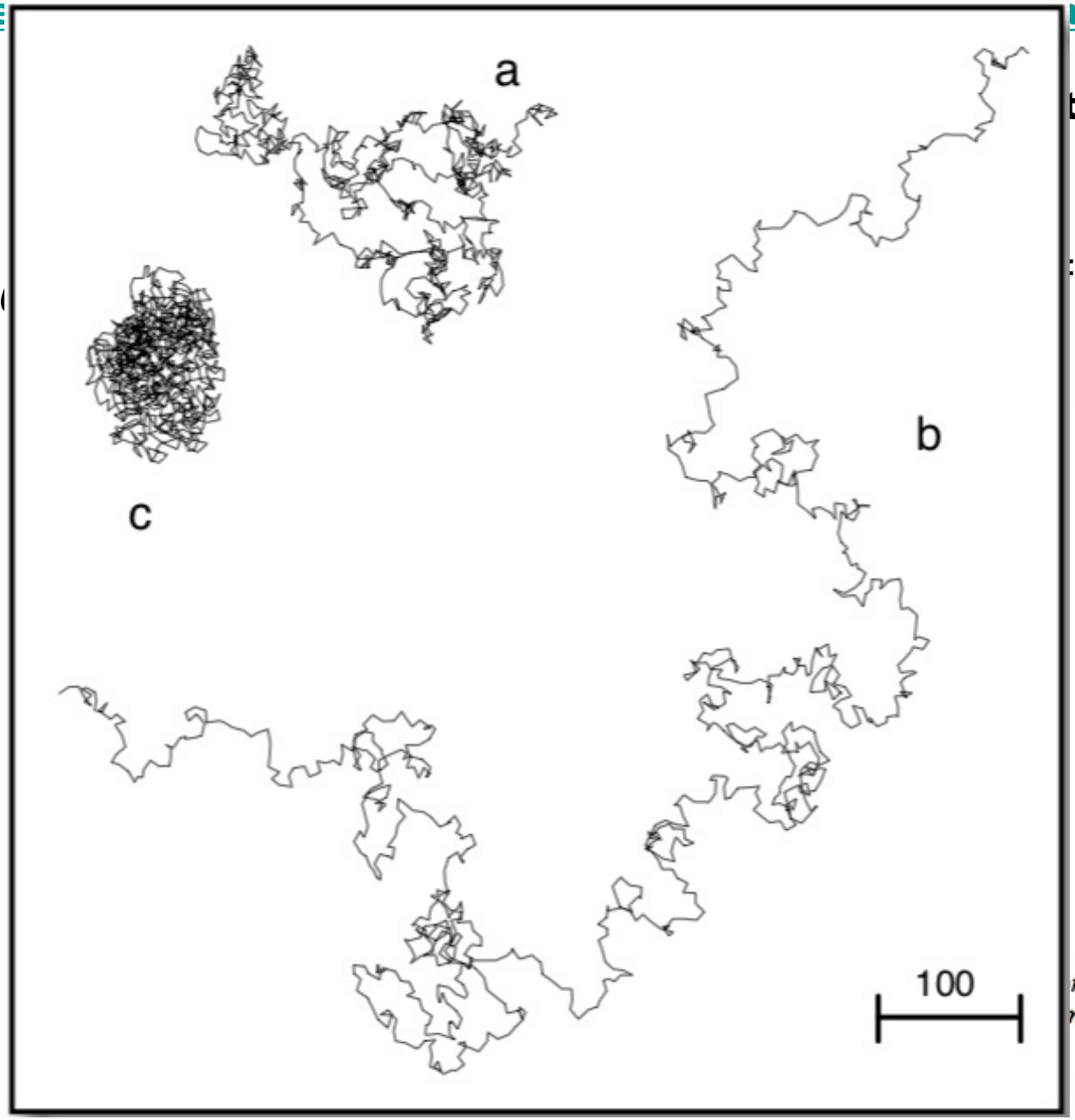

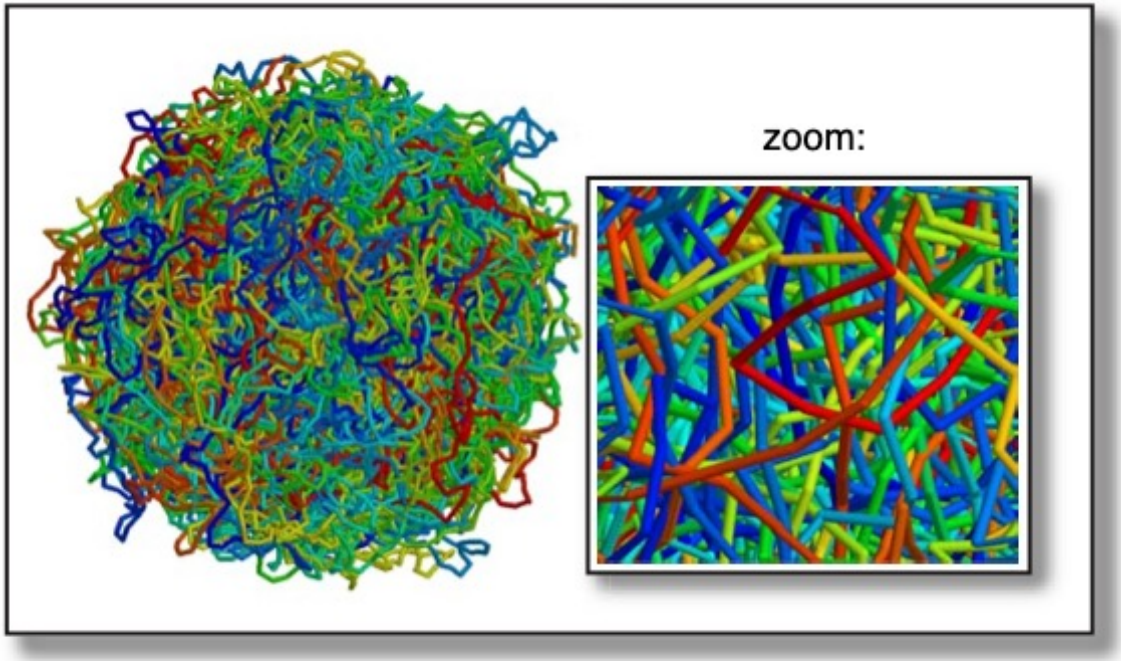

Fig. C9.1 A computer simulated globule of a long chain. Notice that the globule is pretty accurately spherical, its surface consists of loops, while its interior, particularly well seen in the zoomed part, reminds a concentrated solution of different chains (compare Figure C12.3) — even though in reality they are all distant parts of the same chain. The chain is a homopolymer in terms of chain flexibility and monomer–monomer interactions being the same for all monomers. However, to help the eye, the chain is colored, smoothly going through the rainbow colors from one end to the other (e.g., one end is red and the other is violet, with all intermediate colors in between). What one should notice is that any particular color is not located in a particular region of the globule; just the opposite, every color is reasonably uniformly distributed throughout the globule, and the local surrounding of any monomer is full of all sorts of different colors, confirming that very distant parts of the chain form contacts in the globule. The figure is courtesy of L. Mirny.

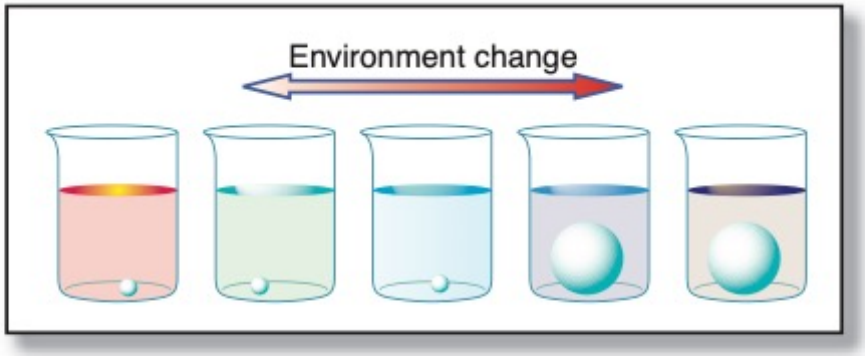

Fig. C9.6 A cartoon showing gel collapse and swelling upon change of environment conditions, such as, e.g., solvent composition, temperature and so on. The figure is courtesy of T. Tanaka.

Fig. C9.10 A variety of factors that can cause gel to collapse. The figure is courtesy of T. Tanaka.

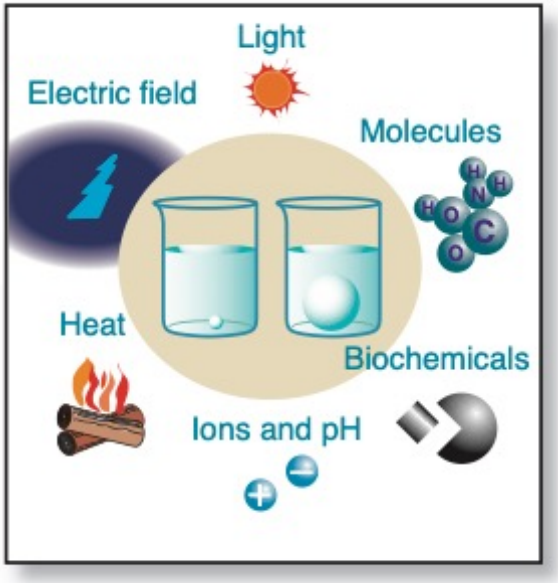

The Flory Krigbaum expression for the free energy of a self-avoiding chain is given by,

$$F(R) = \frac{z^2 V_0 (1-2\chi) kT}{2R^3} + \frac{3R^2 kT}{2zl^2} = U(R) - TS(R) \qquad (1)$$

Equation (1) can be rewritten using the coil expansion coefficient, α,

$$\alpha^2 = \frac{R^2}{R_\theta^2} = \frac{R^2}{zl^2}$$

$$F(\alpha) = \frac{z^{1/2} BkT}{2\alpha^3 l^3} + \frac{3\alpha^2 kT}{2} = U(\alpha) - TS(\alpha) \qquad (3)$$

where B is the second virial coefficient,

$$B = V_0 (1-2\chi)$$

Van der Waals $P = \frac{RT}{V-b} - \frac{a}{V^2}$

$$\frac{pV}{RT} = 1 + \frac{1}{V}\left(b - \frac{a}{RT}\right) + \left(\frac{b}{V}\right)^2 + \left(\frac{b}{V}\right)^3 + \cdots$$

$$p/\rho RT = 1 + B_2 \rho + B_3 \rho^2 + \ldots$$

$$B(T) = b - \frac{a}{RT}$$

Finding the minimum in the free energy expression, equation (3), yields the most probable value for α,

$$\alpha \sim \left(\frac{z^{1/2} B}{l^3}\right)^{1/5} \qquad \mathrm{d}F(\alpha)/\mathrm{d}\alpha = 0 \qquad (5)$$

$$R \sim R_0 \alpha = z^{1/2} b\alpha \sim z^{3/5} B^{1/5} b$$

This is an exact solution by Grosberg's method

Van der Waals' Equation

$p = nRT/(V\text{-}b) - a(n/V)^2 + c\,(n/V)^3$ Van der Waals Equation with repulsive ternary interactions

Compressibility Factor $Z = pV_{molar}/RT = p/\rho RT = 1 + B_2\,\rho + B_3\,\rho^2 + \ldots$ Virial Expansion

B_2 has units of molar volume

$Z_{\mathrm{VdW}} = pV_{molar}/RT = V/(V\text{-}b) - a\rho = 1/(1\text{-}b\rho) - a\rho + c\rho^2$

Geometric series $\Sigma ar^k = a/(1\text{-}r)$ sum from 0 to ∞

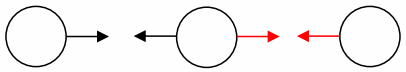

Red detracts from Black

So, $1/(1\text{-}b\rho) = \Sigma ar^k = 1 + b\rho + (b\rho)^2 + \ldots$ and for $b\rho = b/V$ is very small

$Z_{\mathrm{VdW}} = 1/(1\text{-}b\rho) - a\rho = 1 + (b - a/RT)\,\rho + (b^2 + c/\mathrm{RT})\,\rho^2 + \ldots$

Compare with the virial expansion

$Z = pV_{molar}/RT = p/\rho RT = 1 + B_2\,\rho + B_3\,\rho^2 + \ldots$

$B_2 = b - a/RT$ and $B_3 = b^2 + c/\mathrm{RT}$

For an immiscible system B_2 is negative or very small (low temperature)
B_3 can be positive leading to a discrete phase transition or negative leading to a continuous transition

$$F(\alpha) = \frac{z^{1/2} BkT}{2\alpha^3 l^3} + \frac{3\alpha^2 kT}{2} = U(\alpha) - TS(\alpha)$$

$$\alpha^2 = \frac{R^2}{R_0^2} = \frac{R^2}{zl^2}$$

The virial expansion of the enthalpic interactions is given by,

$$U(\alpha) = V_{Coil} kT\left[n^2 B + n^3 C + \ldots\right] \approx V_{Coil} kTn^2 B \sim \frac{kTR^3 Bz^2}{R^6} = \frac{z^{1/2} BkT}{2\alpha^3 l^3} \qquad (6)$$

$n \sim z/R^3$

where n is the segmental density in the coil and V_{Coil} is the volume of the coil. The second virial coefficient describes binary interactions and the third virial coefficient describes ternary interactions. In dilute conditions we can ignore the higher order interactions and use only the second virial coefficient.

B changes sign, positive for miscible, negative for phase separation below the Boyle temperature $T_B = a/b$ ($B = b - a/T$ so "a" (or χ) is negative for miscibility/repulsive pp)

C is always positive, i.e., favors coil expansion.

C is important below the theta temperature to model the coil to globule transition at high monomer density

For simplicity we ignore higher order terms because C is enough to give the gross features of this transition.

Generally, it is known that this transition can be either ***first-order*** for biopolymers such as protein folding, or ***second-order*** for synthetic polymers.

First-order means that the first derivative of the free energy is not continuous, i.e., a jump in free energy at a discrete transition temperature, such as a melting point, heat of melting.

Second order, free energy, volume, entropy etc. are continuous through the transition, slope changes in T (heat capacity, thermal expansion coefficient).

Blob model for coil collapse

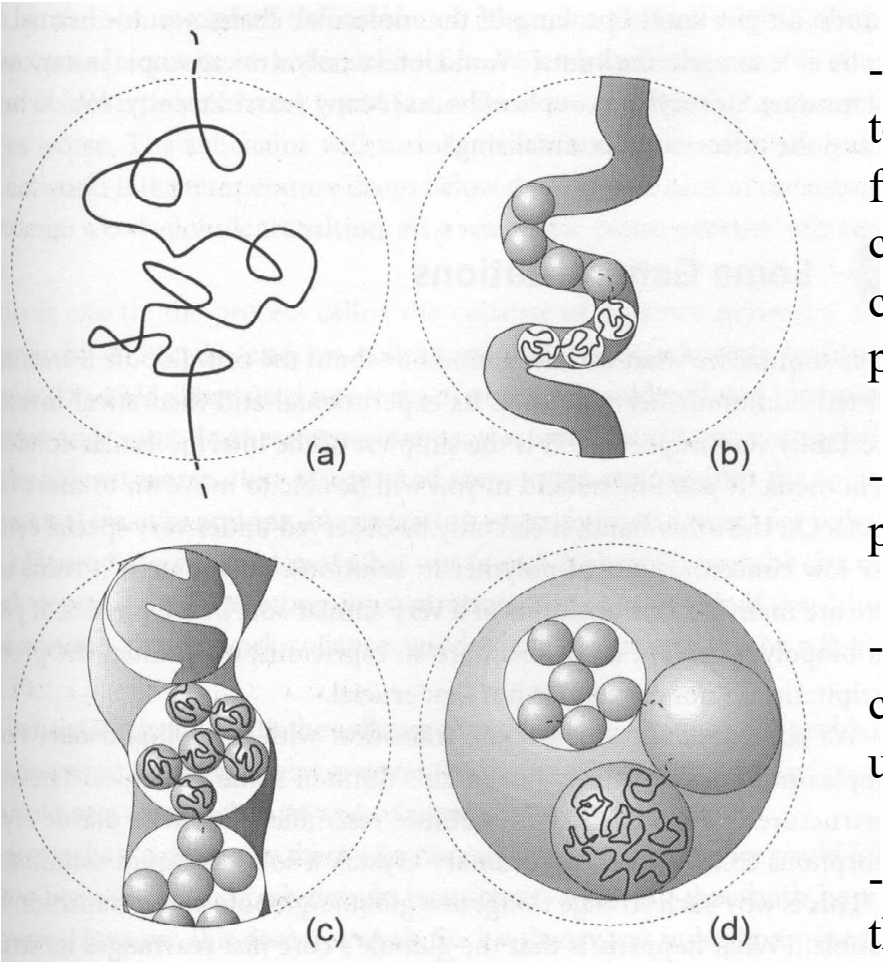

-The expanded coil transitions to a Gaussian chain by locally forming Gaussian "blobs" called "*thermal blobs*" (will cover later). Neutron scattering provides evidence.

-These blobs grow as the theta point is approached.

-Thermally driven structural changes occur from the bottom up.

-Propose a similar model for the collapse of the theta coil using a different kind of "blob".

$d_f = 2$ for coil

$d_f = 3$ for blob

Gaussian Scaling of g^* Blobs

$$R^2 \sim g^*$$

Blob model for coil collapse

$d_f = 2$ for coil
$d_f = 3$ for blob

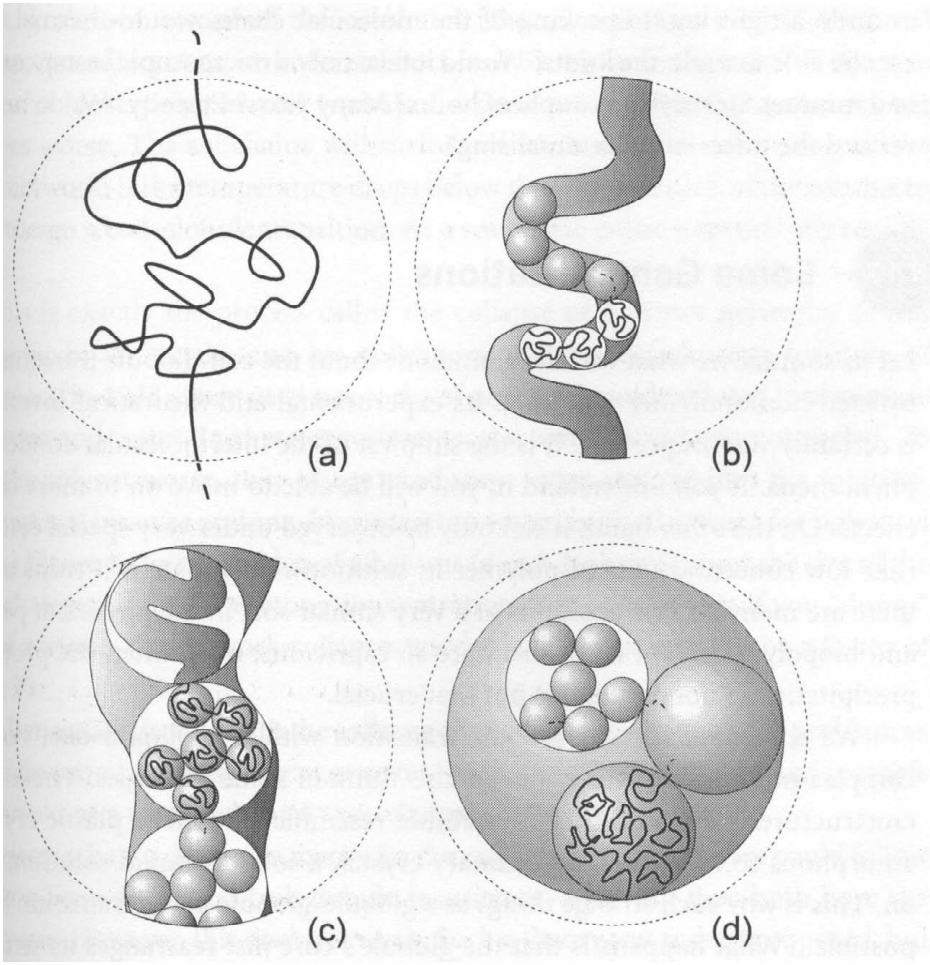

FIGURE 8.6 A few initial stages of the coil-globule transition. This looks self-similar! (Compare with what we write about self-similarity in Chapter 10). *Source:* Courtesy of S. Nechaev.

Number of Blobs = z/g^*

Gaussian Scaling of g^* Blobs

$$R^2 \sim g^*$$

Grosberg and Khokhlov's figure 8.6 shows a model for chain collapse that explains the entropic behavior in terms of blobs of g* chain units associated with a confined chain. We can consider the collapsed chain as composed of z/g* collapsed blobs each with an energy kT.

Entropic Part of Collapse Free Energy

Number of Blobs (z/g^*) times kT is the Confinement Entropy

$$\alpha^2 = \frac{R^2}{R_0^2} = \frac{R^2}{zl^2}$$

$$\left[-TS(\alpha)\right]_{Confinement} \sim kT\frac{z}{g^*} = kT\frac{zl^2}{R^2} = \frac{kT}{\alpha^2} \qquad R^2 \sim g^* \qquad (7)$$

In the absence of confinement (coil collapse) the expression was,

$$\left[-TS(\alpha)\right]_{Expansion} \sim kT\alpha^2 \qquad F(\alpha) = \frac{z^{1/2}BkT}{2\alpha^3 l^3} + \frac{3\alpha^2 kT}{2} = U(\alpha) - TS(\alpha)$$

and a sum of these terms (approximation),

$$-TS(\alpha) = \left[-TS(\alpha)\right]_{Confinement} + \left[-TS(\alpha)\right]_{Expansion} \sim kT\left(\alpha^2 + \alpha^{-2}\right) \qquad (9)$$

Total Collapse Free Energy

$$F(\alpha) \sim kT\left(\alpha^2 + \alpha^{-2}\right) + \frac{kTBz^{1/2}}{2\alpha^3 l^3} + \frac{kTC}{\alpha^6 l^6}$$

$$kT\,C\,n^3 = kT\,C\,z^3/R^3 = kT\,C/(\alpha^6 l^6)$$

$$F(\alpha) = \frac{z^{1/2} BkT}{2\alpha^3 l^3} + \frac{3\alpha^2 kT}{2} = U(\alpha) - TS(\alpha) \qquad (3)$$

Free Energy Including Third Virial Coefficient

$$F(\alpha) \sim kT\left(\alpha^2 + \alpha^{-2}\right) + \frac{kTBz^{1/2}}{2\alpha^3 l^3} + \frac{kTC}{\alpha^6 l^6} \qquad (10).$$

α > 1 for expansion

α < 1 for contraction

Which works for both expansion and collapse. Finding the minimum in this free energy yields the most probable value for α, (equivalent of equation (5)),

$$\alpha^5 - \alpha = x + y\alpha^{-3} \tag{11}$$

where x is related to B and is given by,

$$x = K_1 B z^{1/2} / l^3 \tag{12}$$

and y is related to C and is given by,

$$y = K_2 C / l^6 \tag{13}$$

If α is small you can neglect the terms on the left hand side of equation (11) and solve for R,

$$R \sim \alpha z^{1/2} l \sim \left(\frac{-C}{B}\right)^{1/3} z^{1/3} \tag{14}$$

Ratio of C/B determines behavior
The collapsed coil is 3d

$$\alpha^5 - \alpha = x + y\alpha^{-3} \tag{11}$$

$$x \sim B;\ y \sim C$$
$$B \sim 1/T;\ \alpha \sim V^{1/3}$$

Equation (11) can be understood by plotting the coil expansion factor, α, versus the reduced temperature function x for fixed values of y as shown in Figure 8.3 from Grosberg and Khokhlov reproduced below. In this figure, at large y the chain is flexible and the coil only slightly collapses on cooling (smaller x). The theta temperature occurs at x = 0. For rigid chains with a small value for y, the curve shows three values for a given x just below the θ-temperature.

134 Chapter 8 Coils and Globules

FIGURE 8.3 The dependence $\alpha(x)$ given by equation (8.7) for different values of y; from top to bottom, the curves correspond to the following values of y: 10, 1, 0.1, 1/60, 0.01, 0.001, 0.0001.

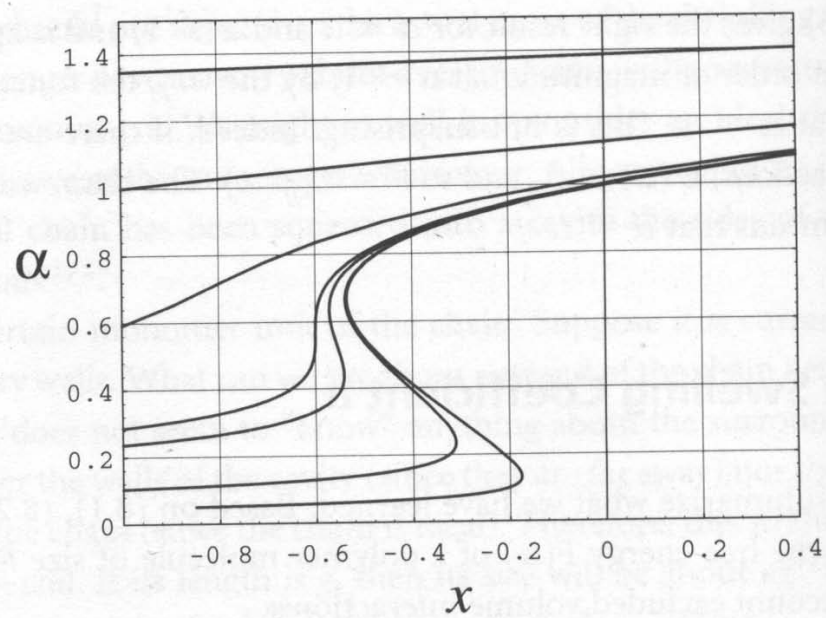

Maxwell Construction

Maxwell Construction

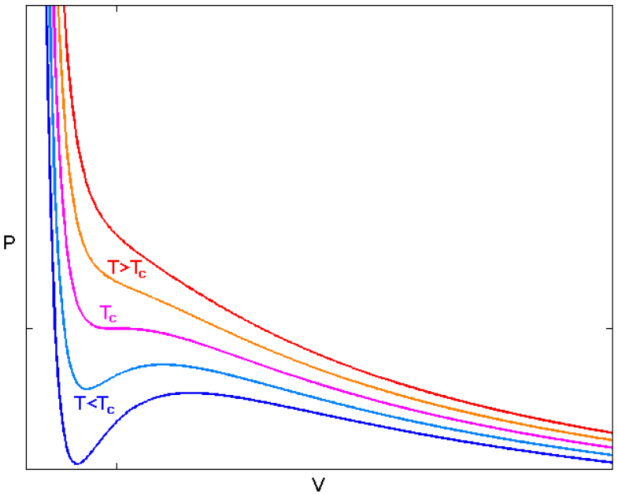

Lieden the Netherlands
van der Waals place

Isotherm of a **Cubic Equation of State**
in the Two-Phase Region of Temperature

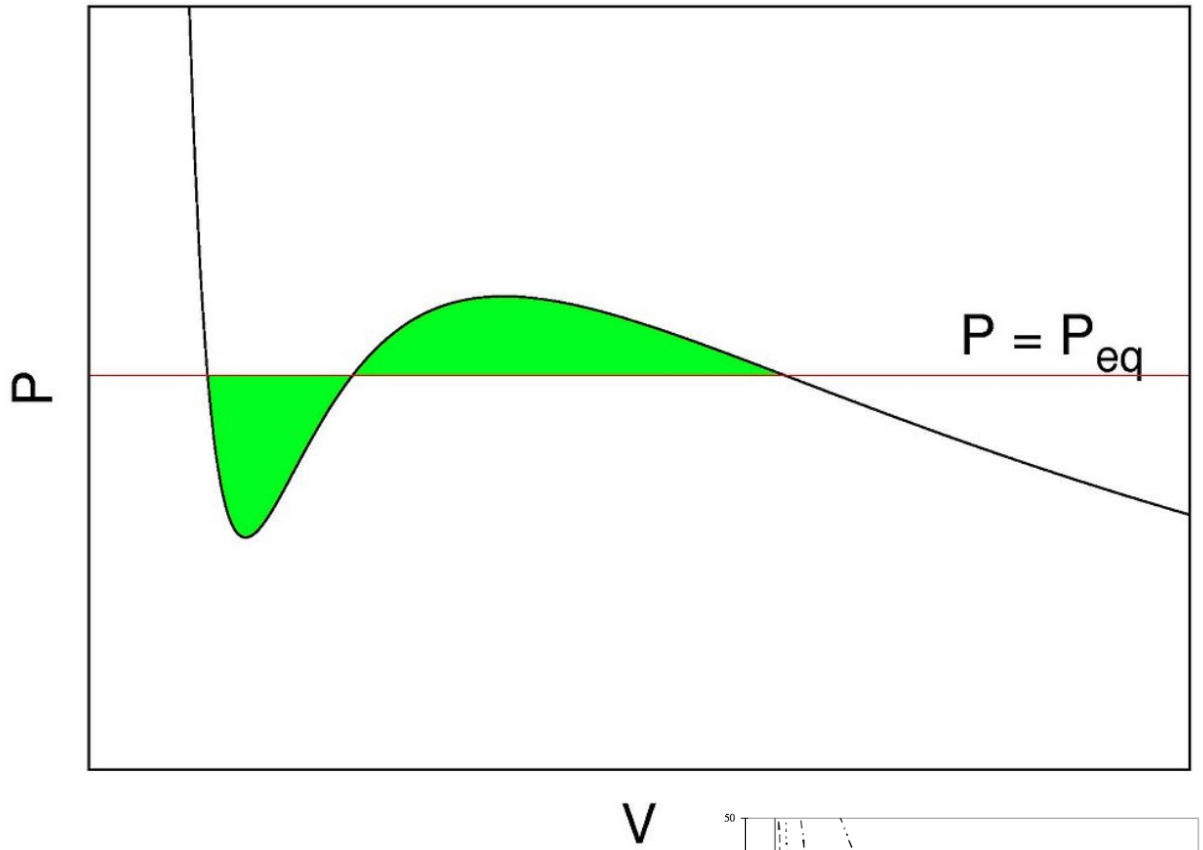

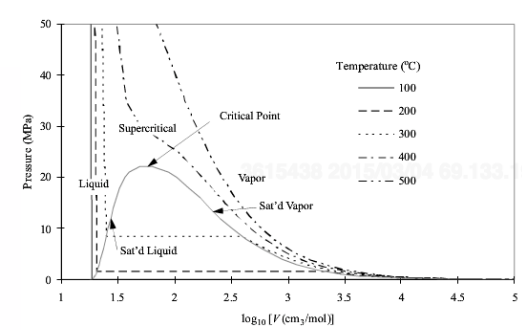

Figure 1.4 *P-V-T behavior of water at the same temperatures used in Fig. 1.3. The plot is prepared from the steam tables in Appendix E.*

There are three possible roots, two points are at equilibrium, middle is not real.

FIGURE 8.3
The dependence $\alpha(x)$ given by equation (8.7) for different values of y; from top to bottom, the curves correspond to the following values of y: 10, 1, 0.1, 1/60, 0.01, 0.001, 0.0001.

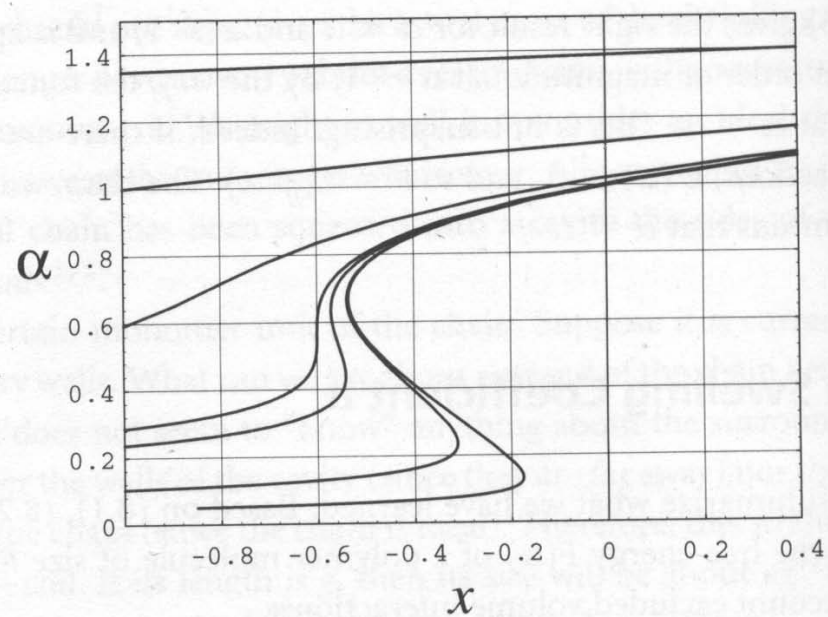

$$x \sim B;\ y \sim C$$

$$B \sim 1/T;\ \alpha \sim V^{1/3}$$

EOS Calculation

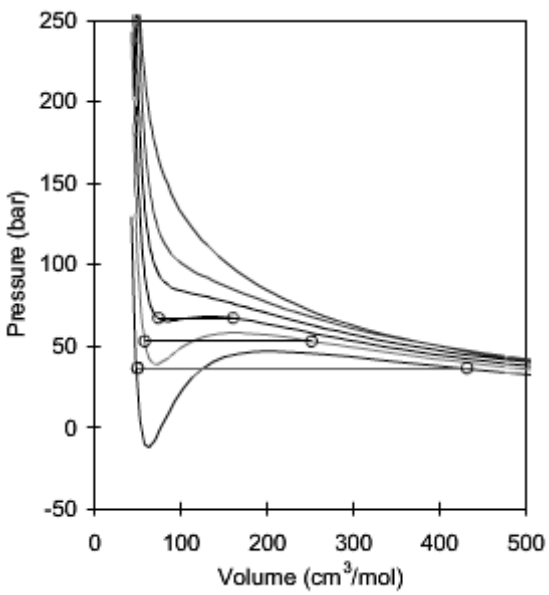

Phase Diagram

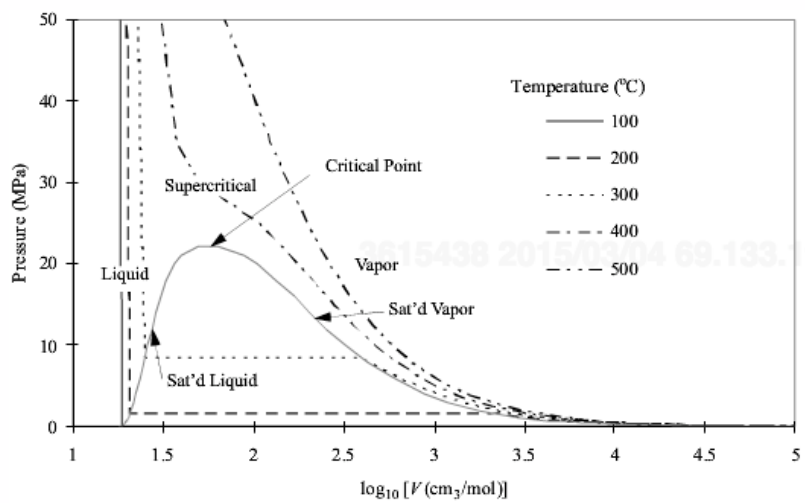

Figure 1.4 *P-V-T behavior of water at the same temperatures used in Fig. 1.3. The plot is prepared from the steam tables in Appendix E.*

FIGURE 8.3
The dependence $\alpha(x)$ given by equation (8.7) for different values of y; from top to bottom, the curves correspond to the following values of y: 10, 1, 0.1, 1/60, 0.01, 0.001, 0.0001.

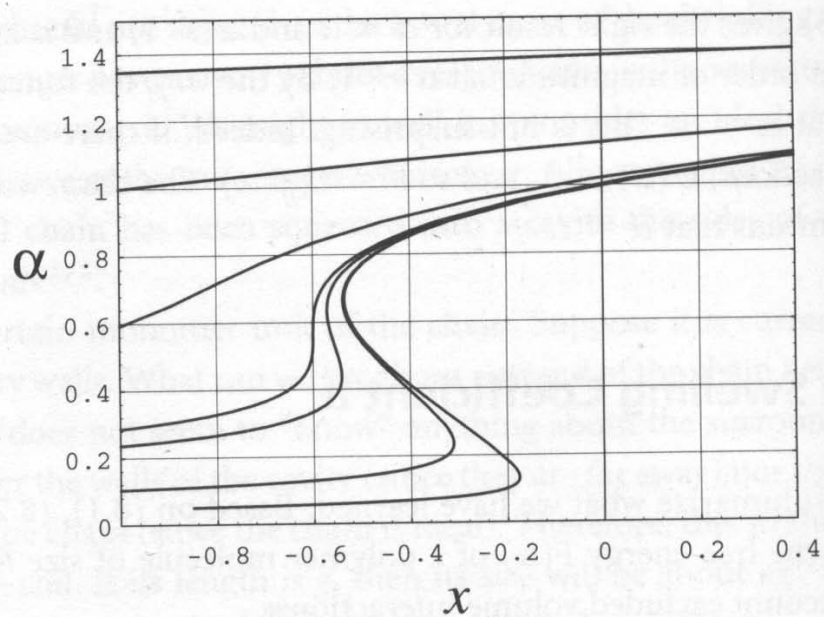

EOS Calculation

$$x \sim B;\ y \sim C$$

$$B \sim 1/T;\ \alpha \sim V^{1/3}$$

Phase Diagram

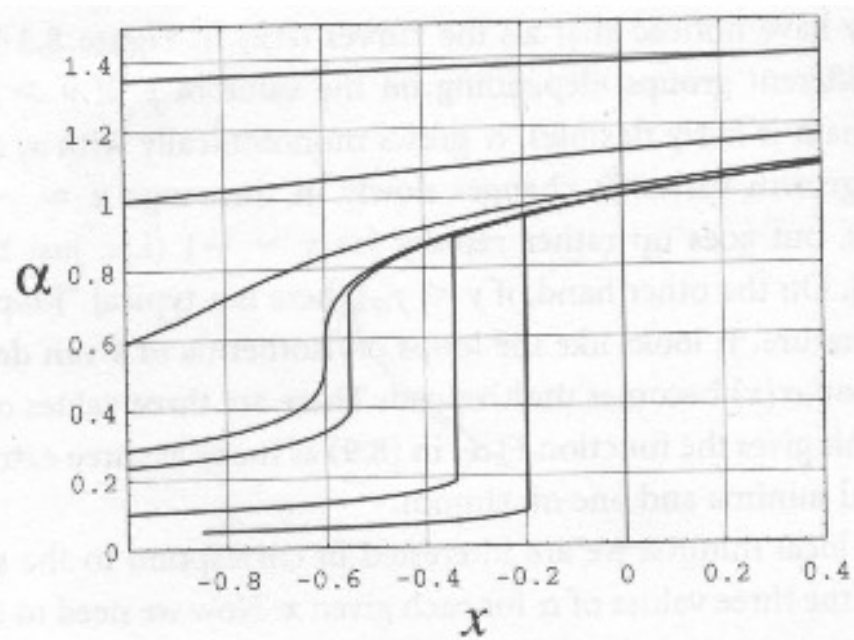

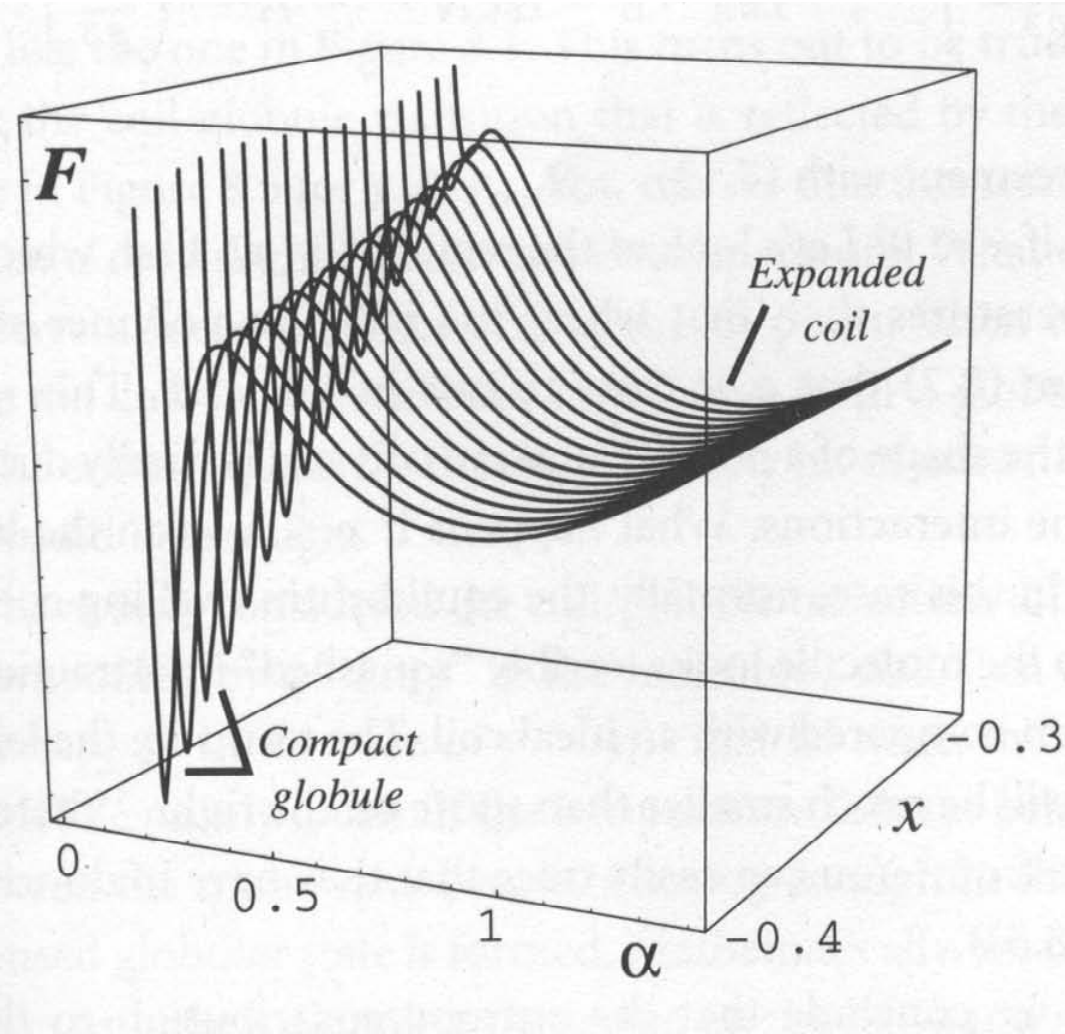

FIGURE 8.4
The dependence $F(\alpha)$ in the case where $\alpha(x)$ is multivalued. As x changes (which can be controlled by, say, temperature change), the shape of the $F(\alpha)$ dependence changes such that one minimum gets deeper at the expense of the other. Deeper minimum corresponds to the more stable state. For this figure, we choose the value $y = 0.001$.

$$x \sim B;\ y \sim C$$

$$B \sim 1/T;\ \alpha \sim V^{1/3}$$

$x \sim B; y \sim C$

$B \sim 1/T; \alpha \sim V^{1/3}$

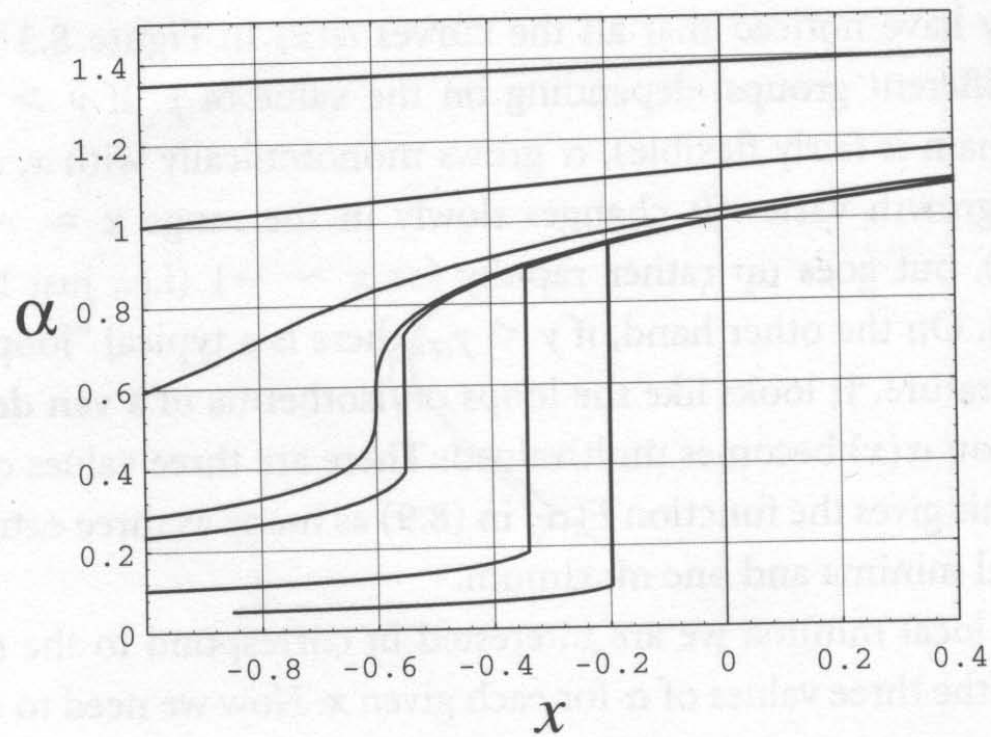

FIGURE 8.5 The curves $\alpha(x)$ in Figure 8.3 are multivalued at some x; in this figure, one solution is selected for each x such that the values of $\alpha(x)$ correspond to the absolute minimum free energy for every x. The values of y are the same as in Figure 8.3.

Generally, it is known that this transition can be either ***first-order*** for biopolymers such as protein folding, or ***second-order*** for synthetic polymers.
First order means that the first derivative of the free energy is not continuous, i.e. a jump in Free energy at a discrete transition temperature, such as a melting point.

$x \sim B; y \sim C$

$B \sim 1/T; \alpha \sim V^{1/3}$

FIGURE 8.5
The curves $\alpha(x)$ in Figure 8.3 are multivalued at some x; in this figure, one solution is selected for each x such that the values of $\alpha(x)$ correspond to the absolute minimum free energy for every x. The values of y are the same as in Figure 8.3.

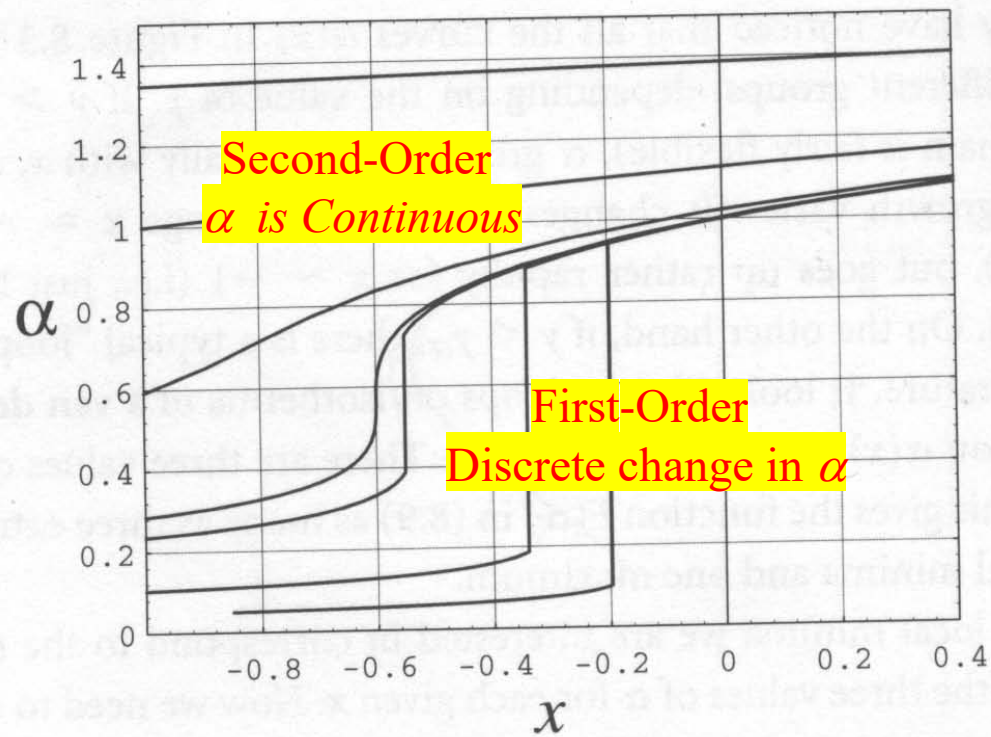

Generally, it is known that this transition can be either ***first-order*** for biopolymers such as protein folding, or ***second-order*** for synthetic polymers.
First order means that the first derivative of the free energy is not continuous, i.e. a jump in Free energy at a discrete transition temperature, such as a melting point.

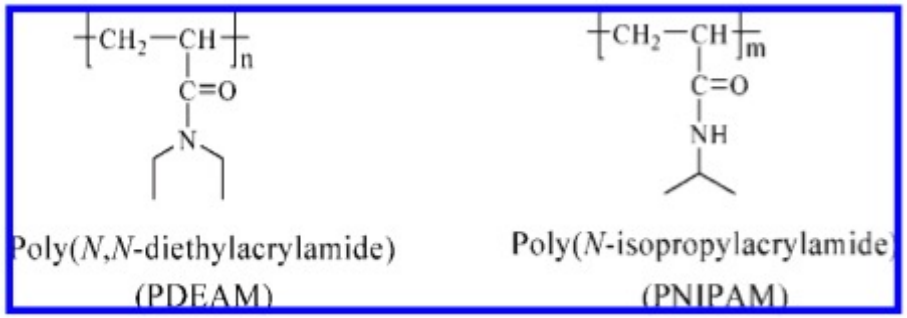

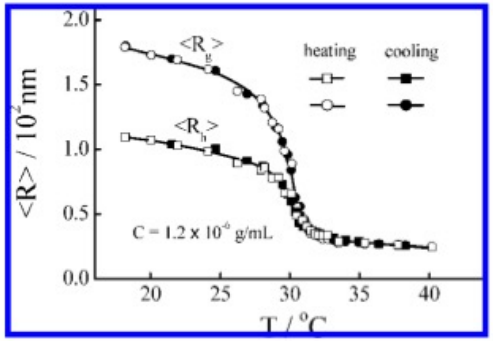

Figure 4. Temperature dependence of average radius of gyration ($\langle R_g \rangle$) and hydrodynamic radius ($\langle R_h \rangle$) of poly(*N*,*N*-diethylacrylamide) (PDEAM) chains in water in one heating-and-cooling cycle.

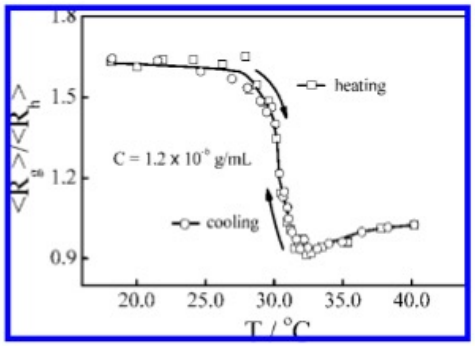

Figure 5. Temperature dependence of ratio of average radius of gyration to average hydrodynamic radius ($\langle R_g \rangle / \langle R_h \rangle$) of poly(*N*,*N*-diethylacrylamide) (PDEAM) chains in water in one heating-and-cooling cycle.

1.5 Theta
1.6 Expanded
0.774 Sphere
0.92 Draining Sphere
(We will Look at this further)

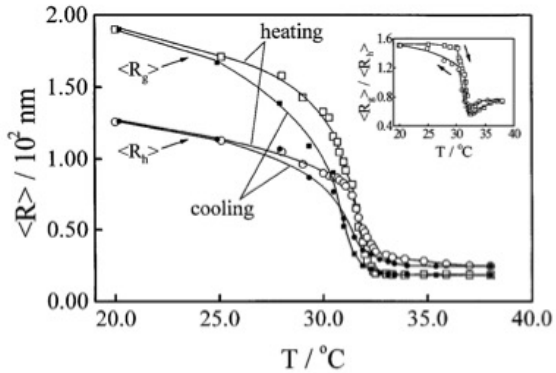

FIG. 2. Temperature dependence of the average radius of gyration $\langle R_g \rangle$ and the average hydrodynamic radius $\langle R_h \rangle$, respectively, in the coil-to-globule (heating) and the globule-to-coil (cooling) processes, where each point was obtained at least 2 h after the solution reached the thermal equilibrium to ensure that the polymer chains were thermodynamically stable. The inset shows the temperature dependence of $\langle R_g \rangle / \langle R_h \rangle$ in the heating and the cooling processes.

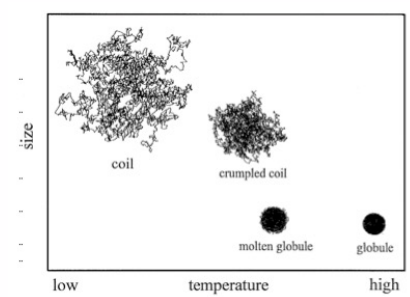

FIG. 3. Schematic of four thermodynamically stable states of a homopolymer chain in the coil-to-globule and the globule-to-coil transitions.

Macromolecules **2008**, *41*, 8927−8931

The Coil-to-Globule-to-Coil Transition of Linear Polymer Chains in Dilute Aqueous Solutions: Effect of Intrachain Hydrogen Bonding

Kejin Zhou,[†] Yijie Lu,[‡] Junfang Li,[‡] Lei Shen,[‡] Guangzhao Zhang,*[,‡] Zuowei Xie,[†,§] and Chi Wu*[,§]

ABSTRACT: Our previous studies of the captioned transition have shown that thermally sensitive poly(*N*-isopropylacrylamide) (PNIPAM) in water can form stable individual single-chain globules, but not for polystyrene (PS) in cyclohexane. In the current study, using poly(*N*,*N*-diethylacrylamide) (PDEAM) ($M_w = 1.7 \times 10^7$ g/mol and $M_w/M_n = 1.06$) with no hydrogen donator site, we intend to find whether the intrachain hydrogen bonding plays a role in stabilizing individual collapsed PNIPAM single-chain globules. We found that PDEAM can also form stable single-chain globules in water even though the transition is less sharp. The resultant individual PDEAM single-chain globules are less compact, reflecting in a lower chain density and a higher ratio of the radius of gyration to hydrodynamic radius, presumably due to the lack of intrachain hydrogen bonding. Our result also shows that, unlike PNIPAM, there is no hysteresis in the transition, indirectly supporting our previous assumption that the hysteresis observed for PNIPAM is due to the formation of some intrachain additional hydrogen bonds formed in the collapsed state.

VOLUME 80, NUMBER 18 PHYSICAL REVIEW LETTERS 4 MAY 1998

Globule-to-Coil Transition of a Single Homopolymer Chain in Solution

Chi Wu[1,2,*] and Xiaohui Wang[1]

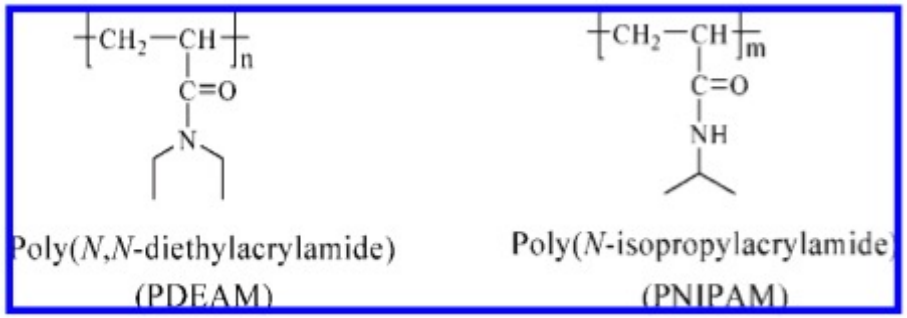

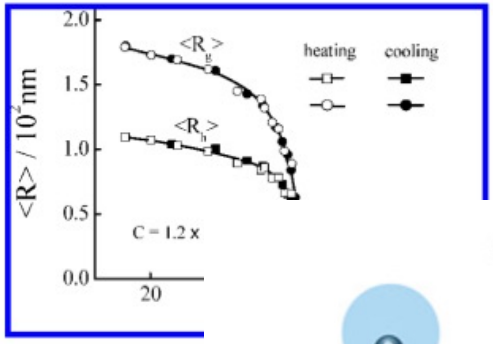

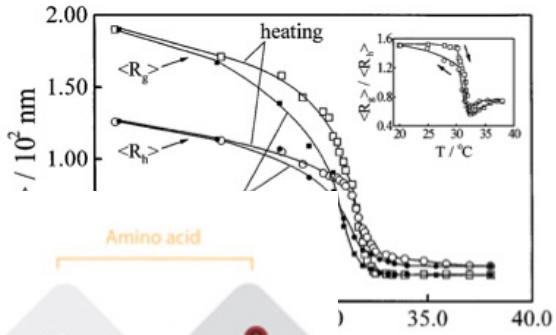

Figure 4. Temperature depend
and hydrodynamic radius ($\langle R_h \rangle$) c
chains in water in one heating

the average radius of
rodynamic radius $\langle R_h \rangle$,
eating) and the globule-
:h point was obtained at
e thermal equilibrium to
ıermodynamically stable.
endence of $\langle R_g \rangle / \langle R_h \rangle$ in

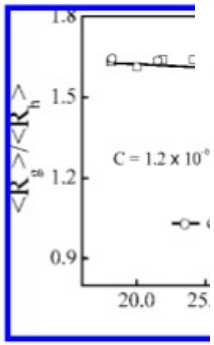

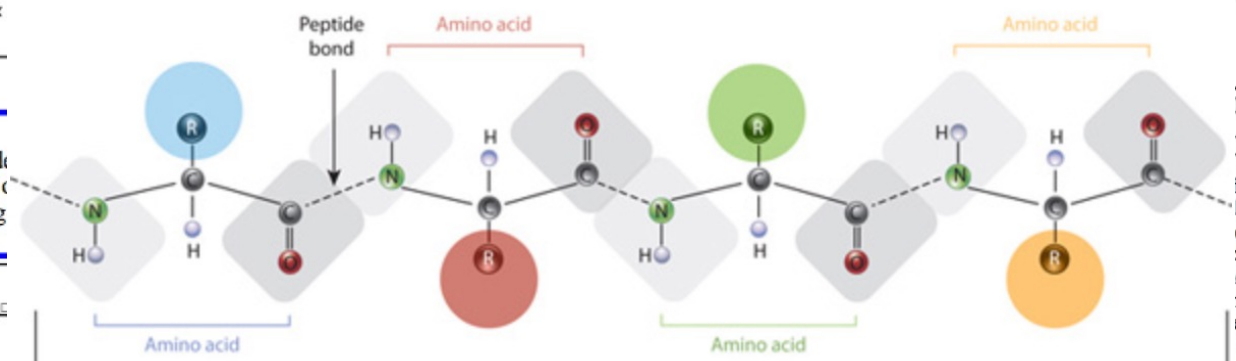

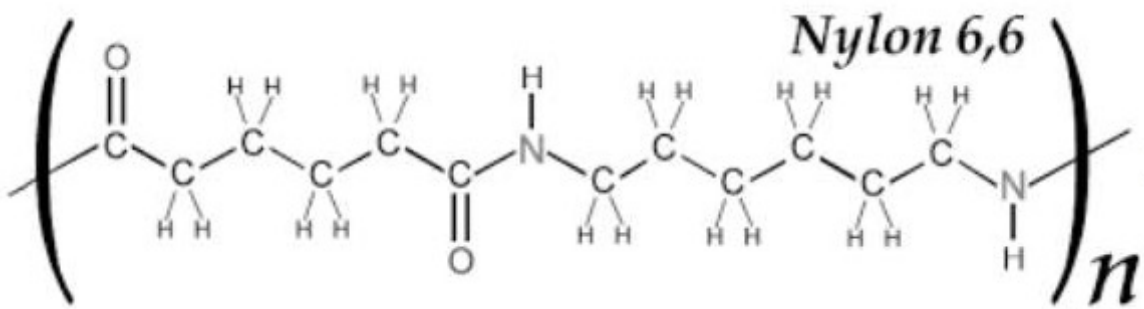

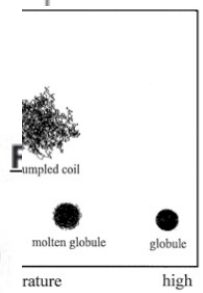

Figure 5. Temperature dependen
to average hydrodynamic radiu
lamide) (PDEAM) chains in wa

odynamically stable states of
a homopolymer chain in the coil-to-globule and the globule-to-
coil transitions.

Macromolecules **2008**, *41*, 8927−8931

The Coil-to-Globule-to-Coil Transition of Linear Polymer Chains in Dilute Aqueous Solutions: Effect of Intrachain Hydrogen Bonding

Kejin Zhou,[†] Yijie Lu,[‡] Junfang Li,[‡] Lei Shen,[‡] Guangzhao Zhang,*[,‡] Zuowei Xie,[†,§] and Chi Wu*[,§]

ABSTRACT: Our previous studies of the captioned transition have shown that thermally sensitive poly(*N*-isopropylacrylamide) (PNIPAM) in water can form stable individual single-chain globules, but not for polystyrene (PS) in cyclohexane. In the current study, using poly(*N,N*-diethylacrylamide) (PDEAM) ($M_w = 1.7 \times 10^7$ g/mol and $M_w/M_n = 1.06$) with no hydrogen donator site, we intend to find whether the intrachain hydrogen bonding plays a role in stabilizing individual collapsed PNIPAM single-chain globules. We found that PDEAM can also form stable single-chain globules in water even though the transition is less sharp. The resultant individual PDEAM single-chain globules are less compact, reflecting in a lower chain density and a higher ratio of the radius of gyration to hydrodynamic radius, presumably due to the lack of intrachain hydrogen bonding. Our result also shows that, unlike PNIPAM, there is no hysteresis in the transition, indirectly supporting our previous assumption that the hysteresis observed for PNIPAM is due to the formation of some intrachain additional hydrogen bonds formed in the collapsed state.

VOLUME 80, NUMBER 18 PHYSICAL REVIEW LETTERS 4 MAY 1998

Globule-to-Coil Transition of a Single Homopolymer Chain in Solution

Chi Wu[1,2,*] and Xiaohui Wang[1]

Size of a Chain, “R”
(You can not directly measure the End-to-End Distance)

What are the measures of Size, "*R*", for a polymer coil?

Radius of Gyration, R_g

$$R_g^2 = \frac{1}{N}\sum_{n=1}^{N}\left\langle (R_n - R_G)^2 \right\rangle \qquad R_G = \frac{1}{N}\sum_{n=1}^{N} R_n$$

$$R_g^2 = \frac{1}{N}\sum_{n=1}^{N}\left\langle \left(R_n - \frac{1}{N}\sum_{m=1}^{N} R_m\right)^2 \right\rangle = \frac{1}{N}\sum_{n=1}^{N}\left\langle \frac{1}{2N}\sum_{m=1}^{N}(R_n - R_m)^2 \right\rangle = \frac{1}{2N^2}\sum_{n=1}^{N}\sum_{m=1}^{N}\left\langle (R_n - R_m)^2 \right\rangle$$

$$\sum_{n=1}^{N}\sum_{m=1}^{N}\left\langle (R_n - R_m)^2 \right\rangle = \sum_{n=1}^{N}\sum_{m=1}^{N}|n-m|b^2 = 2\sum_{n=m}^{N}\sum_{m=1}^{N}(n-m)b^2 = 2b^2\left[Z + 2(Z-1) + 3(Z-2)\ldots(Z-1)2 + Z\right]$$

$Z = N - 1$

$$\sum_{p=1}^{Z}(Z+1-p)p = (Z+1)\sum_{p=1}^{Z}p - \sum_{p=1}^{Z}p^2 = \frac{Z(Z+1)(Z+2)}{6} \cong \frac{N^3}{6}$$

$$\sum_{u=1}^{n}u^p = \frac{n^{p+1}}{p+1} + \frac{n^p}{2} + \frac{pn^{p-1}}{12}$$

for p<3 (other terms needed for higher p's)

http://www.eng.uc.edu/~gbeaucag/Classes/Physics/Chapter1.pdf

What are the measures of Size, "*R*", for a polymer coil?

Radius of Gyration, R_g

$$R_g^2 = \frac{1}{N}\sum_{n=1}^{N}\left\langle (R_n - R_G)^2 \right\rangle \qquad R_G = \frac{1}{N}\sum_{n=1}^{N} R_n$$

$$R_g^2 = \frac{Nb^2}{6} = \frac{R_{RMSeted}^2}{6}$$

R_g is $1/\sqrt{6}$ of the RMS end-to-end distance.

$$2.45\ R_g = R_{eted}$$

R_g is a direct measure of the end-to-end distance for a linear Gaussian chain

http://www.eng.uc.edu/~gbeaucag/Classes/Physics/Chapter1.pdf

Static Light Scattering for R_g

$$I(q) = I_e N n_e^2 \exp\left({-R_g^2 q^2}/{3} \right)$$

Guinier's Law

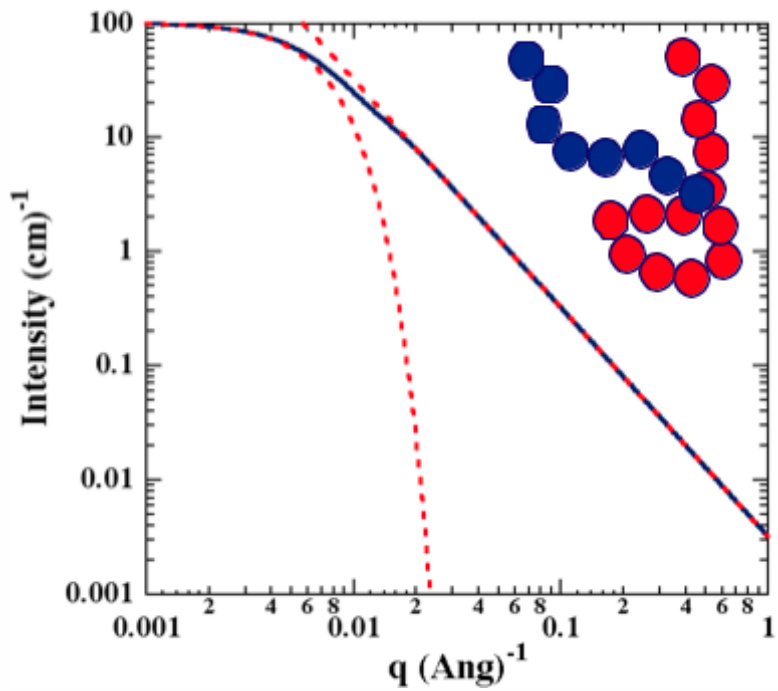

Guinier Plot linearizes this function

$$\ln\left(\frac{I(q)}{G} \right) = -\frac{R_g^2}{3} q^2 \qquad G = I_e N n_e^2$$

The exponential can be expanded at low-q and linearized to make a Zimm Plot

$$\frac{G}{I(q)} = \left(1 + \frac{R_g^2}{3} q^2 \right)$$

Binary Interference Yields Scattering Pattern.

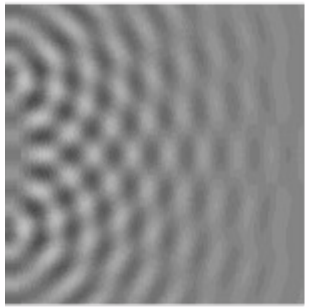

$I(q) \sim N\, n_e^2$

n_e Reflects the density of a Point generating waves

N is total number of points

The Scattering Event

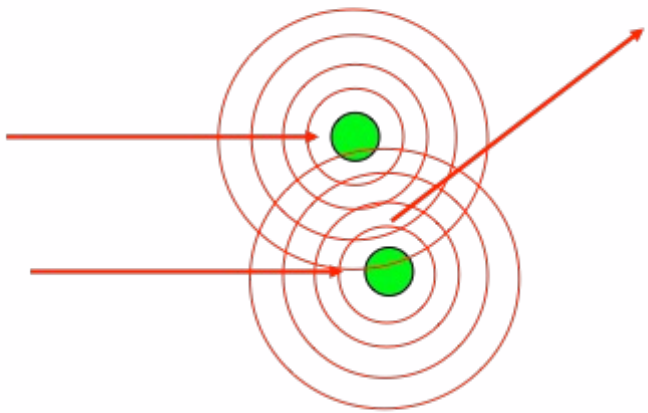

I(q) is related to amount Nn^2

q is related to size/distances

$$q = \frac{4\pi}{\lambda}\sin\left(\theta/2\right)$$

$$d = \frac{2\pi}{q}$$

2) Rather than consider specific structures, we can consider *general scattering laws* by which all scatters are governed under the premises that 1) "Particles" have a size and 2) "Particles" have a surface.

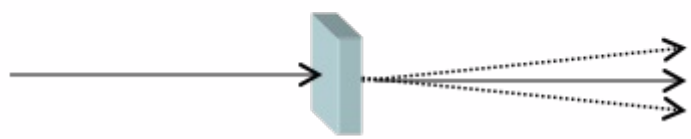

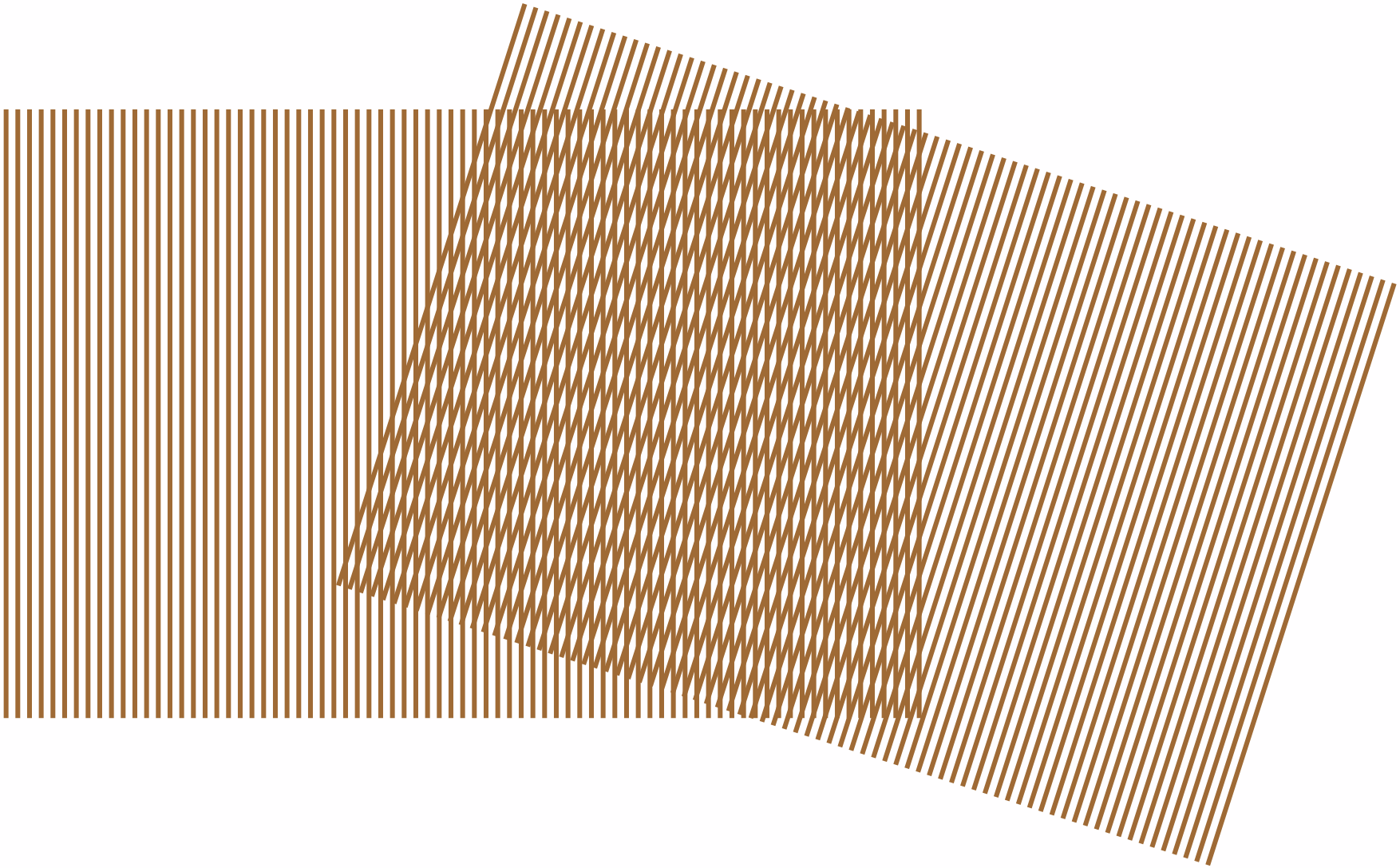

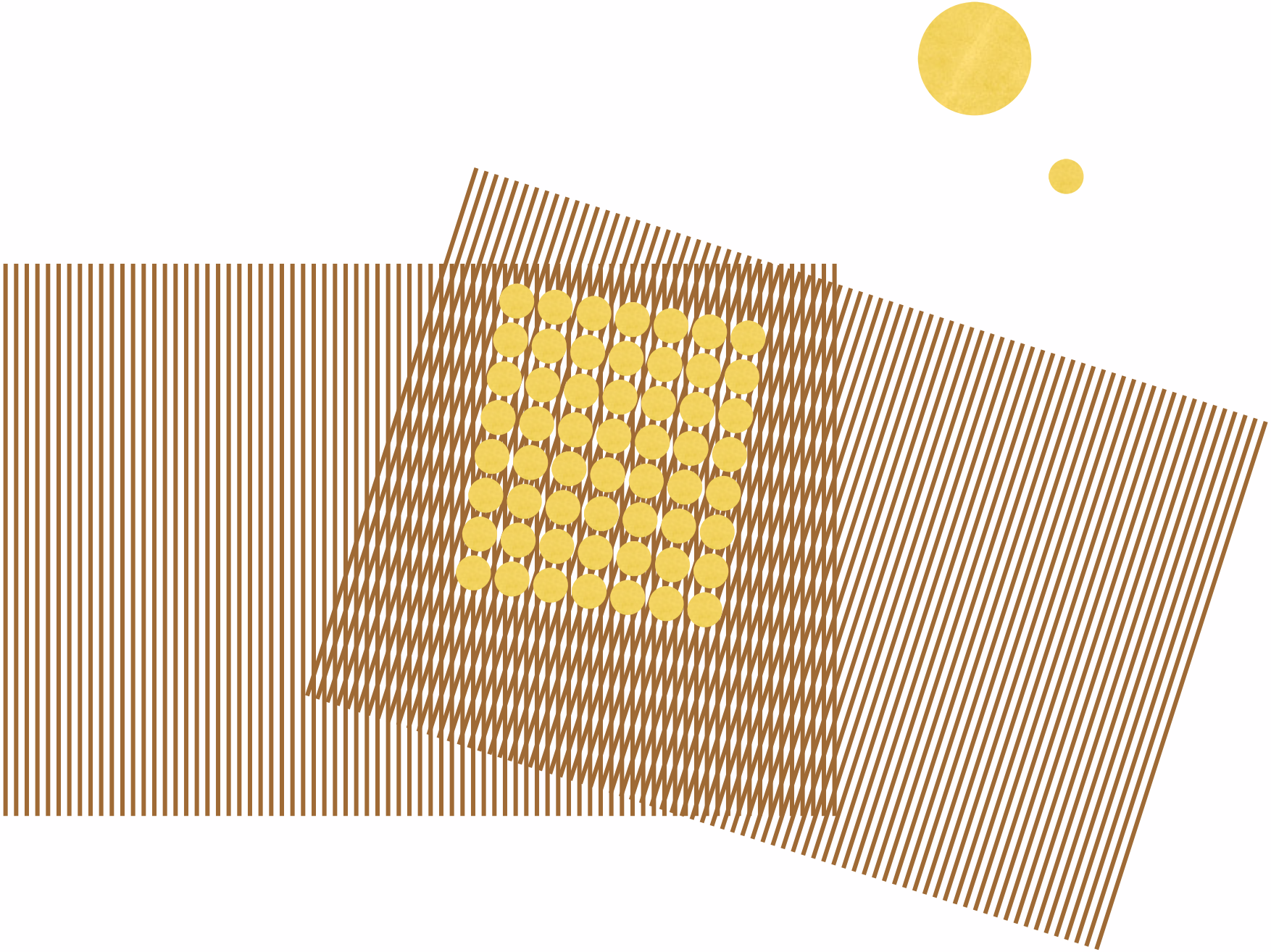

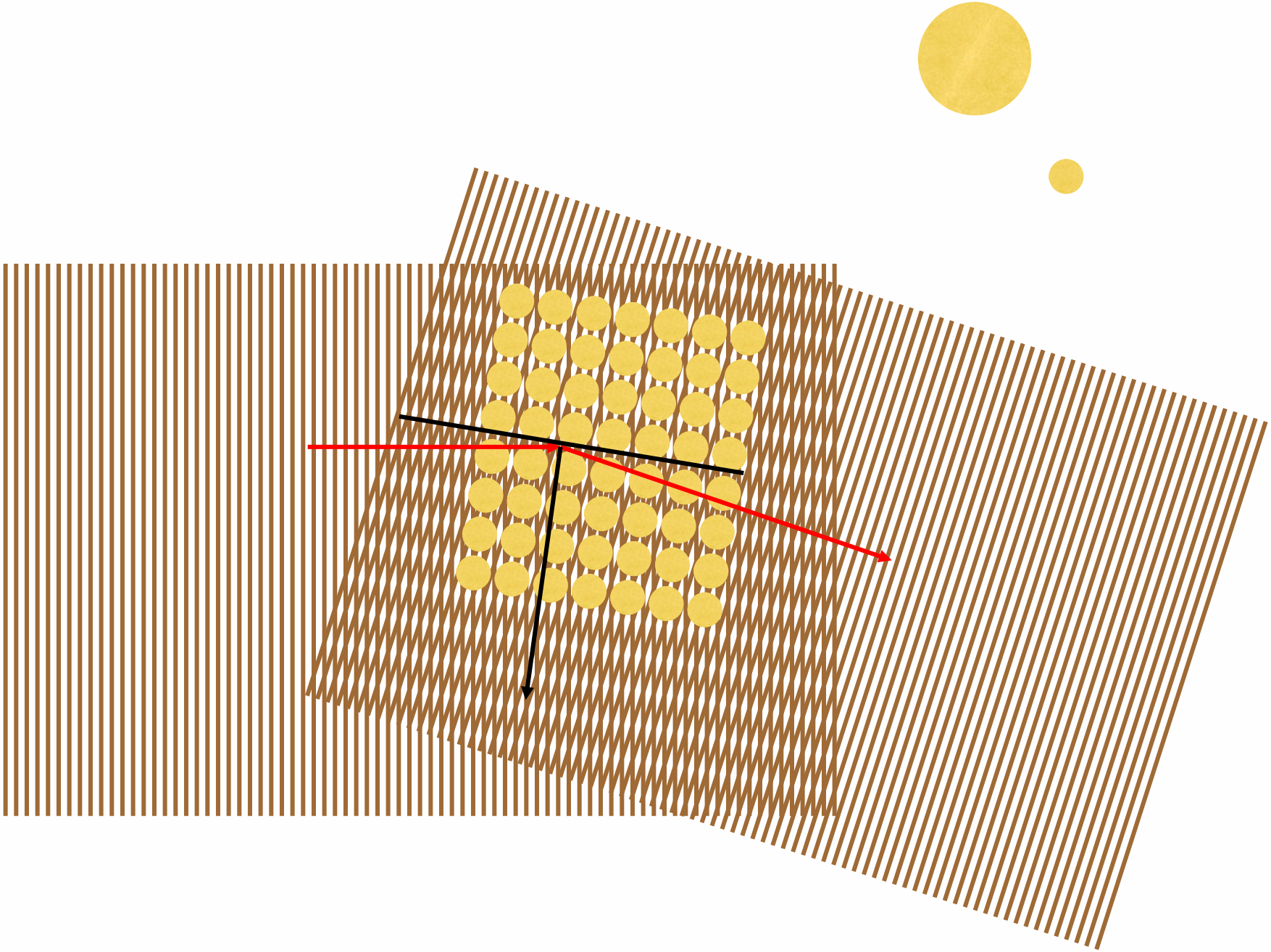

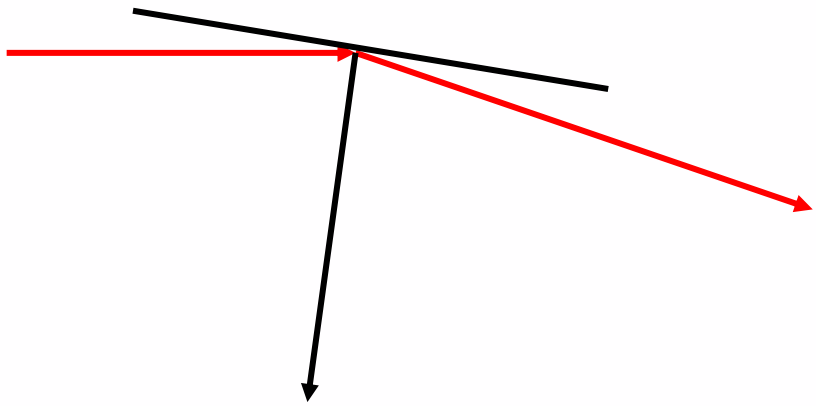

Binary Interference Yields Scattering Pattern.

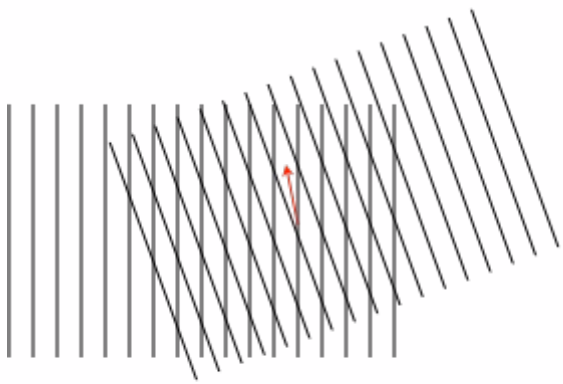

-Consider that an in-phase wave scattered at angle θ was in phase with the incident wave at the source of scattering.

-This can occur for points separated by ***r*** such that

|r| = 2π/|q|

- $q = \frac{4\pi}{\lambda} \sin \frac{\theta}{2}$

Binary Interference Yields Scattering Pattern.

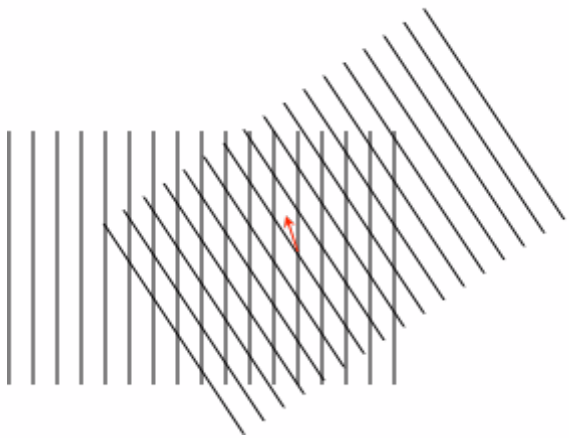

-For high θ, ***r*** is small

Binary Interference Yields Scattering Pattern.

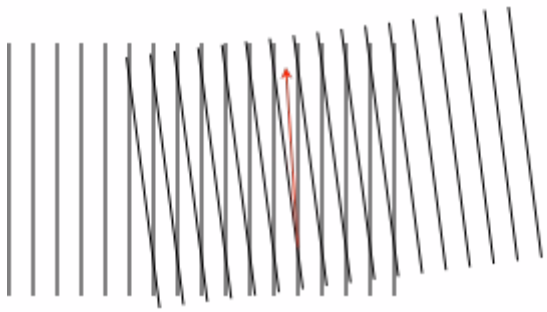

-For small θ, ***r*** is large

For an isotropic sample we consider scattering as arising from the probability of the random placement of a vector ***r*** in the scattering phase.

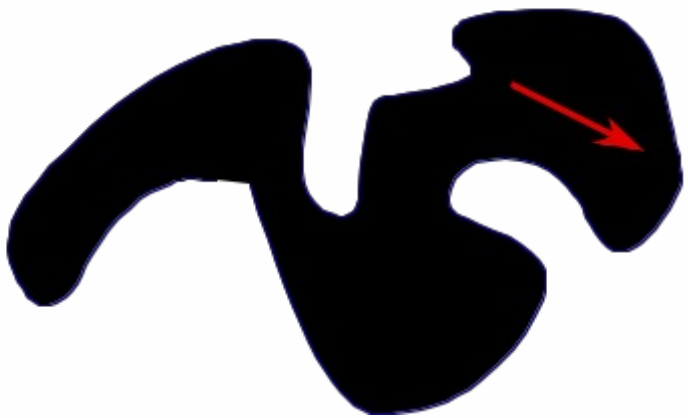

For an isotropic sample we consider scattering as arising from the probability of the random placement of a vector ***r*** in the scattering phase.

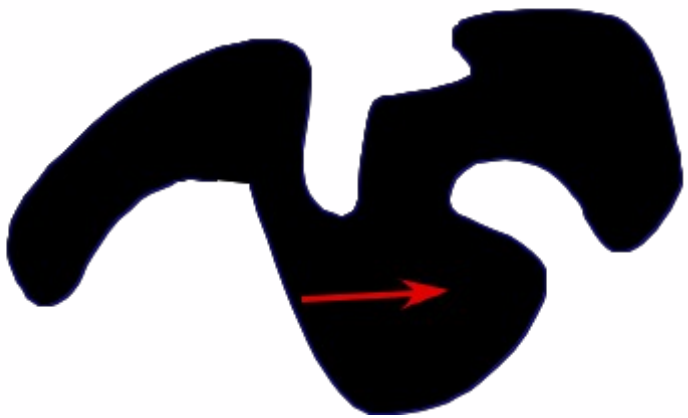

For an isotropic sample we consider scattering as arising from the probability of the random placement of a vector ***r*** in the scattering phase.

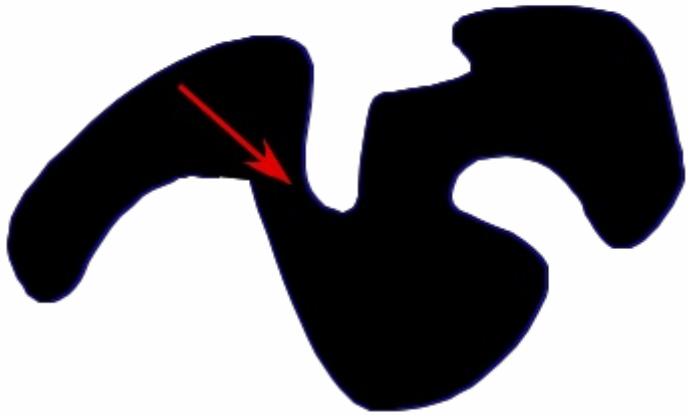

Rather than random placement of the vector we can hold The vector fixed and rotate the particle

For an isotropic sample we consider scattering as arising from the probability of the random placement of a vector ***r*** in the scattering phase.

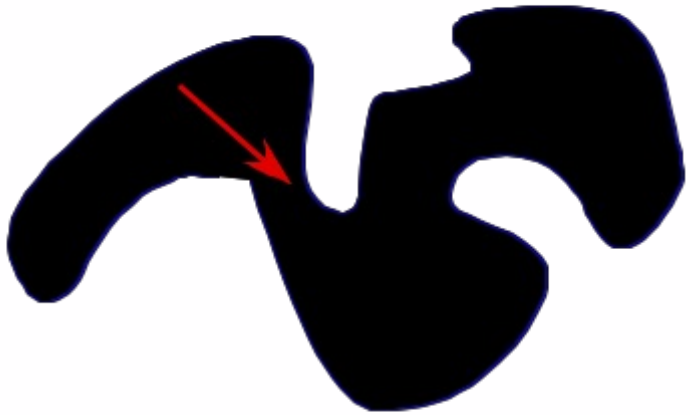

Rather than random placement of the vector we can hold The vector fixed and rotate the particle

For an isotropic sample we consider scattering as arising from the probability of the random placement of a vector ***r*** in the scattering phase.

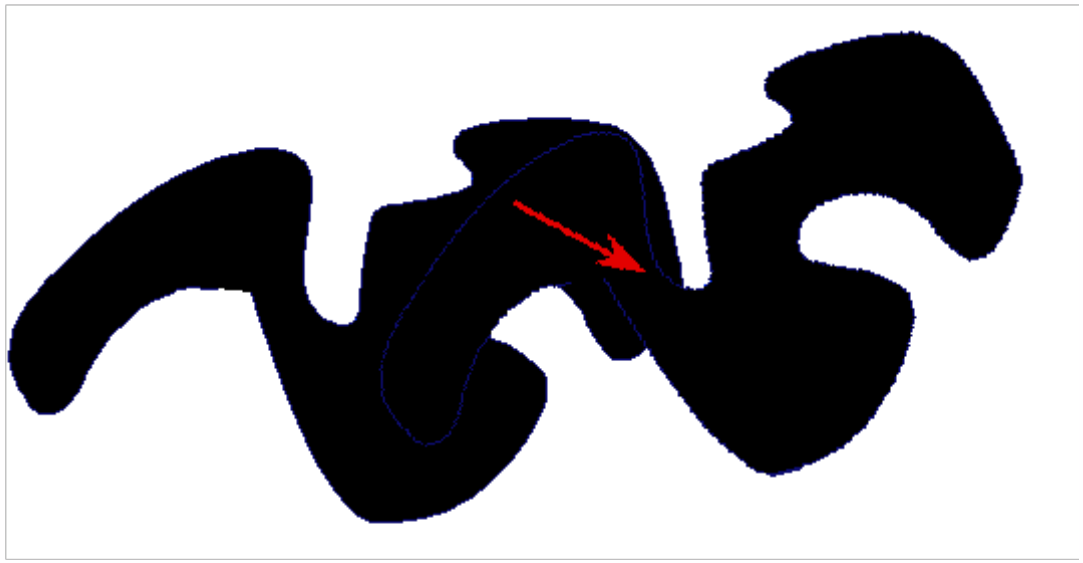

Rather than random placement of the vector we can hold The vector fixed and rotate the particle

For an isotropic sample we consider scattering as arising from the probability of the random placement of a vector ***r*** in the scattering phase.

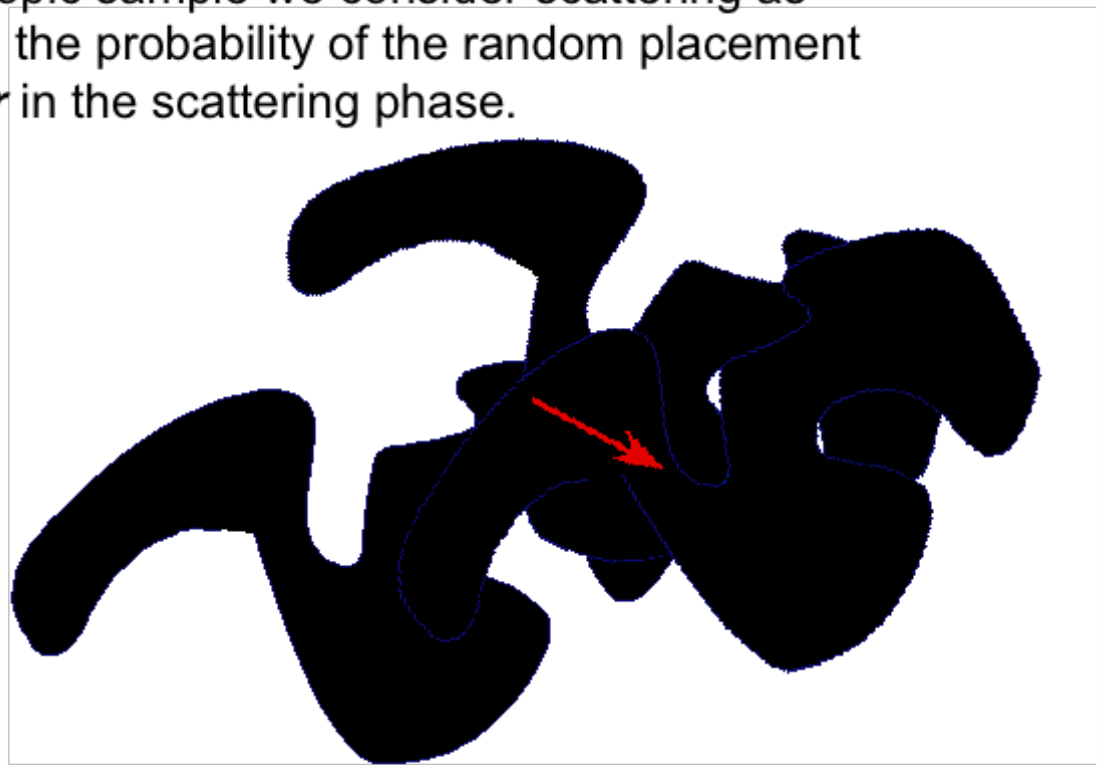

Rather than random placement of the vector we can hold The vector fixed and rotate the particle

The particle becomes a probability density function from the center of mass.

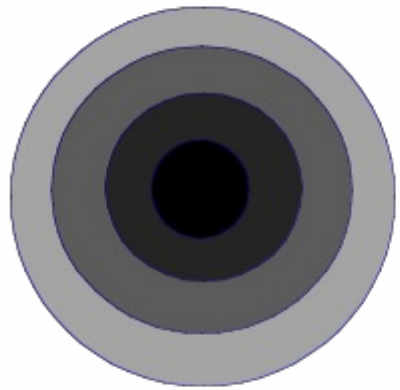

That follows a Gaussian Distribution.

$$p(r) = \exp\left(\frac{-3r^2}{4R_g^2}\right)$$

The particle becomes a probability density function from the center of mass.

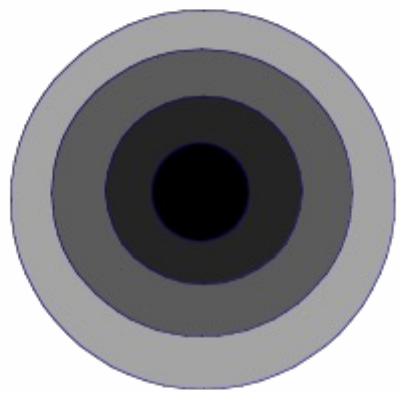

Whose Fourier Transform is Guinier's Law.

$$p(r) = \exp\left(\frac{-3r^2}{4R_g^2}\right) \quad \Rightarrow \quad \mathrm{I(q)} = G\exp\left(-\frac{q^2R_g^2}{3}\right)$$

$$\mathrm{G} = \mathrm{Nn_e^2}$$

Static Light Scattering for Radius of Gyration

Consider binary interference at a distance "r" for a particle with arbitrary orientation
Rotate and translate a particle so that two points separated by r lie in the particle for all rotations and average the structures at these different orientations

Guinier's Law

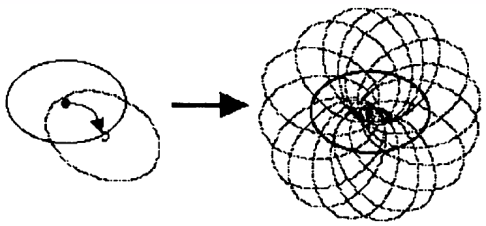

Fig. 4. Averaging of a particle about the origin of the vector **r** in analogy to random translations and rotations of the particle about the origin of **r**. In (*a*), a single rotation and a single translation are considered. In (*b*), the superposition of a number of such translations and rotations in random directions leads to a Gaussian distribution of scattering density $\rho(r)$.

$$\gamma_{Gaussian}(r) = \exp\left(-3r^2 \big/ 2\sigma^2\right)$$

Binary Autocorrelation Function

$$\sigma^2 = \frac{\sum_{i=1}^{N}(x_i - \mu)^2}{N-1} = 2R_g^2$$

$$I(q) = I_e N n_e^2 \exp\left(-R_g^2 q^2 \big/ 3\right)$$

Lead Term is

$$I(0) = N n_e^2$$

$$I(1/r) \sim N(r) n(r)^2$$

Scattered Intensity is the Fourier Transform of The Binary Autocorrelation Function

$$\gamma_0(r) = 1 - \frac{S}{4V} r + \ldots$$

$$\exp\left(\frac{-3r^2}{4R_g^2}\right) \approx 1 - \frac{3r^2}{4R_g^2} + \ldots$$

$$r \Rightarrow 0 \text{ then } d\left(\gamma_{Gaussian}(r)\right) \big/ dr \Rightarrow 0$$

A particle with no surface

Beaucage G *J. Appl. Cryst.* **28** 717-728 (1995).

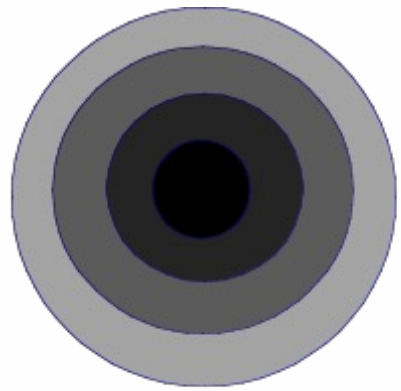

Guinier's Law Pertains to a Particle with no Surface.

$$p(r) = \exp\left(\frac{-3r^2}{4R_g^2}\right) \quad \Rightarrow \quad \mathrm{I(q)} = G\exp\left(-\frac{q^2R_g^2}{3}\right)$$

$$\mathrm{G} = \mathrm{Nn_e^2}$$

Any "Particle" can be Approximated as a Gaussian probability distribution in this context.

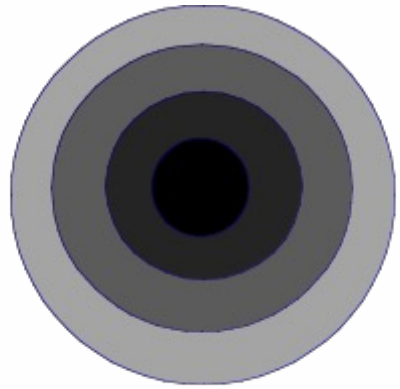

$$p(r) = \exp\left(\frac{-3r^2}{4R_g^2}\right) \quad \Rightarrow \quad \mathrm{I(q)} = G\exp\left(-\frac{q^2R_g^2}{3}\right)$$

$$\mathrm{G} = \mathrm{Nn_e^2}$$

Guinier's Law can be thought of as the
First Premise of Scattering:
All "Particles" have a size reflected by the radius of gyration.

Table 3.1. Radii of Gyration of Some Homogeneous Bodies

Sphere of radius R	$R_g^2 = \frac{3}{5} R^2$
Spherical shell with radii $R_1 > R_2$	$R_g^2 = \frac{3}{5} \frac{R_1^5 - R_2^5}{R_1^3 - R_2^3}$
Ellipse with semiaxes a and b	$R_g^2 = \frac{a^2 + b^2}{4}$
Ellipsoid with semiaxes a, b, and c	$R_g^2 = \frac{a^2 + b^2 + c^2}{5}$
Prism with edges A, B, and C	$R_g^2 = \frac{A^2 + B^2 + C^2}{12}$
Elliptical cylinder with semiaxes a and b and height h	$R_g^2 = \frac{a^2 + b^2}{4} + \frac{h^2}{12}$
Hollow circular cylinder with radii $R_1 > R_2$ and height h	$R_g^2 = \frac{R_1^2 + R_2^2}{2} + \frac{h^2}{12}$

semi axis is a radius

Debye Scattering Function for Gaussian Polymer Coil

Consider a chain of length N whose average end to end distance is $N^{1/2}$ b, where b is the effective step length for the chain which has no long-range interactions. For the n'th chain step, $g_n(r)$ is the average density of segments at a radial position r from step n. R_n is here the position vector for the segments of the chain. It is important to keep clear that r_n is a radial position relative to segment "n" while R_n is the segmental position relative to a coordinate system based at the first segment where n = 1. n can have values from 1 to N. Then,

$$g_n(r_n) = \frac{\sum_{m=1}^{N} \langle \delta(r_n - (R_m - R_n)) \rangle}{N}$$

where the del operator has a value of 1 when the position vector difference (R's) is equal to r. $g_n(r)$ will have values between 0 for r's larger than the chain to 1 for r = 0.

Since $g_n(r)$ only considers a single segment, "n", it must be averaged over all segments in order to obtain a statistical description of the spatial distribution of chain segments for the entire coil. This averaging results in the pair correlation function, g(r) for the coil,

$$g(r) = \frac{1}{2N^2} \sum_{n=1}^{N} g_n(r_n) = \frac{1}{2N^2} \sum_{n=1}^{N} \sum_{m=1}^{N} \langle \delta(r - (R_m - R_n)) \rangle$$

The pair correlation function, g(r), is directly related to the intensity scattered by light, neutrons or x-rays from a polymer coil. The scattered intensity is measured as a function of scattering angle, θ, and is usually plotted against the reduced parameter, $q = |q| = 4\pi/\lambda \sin(\theta/2)$, which is called the scattering vector. "q" is the inverse space vector and is related to the Bragg spacing, d, by $d = 2\pi/q$.

What are the measures of Size, "R", for a polymer coil?

Radius of Gyration, R_g

$$R_g^2 = \frac{1}{N}\sum_{n=1}^{N}\left\langle (R_n - R_G)^2 \right\rangle \qquad R_G = \frac{1}{N}\sum_{n=1}^{N} R_n$$

$$R_g^2 = \frac{1}{N}\sum_{n=1}^{N}\left\langle \left(R_n - \frac{1}{N}\sum_{m=1}^{N} R_m\right)^2 \right\rangle = \frac{1}{N}\sum_{n=1}^{N}\left\langle \frac{1}{2N}\sum_{m=1}^{N}(R_n - R_m)^2 \right\rangle = \frac{1}{2N^2}\sum_{n=1}^{N}\sum_{m=1}^{N}\left\langle (R_n - R_m)^2 \right\rangle$$

$$\sum_{n=1}^{N}\sum_{m=1}^{N}\left\langle (R_n - R_m)^2 \right\rangle = \sum_{n=1}^{N}\sum_{m=1}^{N}|n-m|b^2 = 2\sum_{n=m}^{N}\sum_{m=1}^{N}(n-m)b^2 = 2b^2\left[Z + 2(Z-1) + 3(Z-2)\ldots(Z-1)2 + Z\right]$$

$Z = N - 1$

$$\sum_{p=1}^{Z}(Z+1-p)p = (Z+1)\sum_{p=1}^{Z}p - \sum_{p=1}^{Z}p^2 = \frac{Z(Z+1)(Z+2)}{6} \cong \frac{N^3}{6}$$

$$\sum_{u=1}^{n}u^p = \frac{n^{p+1}}{p+1} + \frac{n^p}{2} + \frac{pn^{p-1}}{12}$$

for p<3 (other terms needed for higher p's)

http://www.eng.uc.edu/~gbeaucag/Classes/Physics/Chapter1.pdf

Scattered Intensity = K g(q) where K is a constant for a given system which includes the contrast and instrumental parameters. g(q) is the Fourier Transform of g(r),

$$g(q) = \int dr g(r) \exp(iq \bullet r) = \frac{1}{2N^2} \sum_{n=1}^{N} \sum_{m=1}^{N} \left\langle \exp\left(iq \bullet (R_m - R_n)\right) \right\rangle$$

For a Gaussian polymer coil the solution to this double summation is the Debye Equation for Polymer Coils which was first solved in 1946 by P. Debye.

$$g(q)_{Gaussian} = \frac{2}{Q^2}\left[Q - 1 + \exp(-Q)\right]$$

where $Q = q^2 N b^2/6 = q^2 R_g^{\ 2}$

The Debye function for polymer coils describes a decay of scattered intensity following a power-law of -2 at high-q and a constant value for intensity at low-q (below R_g).

Debye Paper Deriving this Equation

Low-q and High-q Limits of Debye Function

$$g(q)_{Gaussian} = \frac{2}{Q^2}\left[Q - 1 + \exp(-Q)\right]$$

where $Q = q^2Nb^2/6 = q^2R_g^{\ 2}$

At high q the last term => 0

Q-1 => Q

g(q) => $2/Q \sim q^{-2}$

Which is a mass-fractal scaling law with $d_f = 2$

At low q, $\exp(-Q) \Rightarrow 1-Q+Q^2/2-Q^3/6+\ldots$

Bracketed term => $Q^2/2-Q^3/6+\ldots$

$g(q) \Rightarrow 1-Q/3+\ldots \sim \exp(-Q/3) = \exp(-q^2R_g^2/3)$

Which is Guinier's Law

Ornstein-Zernike Function, Limits and Related Functions

The Zimm equation involves a truncated form of the Guinier Expression intended For use at extremely low-qR_g:

$$\frac{\phi}{S(qR_g << 1)} = \left(\frac{1}{N} + (1-2\chi)\phi\right)\left(1 + \frac{q^2 R_g^2}{3}\right) \qquad (6).$$

If this expression is generalized for a fixed composition and all q, R_g is no longer the size parameter and the equation is empirical (no theoretical basis) but has a form similar to the Debye Function for polymer coils:

$$I(q) = \frac{G}{1 + q^2 \xi^2}$$

This function is called the Ornstein-Zernike function and ξ is called a correlation length.

The inverse Fourier transform of this function can be solved and is given by (Benoit-Higgins *Polymers and Neutron Scattering* p. 233 1994):

$$p(r) = \frac{K}{r} \exp\left(-\frac{r}{\xi}\right)$$

This function is empirical and displays the odd (impossible) feature that the correlation function for a "random" system is not symmetric about 0, that is + and – values for r are not equivalent even though the system is random. (Compare with the normal behavior of the Guinier correlation function.)

$$p(r) = K \exp\left(-\frac{3r^2}{4R_g^2}\right)$$

The Flory Expression indicates a linear dependence of osmotic pressure in concentration at low concentration and a dependence on concentration to the power 2 at high concentration.

$$\Pi = \frac{kT}{V_c}\left(\frac{\phi}{N} + \left(\frac{1}{2} - \chi\right)\phi^2 + \ldots\right)$$

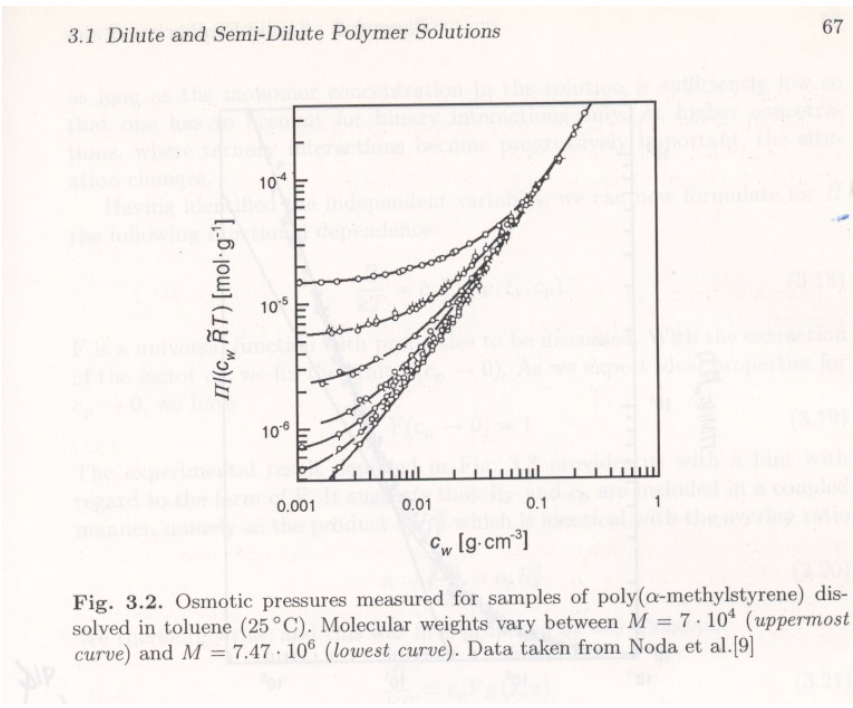

Fig. 3.2. Osmotic pressures measured for samples of poly(α-methylstyrene) dissolved in toluene (25 °C). Molecular weights vary between $M = 7 \cdot 10^4$ (*uppermost curve*) and $M = 7.47 \cdot 10^6$ (*lowest curve*). Data taken from Noda et al.[9]

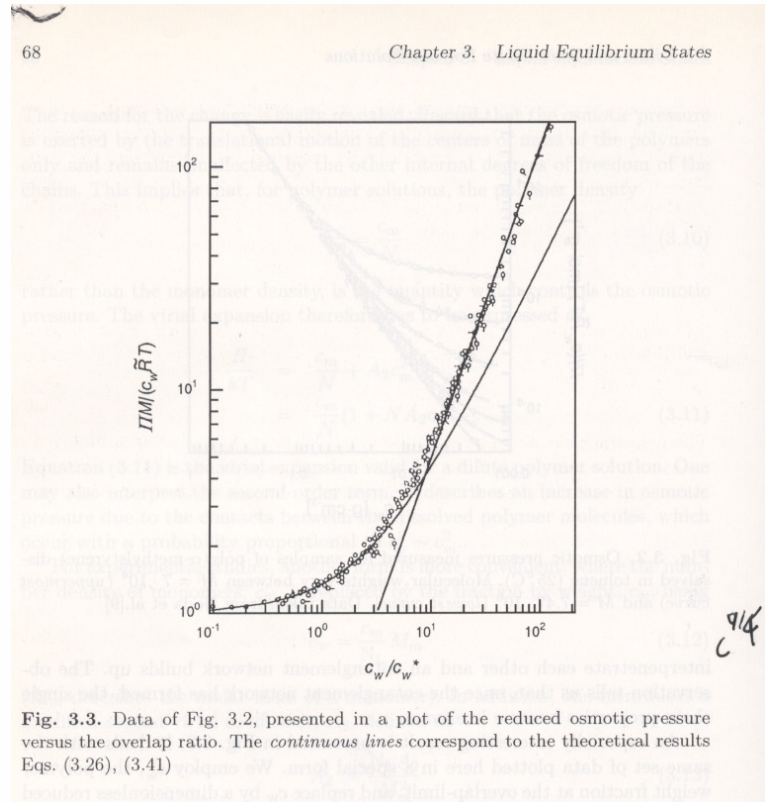

Fig. 3.3. Data of Fig. 3.2, presented in a plot of the reduced osmotic pressure versus the overlap ratio. The *continuous lines* correspond to the theoretical results Eqs. (3.26), (3.41)

From Gert Strobl, Polymer Physics

Ornstein-Zernike Function, Limits and Related Functions

Ornstein-Zernike (Empirical)

$$I(q) = \frac{G}{1 + q^2\xi^2}$$

Debye (Exact)

$$g(q)_{Gaussian} = \frac{2}{Q^2}\left[Q - 1 + \exp(-Q)\right]$$

where $Q = q^2Nb^2/6 = q^2R_g^{\ 2}$

High-q limit

$$I(q) = \frac{G}{q^2\xi^2}$$

$$2\xi^2 = R_g^2$$

$$I(q) = \frac{2G}{q^2R_g^2}$$

Low-q limit

$$I(q) \sim G\exp\left(-q^2\xi^2\right)$$

$$3\xi^2 = R_g^2$$

$$I(q) \sim G\left(1 - \frac{q^2R_g^2}{3}\right) \sim G\exp\left(-\frac{q^2R_g^2}{3}\right)$$

Ornstein-Zernike Function, Limits and Related Functions

Empirical Correlation Function		Transformed Empirical Scattering Function
$p(r)=\frac{K}{r}\exp\left(-\frac{r}{\xi}\right)$	Ornstein-Zernike Function	$I(q)=\frac{G}{1+q^2\xi^2}$
$p(r)=K\exp\left(-\frac{r}{\xi}\right)$	Debye-Bueche Function	$I(q)=\frac{G}{1+q^4\xi^4}$
$p(r)=\frac{K}{r}\exp\left(-\frac{r}{\xi}\right)\sin\left(\frac{2\pi r}{d}\right)$	Teubner-Strey Function (F Brochard and JF Lennon 1975 J. de Phy. 36(11) 1035)	$I(q)=\frac{G}{1+q^2c_2+q^4c_3}$ c_2 is negative to create a peak
$p(r)=\frac{K}{r^{3-d_f}}\exp\left(-\frac{r}{\xi}\right)$	Sinha Function	$I(q)=\frac{G\sin\left[\left(d_f-1\right)\arctan\left(q\xi\right)\right]}{q\xi\left(1+q^2\xi^2\right)^{\left(d_f-1\right)/2}}$

Correlation function in all of these cases is not symmetric about 0 which is physically impossible for a random system. The resulting scattering functions can be shown to be non-physical, that is they do not follow fundamental rules of scattering. Fitting parameters have no physical meaning.

Mean-Field Interactions

The license of the image source clearly states that it can be used for commercial and noncommercial purposes and there is no need to ask permission from or provide credit to the photographer or Unsplash, although it is appreciated when possible.

Specific Interactions

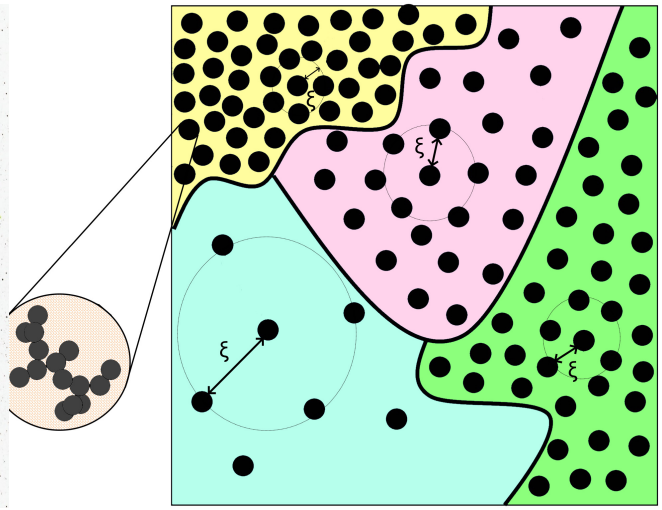

Reprinted (adapted) with permission from McGlasson, A.; Rishi, K.; Beaucage, G.; Chauby, M.; Kuppa, V.; Ilavsky, J.; Rackaitis, M. Quantification of Dispersion for Weakly and Strongly Correlated Nanofillers in Polymer Nanocomposites. ***Macromolecules* 2020,** https://doi.org/10.1021/acs.macromol.9b02429. Copyright 2020 American Chemical Society

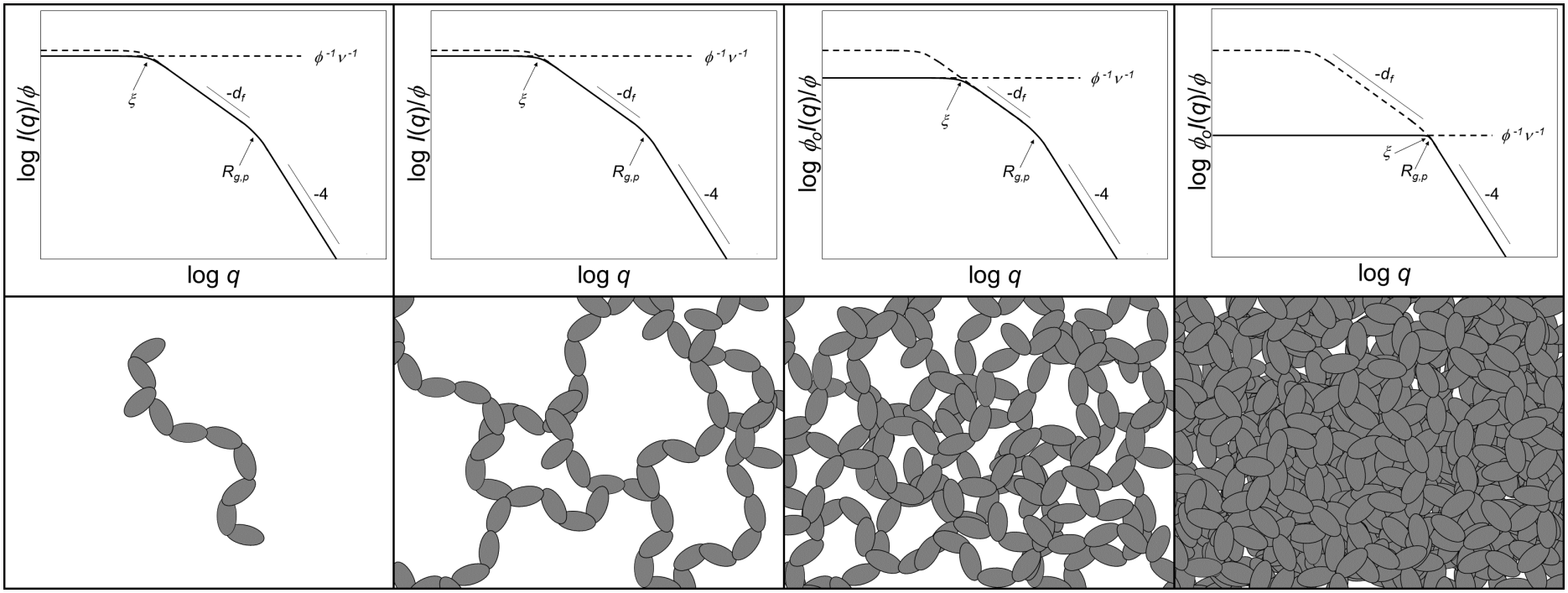
log I(q)/ϕ
log q
ϕ⁻¹ν⁻¹
ξ
-d_f
R_g,p
-4
log ϕ_o I(q)/ϕ

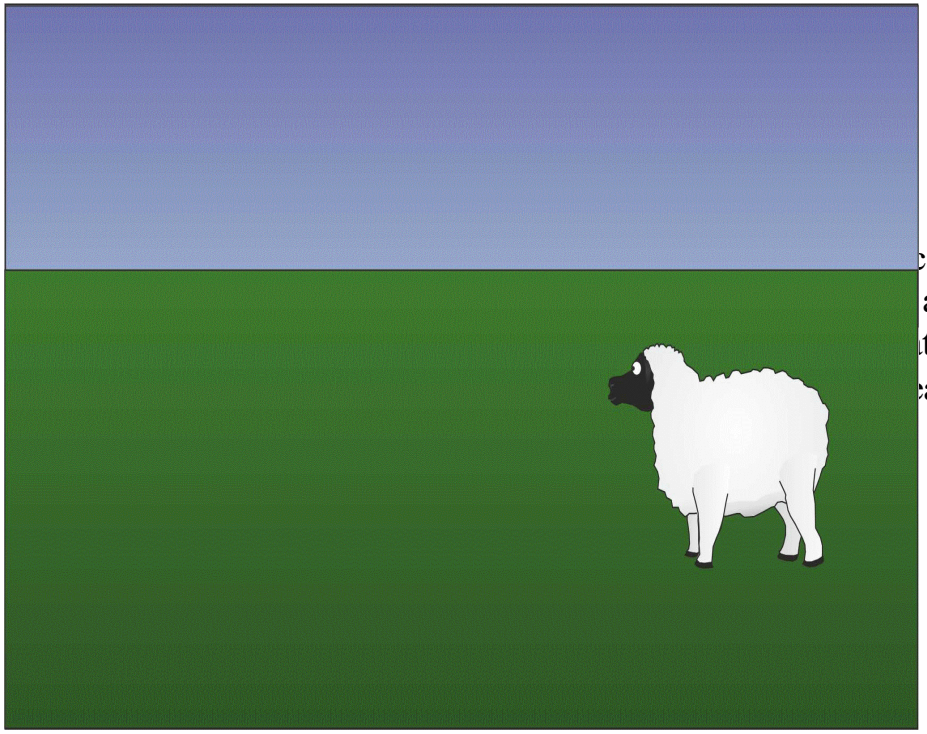

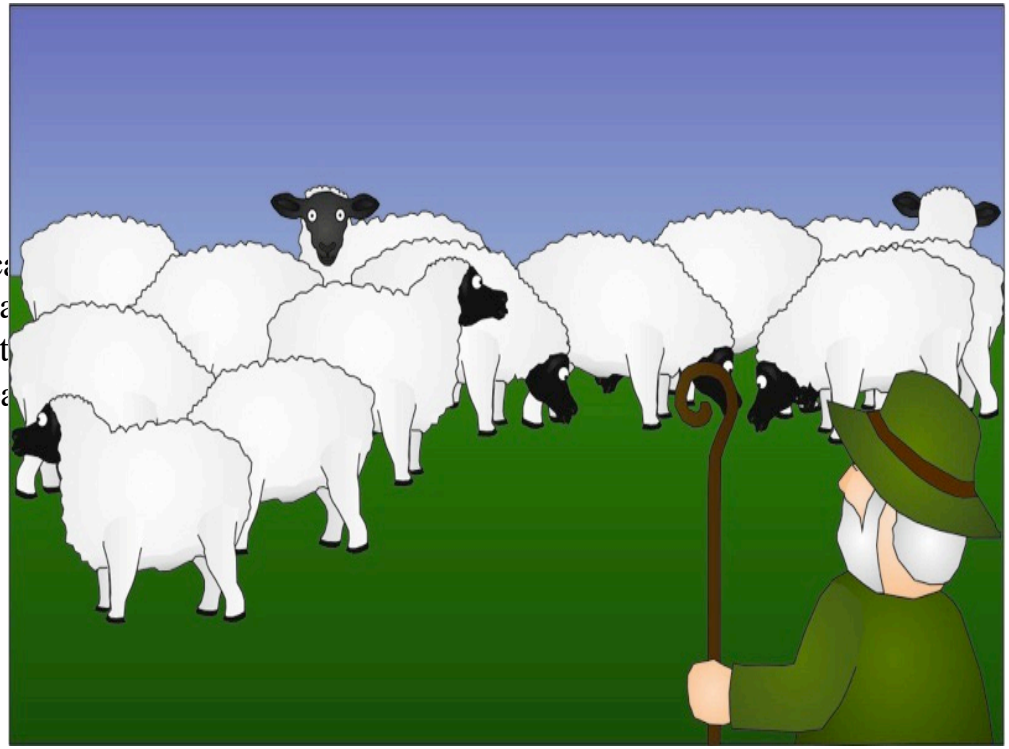

Progr Colloid Polym Sci (2005) 130: 70–78
DOI 10.1007/b107350
Published online: 3 June 2005
© Springer-Verlag 2005

Jan Skov Pedersen
Cornelia Sommer

Temperature dependence of the virial coefficients and the chi parameter in semi-dilute solutions of PEG

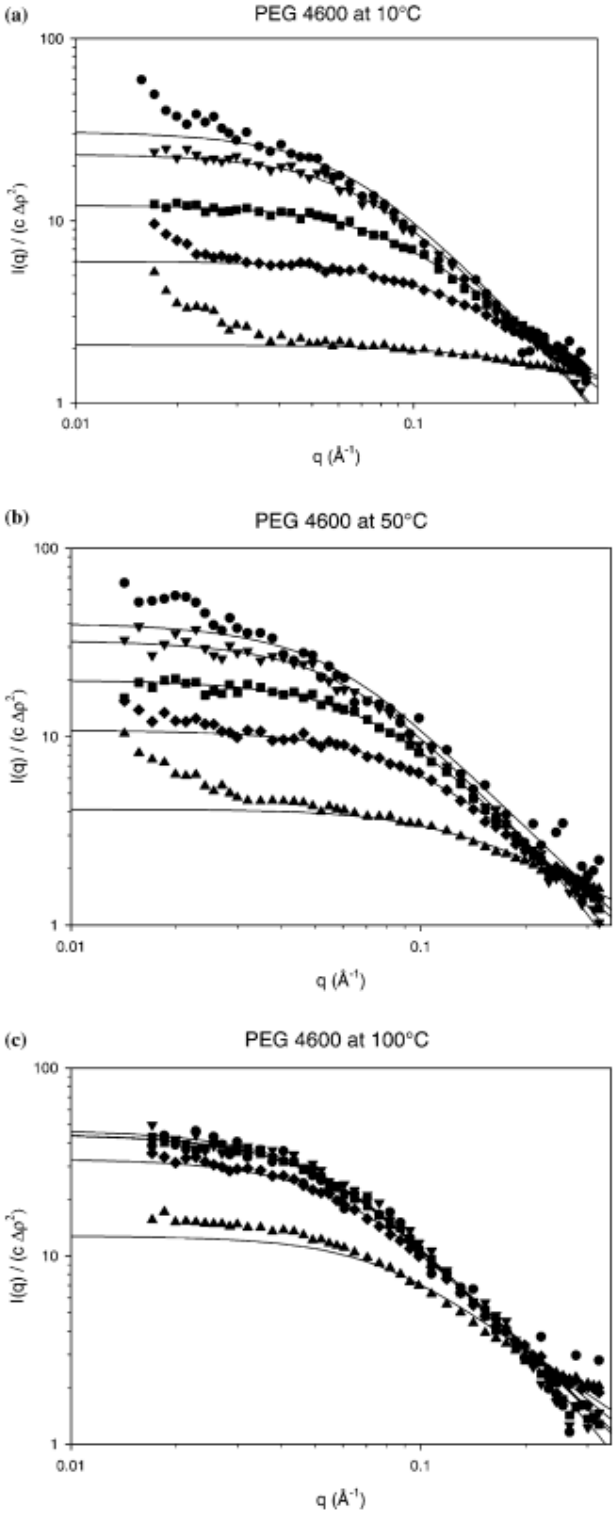

Fig. 1 SAXS data with fits (curves) for PEG 4600 solutions at fixed temperature as a function of concentration. (a) 10°C (b) 50° C (c) 100° C. Signatures: 1 wt% circles, 2 wt% triangle down, 5 wt% square, 10 wt% diamond, 20 wt% triangle up. The data have been divided by the square of the excess electron density ($\Delta\rho$ was in units of e/Å^3) of the PEG chains in order to eliminate the influence in the plot of the change in contrast with temperature

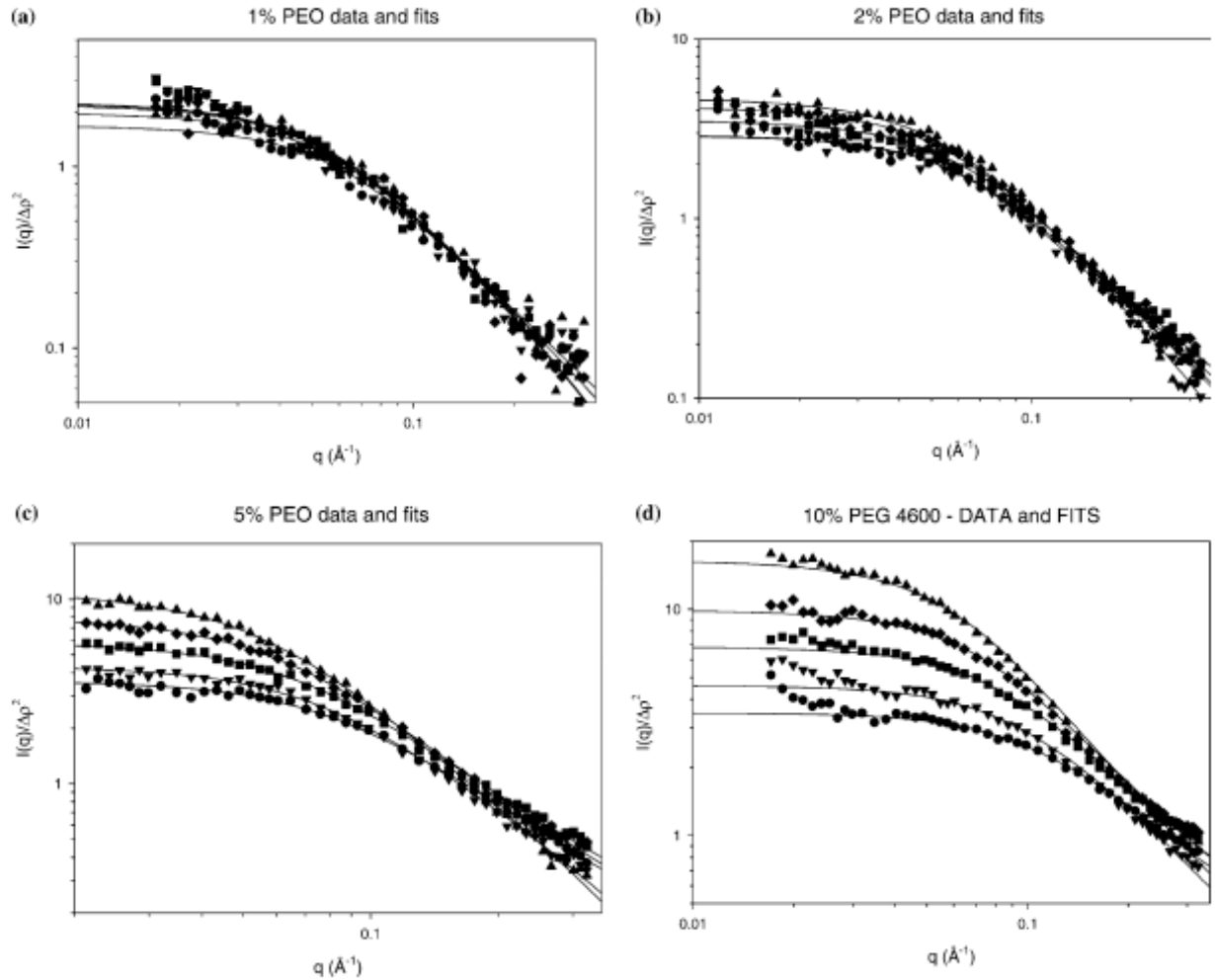

Fig. 2 SAXS data with fits (curves) for PEG 4600 solutions at fixed concentration as a function of temperature. (a) 1 wt% (b) 2 wt% (c) 5 wt% (d) 10 wt%. Signatures: 20°C circles, 40°C triangles down, 60°C squares, 80°C diamonds and 100°C triangles. The data have been divided by the square of the excess electron density of the PEG chains in order to eliminate the influence in the plot of the change in contrast with temperature

Pedersen Sommer Paper 2005

Random Phase Approximation (RPA) Equation

$$\frac{\phi}{I(q)} = \frac{\phi_0}{I_0(q)} - 2\chi\phi \qquad \text{Polymer in Solution}$$

At high-q, $I_0(q)$ is small and $1/I_0(q)$ is much larger than 2χ.

At low-q, $I_0(q)$ is large, and 2χ is much larger than $1/I_0(q)$.

Negative 2χ indicates miscibility, positive, phase separation.

Concentration

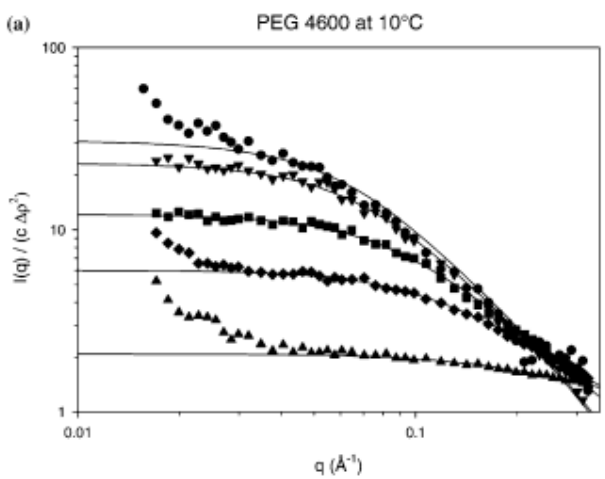

Temperature, $\chi \sim B/T$, high T small χ

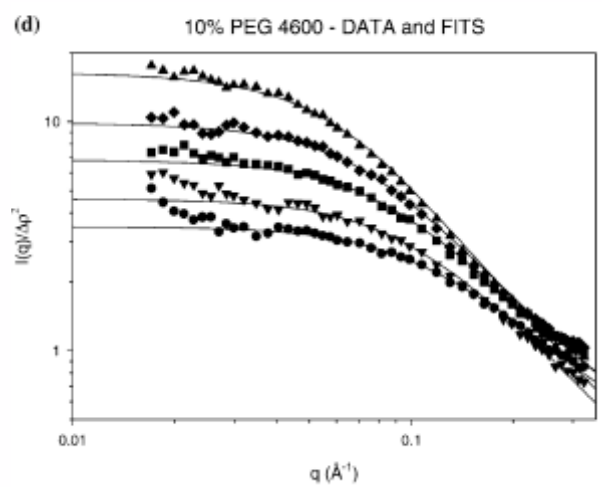

How to observe the concentration blob?

Concentration

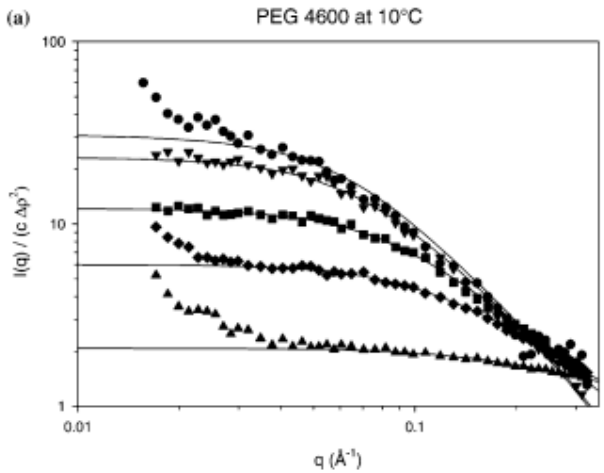

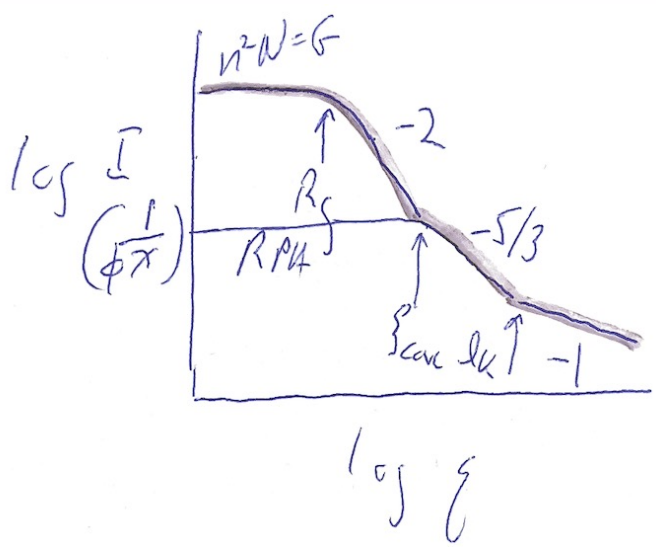

Contrast match the solvent with a mixture of deuterated and hydrogenous solvents
Tag one chain by deuteration (1% of chains)

$$\frac{\phi}{I(q)} = \frac{\phi_0}{I_0(q)} - 2\chi\phi$$

Zimm Plot

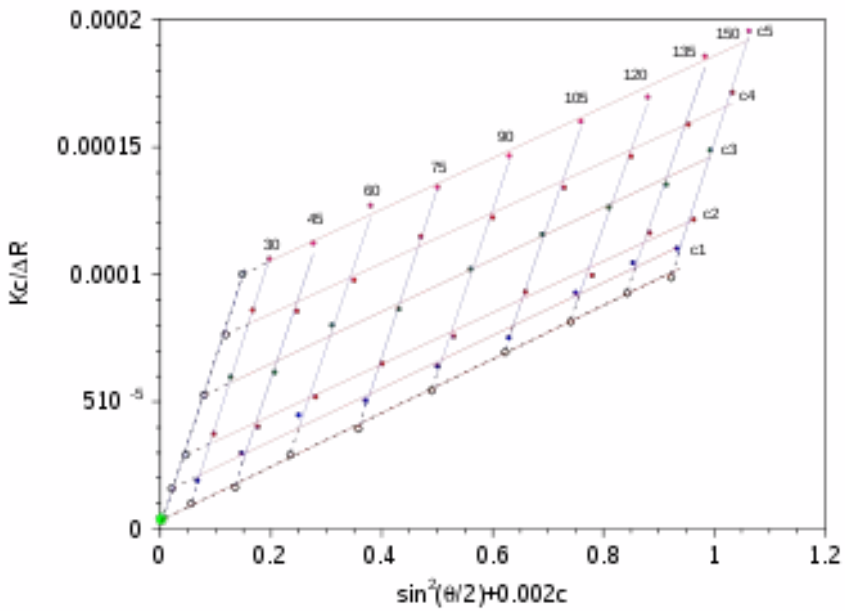

$$I(q) = \frac{G}{\exp\left(\frac{q^2 R_g^2}{3}\right)}$$

$$\frac{G}{I(q)} = \exp\left(\frac{q^2 R_g^2}{3}\right) \approx 1 + \frac{q^2 R_g^2}{3} + \ldots$$

Plot is linearized by $G/I(q)$ versus q^2

$$q = \frac{4\pi}{\lambda}\sin\left(\frac{\theta}{2}\right)$$

$$\frac{\phi}{S(qR_g << 1)} = \left(\frac{1}{N} + (1-2\chi)\phi\right)\left(1 + \frac{q^2 R_g^2}{3}\right) \qquad (6).$$

At q => 0 this is 1/osmotic compressibility, $d\Pi/d\phi = 1/N + \phi B_2 = (1/N + (1-2\chi)\phi)$

Zimm Plot

$$\frac{\phi}{S(qR_g << 1)} = \left(\frac{1}{N} + (1-2\chi)\phi\right)\left(1 + \frac{q^2 R_g^2}{3}\right) \qquad (6).$$

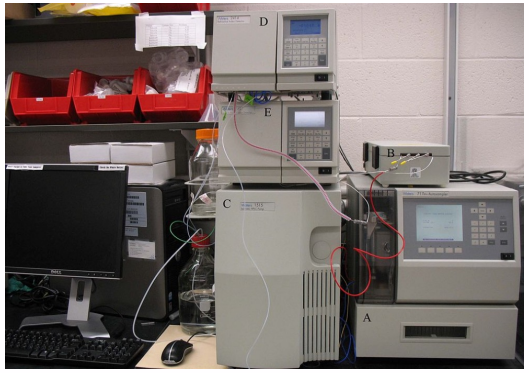

In a GPC you have $\phi \sim 0$ for each fraction Measure light scattering at a few angles and extrapolate q^2 to 0 to find weight average MW for each fraction. For each fraction the polydispersity, $M_w/M_n \sim 1$ so $M_w = M_n = M_z$

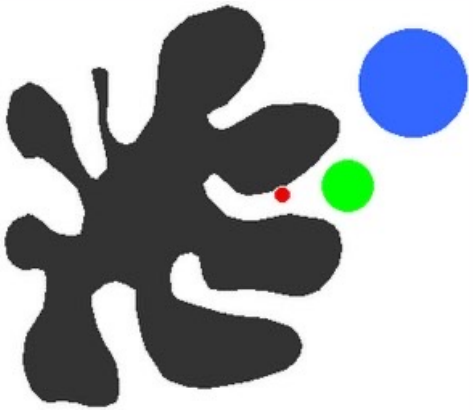

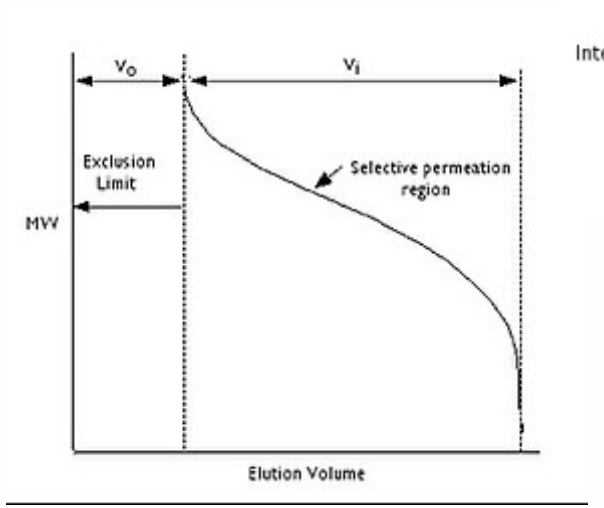

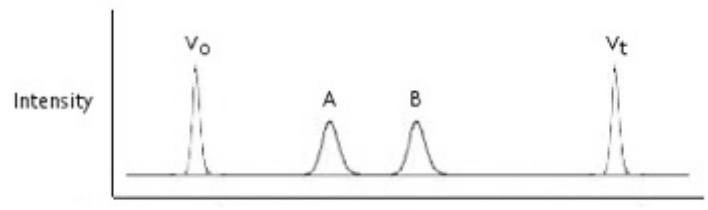

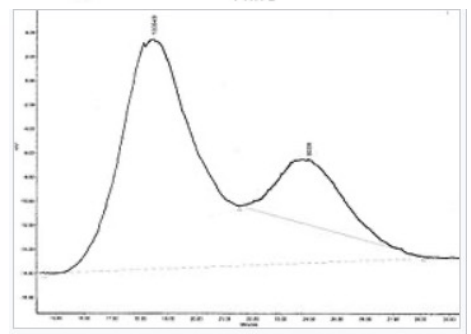

GPC Separation of Free-Radical Synthesized Polystyrene; M_n=24,000 g/mol, $Đ$=4.96

Two types of correlation: Mean Field and Specific Interactions are Experimentally Observed

Progr Colloid Polym Sci (2005) 130: 70–78
DOI 10.1007/b107350
Published online: 3 June 2005
© Springer-Verlag 2005

Jan Skov Pedersen
Cornelia Sommer

Temperature dependence of the virial coefficients and the chi parameter in semi-dilute solutions of PEG

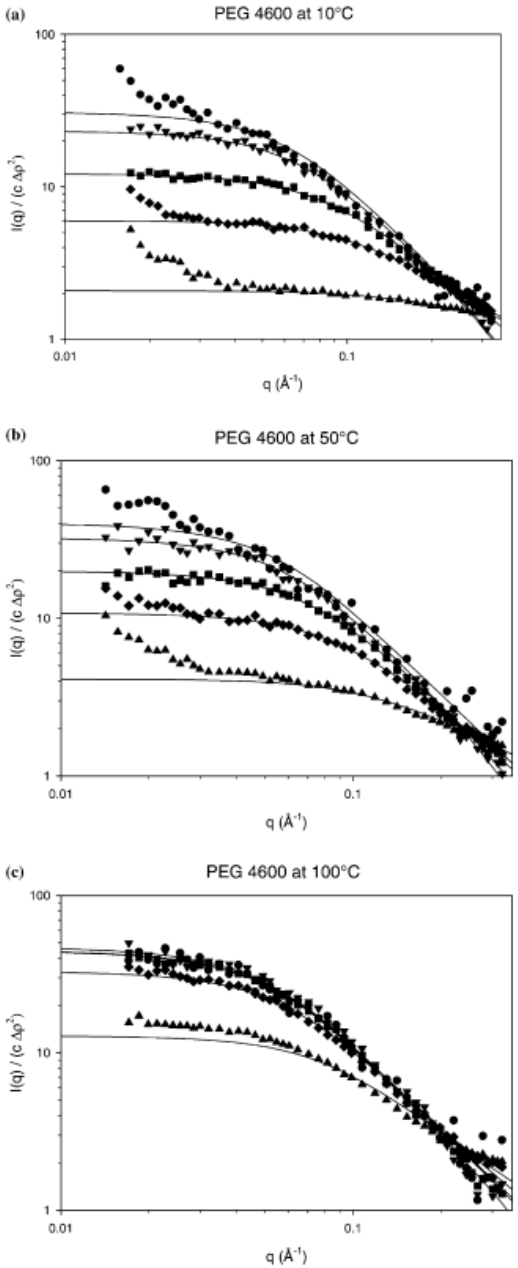

Soft Matter

Dynamic Article Links

Cite this: *Soft Matter*, 2011, **7**, 2725

www.rsc.org/softmatter

PAPER

Mechanical reinforcement of polymer nanocomposites: theory and ultra-small angle X-ray scattering (USAXS) studies†

Maura E. McEwan,[a] Sergei A. Egorov,[b] Jan Ilavsky,[c] David L. Green*[a] and Yang Yang[a]

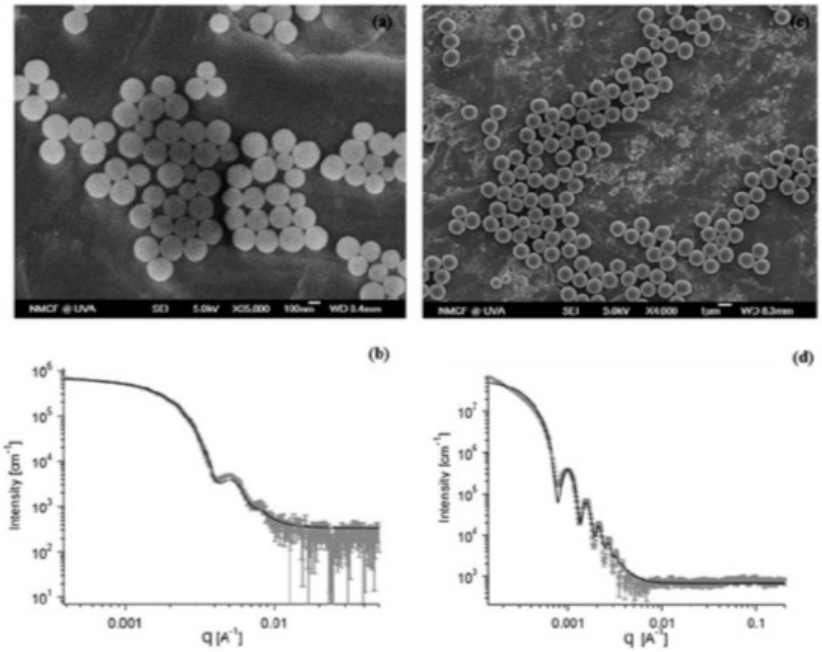

Fig. 2 SEM micrographs of the silica cores used in this study and USAXS scattering curves of the cores grafted with 25 kg mol^{-1} PDMS in PDMS: (a) SEM of radius $R \approx 100$ nm nanoparticles; (b) USAXS scattering intensity $I(q)$ of $R \approx 100$ nm nanoparticles in 2 kg mol^{-1} PDMS at a particle core volume fraction of $\phi_c = 0.02$; (c) SEM of $R \approx 600$ nm silica particles; and (d) $I(q)$ of $R \approx 600$ nm particles in 8 kg mol^{-1} PDMS at $\phi_c = 0.01$. Lines in (b) and (d) are fits of eqn (12) to $I(q)$.

Progr Colloid Polym Sci (2005) 130: 70–78
DOI 10.1007/b107350
Published online: 3 June 2005
© Springer-Verlag 2005

Jan Skov Pedersen
Cornelia Sommer

Temperature dependence of the virial coefficients and the chi parameter in semi-dilute solutions of PEG

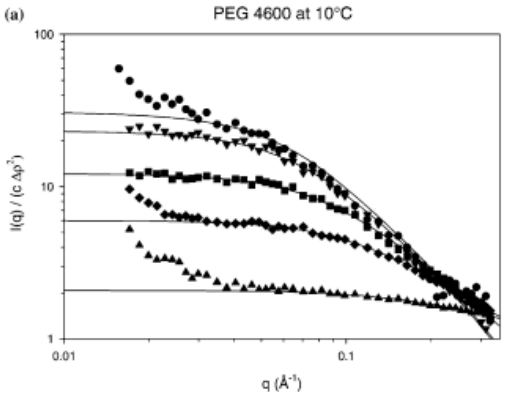

These are related to Thermodynamics:
Virial Coefficient = Mean Field = FH χ
EOS like Van der Waals = Specific Interaction
(There is overlap)

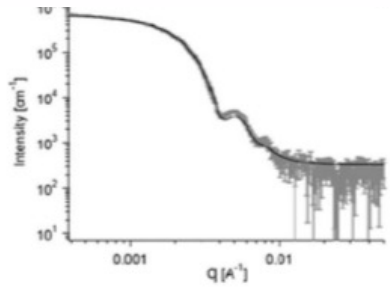

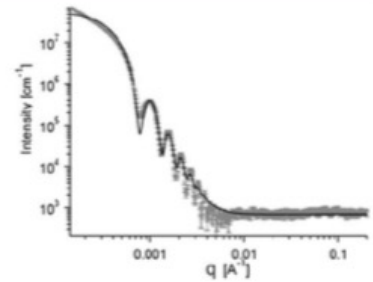

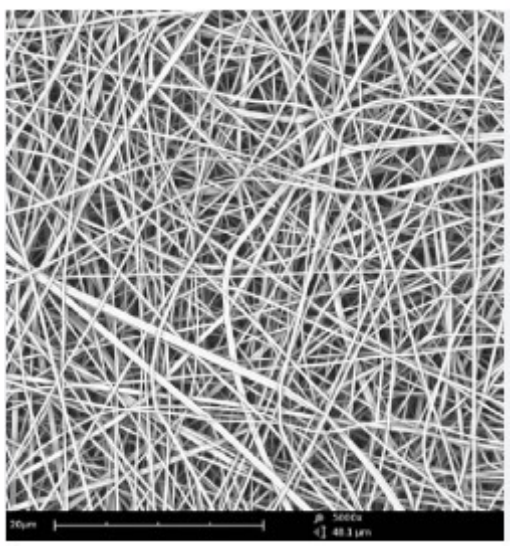

Non-woven fabric
(fleece, tissue, paper)

At large-scale (q => 0)
they appear the same.
We expect I/ϕ(q=>0) to drop
at higher concentrations as a
measure of $1/(\phi\ B_2)$ for both.

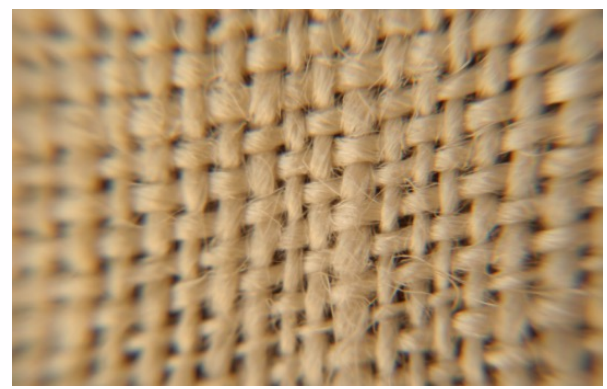

Woven
fabric

Critical ordering (

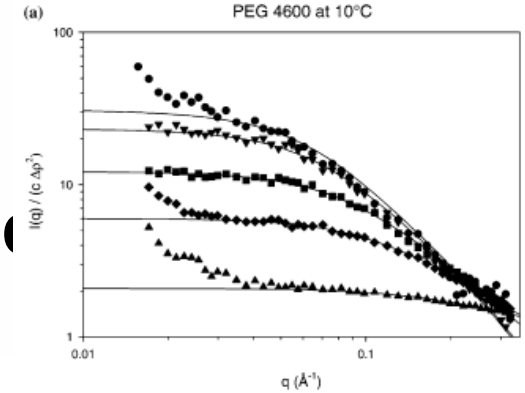

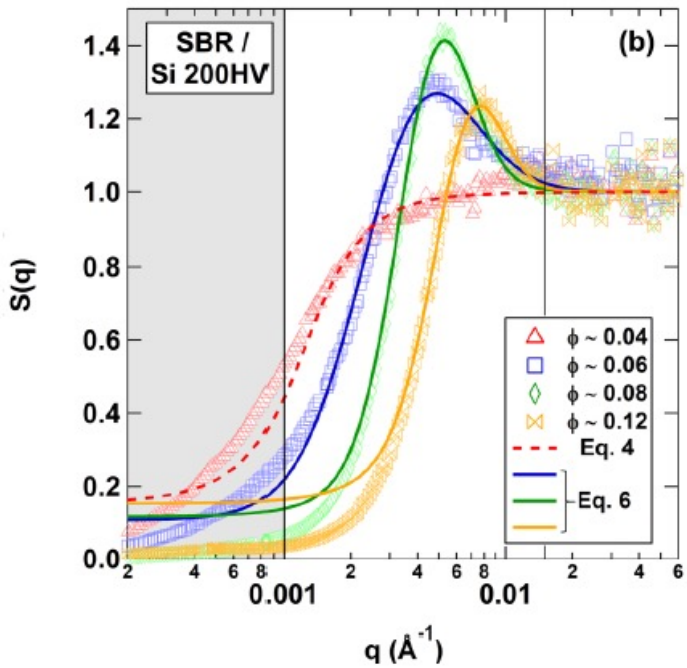

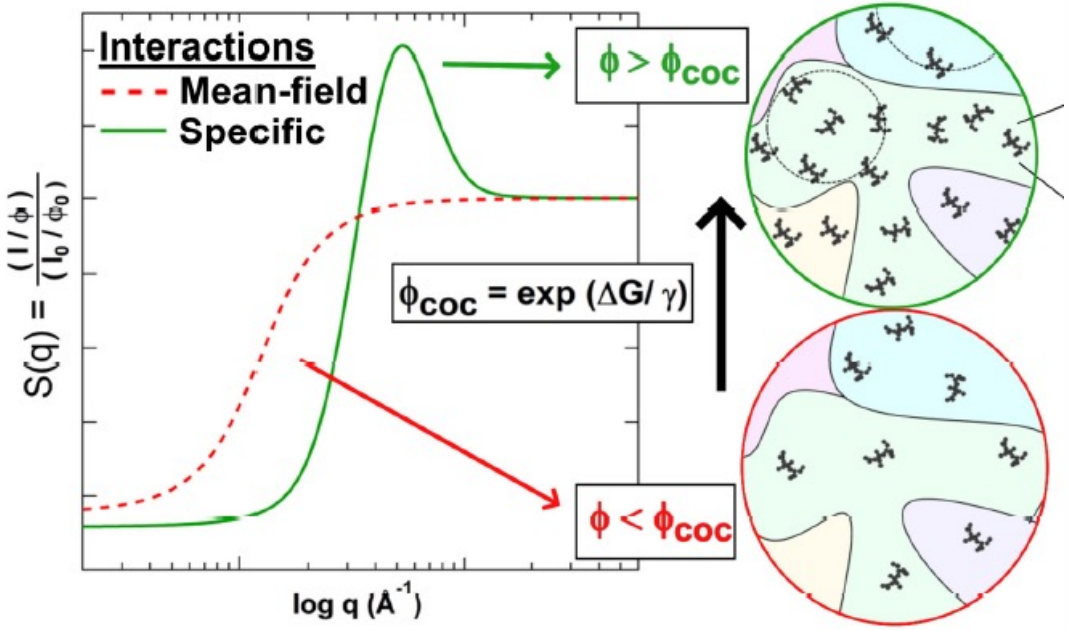

Rishi, K.; Pallerla, L.; Beaucage, G.; Tang, A. Dispersion of Surface-Modified, Aggregated, Fumed Silica in Polymer Nanocomposites. J. Appl. Phys. 2020, 127 (17), 174702.

Soft Matter

Dynamic Article Links

Cite this: *Soft Matter*, 2011, **7**, 2725

www.rsc.org/softmatter

PAPER

Mechanical reinforcement of polymer nanocomposites: theory and ultra-small angle X-ray scattering (USAXS) studies†

Maura E. McEwan,[a] Sergei A. Egorov,[b] Jan Ilavsky,[c] David L. Green*[a] and Yang Yang[a]

$$I(q) = \phi_c V_p (\Delta\rho)^2 P(q) S(q)$$

$$S(q) = 1 + 4\pi\rho_p \int_0^\infty (g(r) - 1) r^2 \frac{\sin(qr)}{qr} \mathrm{d}r$$

$$P(qR) = \left(3 \frac{\sin(qR) - qR\cos(qR)}{(qR)^3} \right)^2$$

$$S(q) = \frac{I(q)_{conc} \phi_{c,dil}}{I(q)_{dil} \phi_{c,conc}}$$

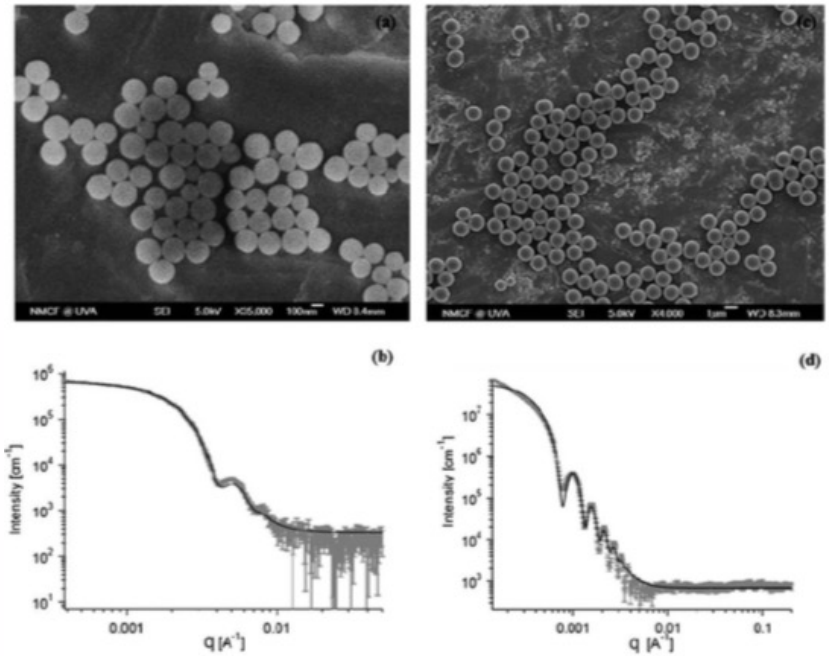

Soft Matter

Dynamic Article Links

Cite this: *Soft Matter*, 2011, **7**, 2725

www.rsc.org/softmatter

PAPER

Mechanical reinforcement of polymer nanocomposites: theory and ultra-small angle X-ray scattering (USAXS) studies†

Maura E. McEwan,[a] Sergei A. Egorov,[b] Jan Ilavsky,[c] David L. Green*[a] and Yang Yang[a]

$$I(q) = \phi_c V_p (\Delta\rho)^2 P(q) S(q)$$

$$S(q) = 1 + 4\pi\rho_p \int_0^\infty (g(r) - 1) r^2 \frac{\sin(qr)}{qr} \mathrm{d}r$$

$$P(qR) = \left(3 \frac{\sin(qR) - qR\cos(qR)}{(qR)^3} \right)^2$$

$$S(q) = \frac{I(q)_{\mathrm{conc}} \phi_{\mathrm{c,dil}}}{I(q)_{\mathrm{dil}} \phi_{\mathrm{c,conc}}}$$

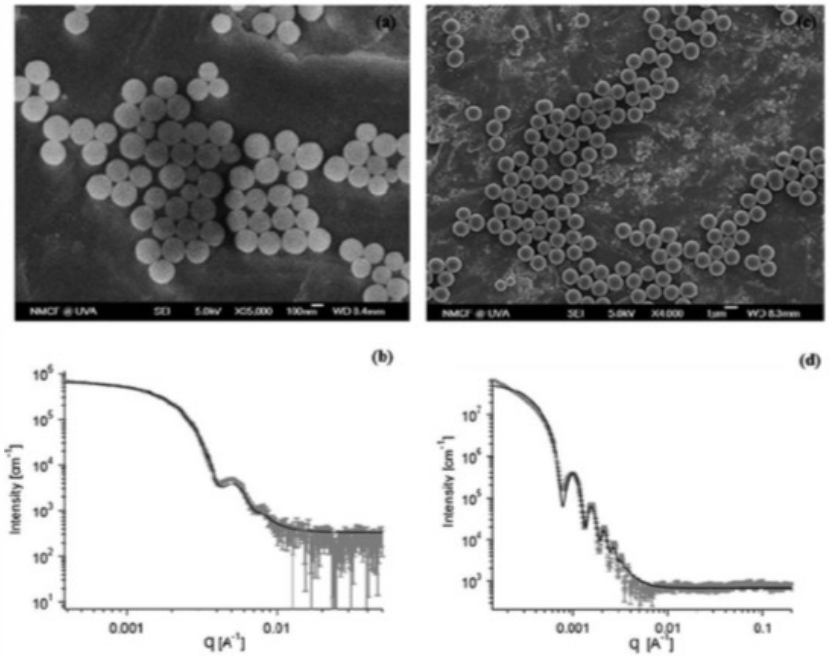

$$\sin(x) = x - \frac{x^3}{3!} + \frac{x^5}{5!} - \frac{x^7}{7!} + \cdots$$

$$\cos(x) = 1 - \frac{x^2}{2!} + \frac{x^4}{4!} - \frac{x^6}{6!} + \cdots$$

$N - 2$ remaining particles through the Ornstein–Zernike (OZ) relation which decomposes the total correlation function, $h(r) = g(r) - 1$, into direct and indirect contributions, $c(r)$ and $\gamma(r)$, respectively, through:

$$\gamma(r) = h(r) - c(r) = \rho_{\mathrm{P}} \int h(r')c(|r - r'|)\mathrm{d}r' \tag{5}$$

To solve the OZ equation, an appropriate closure relation is needed to approximate how particle interactions through $U(r)$ impact the local microstructure through $g(r)$, $h(r)$, and $c(r)$. To this end, we chose the Percus–Yevick (PY) approximation in eqn (6),

$$g(r) = \exp\left[\frac{-U(r)}{k_{\mathrm{B}}T}\right](1 + \gamma(r))$$

$$U(r) = U_0\left[\begin{array}{c} U(r) = \infty; \\ -\ln(y) - \frac{9}{5}(1-y) + \frac{1}{3}(1-y^3) - \frac{1}{30}(1-y^6) \\ U(r) = 0; \end{array}\right]; \quad \begin{array}{c} y \leq 0 \\ 0 < y \leq 1 \\ y > 1 \end{array} \tag{7}$$

where dimensionless separation distance $y = (r - 2R/2L)$ and prefactor $U_0 = (\pi^3/12)(\Sigma RL^3/a^2N_{\mathrm{in}})k_{\mathrm{B}}T$ for monomer size a,

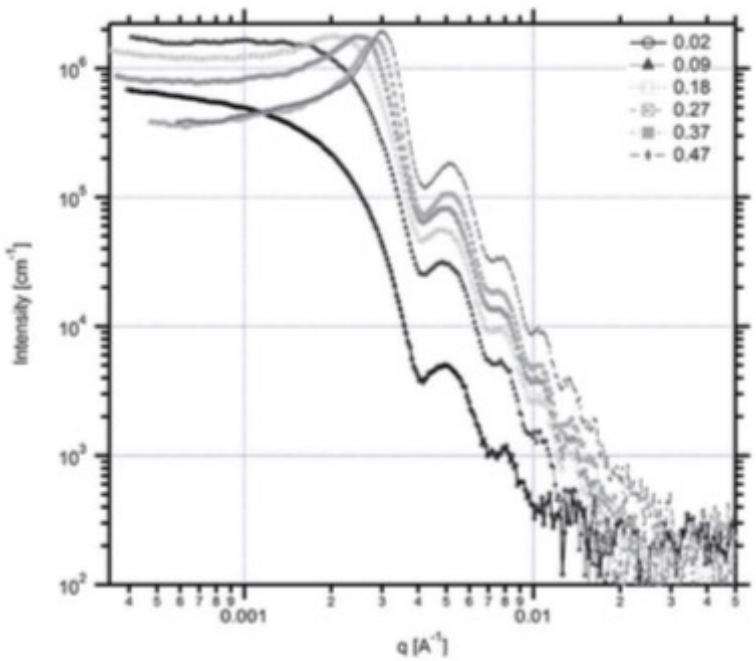

Fig. 3 USAXS scattering intensity $I(q)$ of radius $R \approx 100$ nm silica nanoparticles grafted with 25 kg mol^{-1} in 13 kg mol^{-1} PDMS. The silica core volume fraction range from $\phi_c = 0.02$–0.47.

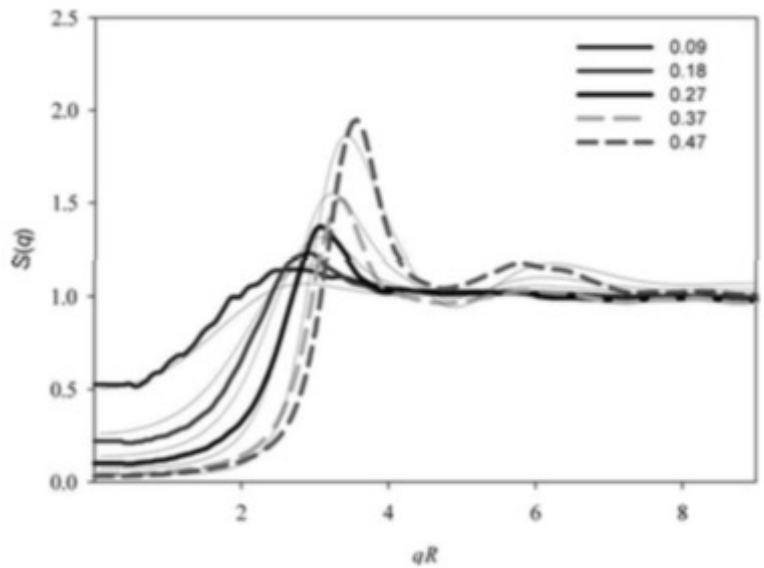

Fig. 4 Comparison of experimental and theoretical structure factors $S(q)$ for radius $R \approx 100$ nm silica nanoparticles grafted with 25 kg mol^{-1} PDMS in 13 kg mol^{-1} PDMS with varying core volume fractions $\phi_c = 0.09$–0.47. Thin solid lines are predictions of $S(q)$ from Percus–Yevick closure from eqn (13) for particles with a size distribution of 109 ± 13 nm obtained from analysis of USAXS intensities.

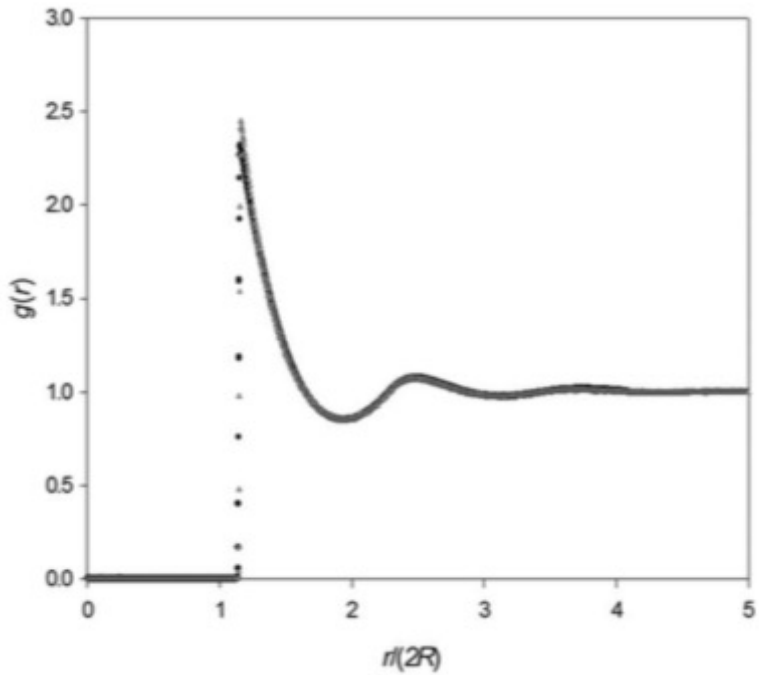

Fig. 6 Correspondence between the radial distribution function $g(r)$ predicted with Percus–Yevick closure (black) and Monte Carlo simulations (gray) for radius $R \approx 100$ nm silica nanoparticles grafted with 25 kg mol^{-1} PDMS in 13 kg mol^{-1} PDMS at $\phi_c = 0.20$. The interactions of the polymer-grafted nanoparticles in the melts were simulated with Mewis–Russell potential in eqn (7).

Go to slides 2 second half

Measurement of the Hydrodynamic Radius, R_h

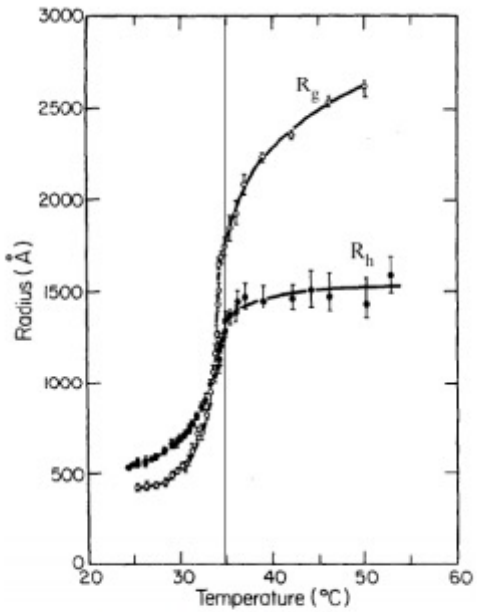

Figure 3. *Radius of gyration, R_g, and hydrodyamic radius R_h versus temperature for polystyrene in cyclohexane. Vertical line indicates the phase separation temperature. From Reference [21].*

$$[\eta] = \frac{4/3\pi R_H^3}{N} \qquad R_H = \frac{kT}{6\pi\eta D} \qquad \frac{1}{R_H} = \frac{1}{2N^2}\sum_{i=1}^{N}\sum_{j=1}^{N}\left\langle \frac{1}{|r_i - r_j|} \right\rangle$$

Kirkwood, J. Polym. Sci. **12** 1(1953).

http://theor.jinr.ru/~kuzemsky/kirkbio.html

http://www.eng.uc.edu/~gbeaucag/Classes/Properties/HydrodyamicRadius.pdf

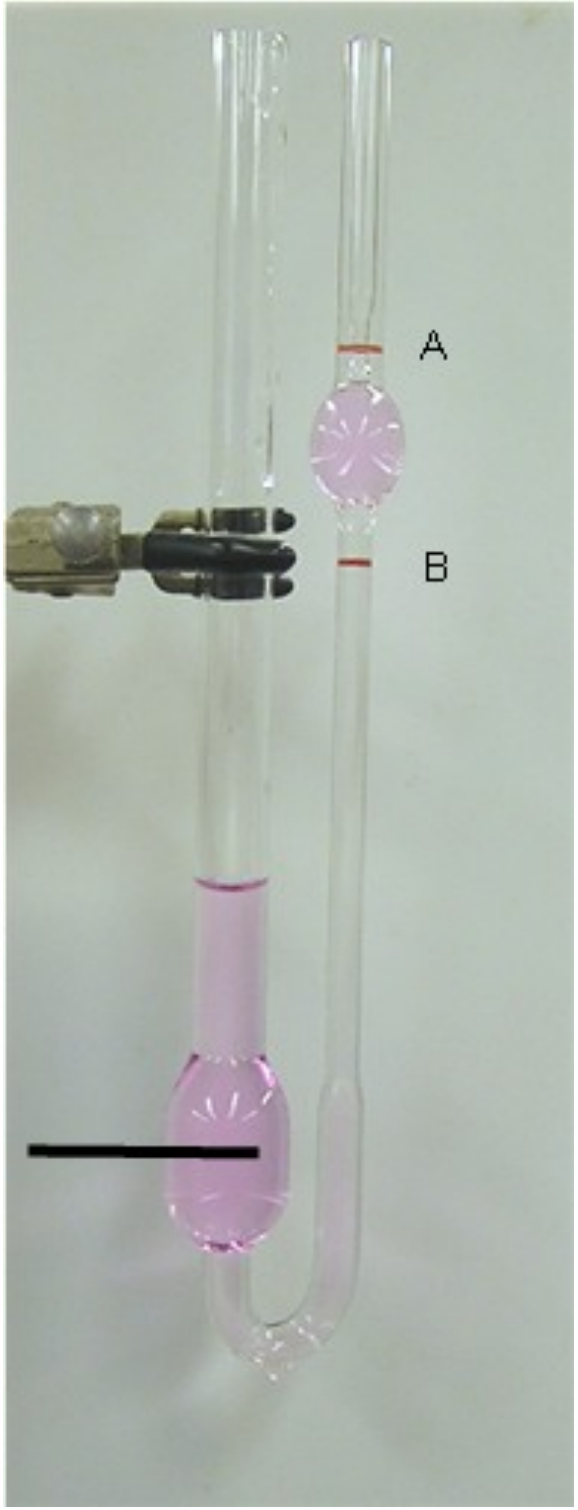

Viscosity

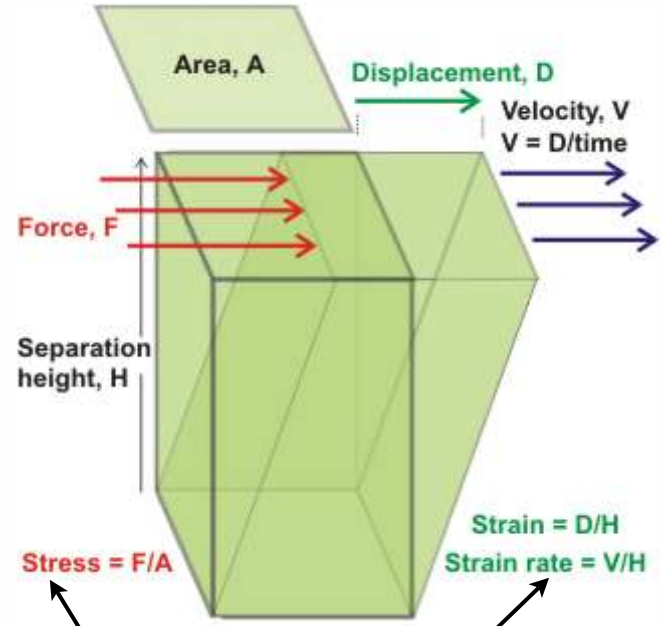

$$\tau = \eta\dot{\gamma}$$

$$\eta_s = \eta_0\left(1+[\eta]\phi\right)$$

$$[\eta] \approx \frac{V_{Molecule}}{M_{Moledule}}$$

Native state has the smallest volume

Intrinsic, specific & reduced "viscosity"

$\tau_{xy} = \eta \dot{\gamma}_{xy}$ Shear Flow (may or may not exist in a capillary/Couette geometry)

$$\eta = \eta_0 \left(1 + \phi[\eta] + k_1 \phi^2 [\eta]^2 + k_2 \phi^3 [\eta]^3 + \cdots + k_{n-1} \phi^n [\eta]^n\right) \qquad (1)$$

n = order of interaction (2 = binary, 3 = ternary etc.)

$$\frac{1}{\phi}\left(\frac{\eta - \eta_0}{\eta_0}\right) = \frac{1}{\phi}(\eta_r - 1) = \frac{\eta_{sp}}{\phi} \xrightarrow{\text{Limit } \phi => 0} [\eta] = \frac{V_H}{M}$$

We can approximate (1) as:

$$\eta_r = \frac{\eta}{\eta_0} = 1 + \phi[\eta]\exp\left(K_M \phi[\eta]\right)$$ Martin Equation

Utracki and Jamieson "Polymer Physics From Suspensions to Nanocomposites and Beyond" 2010 Chapter 1

Intrinsic, specific & reduced "viscosity"

$$\eta = \eta_0 \left(1 + c[\eta] + k_1 c^2 [\eta]^2 + k_2 c^3 [\eta]^3 + \cdots + k_{n-1} c^n [\eta]^n\right) \qquad (1)$$

n = order of interaction (2 = binary, 3 = ternary etc.)

$$\frac{1}{c}\left(\frac{\eta - \eta_0}{\eta_0}\right) = \frac{1}{c}(\eta_r - 1) = \frac{\eta_{sp}}{c} \xrightarrow{\text{Limit } c \Rightarrow 0} [\eta] = \frac{V_H}{M}$$

Concentration Effect

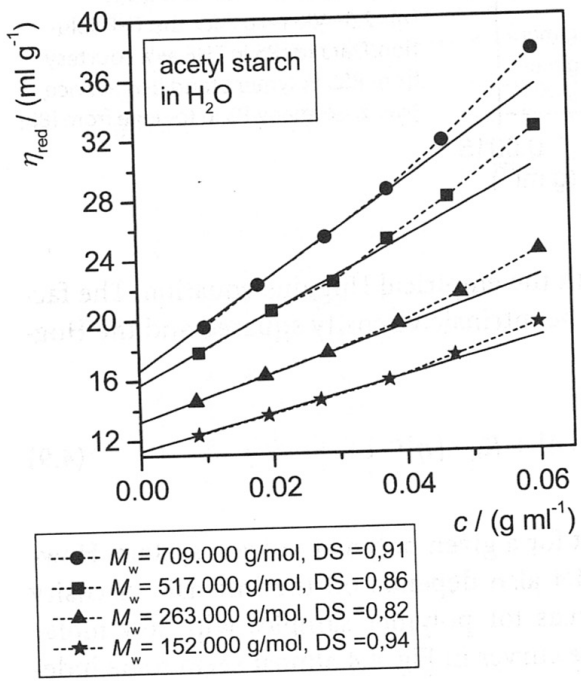

Fig. 4.5. Reduced viscosity η_{red} as a function of the concentration c for acetyl starch of different molar masses in aqueous solution at T=25 °C. The degree of substitution (DS) with acetyl groups is nearly constant at DS≈0.9. Due to the compact structure of the polymer coil the concentrations of the dilution series are relatively high to reach the required relative viscosity range of η_r=1.2–2.5

Kulicke & Clasen "Viscosimetry of Polymers and Polyelectrolytes (2004)

Intrinsic, specific & reduced "viscosity"

$$\eta = \eta_0 \left(1 + c[\eta] + k_1 c^2 [\eta]^2 + k_2 c^3 [\eta]^3 + \cdots + k_{n-1} c^n [\eta]^n\right) \qquad (1)$$

n = order of interaction (2 = binary, 3 = ternary etc.)

$$\frac{1}{c}\left(\frac{\eta - \eta_0}{\eta_0}\right) = \frac{1}{c}(\eta_r - 1) = \frac{\eta_{sp}}{c} \xrightarrow{\text{Limit } c=>0} [\eta] = \frac{V_H}{M}$$

Concentration Effect, c*

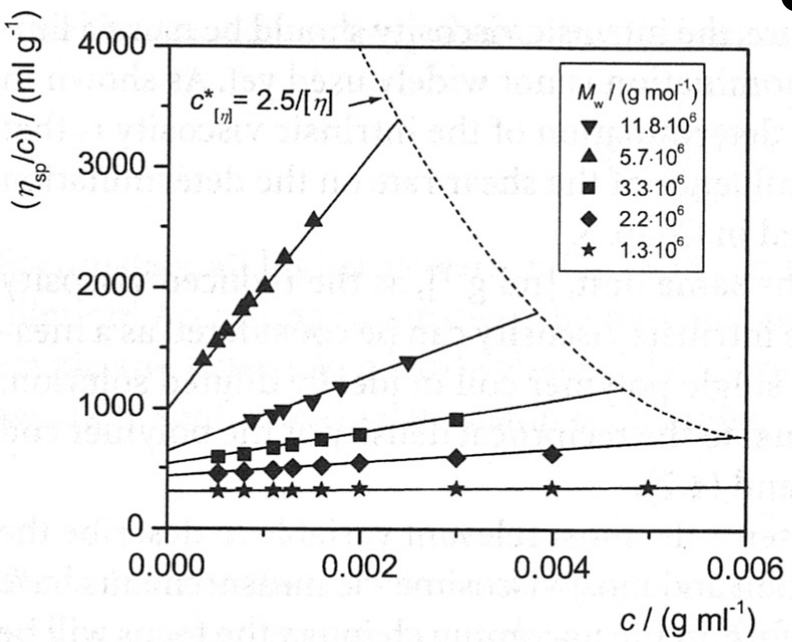

Fig. 4.2. Reduced viscosity η_{red} as a function of the concentration c for different molar masses of the polycation poly(acrylamide-*co*-(*N,N,N*-trimethyl-*N*-[2-methacryloethyl]-ammoniumchloride) (PTMAC) in 0.1 mol/l $NaNO_3$ solution. Data from [87]. All data points are measured at concentrations below the critical concentration $c^*_{[\eta]}$. The copolymer consists of 8 mol% TMAC and 92 mol% AAm

Kulicke & Clasen "Viscosimetry of Polymers and Polyelectrolytes (2004)

Intrinsic, specific & reduced "viscosity"

$$\eta = \eta_0 \left(1 + c[\eta] + k_1 c^2 [\eta]^2 + k_2 c^3 [\eta]^3 + \cdots + k_{n-1} c^n [\eta]^n\right) \qquad (1)$$

n = order of interaction (2 = binary, 3 = ternary etc.)

$$\frac{1}{c}\left(\frac{\eta - \eta_0}{\eta_0}\right) = \frac{1}{c}(\eta_r - 1) = \frac{\eta_{sp}}{c} \xrightarrow{\text{Limit } c \Rightarrow 0} [\eta] = \frac{V_H}{M}$$

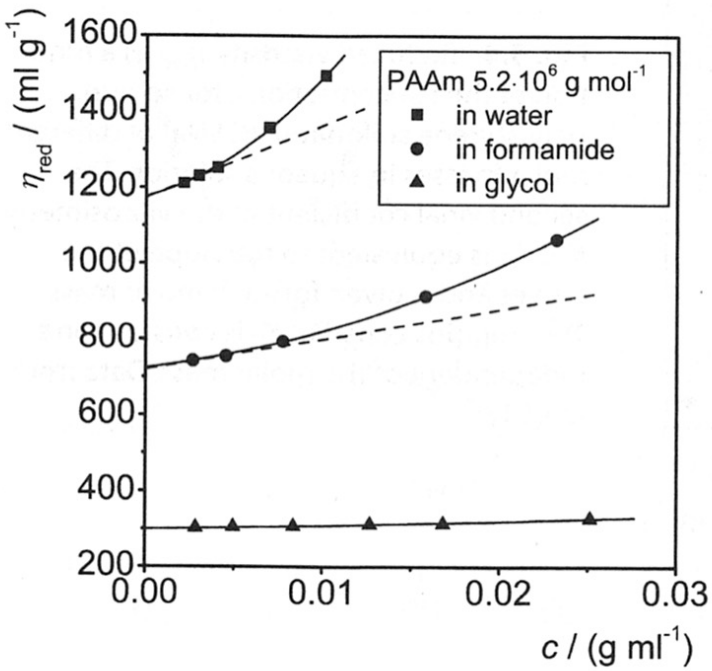

Solvent Quality

Fig. 5.3. Reduced viscosity η_{red} as a function of the concentration c for a poly(acrylamide) (PAAm) in the solvents H_2O, formamide and ethylene glycol at T=25 °C. Data from [89, 90]. The intrinsic viscosity (intersection with the Y-axis) rises with the solvent quality

Kulicke & Clasen "Viscosimetry of Polymers and Polyelectrolytes (2004)

Intrinsic, specific & reduced "viscosity"

$$\eta = \eta_0 \left(1 + c[\eta] + k_1 c^2 [\eta]^2 + k_2 c^3 [\eta]^3 + \cdots + k_{n-1} c^n [\eta]^n\right) \qquad (1)$$

n = order of interaction (2 = binary, 3 = ternary etc.)

$$\frac{1}{c}\left(\frac{\eta - \eta_0}{\eta_0}\right) = \frac{1}{c}(\eta_r - 1) = \frac{\eta_{sp}}{c} \xrightarrow{\text{Limit } c=>0} [\eta] = \frac{V_H}{M}$$

Molecular Weight Effect

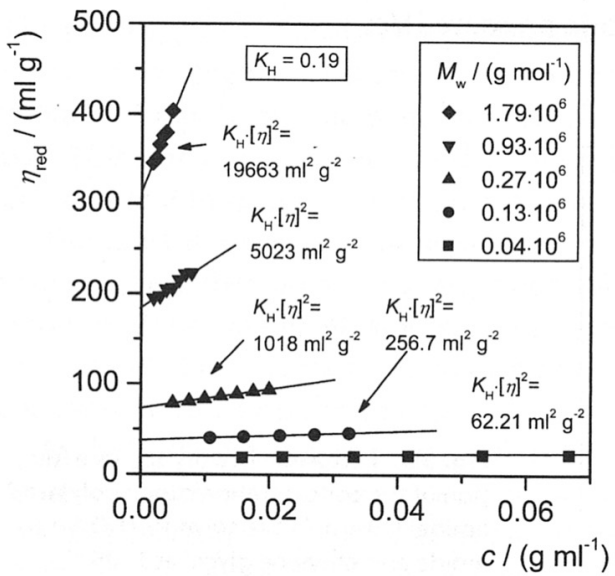

Fig. 5.4. Reduced viscosity η_{red} as a function of the concentration c for sodium poly(styrene sulfonate) (PSSNa) of different molar masses in aqueous solution. The second virial coefficient of the viscosimetry, $K_H \cdot [\eta]^2$, is equivalent to the slope of the curves and is given for each molar mass. The Huggins constant K_H is constant and independent of the molar mass. Data from [35, 91]

$$[\eta] = KM^a$$

Kulicke & Clasen "Viscosimetry of Polymers and Polyelectrolytes (2004)

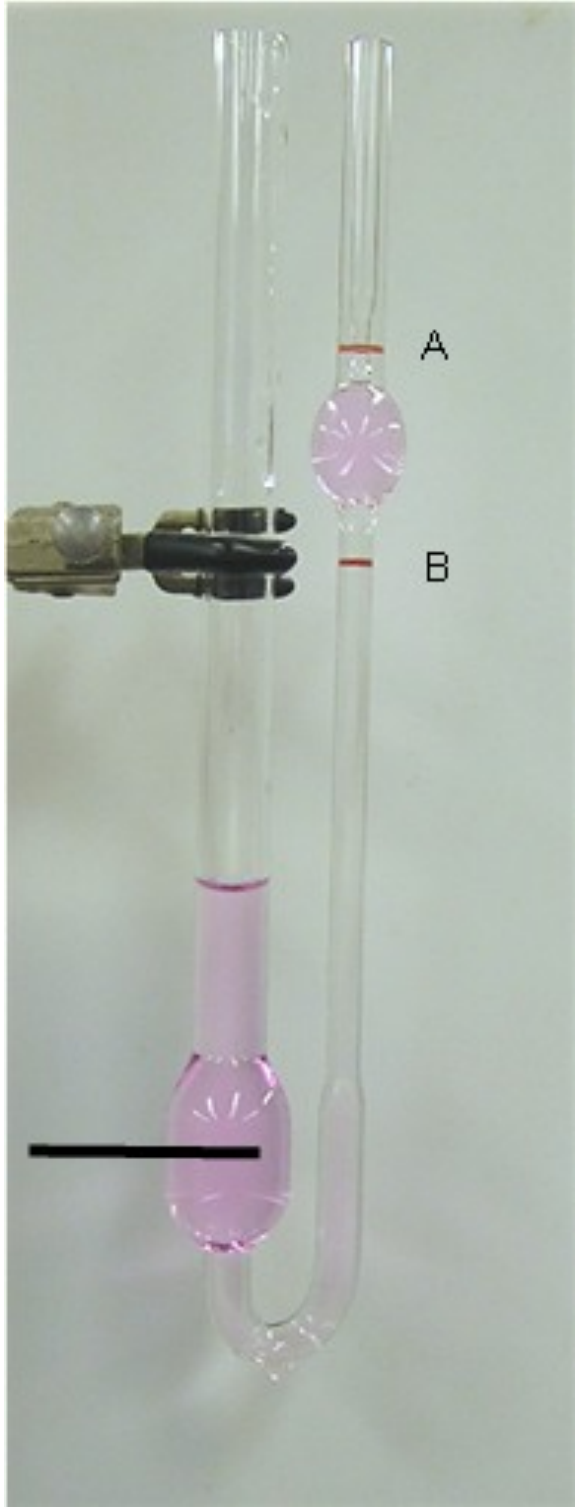

Viscosity

$$\eta_s = \eta_0 \left(1 + [\eta]\phi\right)$$

$$[\eta] \approx \frac{V_{Molecule}}{M_{Moledule}}$$

For the Native State Mass ~ $\rho V_{Molecule}$

Einstein Equation (for Suspension of 3d Objects)

$$\eta_s = \eta_0 \left(1 + 2.5\phi\right)$$

For "Gaussian" Chain Mass ~ Size^2 ~ $V^{2/3}$

V ~ Mass$^{3/2}$

For "Expanded Coil" Mass ~ Size$^{5/3}$ ~ $V^{5/9}$

V ~ Mass$^{9/5}$

For "Fractal" Mass ~ Size^{df} ~ $V^{df/3}$

V ~ Mass$^{3/df}$

$$[\eta] \sim M_{Molecule}^{\frac{3}{d_f}-1}$$

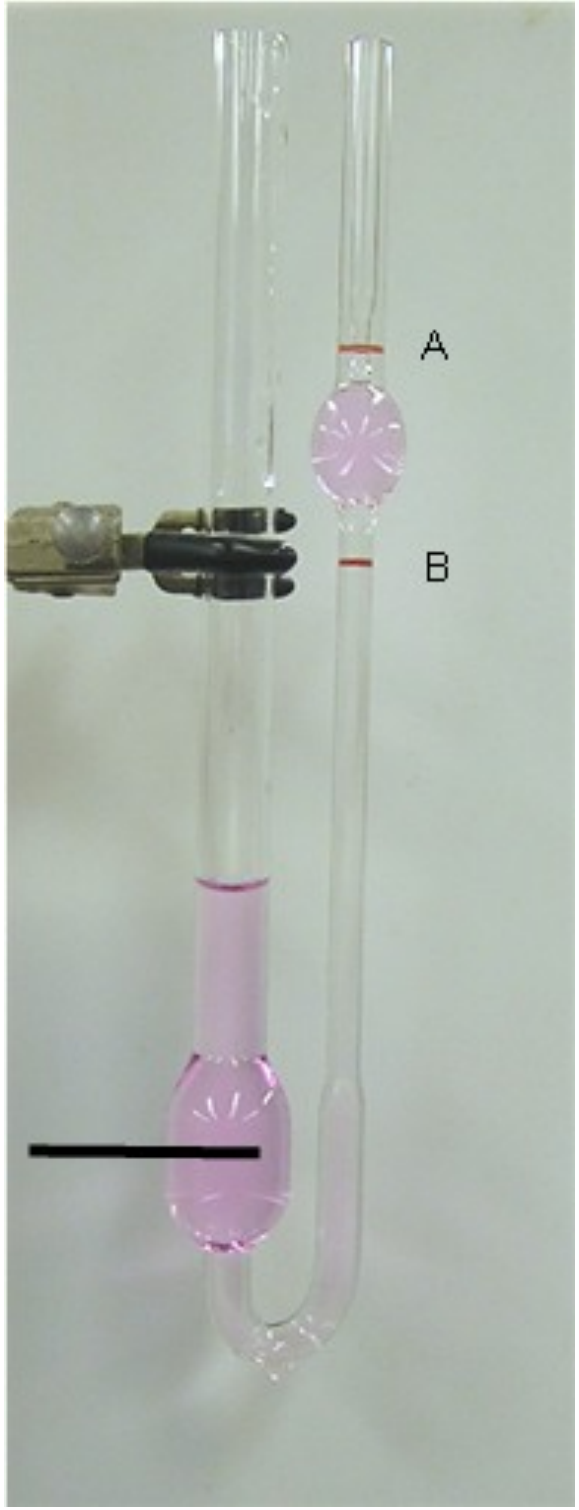

Viscosity

$$\eta_s = \eta_0 \left(1 + [\eta]\phi\right)$$

$$[\eta] \approx \frac{V_{Molecule}}{M_{Moledule}}$$

For the Native State Mass ~ $\rho V_{Molecule}$

Einstein Equation (for Suspension of 3d Objects)

$$\eta_s = \eta_0 \left(1 + 2.5\phi\right)$$

"Size" is the "Hydrodynamic Size"

For "Gaussian" Chain Mass ~ $Size^2 \sim V^{2/3}$

$V \sim Mass^{3/2}$

For "Expanded Coil" Mass ~ $Size^{5/3} \sim V^{5/9}$

$V \sim Mass^{9/5}$

For "Fractal" Mass ~ $Size^{df} \sim V^{df/3}$

$V \sim Mass^{3/df}$

$$[\eta] \sim M_{Molecule}^{\frac{3}{d_f}-1}$$

Intrinsic, specific & reduced "viscosity"

$$\eta = \eta_0 \left(1 + c[\eta] + k_1 c^2 [\eta]^2 + k_2 c^3 [\eta]^3 + \cdots + k_{n-1} c^n [\eta]^n\right) \qquad (1)$$

n = order of interaction (2 = binary, 3 = ternary etc.)

$$\frac{1}{c}\left(\frac{\eta - \eta_0}{\eta_0}\right) = \frac{1}{c}(\eta_r - 1) = \frac{\eta_{sp}}{c} \xrightarrow{\text{Limit } c=>0} [\eta] = \frac{V_H}{M}$$

Temperature Effect

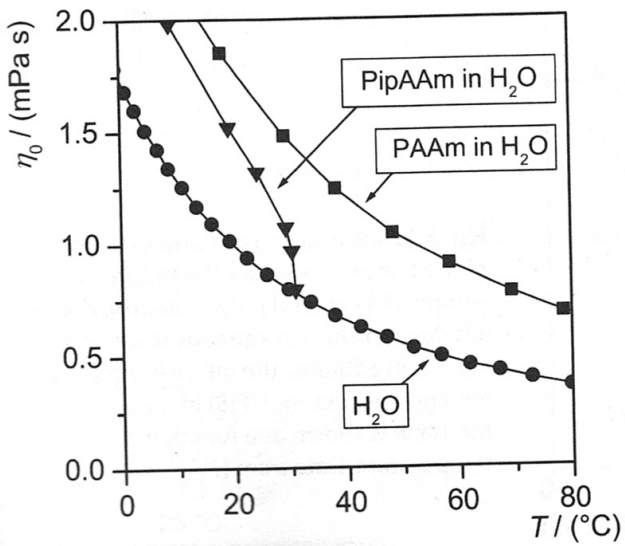

Fig. 5.5. Zero-shear viscosity η_0 as a function of the temperature T for poly (acrylamide) (PAAm) and poly(N-iso-propyl-acrylamide) (PipAAm) in aqueous solution (c=0.1 wt%). The viscosity for the solvent water as a function of the temperature is plotted as well. Data from [77]

$$\eta_0 = A \exp\left(\frac{E}{k_B T}\right)$$

Kulicke & Clasen "Viscosimetry of Polymers and Polyelectrolytes (2004)

Intrinsic, specific & reduced "viscosity"

$$\eta = \eta_0 \left(1 + c[\eta] + k_1 c^2 [\eta]^2 + k_2 c^3 [\eta]^3 + \cdots + k_{n-1} c^n [\eta]^n\right) \qquad (1)$$

n = order of interaction (2 = binary, 3 = ternary etc.)

$$\frac{1}{c}\left(\frac{\eta - \eta_0}{\eta_0}\right) = \frac{1}{c}(\eta_r - 1) = \frac{\eta_{sp}}{c} \xrightarrow{\text{Limit } c=>0} [\eta] = \frac{V_H}{M}$$

We can approximate (1) as:

$$\eta_r = \frac{\eta}{\eta_0} = 1 + c[\eta]\exp\left(K_M c[\eta]\right)$$ Martin Equation

$$\frac{\eta_{sp}}{c} = [\eta] + k_1 [\eta]^2 c$$ Huggins Equation

$$\frac{\ln(\eta_r)}{c} = [\eta] + k_1' [\eta]^2 c$$ Kraemer Equation (exponential expansion)

Utracki and Jamieson "Polymer Physics From Suspensions to Nanocomposites and Beyond" 2010 Chapter 1

Intrinsic "viscosity" for colloids (Simha, Case Western)

$$\eta = \eta_0 \left(1 + v\phi\right) \qquad \eta = \eta_0 \left(1 + [\eta] c\right)$$

$$[\eta] = \frac{v N_A V_H}{M}$$

For a solid object with a surface v is a constant in molecular weight, depending only on shape

For a symmetric object (sphere) *v* = 2.5 (Einstein) $[\eta] = \frac{2.5}{\rho} \; ml/g$

For ellipsoids *v* is larger than for a sphere,

$$v = \frac{J^2}{15\left(\ln(2J) - 3/2\right)}$$

prolate

a, b, b :: a>b

J = a/b

$$v = \frac{16J}{15\tan^{-1}(J)}$$

oblate

a, a, b :: a<b

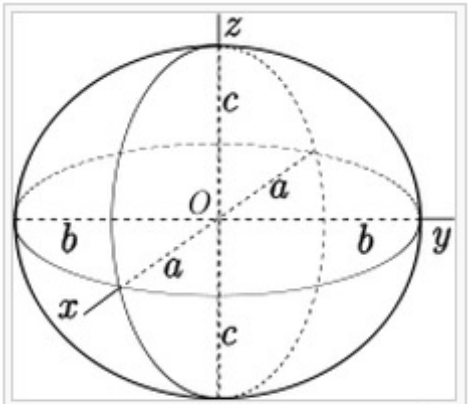

Tri-axial ellipsoid with distinct semi-axes *a*, *b* and *c*

Intrinsic "viscosity" for colloids (Simha, Case Western)

$$\eta = \eta_0 \left(1 + v\phi\right) \qquad \eta = \eta_0 \left(1 + [\eta] c\right)$$

$$[\eta] = \frac{v N_A V_H}{M}$$

Hydrodynamic volume for "bound" solvent

$$V_H = \frac{M}{N_A}\left(\bar{v}_2 + \delta_S v_1^0\right)$$

Partial Specific Volume	$\bar{v}_2$
Bound Solvent (g solvent/g polymer)	δ_S
Molar Volume of Solvent	v_1^0

Intrinsic "viscosity" for colloids (Simha, Case Western)

$$\eta = \eta_0 \left(1 + v\phi\right) \qquad \eta = \eta_0 \left(1 + [\eta] c\right)$$

$$[\eta] = \frac{v N_A V_H}{M}$$

Long cylinders (TMV, DNA, Nanotubes)

$$[\eta] = \frac{2}{45} \frac{\pi N_A L^3}{M\left(\ln J + C_\eta\right)}$$

J=L/d

C_η End Effect term ~ 2 ln 2 – 25/12 Yamakawa 1975

Shear Rate Dependence for Polymers

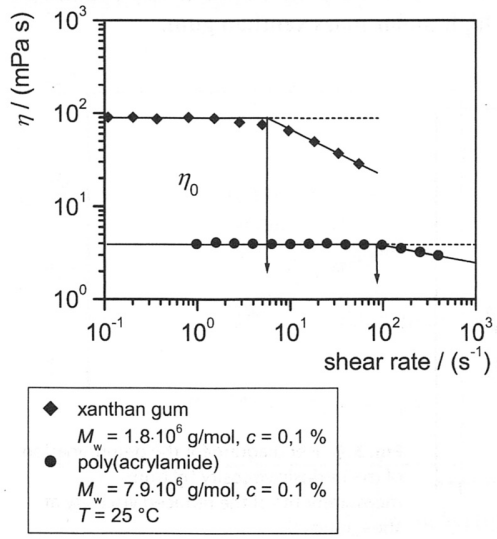

Fig. 5.8. Dynamic viscosity η as a function of the shear rate $\dot{\gamma}$ for an aqueous xanthan gum and an aqueous poly(acrylamide) solution of a comparable degree of polymerization and the same concentration c=0.1 wt% data from [92]. The viscosity depends on the shear rate above a critical shear rate $\dot{\gamma}_{crit}$

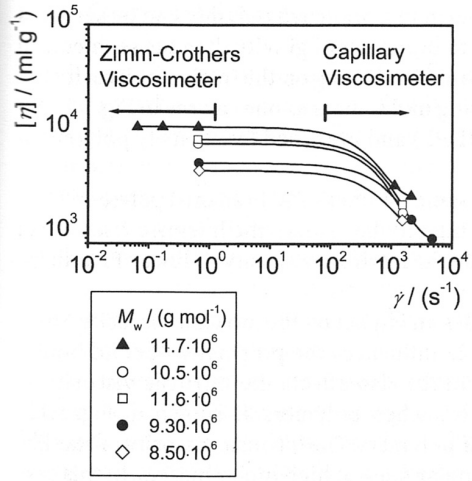

Fig. 5.10. Intrinsic viscosity $[\eta]$ determined at high shear rates $\dot{\gamma}$ with a capillary viscosimeter and at lower shear rates with a Zimm-Crothers viscosimeter for different xanthan gums in 0.1 mol/l sodium chloride (NaCl) solution at 25 °C. Data from [93]. For strongly shear thinning polymer solutions, only low shear viscosimeters reach the shear rate independent viscosity region

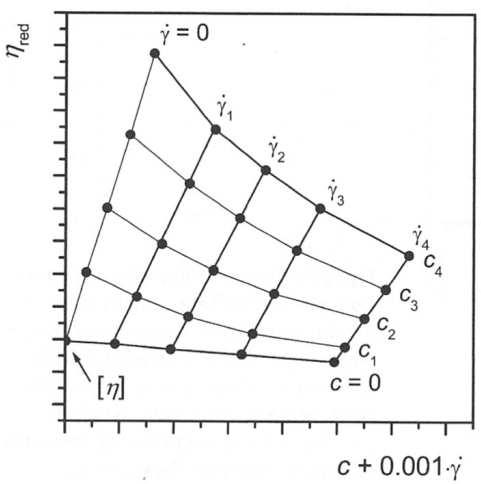

Fig. 5.9. Net diagram for the determination of the intrinsic viscosity $[\eta]$ from measurements of the reduced viscosity at shear rates≠0

Capillary Viscometer

$$\frac{Volume}{time} = \frac{\pi R^4 \Delta p}{8\eta l}$$

$$\Delta p = \rho g h$$

$$\dot{\gamma}_{Max} = \frac{4Volume}{\pi R^3 time}$$

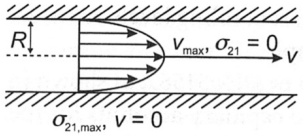

Fig. 3.2. Velocity profile in a capillary viscosimeter. The fluid velocity v has a parabolic profile with a maximum in the middle of the capillary; the shear rate $\dot{\gamma}$ and the shear stress τ have a maximum at the capillary wall and are zero in the middle of the capillary

Kulicke & Clasen "Viscosimetry of Polymers and Polyelectrolytes (2004)

Branching and Intrinsic Viscosity

5.5 Branching

Branching in a polymer coil leads for polymers of the same molar mass to changes of the intrinsic viscosity. Although the chemical composition is the same, branched polymers have a higher density ρ_{equ} in solution than linear polymers and therefore

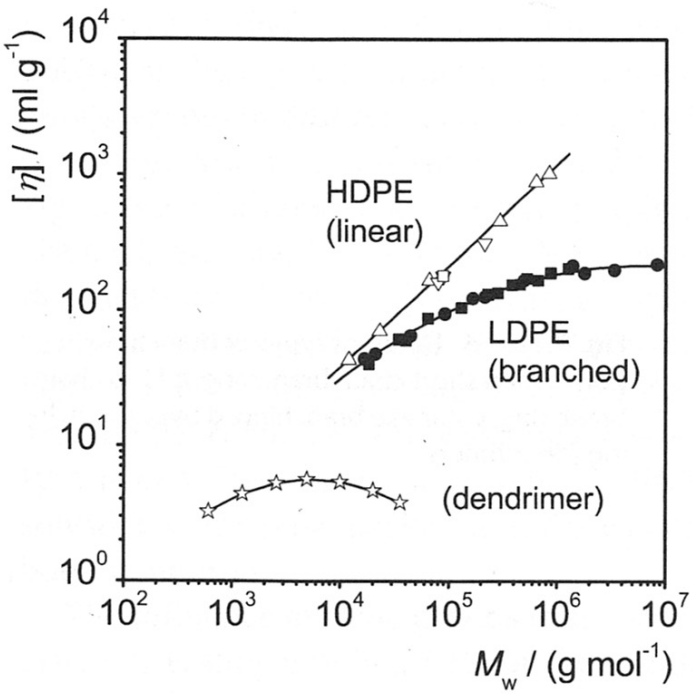

Fig. 5.11. Intrinsic viscosity [η] as a function of the molar mass M for linear poly(ethylene) (high density poly(ethylene), HDPE) and longchain branched poly(ethylene) (low density poly(ethylene), LDPE) in tetraline at T=120 °C (data from [47, 94]) as well as for a dendrimer with 3,5-dioxybenzylidene units in tetrahydrofuran at T=30 °C (data from [47, 95])

Kulicke & Clasen "Viscosimetry of Polymers and Polyelectrolytes (2004)

Branching and Intrinsic Viscosity

$$R^2_{g,b,M} \leq R^2_{g,l,M}$$

$$g = \frac{R^2_{g,b,M}}{R^2_{g,l,M}}$$

$$g = \frac{3f-2}{f^2}$$

$$g_\eta = \frac{[\eta]_{b,M}}{[\eta]_{l,M}} = g^{0.58} = \left(\frac{3f-2}{f^2}\right)^{0.58}$$

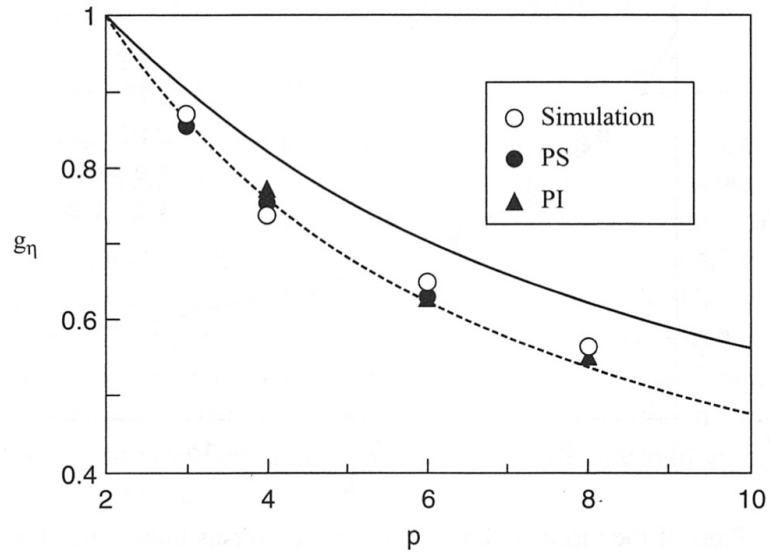

FIGURE 1.7 Plots of viscometric branching parameter, g_η, versus branch functionality, p, for star chains on a simple cubic lattice (unfilled circles), together with experimental data for star polymers in theta solvents: ●, polystyrene in cyclohexane; ▲, polyisoprene in dioxane. Solid and dashed lines represent calculated values via Eqs. (1.70) and (1.71), respectively. (Adapted from Shida et al. [2004].)

Utracki and Jamieson "Polymer Physics From Suspensions to Nanocomposites and Beyond" 2010 Chapter 1

Polyelectrolytes and Intrinsic Viscosity

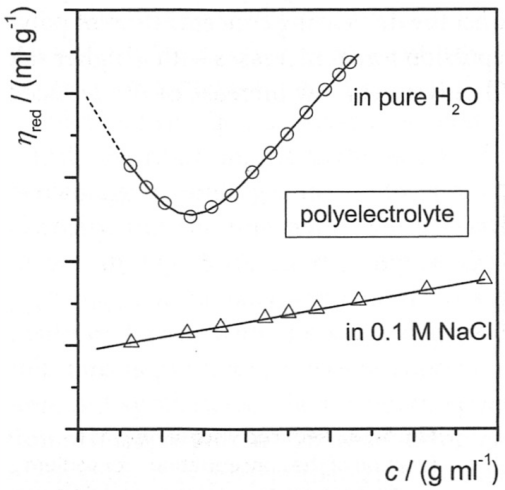

Fig. 5.16. Different behavior of a polyelectrolyte in aqueous solution and a salt solution. At high concentrations of the polyelectrolyte in aqueous solution is the concentration of counter ions inside the polymer coil higher than outside, leading to an expansion of the coil due to osmotic pressure. At low concentrations of the polyelectrolyte in aqueous solution, the polyelectrolyte is highly dissociated, leading to an expansion of the coil due to coulomb repulsion forces. Both expansion effects are compensated in the salt solution

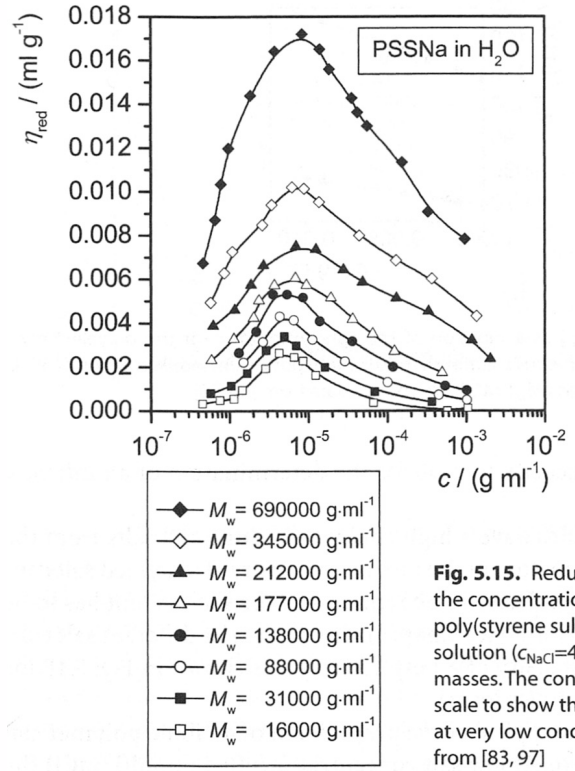

Fig. 5.15. Reduced viscosity η_{red} as a function of the concentration c for the polyelectrolyte sodium poly(styrene sulfonate) in nearly salt free aqueous solution (c_{NaCl}=4×10^{-6} mol l^{-1}) and for different molar masses. The concentration is plotted on a logarithmic scale to show the maximum behavior of the viscosity at very low concentrations of the polyelectrolyte. Data from [83, 97]

Kulicke & Clasen "Viscosimetry of Polymers and Polyelectrolytes (2004)

Polyelectrolytes and Intrinsic Viscosity

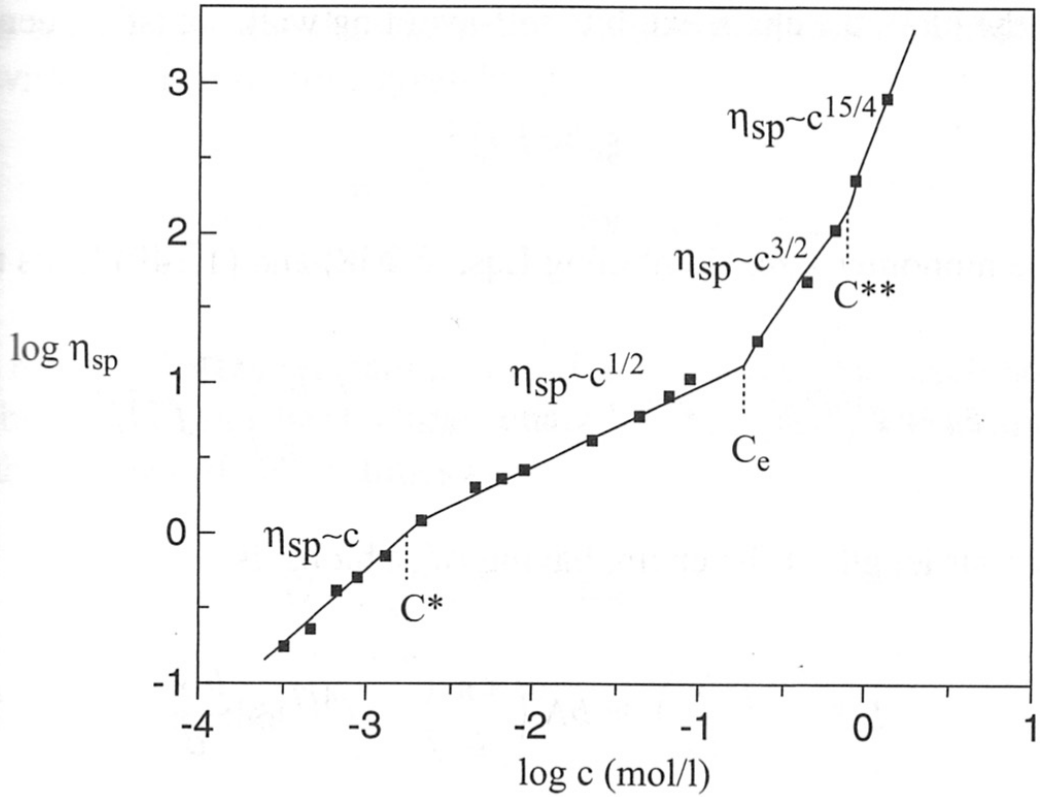

FIGURE 1.16 Determination of the chain overlap concentration c^*, the entanglement concentration c_e, the electrostatic blob overlap concentration c^{**} from the concentration dependence of specific viscosity for a 17%-quaternized P2VP copolymer (17PMVP-Cl) in solution in ethylene glycol at 25°C. Symbols are experimental data and solid lines represent the power laws predicted from scaling theory. (Adapted from Dou and Colby [2006].)

Kulicke & Clasen "Viscosimetry of Polymers and Polyelectrolytes (2004)

Hydrodynamic Radius from Dynamic Light Scattering

http://www.eng.uc.edu/~gbeaucag/Classes/Properties/HiemenzRajagopalanDLS.pdf

http://www.eng.uc.edu/~gbeaucag/Classes/Physics/DLS.pdf

http://www.eng.uc.edu/~gbeaucag/Classes/Properties/HydrodyamicRadius.pdf

Consider motion of molecules or nanoparticles in solution

Particles move by Brownian Motion/Diffusion
The probability of finding a particle at a distance x from the starting point at t = 0 is a Gaussian Function that defines the diffusion Coefficient, D

$$\rho(x,t) = \frac{1}{(4\pi Dt)^{1/2}} e^{-x^2/2(2Dt)}$$

$$\langle x^2 \rangle = \sigma^2 = 2Dt$$

The Stokes-Einstein relationship states that D is related to R_H,

$$D = \frac{kT}{6\pi\eta R_H}$$

A laser beam hitting the solution will display a fluctuating scattered intensity at "q" that varies with q since the particles or molecules move in and out of the beam
I(q,t)
This fluctuation is related to the diffusion of the particles

For static scattering p(r) is the binary spatial auto-correlation function

We can also consider correlations in time, binary temporal correlation function
$g_I(q,\tau)$

For dynamics we consider a single value of q or r and watch how the intensity changes with time
$I(q,t)$

We consider correlation between intensities separated by t
We need to subtract the constant intensity due to scattering at different size scales
and consider only the fluctuations at a given size scale, r or $2\pi/r = q$

Dynamic Light Scattering

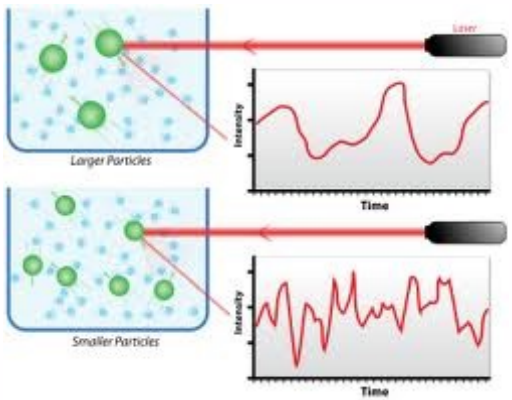

$$g^2(q;\tau) = \frac{\langle I(t)I(t+\tau)\rangle}{\langle I(t)\rangle^2}$$

$$g^2(q;\tau) = 1 + \beta\left[g^1(q;\tau)\right]^2$$

$$q = \frac{4\pi n_0}{\lambda}\sin\left(\frac{\theta}{2}\right)$$

$$g^1(q;\tau) = \exp(-\Gamma\tau)$$

$$\Gamma = q^2 D_t$$

$$D = k_B T / 6\pi\eta a$$

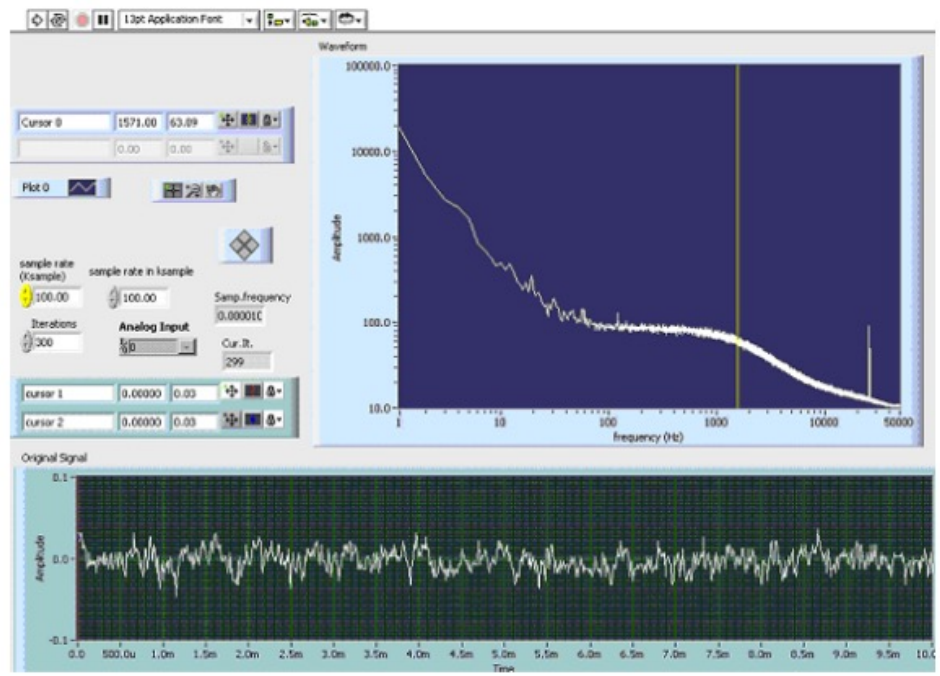

a = R_H = Hydrodynamic Radius

The radius of an equivalent sphere following Stokes' Law

Dynamic Light Scattering

my DLS web page

http://www.eng.uc.edu/~gbeaucag/Classes/Physics/DLS.pdf

Wiki

http://webcache.googleusercontent.com/search?q=cache:eY3xhiX117IJ:en.wikipedia.org/wiki/Dynamic_light_scattering+&cd=1&hl=en&ct=clnk&gl=us

Wiki Einstein Stokes

http://webcache.googleusercontent.com/search?q=cache:yZDPRbqZ1BIJ:en.wikipedia.org/wiki/Einstein_relation_(kinetic_theory)+&cd=1&hl=en&ct=clnk&gl=us

Diffusing Wave Spectroscopy (DWS)

Will need to come back to this after introducing dynamics
And linear response theory

http://www.formulaction.com/technology-dws.html

Static Scattering for Fractal Scaling

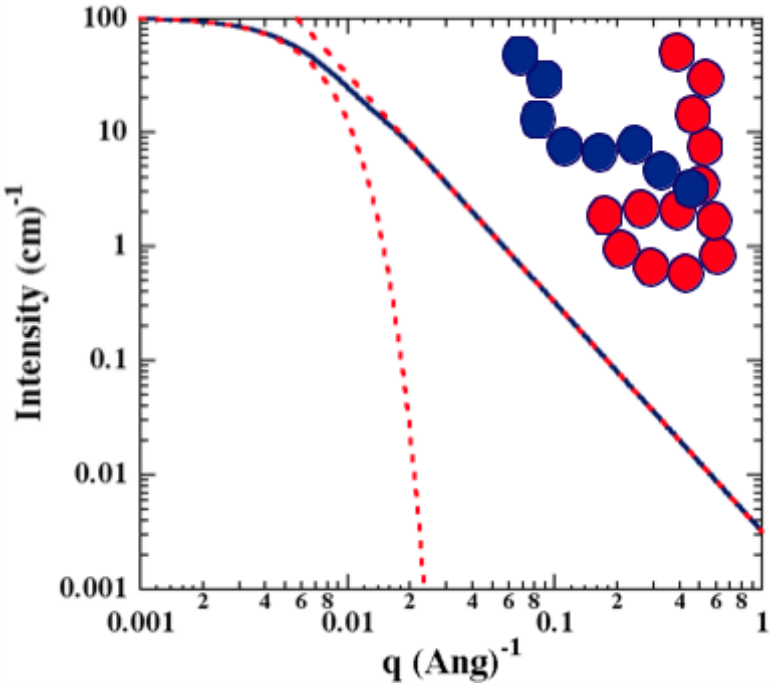

At intermediate sizes the chain is “self-similar”

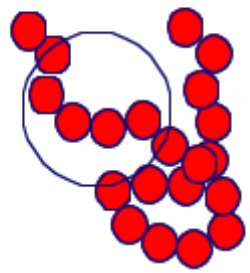

$$Mass \sim Size^{d_f}$$

$$z \sim \left(\frac{R_2}{R_1} \right)^{d_f}$$

At intermediate sizes the chain is "self-similar"

$I(q) \sim N\, n_e^2$

N = Number of Intermediate Spheres in the Aggregate

n_e = Mass of inter. sphere

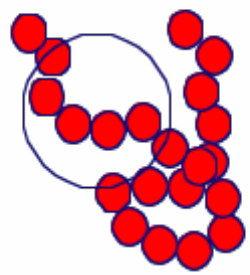

$I(q) \sim N\, n_e^2$

$$N \sim \left(\frac{R_2}{r_{\text{int}}}\right)^{d_f}$$

$$n_e \sim \left(\frac{r_{\text{int}}}{R_1}\right)^{d_f}$$

$$N n_e^2 \sim \left(\frac{r_{\text{int}}}{R_1}\right)^{d_f} \left(\frac{R_2}{R_1}\right)^{d_f} \quad \Rightarrow \quad \mathrm{I(q)} \sim \left(\frac{R_2}{R_1^2}\right)^{d_f} q^{-d_f}$$

The Debye Scattering Function for a Polymer Coil

$$I(Q) = \frac{2}{Q^2}\left(Q - 1 + \exp(-Q)\right)$$

$$Q = q^2 R_g^2$$

For $qR_g << 1$

$$\exp(-Q) = 1 - Q + \frac{Q^2}{2!} - \frac{Q^3}{3!} + \frac{Q^4}{4!} - \ldots$$

$$I(q) = 1 - \frac{Q}{3} + \ldots \approx \exp\left(-\frac{q^2 R_g^2}{3}\right)$$

Guinier's Law!

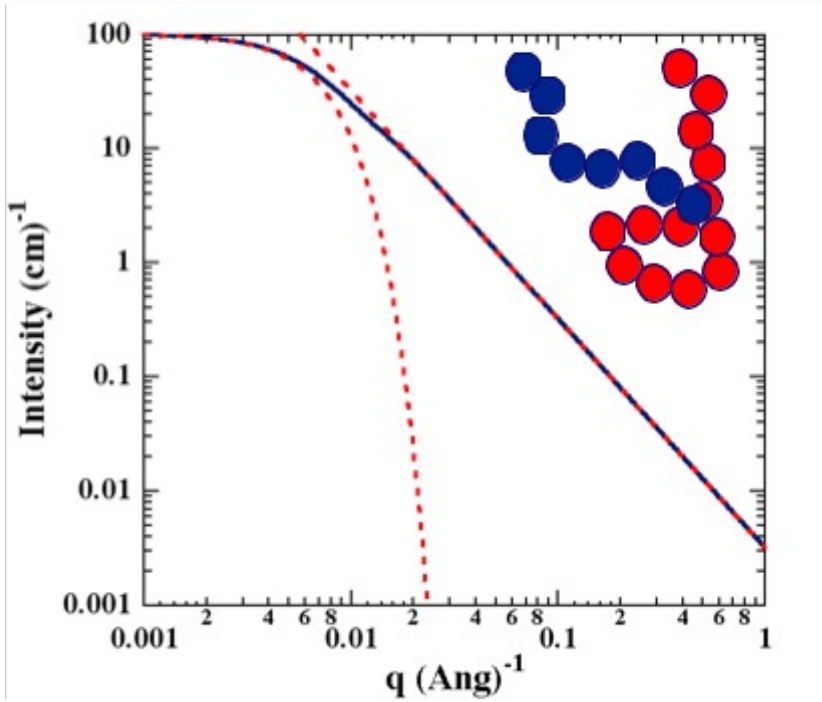

The Debye Scattering Function for a Polymer Coil

$$I(Q) = \frac{2}{Q^2}\left(Q - 1 + \exp(-Q)\right)$$

$$Q = q^2 R_g^2$$

For $qR_g >> 1$

$$I(Q) = \frac{2}{Q} = \frac{2}{q^2 R_g^2} \sim q^{-d_f}$$

$d_f = 2$

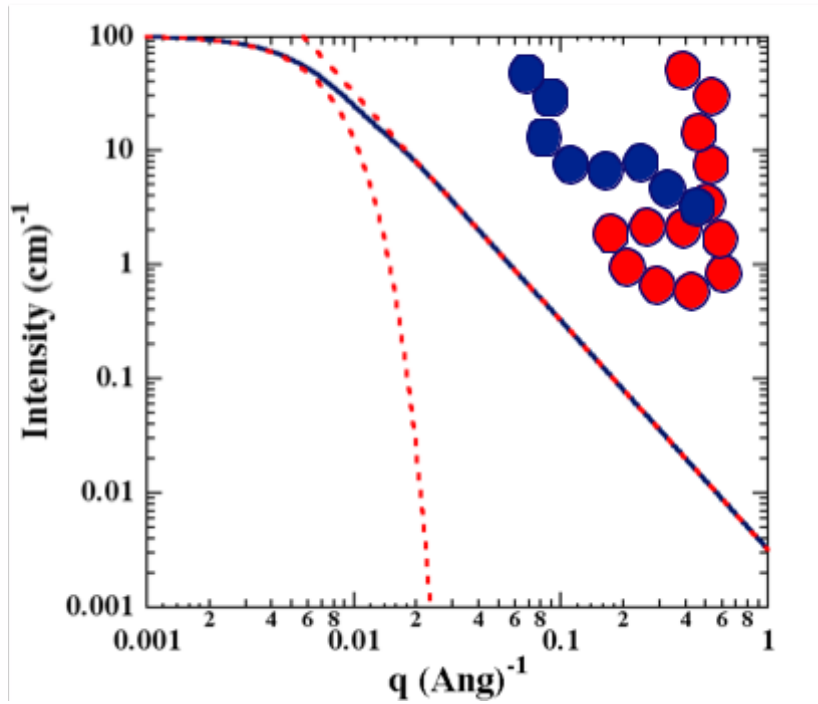

Ornstein-Zernike Equation

$$I(q) = \frac{G}{1 + q^2 \xi^2} \qquad I(q => \infty) = \frac{G}{q^2 \xi^2}$$

Has the correct functionality at high q

Debye Scattering Function =>

$$I(q) = \frac{2}{q^2 R_g^2}\left(q^2 R_g^2 - 1 + \exp\left(-q^2 R_g^2\right)\right) \qquad I(q => \infty) = \frac{2G}{q^2 R_g^2}$$

So, $$R_g^2 = 2\zeta^2$$

Ornstein-Zernike Equation

$$I(q) = \frac{G}{1 + q^2 \xi^2} \qquad I(q => 0) = G \exp\left(-q^2 \xi^2\right)$$

Has the correct functionality at low q
Debye =>

$$I(q) = \frac{2}{q^2 R_g^2}\left(q^2 R_g^2 - 1 + \exp\left(-q^2 R_g^2\right)\right) \qquad I(q => 0) = G \exp\left(-\frac{q^2 R_g^2}{3}\right)$$

$$R_g^2 = 3\zeta^2$$

The relatoinship between R_g and correlation length differs for the two regimes.

How does a polymer chain respond to external perturbation?

The Gaussian Chain

Boltzman Probability
For a Thermally Equilibrated System

$$P_B(R) = \exp\left(-\frac{E(R)}{kT}\right)$$

Gaussian Probability
For a Chain of End to End Distance R

$$P(R) = \left(\frac{3}{2\pi\sigma^2}\right)^{3/2} \exp\left(-\frac{3(R)^2}{2(\sigma)^2}\right)$$

By Comparison The Energy to stretch a Thermally Equilibrated Chain Can be Written

$$E = kT\frac{3R^2}{2nl_K^2}$$

Force

Force

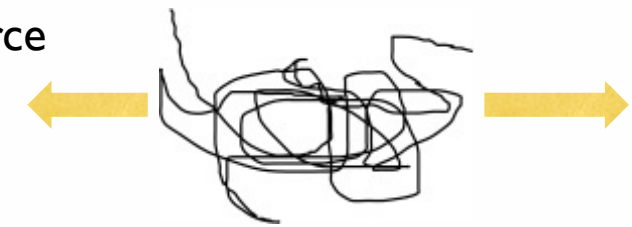

$$F = \frac{dE}{dR} = \frac{3kT}{nl_K^2}R = k_{spr}R$$

Assumptions:
-Gaussian Chain
-Thermally Equilibrated
-**Small Perturbation** of Structure (so it is still Gaussian after the deformation)

Tensile Blob

For **Larger Perturbations** of Structure

-At small scales, small lever arm, structure remains Gaussian

-At large scales, large lever arm, structure becomes linear

Perturbation of Structure leads to a structural transition at a size scale ξ

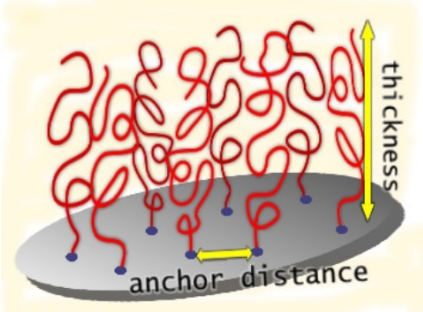

$$E = kT\frac{3R^2}{2nl_K^2} \qquad F = \frac{dE}{dR} = \frac{3kT}{nl_K^2}R$$

For weak perturbations of the chain $R \approx n^{1/2} l_K \equiv \xi_{Tensile}$

$$\xi_{Tensile} = \frac{3kT}{F}$$

Application of an external stress to the ends of a chain create a transition size where the coil goes from Gaussian to Linear called the Tensile Blob.

$$F = k_{spr} R = \frac{3kT}{R^{*2}} R$$

$$\xi_{Tensile} \sim \frac{R^{*2}}{R} = \frac{3kT}{F}$$

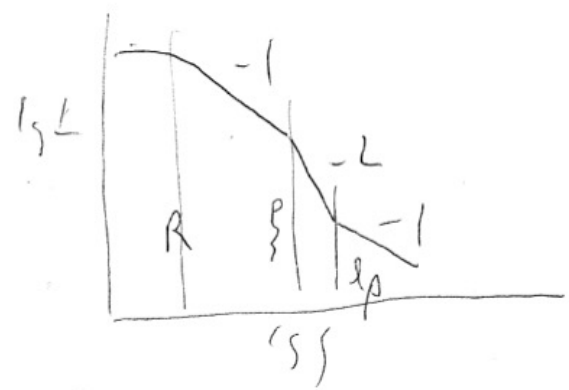

For sizes larger than the blob size the structure is linear, one conformational state so the conformational entropy is 0. For sizes smaller the blob has the minimum spring constant so the weakest link governs the mechanical properties and the chains are random below this size.

Semi-Dilute Solution Chain Statistics

In dilute solution the coil contains a concentration $c^* \sim 1/[\eta]$

$$c^* = k\, n/R^3 = k\, n^{-4/5}$$ for good solvent conditions

For semi-dilute solution the coil contains a concentration $c > c^*$

At large sizes the coil acts as if it were in a concentrated solution ($c >>> c^*$), $d_f = 2$. At small sizes the coil acts as if it were in a dilute solution, $d_f = 5/3$. There is a size scale, ξ, where this "scaling transition" occurs.

We have a primary structure of rod-like units, a secondary structure of expanded coil and a tertiary structure of Gaussian Chains.

What is the value of ξ?

ξ is related to the coil size R since it has a limiting value of R for $c < c^*$ and has a scaling relationship with the reduced concentration c/c^*

$$\xi \sim R\,(c/c^*)^P \sim n^{(3+4P)/5}$$

There are no dependencies on n above c^* so $(3+4P)/5 = 0$ and $P = -3/4$

$$\xi \sim R\,(c/c^*)^{-3/4}$$

Coil Size in terms of the concentration

$$\xi = b\left(\frac{N}{n_\xi}\right)^{3/5} \sim \left(\frac{c}{c^*}\right)^{-3/4}$$

$$n_\xi \sim \left(\frac{c}{c^*}\right)^{(3/4)(5/3)} = \left(\frac{c}{c^*}\right)^{(5/4)}$$

$$R = \xi n_\xi^{1/2} \sim \left(\frac{c}{c^*}\right)^{-3/4}\left(\frac{c}{c^*}\right)^{(5/8)} = \left(\frac{c}{c^*}\right)^{-1/8}$$

$$R = \xi\, n_\xi^{1/2} = R_{F0}\,(c/c^*)^{-3/4}\,(c/c^*)^{5/8} = R_{F0}\,(c/c^*)^{-1/8}$$

This is called the "Concentration Blob"

Three regimes of chain scaling in concentration.

In dilute solution the chain displays good solvent scaling in most cases, $d_f = 5/3$. When the concentration is increased above the overlap concentration, c*, a concentration blob, ξ_c, is introduced between R_g and l_p. For sizes larger than the blob size, screening of interactions leads to Gaussian scaling, $d_f = 2$. For sizes smaller than the screening length of blob size, the chains are not screened and good solvent scaling is observed. The blob size follows $\xi \sim R\left(\frac{c}{c^*}\right)^{-3/4}$ until a concentration where $\xi = l_p$. At that concentrations above c**, $c^{**} \sim c^*\left(\frac{R}{l_p}\right)^{4/3}$, the chain is in a concentrated condition and all interactions are screened so that the chain has a Gaussian configuration, $d_f = 2$.

Thermal Blob

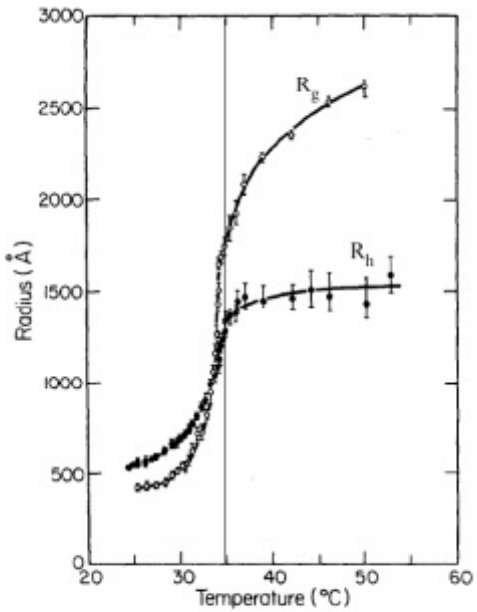

Figure 3. *Radius of gyration, R_g, and hydrodyamic radius R_h versus temperature for polystyrene in cyclohexane. Vertical line indicates the phase separation temperature. From Reference [21].*

Chain expands from the theta condition to fully expanded gradually.
At small scales it is Gaussian, at large scales expanded (opposite of concentration blob).

$$E = kT\left(\frac{3R^2}{2nl_K^2} + \frac{n^2V_c}{2R^3}\right)$$

$$E = kT\left(\frac{3R^2}{2nl_K^2} + \frac{n^2V_c(1-2\chi)}{2R^3}\right)$$

Thermal Blob

$$\Delta\varepsilon = \left(\varepsilon_{PP} + \varepsilon_{SS}\right)/2 - \varepsilon_{PS}$$

$$\chi = \frac{z\Delta\varepsilon}{kT}$$

$$V_{c,enthalpic} = V_c\left(1 - 2\chi\right)$$

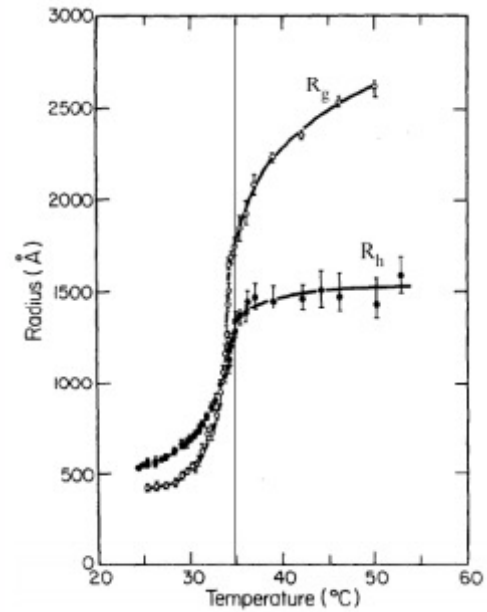

$$E = kT\left(\frac{3R^2}{2nl_K^2} + \frac{n^2V_c}{2R^3}\right)$$

$$E = kT\left(\frac{3R^2}{2nl_K^2} + \frac{n^2V_c\left(1-2\chi\right)}{2R^3}\right)$$

Thermal Blob

$$E = kT\left(\frac{3R^2}{2nl_K^2} + \frac{n^2V_c(1-2\chi)}{2R^3}\right)$$

Energy Depends on n, a chain with a mer unit of length 1 and n = 10000
could be re cast (renormalized) as a chain of unit length 100 and n = 100
The energy changes with n so depends on the definition of the base unit

Smaller chain segments have less entropy so phase separate first.
We expect the chain to become Gaussian on small scales first.
This is the opposite of the concentration blob.

Cooling an expanded coil leads to local chain structure collapsing to a Gaussian structure first.
As the temperature drops further the Gaussian blob becomes larger until the entire chain is Gaussian at the theta temperature.

Thermal Blob

$$R = N_T^{3/5}\xi_T = \left(N/n_T\right)^{3/5}\xi_T = \left(N\Big/\left(\xi_T/l\right)^2\right)^{3/5}\xi_T = N^{3/5}\xi_T^{-1/5}l^{6/5}$$

Flory-Krigbaum Theory yields: $R = V_c^{1/5}\left(1-2\chi\right)^{1/5}N^{3/5}l^{2/5}$

By equating these:

$$\xi_T = \frac{l}{\left(1-2\chi\right)}$$

Fractal Aggregates and Agglomerates

Growth of Nanoparticles

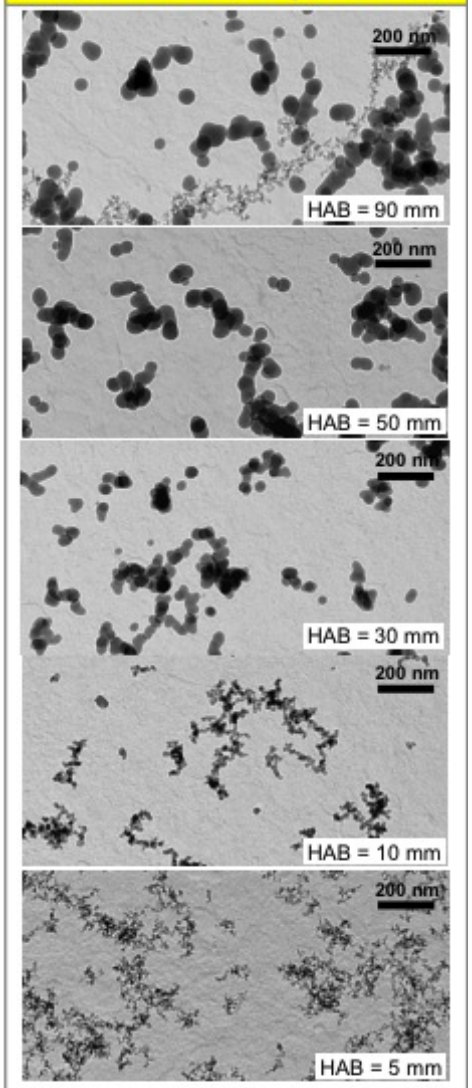

Fig. 1: Silica particles as collected by conventional thermophoretic sampling (TS) along the axis of a premixed flame of hexamethyldisiloxane and oxygen [1,2]. Using aluminum foil in-stead of TEM grids and performing multiple sampling from the same location in the flame, the Al-probe was covered with ***a silica monolayer*** *[1] (as indicated in Fig. 2).*

Spray Flame Appearance

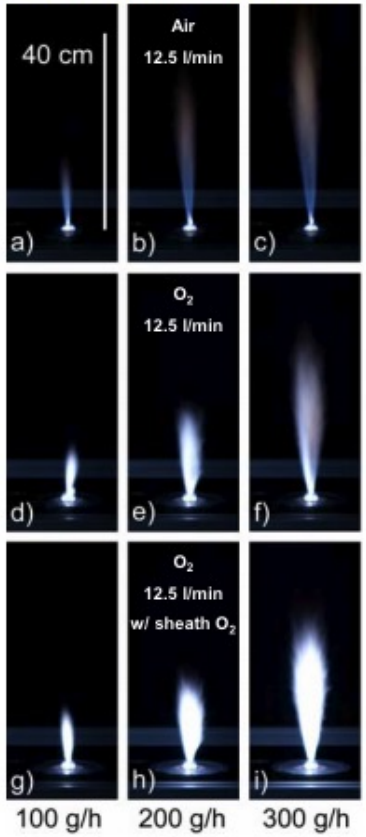

Fig. 3: Spray flames (1.26 M HMDSO in EtOH) producing 100, 200 and 300 g/h of silica using 12.5 l/min air (a-c) or O_2 as dispersion gas without (d-f) and with (g-i) additional 25 l/min of O_2 sheath flow at 1 bar pressure drop across the nozzle tip.

Powder Morphology

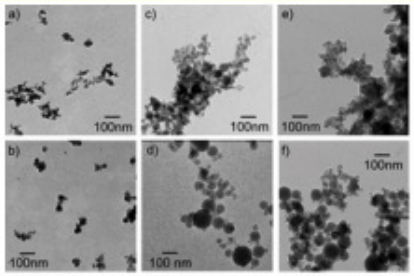

Fig. 4: Transmission electron micrographs of silica nanoparticles at production rates of 150 (top row) and 300 g/h (bottom row) using 12.5 l/min air (a,b) or O_2 as dispersion gas without (c,d) and with (e,f) additional 25 l/min of O_2 sheath flow using 1.26 M HMDSO in EtOH.

Powder Morphology

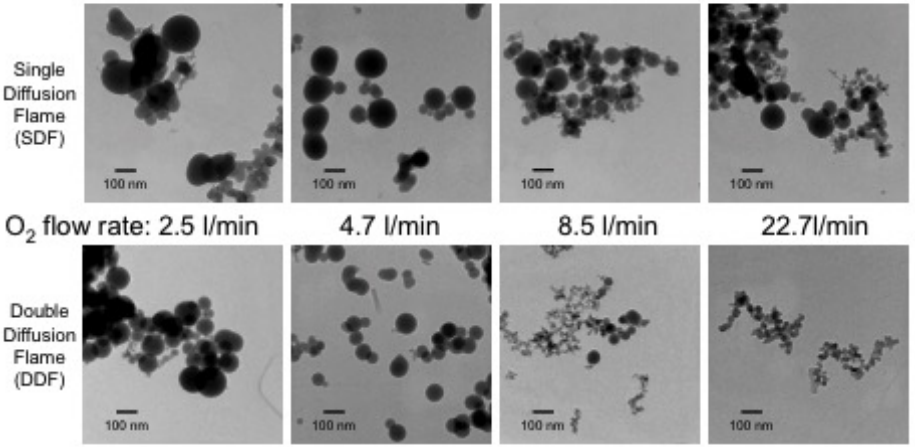

Fig. 5: Transmission Electron Micrographs (TEM) of SiO_2 synthesized in SDF and DDF at different oxygen flow rates. Particles made in flames at low oxygen flow rates stay longer at high temperatures leading to the formation of rather big spherical, non-agglomerated particles with diameters of about 100 nm. At high oxygen flow rates the particles are agglomerates of small primary particles. Particles synthesized in DDF have narrower size distributions indicated by TEM compared to those made in SDF.

Flame Structure

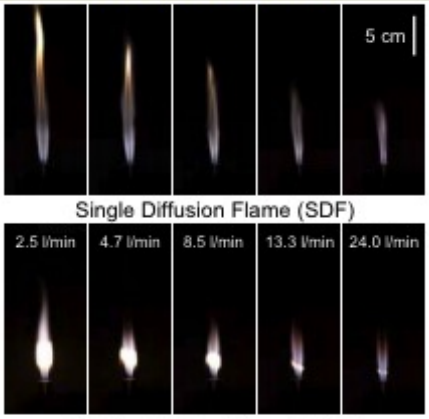

Fig. 3: Effect of oxygen flow rate on flame structure of a SDF and DDF. Increasing the oxygen flow rate decreases the flame height of the HMDSO-methane-oxygen diffusion flame as turbulence accelerates the mixing of fuel and oxidant.

Polymer Chains are Mass-Fractals

$R_{RMS} = n^{1/2}\, l$	Mass ~ Size^2
3-d object	Mass ~ Size^3
2-d object	Mass ~ Size^2
1-d object	Mass ~ Size^1
d_f-object	Mass ~ Size^{df}

This leads to odd properties:

density $$\rho = \frac{Mass}{Volume} = \frac{Mass}{Size^3} = \frac{Size^{d_f}}{Size^3} \sim Size^{d_f - 3}$$

For a 3-d object density doesn't depend on size,
For a 2-d object density drops with Size
Larger polymers are less dense

How Complex Mass Fractal Structures Can be Decomposed

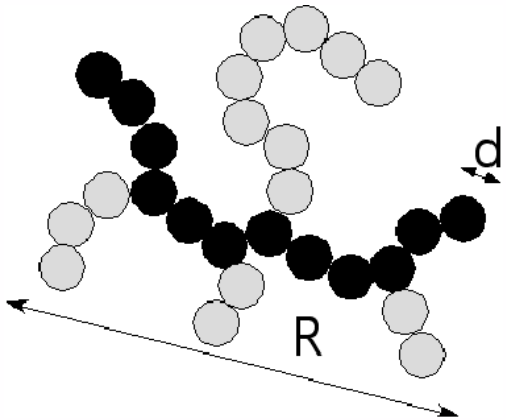

Tortuosity

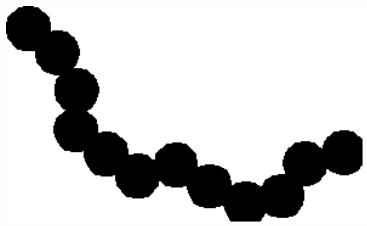

Connectivity

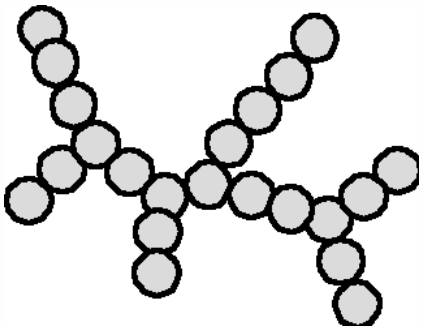

$$z \sim \left(\frac{R}{d}\right)^{d_f} \sim p^c \sim s^{d_{\min}}$$

$$p \sim \left(\frac{R}{d}\right)^{d_{\min}}$$

$$s \sim \left(\frac{R}{d}\right)^{c}$$

$$d_f = d_{\min} c$$

z	d_f	p	d_{min}	s	c	R/d
27	1.36	12	1.03	22	1.28	11.2

Disk

$$d_f = 2$$

$$d_{\min} = 1$$

$$c = 2$$

Extended β-sheet
(misfolded protein)

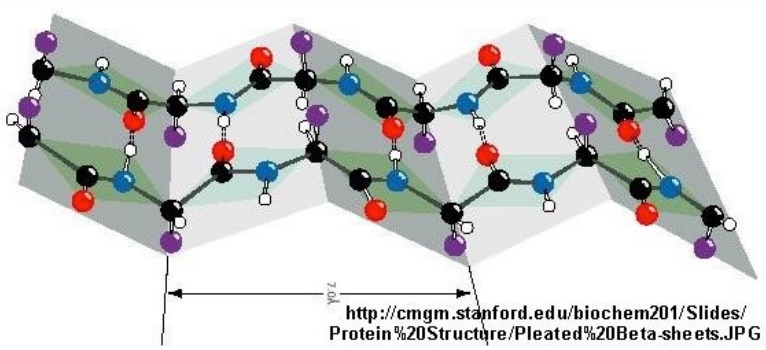

Random Coil

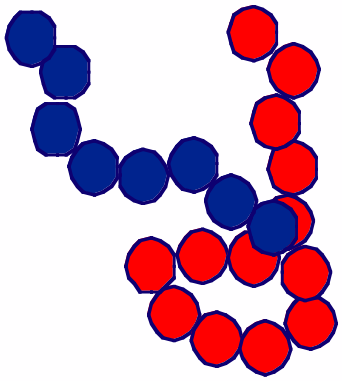

$$d_f = 2$$

$$d_{\min} = 2$$

$$c = 1$$

Unfolded Gaussian chain

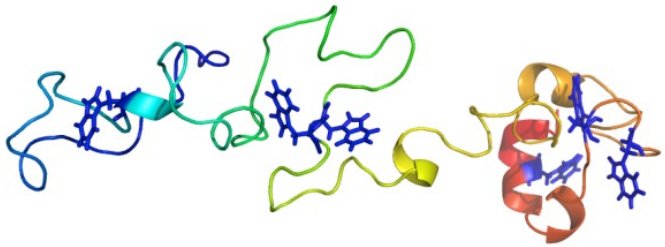

Primary Size for Fractal Aggregates

Primary Size for Fractal Aggregates

- Particle counting from TEM
- Gas adsorption V/S => d_p
- Static Scattering R_g, d_p
- Dynamic Light Scattering

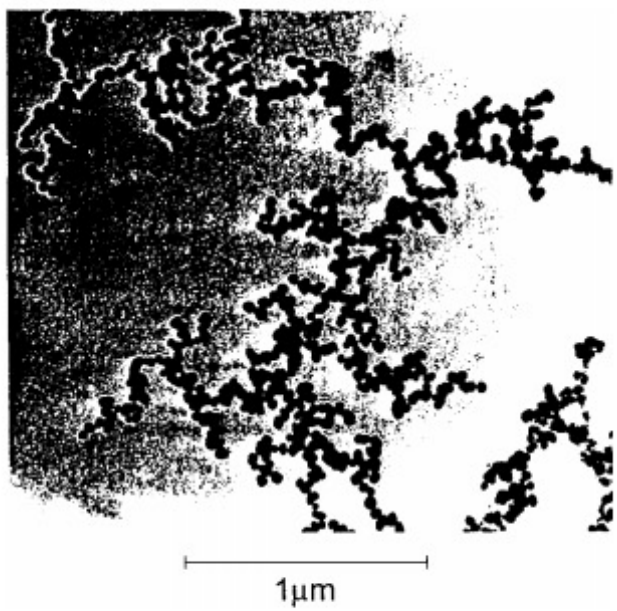

Figure 2. TEM picture of titania (TiO_2) fractal aggregates with $D \simeq 1.8$ produced by pyrolysis of Titanium Isopropoxide.

http://www.phys.ksu.edu/personal/sor/publications/2001/light.pdf

Cryo Scanning Electron Microscopy

A scanning electron micrograph of a frozen sample was taken. The sizes of the particles visible on the picture were measured individually with a ruler and used to calculate a number-mean, D(1,0), a volume-mean, D(4,3) and a number-distribution.

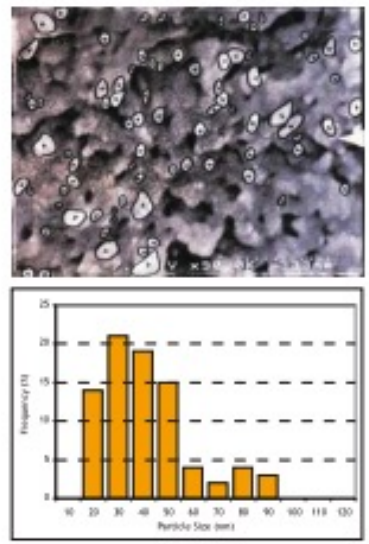

Number Mean - D(1,0) = 45.2 nm
Volume Mean - D(4,3) = 68.0 nm

Note : due to the limited number (82) of particles measured this result is only indicative.

http://www.koboproductsinc.com/Downloads/PS-Measurement-Poster-V40.pdf

Primary Size for Fractal Aggregates

- Particle counting from TEM
- Gas adsorption V/S => d_p
- Static Scattering R_g, d_p
- Dynamic Light Scattering

Dynamic Light Scattering

To evaluate repeatability and robustness, the measure was made 8 times, using 3 different dilutions. The following graph presents one of these measures, expressed as intensity-distribution, volume-distribution and number (length)-distribution.

Measure on Nicomp Model 370 - samples diluted in chloroform to 200-350 kHz.

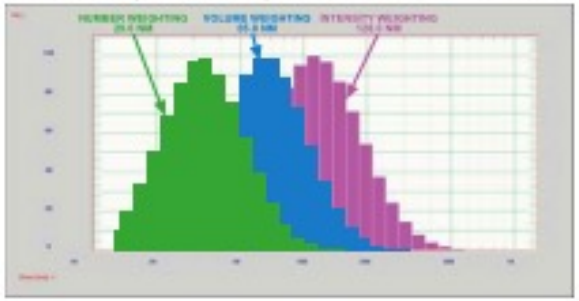

The following table shows the averaged results for the 8 measurements. Precision is calculated as the Relative Standard Deviation of the measurements.

Mean Calculation	Particle Size	Precision
Intensity Weighting	127.9 nm	2 %
Volume Weighting	71.6 nm	16 %
Number Weighting	36.2 nm	25 %

http://www.koboproductsinc.com/Downloads/PS-Measurement-Poster-V40.pdf

For static scattering p(r) is the binary spatial auto-correlation function

We can also consider correlations in time, binary temporal correlation function
$g_I(q,\tau)$

For dynamics we consider a single value of q or r and watch how the intensity changes with time
$I(q,t)$

We consider correlation between intensities separated by t
We need to subtract the constant intensity due to scattering at different size scales
and consider only the fluctuations at a given size scale, r or $2\pi/r = q$

Dynamic Light Scattering

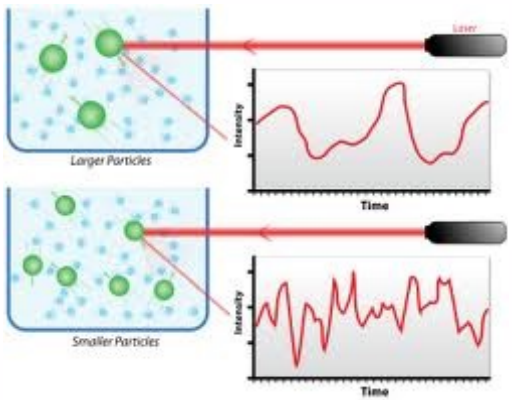

$$g^2(q;\tau) = \frac{\langle I(t)I(t+\tau)\rangle}{\langle I(t)\rangle^2}$$

$$g^2(q;\tau) = 1 + \beta\left[g^1(q;\tau)\right]^2$$

$$q = \frac{4\pi n_0}{\lambda}\sin\left(\frac{\theta}{2}\right)$$

$$g^1(q;\tau) = \exp(-\Gamma\tau)$$

$$\Gamma = q^2 D_t$$

$$D = k_B T / 6\pi\eta a$$

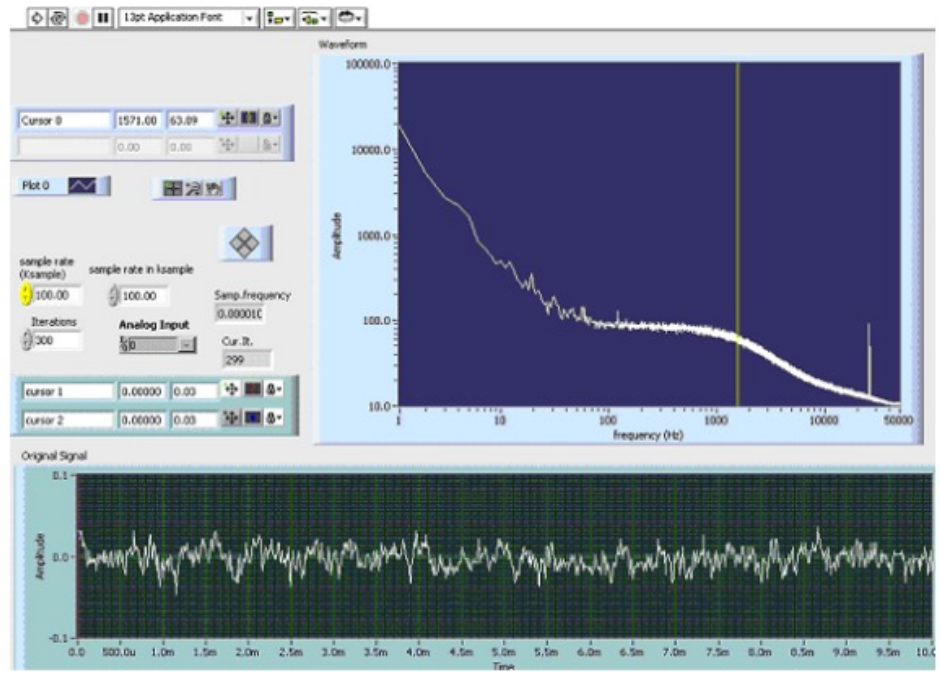

a = R_H = Hydrodynamic Radius

Dynamic Light Scattering

my DLS web page

http://www.eng.uc.edu/~gbeaucag/Classes/Physics/DLS.pdf

Wiki

http://webcache.googleusercontent.com/search?q=cache:eY3xhiX117IJ:en.wikipedia.org/wiki/Dynamic_light_scattering+&cd=1&hl=en&ct=clnk&gl=us

Wiki Einstein Stokes

http://webcache.googleusercontent.com/search?q=cache:yZDPRbqZ1BIJ:en.wikipedia.org/wiki/Einstein_relation_(kinetic_theory)+&cd=1&hl=en&ct=clnk&gl=us

Gas Adsorption

$$\theta = \frac{\text{adsorbed sites}}{\text{total sites (N)}}$$

A + S <=> AS

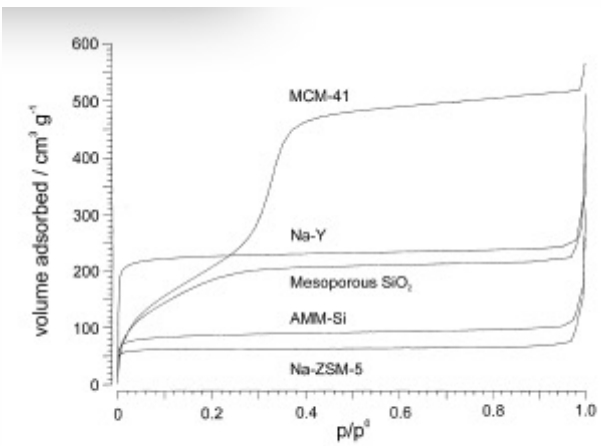

Fig. 2. Adsorption isotherms of the samples tested with Ar at 87.5 K.

Adsorption

$$\frac{d\theta}{dt} = k_a p N (1-\theta)$$

Equilibrium

=

Desorption

$$\frac{d\theta}{dt} = k_d N \theta$$

$$\theta = \frac{Kp}{1+Kp}$$

$$K = k_a / k_d$$

$$\frac{\partial \ln K}{\partial T} = \frac{\Delta H_{abs}}{RT^2}$$

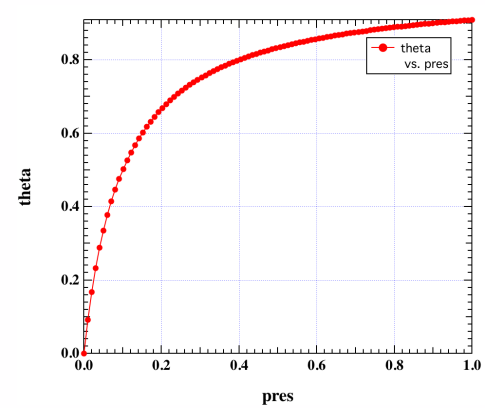

http://www.chem.ufl.edu/~itl/4411L_f00/ads/ads_I.html

Gas Adsorption

Multilayer adsorption

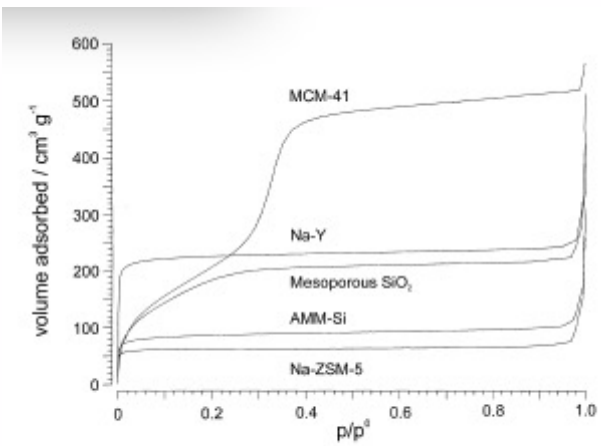

Fig. 2. Adsorption isotherms of the samples tested with Ar at 87.5 K.

BET Isotherm

Various Values of c

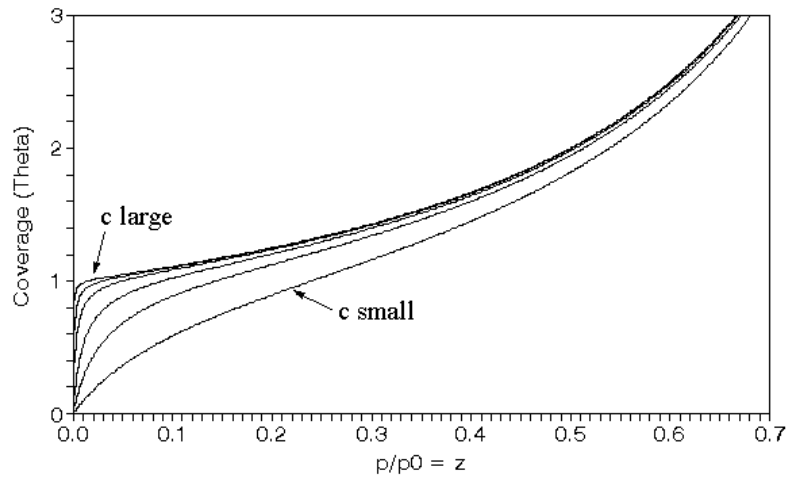

$$\frac{n}{n_{mono}} = \frac{cz}{(1-z)\,[1 - z(1-c)]} = (\theta)$$

$$c \approx \frac{e^{-\Delta H_{ads}/RT}}{e^{\Delta H_{vap}/RT}}$$

http://www.chem.ufl.edu/~itl/4411L_f00/ads/ads_I.html

S. Storck et al. / Applied Catalysis A: General 174 (1998) 137–146

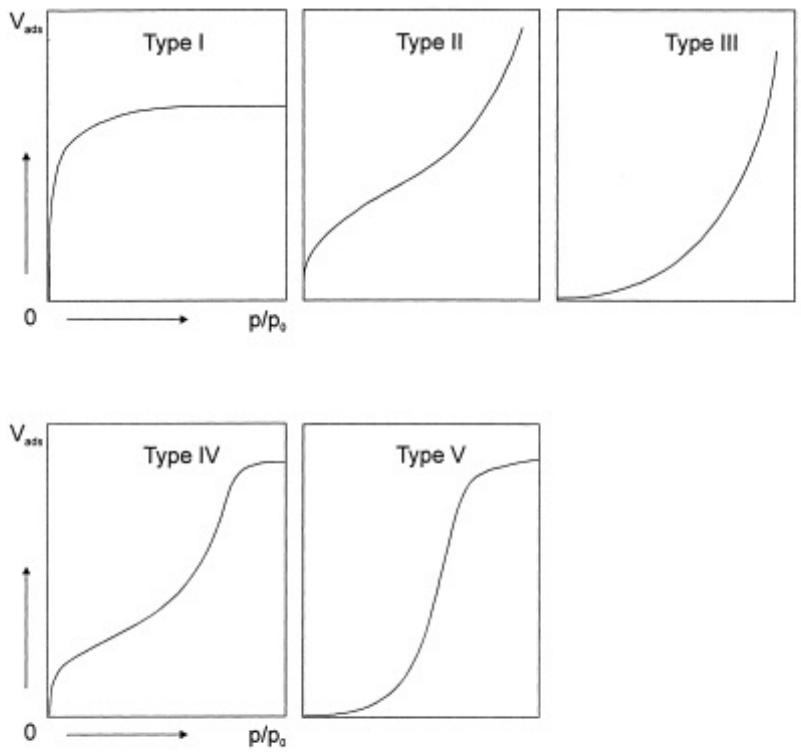

Fig. 1. Adsorption isotherm types defined by Brunauer [6].

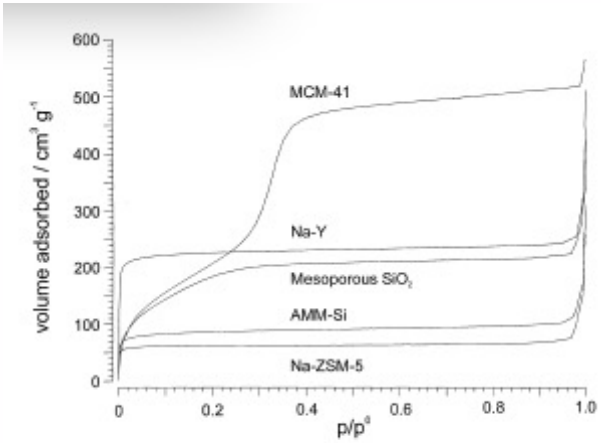

Fig. 2. Adsorption isotherms of the samples tested with Ar at 87.5 K.

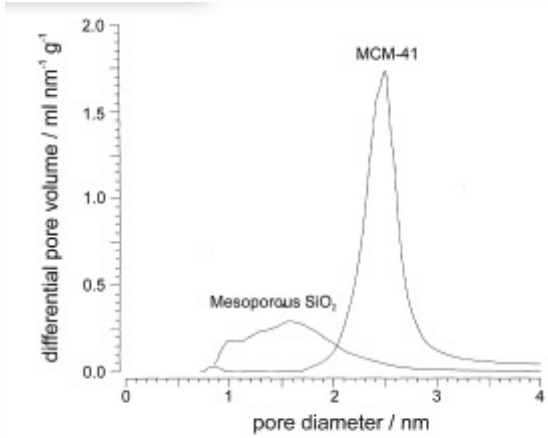

Fig. 3. Pore-size distribution according to the BJH method.

http://www.eng.uc.edu/~gbeaucag/Classes/Nanopowders/GasAdsorptionReviews/ReviewofGasAdsorptionGOodOne.pdf

From gas adsorption obtain surface area by number of gas atoms times an area for the adsorbed gas atoms in a monolayer

Have a volume from the mass and density.

So you have S/V or V/S

Assume sphere $S = 4\pi R^2$, $V = 4/3\ \pi R^3$

So $d_p = 6V/S$

Sauter Mean Diameter $d_p = \langle R^3 \rangle / \langle R^2 \rangle$

Log-Normal Distribution

$$f(R) = \frac{1}{R\sigma(2\pi)^{1/2}} \exp\left\{ -\frac{[\log(R/m)]^2}{2\sigma^2} \right\},$$

$$\langle R^r \rangle = m^r \exp\left(r^2\sigma^2/2\right) = \exp\left(r\mu + r^2\sigma^2/2\right)$$

$$\langle R \rangle = m \exp\left(\sigma^2/2\right)$$

Mean

$$\sigma_g = \exp(\sigma) \qquad x_g = \exp(m)$$

Geometric standard deviation and geometric mean (median)

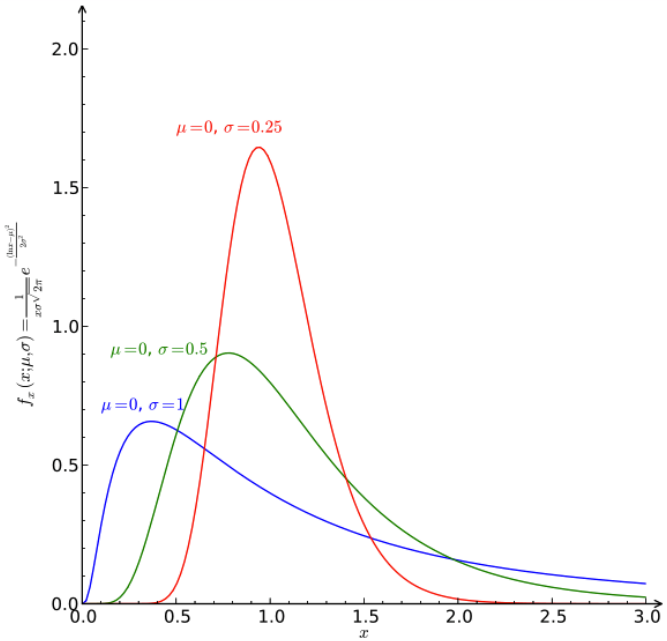

Gaussian is centered at the Mean and is symmetric. For values that are positive (size) we need an asymmetric distribution function that has only values for greater than 1. In random processes we have a minimum size with high probability and diminishing probability for larger values.

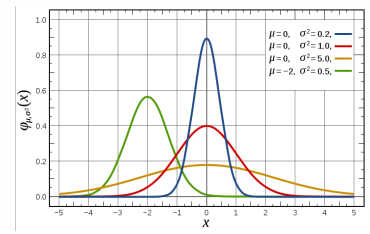

http://www.eng.uc.edu/~gbeaucag/PDFPapers/ks5024%20Japplcryst%20Beaucage%20PSD.pdf

http://en.wikipedia.org/wiki/Log-normal_distribution

Log-Normal Distribution

$$f(R) = \frac{1}{R\sigma(2\pi)^{1/2}} \exp\left\{-\frac{[\log(R/m)]^2}{2\sigma^2}\right\},$$

$$\langle R^r \rangle = m^r \exp\left(r^2\sigma^2/2\right) = \exp\left(r\mu + r^2\sigma^2/2\right)$$

$$\langle R \rangle = m \exp\left(\sigma^2/2\right)$$

Mean

$$\sigma_g = \exp(\sigma) \quad x_g = \exp(m)$$

Geometric standard deviation and geometric mean (median)

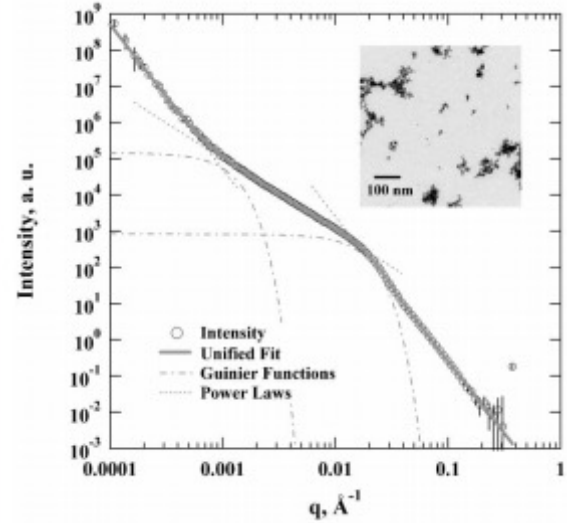

Static Scattering Determination of Log Normal Parameters

$$\ln \sigma_g = \sigma = \left\{\frac{\ln\left[B(R_g^2)^2/(1.62G)\right]}{12}\right\}^{1/2} = \left(\frac{\ln \mathrm{PDI}}{12}\right)^{1/2} \quad (17)$$

and

$$m = \left\{5R_g^2/[3\exp(14\sigma^2)]\right\}^{1/2}, \quad (18)$$

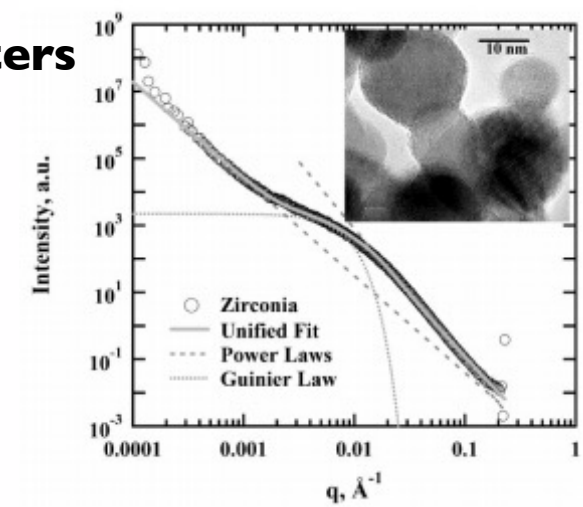

http://www.eng.uc.edu/~gbeaucag/PDFPapers/ks5024%20Japplcryst%20Beaucage%20PSD.pdf

Primary Size for Fractal Aggregates

- Particle counting from TEM
- Gas adsorption V/S => d_p
- Static Scattering R_g, d_p
- Dynamic Light Scattering

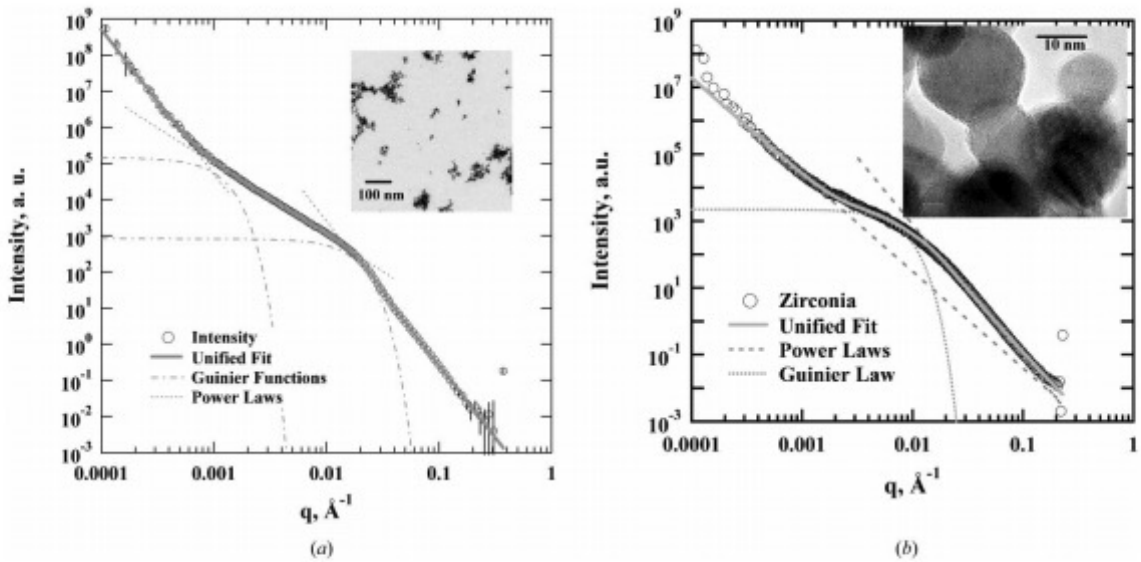

Figure 2
USAXS data from aggregated nanoparticles (circles) showing unified fits (bold grey lines), primary particle Guinier and Porod functions at high q, the intermediate mass fractal scaling regime and the aggregate Guinier regime (dashed lines). (*a*) Fumed titania sample with multi-grain particles and low-q excess scattering due to soft agglomerates. d_{VIS} = 16.7 nm (corrected to 18.0 nm), PDI = 3.01 (σ_g = 1.35), R_g = 11.2 nm, d_f = 1.99, $z_{2:1}$ = 175, z_{R_g} = 226, R_{gz} = 171 nm. From gas adsorption, d_p = 16.2 nm. (*b*) Fumed zirconia sample (Mueller *et al.*, 2004) with single-grain particles, as shown in the inset. The primary particles for this sample have high polydispersity leading to the observed hump near the primary particle scattering regime. d_{VIS} = 20.3 nm, PDI = 10.8 (σ_g = 1.56), R_g = 26.5 nm, d_f = 2.90. From gas adsorption, d_p = 19.7 nm.

http://www.eng.uc.edu/~gbeaucag/PDFPapers/ks5024%20Japplcryst%20Beaucage%20PSD.pdf

Primary Size for Fractal Aggregates

- **Particle counting from TEM**
- **Gas adsorption V/S => d_p**
- **Static Scattering R_g, d_p**

Smaller Size = Higher S/V

(Closed Pores or similar issues)

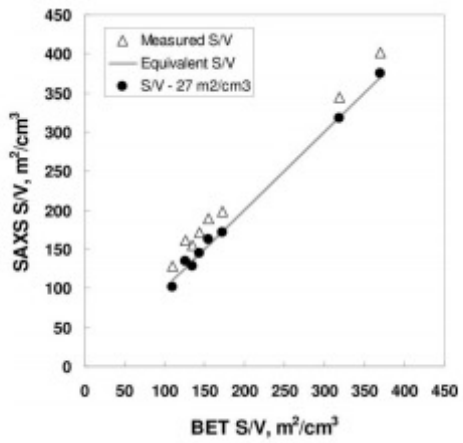

(a)

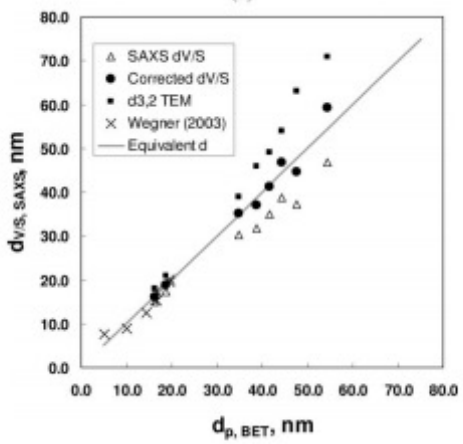

(b)

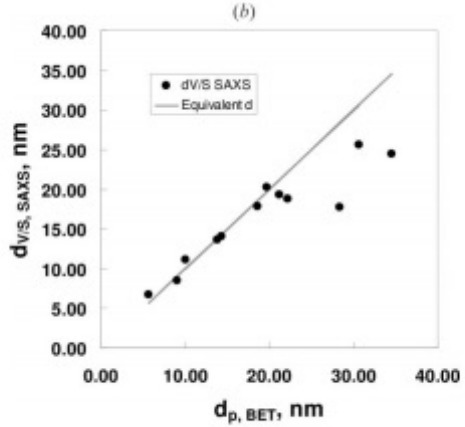

(c)

Figure 3
(*a*) *S/V* from SAXS for titania particles produced by vapor-phase pyrolysis of titania tetraisopropoxide by Kammler *et al.* (2002, 2003). The SAXS *S/V* can be made to agree with the BET value by subtraction of 27 $m^2\ cm^{-3}$. (*b*) $d_{V/S}$ from USAXS [and corrected from (*a*)] *versus* d_p from BET analysis of gas adsorption data for a series of titania samples produced by Kammler (triangles and filled circles), and samples made in a quenched-spray flame from Wegner & Pratsinis (2003) (crosses, single-grain particles). The calculated $d_{3,2}$ from TEM micrographs for the Kammler samples is also shown (filled squares). (*c*) $d_{V/S}$ from USAXS *versus* d_p from BET for fumed zirconia samples of Mueller *et al.* (2004).

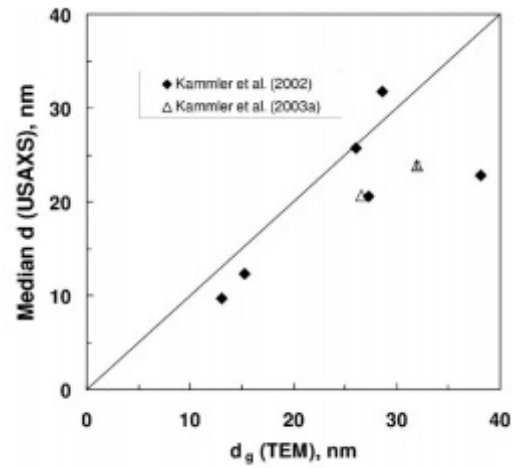

(a)

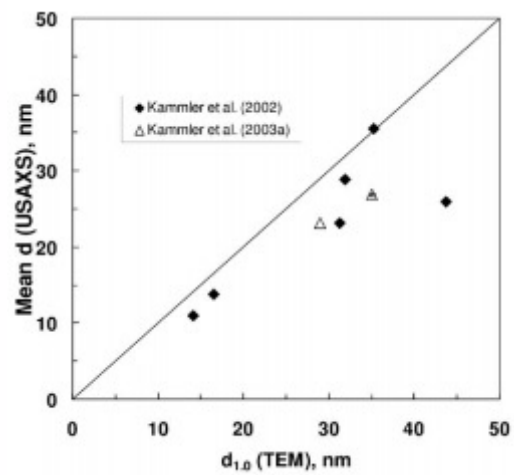

(b)

http://www.eng.uc.edu/~gbeaucag/PDFPapers/ks5024%20Japplcryst%20Beaucage%20PSD.pdf

(a) (b)

Figure 4
(*a*) Comparison of the median particle size from exp *m*, with *m* defined by equation (18), and the median particle size calculated from an analysis of TEM data on TiO_2. (*b*) Mean particle size, ⟨*R*⟩ from USAXS, equation (2) with *r* = 1, and from TEM (Kammler *et al.*, 2003) for the same samples as Figs. 3(*a*) and 3(*b*).

Fractal Aggregates and Agglomerates

Primary Size for Fractal Aggregates

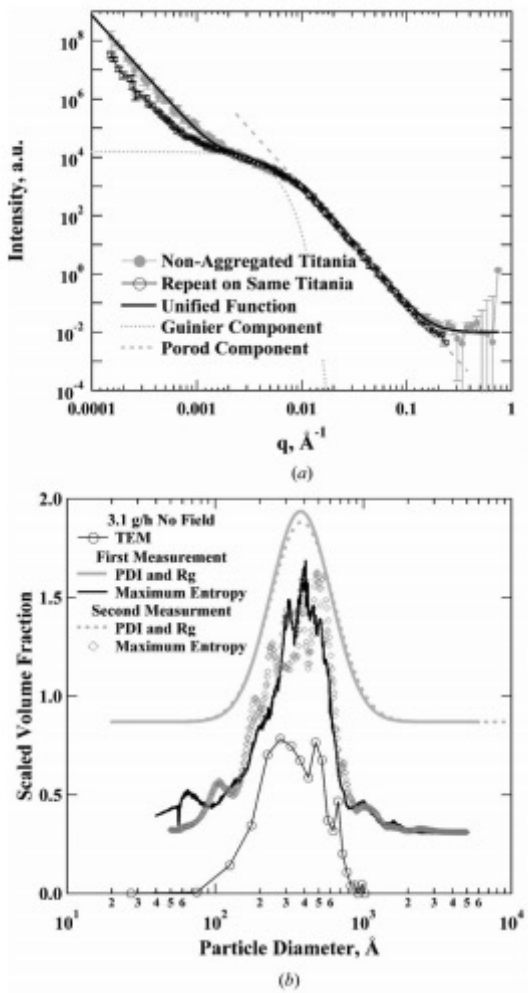

Figure 5
3.1 g h^{-1} titania. (*a*) Repeat USAXS runs on a non-aggregated titania powder (Fig. 1). (*b*) Particle size distributions from TEM (circles; Kammler *et al.*, 2003), equations (1), (2), (17) and (18) using PDI and R_g, and using the maximum-entropy program of Jemian (Jemian *et al.*, 1991). Distribution curves are shifted vertically for clarity. $d_{V/S}$ = 34.9 nm, PDI = 14.4 (σ_g = 1.60), R_g = 44.2 nm.

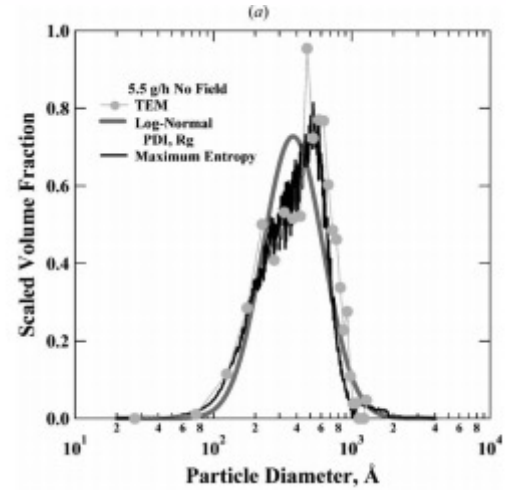

Fractal Aggregate Primary Particles

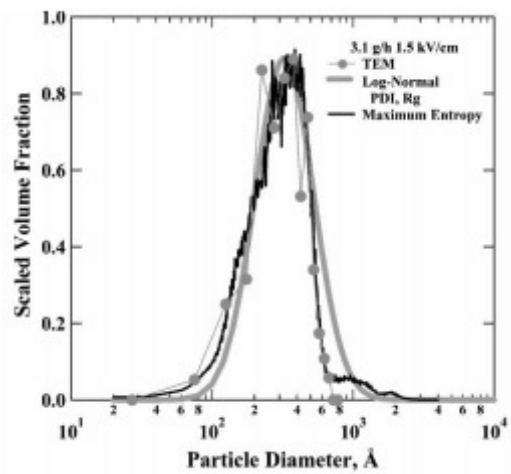

http://www.eng.uc.edu/~gbeaucag/PDFPapers/ks5024%20Japplcryst%20Beaucage%20PSD.pdf

Fractal Aggregates and Agglomerates
Aggregate growth
Some Issues to Consider for Aggregation/Agglomeration

Path of Approach, Diffusive or Ballistic (Persistence of velocity for particles)
Concentration of Monomers
persistence length of velocity compared to mean separation distance
Branching and structural complexity

What happens when monomers or clusters get to a growth site:
Diffusion Limited Aggregation
Reaction Limited Aggregation

Chain Growth (Monomer-Cluster), Step Growth (Monomer-Monomer to Cluster-Cluster)
or a Combination of Both (mass versus time plots)

Cluster-Cluster Aggregation
Monomer-Cluster Aggregation
Monomer-Monomer Aggregation

DLCA Diffusion Limited Cluster-Cluster Aggregation
RLCA Reaction Limited Cluster Aggregation

Post Growth: Internal Rearrangement/Sintering/Coalescence/Ostwald Ripening
http://www.eng.uc.edu/~gbeaucag/Classes/Nanopowders/AggregateGrowth.pdf

Fractal Aggregates and Agglomerates

Aggregate growth

Consider what might effect the dimension of a growing aggregate.

Transport Diffusion/Ballistic
Growth Early/Late (0-d point => Linear 1-d => Convoluted 2-d => Branched 2+d)
Speed of Transport Cluster, Monomer
Shielding of Interior
Rearrangement
Sintering
Primary Particle Shape

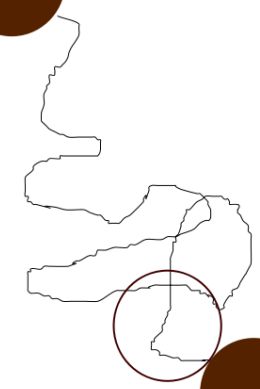

DLA df = 2.5 Monomer-Cluster (Meakin 1980 Low Concentration)
DLCA df = 1.8 (Higher Concentration Meakin 1985)

Ballistic Monomer-Cluster (low concentration) df = 3
Ballistic Cluster-Cluster (high concentration) df = 1.95

Fractal Aggregates and Agglomerates

Aggregate growth

Colloids with Strongly attractive forces

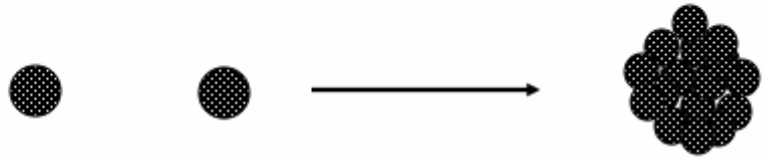

NEAR EQUILIBRIUM: Ostwald Ripening

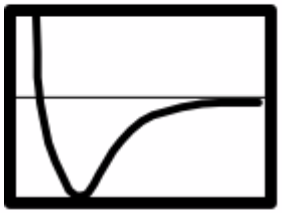

Kinetic Growth: DIFFUSION LIMITED

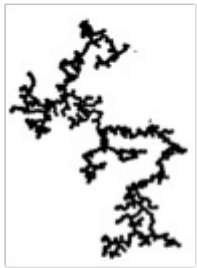

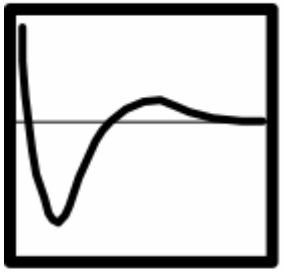

Kinetic Growth: CHEMICALLY LIMITED

Reaction Limited,
Short persistence of velocity

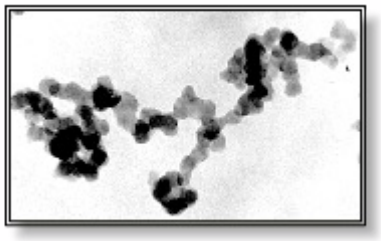

Precipitated Silica

From DW Schaefer Class Notes

Fractal Aggregates and Agglomerates

Aggregate growth

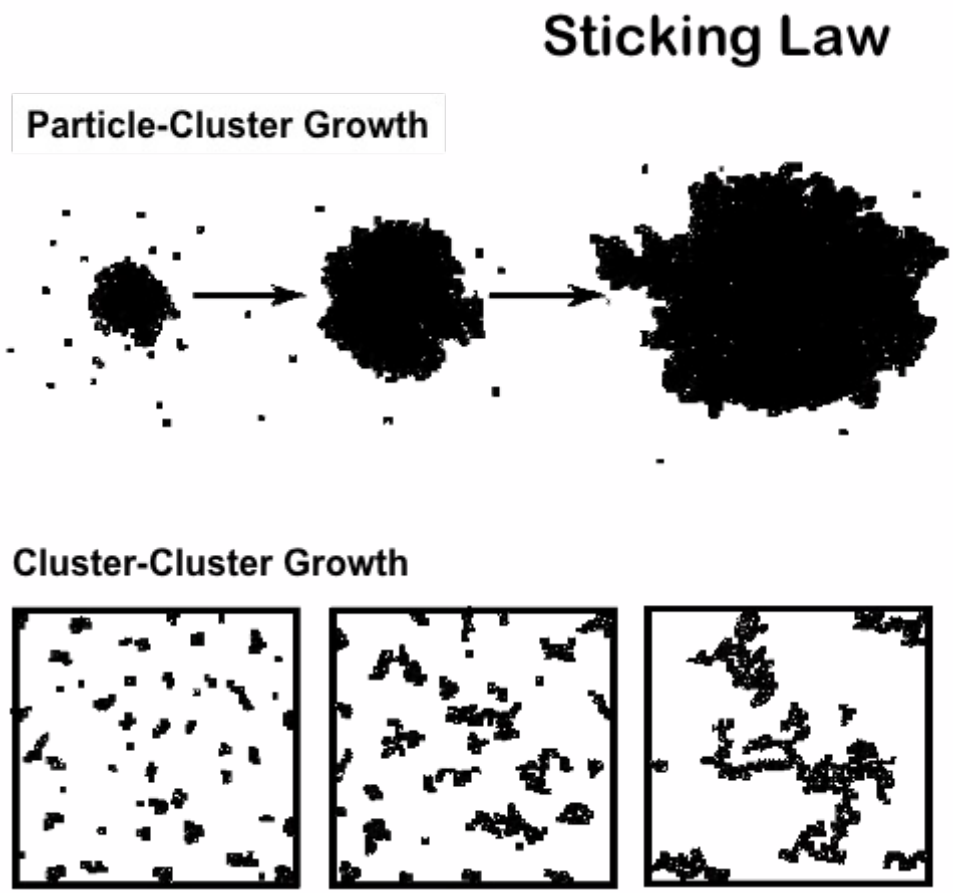

From DW Schaefer Class Notes

Fractal Aggregates and Agglomerates

Aggregate growth

Transport

Diffusion-Limited

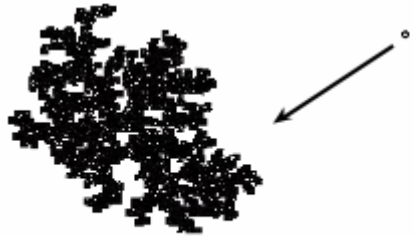

Ballistic

Reaction-Limited
(Independent of transport)

From DW Schaefer Class Notes

Fractal Aggregates and Agglomerates

Aggregate growth

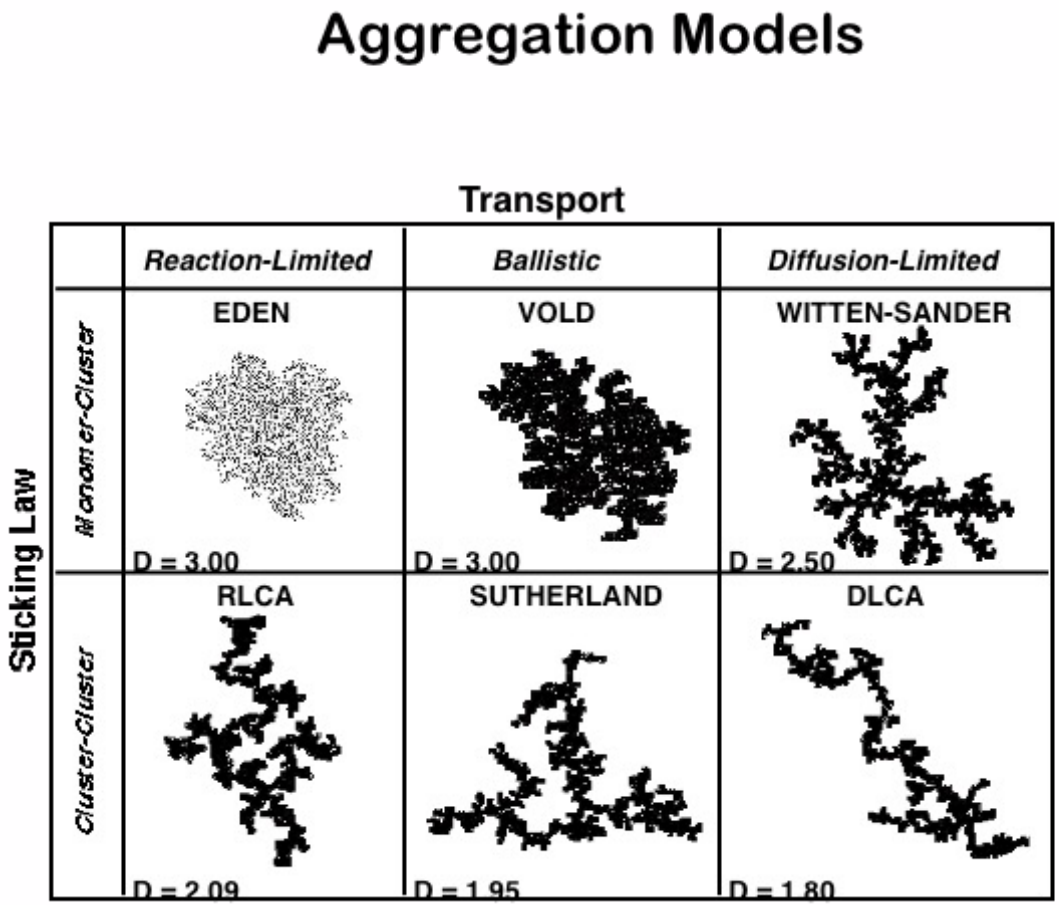

Eden Model particles are added at random with equal probability to any unoccupied site adjacent to one or more occupied sites (Surface Fractals are Produced)

Vold-Sutherland Model particles with random **linear** trajectories are added to a growing cluster of particles at the position where they first contact the cluster

Witten-Sander Model particles with random **Brownian** trajectories are added to a growing cluster of particles at the position where they first contact the cluster

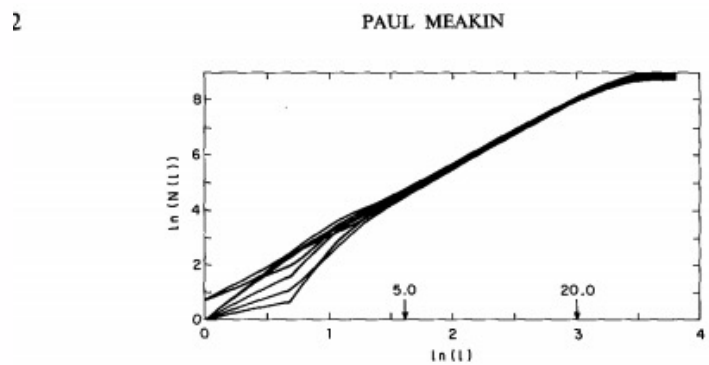

FIG. 8. Dependence of ln ($N(l)$) on ln (l) for eight clusters grown using the WS model of diffusion-limited cluster formation on a three-dimensional cubic lattice.

In RLCA a "sticking probability is introduced in the random growth process of clusters. This increases the dimension.

Sutherland Model pairs of particles are assembled into randomly oriented dimers. Dimers are coupled at random to construct tetramers, then octoamers etc. This is a step-growth process except that all reactions occur synchronously (monodisperse system).

In DLCA the "sticking probability is 1. Clusters follow random walk.

http://www.eng.uc.edu/~gbeaucag/Classes/MorphologyofComplexMaterials/MeakinVoldSunderlandEdenWittenSanders.pdf

From DW Schaefer Class Notes

Fractal Aggregates and Agglomerates

Aggregate growth

Analysis of Fractals

$$\mathrm{Log}(N) = D\,\mathrm{Log}(R)$$

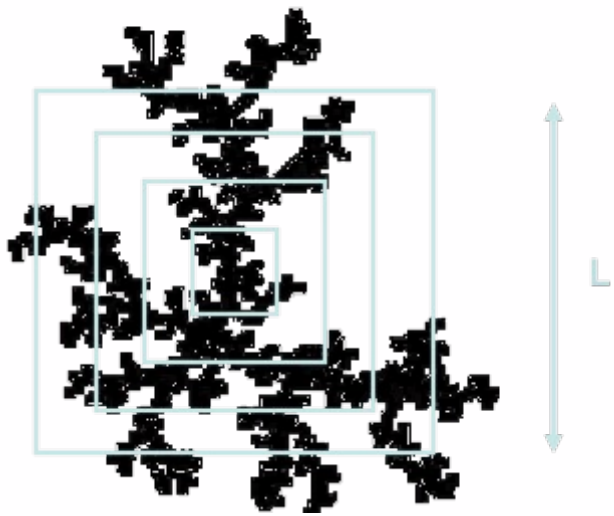

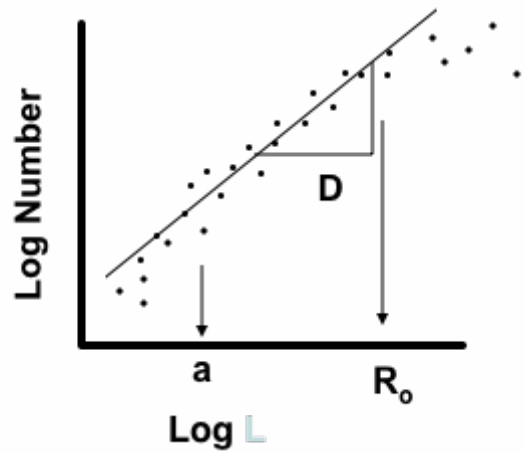

From DW Schaefer Class Notes

Fractal Aggregates and Agglomerates

Aggregate growth

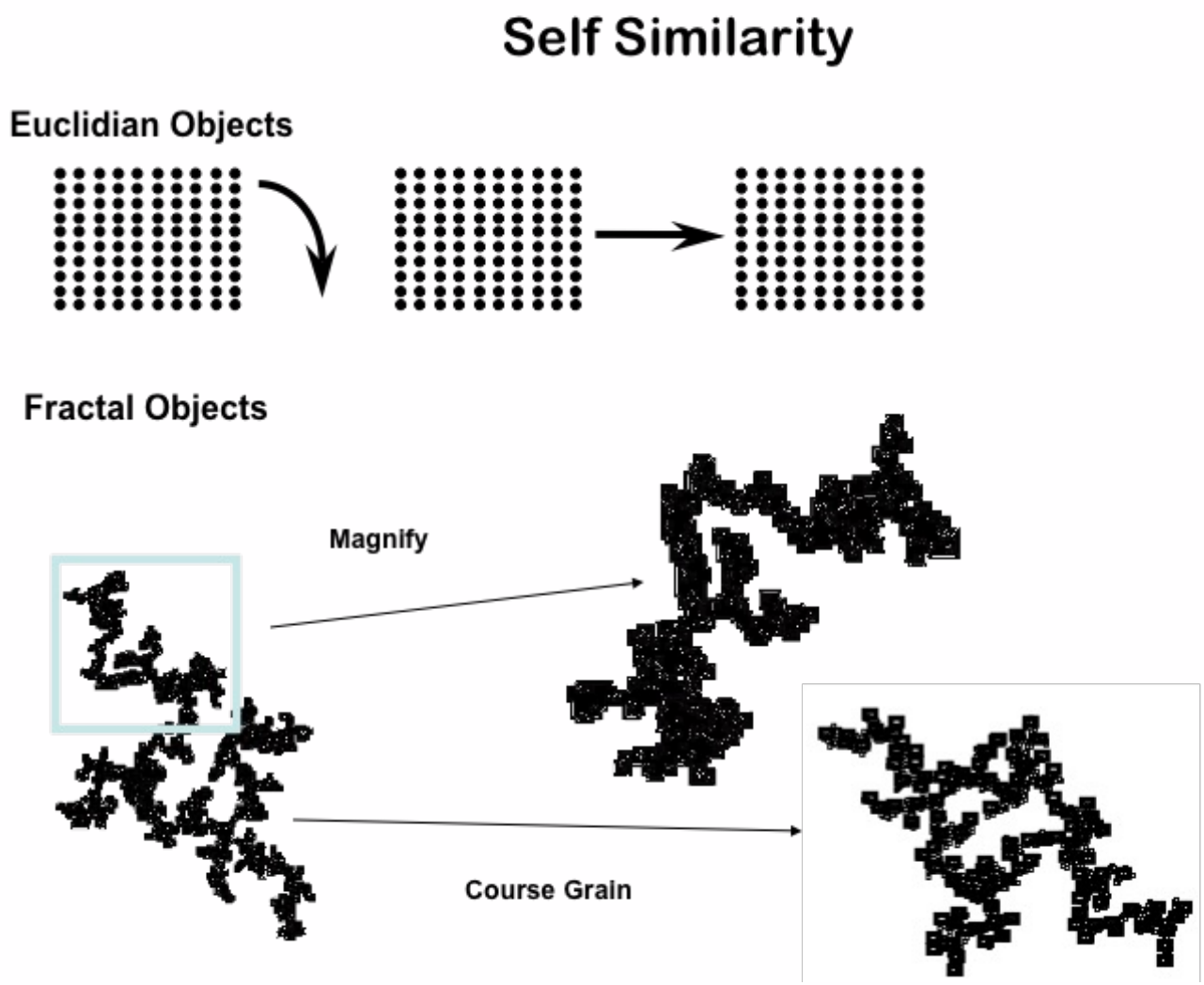

From DW Schaefer Class Notes

Fractal Aggregates and Agglomerates

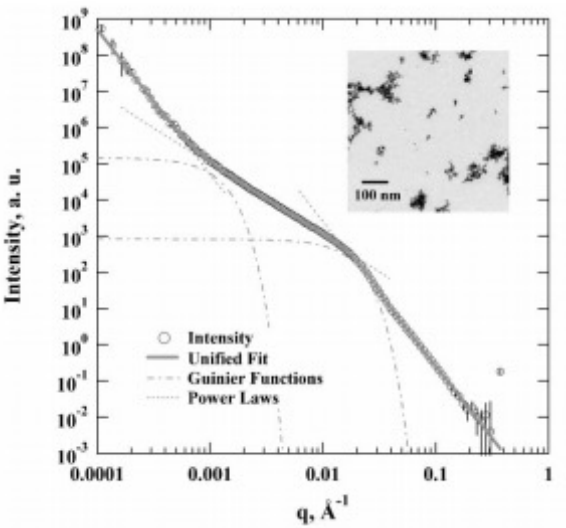

Primary: Primary Particles
Secondary: Aggregates
Tertiary: Agglomerates

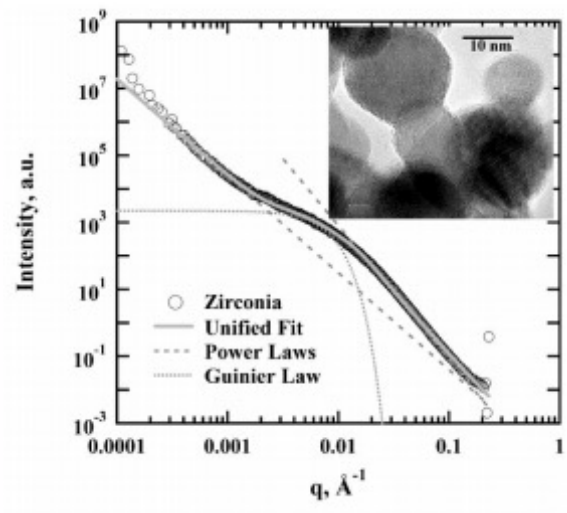

Primary: Primary Particles

Tertiary: Agglomerates

From DW Schaefer Class Notes

http://www.eng.uc.edu/~gbeaucag/PDFPapers/ks5024%20Japplcryst%20Beaucage%20PSD.pdf

Hierarchy of Polymer Chain Dynamics

Dilute Solution Chain

Dynamics of the chain

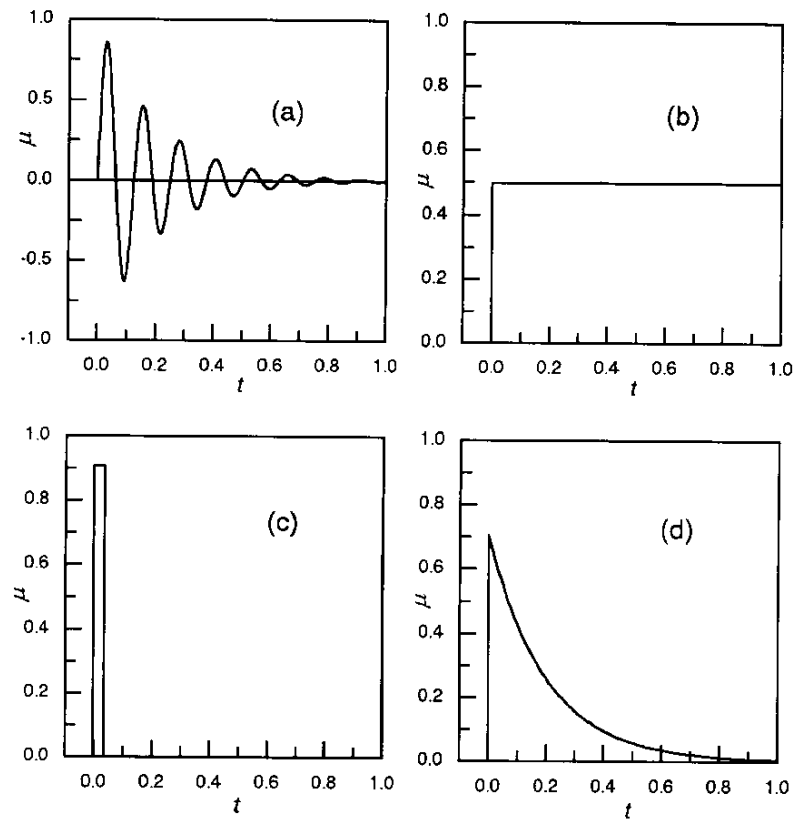

Fig. 5.4. Primary response function of a damped harmonic oscillator (a), a perfectly viscous body (b), a Hookean solid (c), a simple relaxatory system (d)

$$x(t) = \int_{-\infty}^{t} dt' \exp\left(-k_{spr}\left(t-t'\right)/\xi\right) g\left(t'\right)$$

The exponential term is the "response function"
response to a pulse perturbation

Dilute Solution Chain

Dynamics of the chain

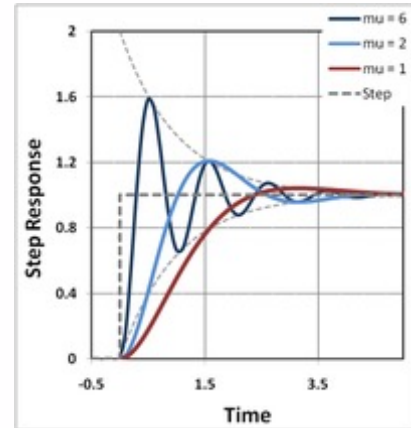

Damped Harmonic Oscillator

$$x(t) = \int_{-\infty}^{t} dt' \exp\left(-k_{spr}(t-t')/\xi\right) g(t')$$

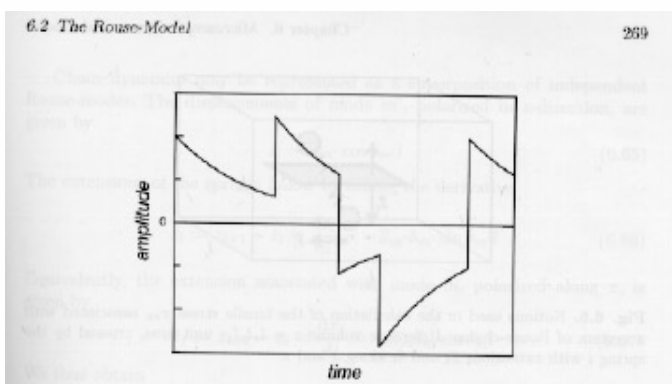

Fig. 6.4. Time dependence of the amplitude $Z_{\nu n}$ of a Rouse mode (schematic)

For Brownian motion
of a harmonic bead in a solvent
this response function can be used to calculate the
time correlation function <x(t)x(0)>
for DLS for instance

$$\langle x(t)x(0)\rangle = \int_{-\infty}^{t} dt_1 \int_{-\infty}^{0} dt_2 \exp\left[-k_{spr}(t-t_1-t_2)/\xi\right]\langle g(t_1)g(t_2)\rangle$$

$$\langle g(t_1)g(t_2)\rangle = \frac{2kT}{\xi}\partial(t_1-t_2)$$

$$\langle x(t)x(0)\rangle = \frac{kT}{k_{spr}}\exp(-t/\tau)$$

τ is a relaxation time.

$$\tau = \frac{\xi}{k_{spr}}$$

Dilute Solution Chain

Dynamics of the chain

Rouse Motion

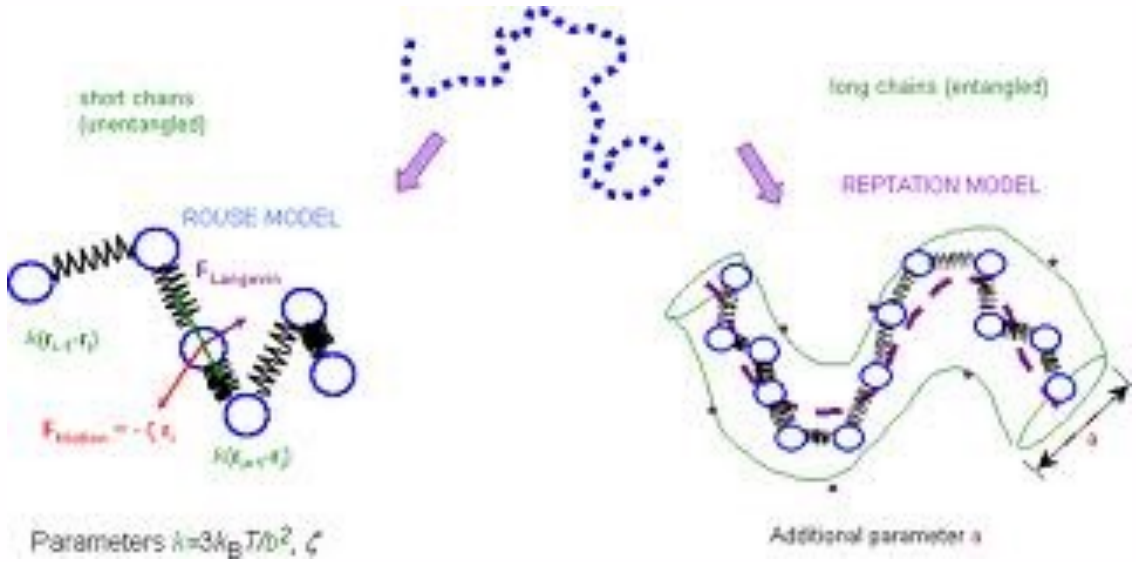

$$E = \frac{k_{spr}}{2}\sum_{i=1}^{N}\left(R_i - R_{i-1}\right)^2$$

$$\frac{dR_i}{dt} = \frac{-\left(dE/dR_i\right)}{\xi} + g_i(t)$$

$$\xi = 6\pi\eta_{solvent}a$$

Beads 0 and N are special

For Beads 1 to N-1

$$\frac{dR_i}{dt} = \frac{-k_{spr}}{\xi}\left(R_{i+1} + R_{i-1} - 2R_i\right) + g_i(t)$$

For Bead 0 use $R_{-1} = R_0$ and for bead N $R_{N+1} = R_N$

This is called a closure relationship

Dilute Solution Chain

Dynamics of the chain

Rouse Motion

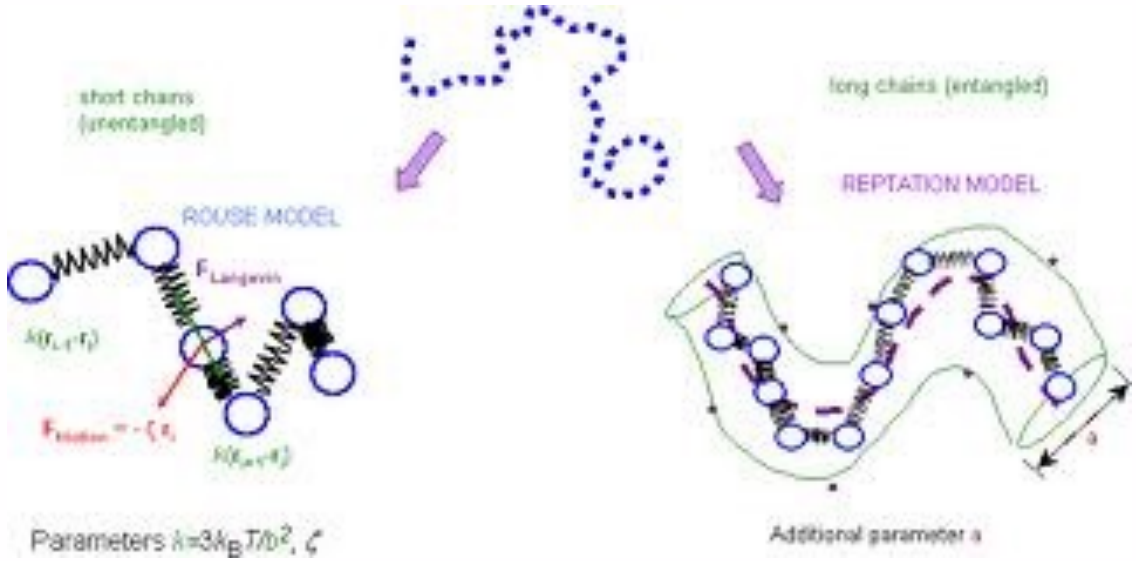

$$\frac{dR_i}{dt} = \frac{-k_{spr}}{\xi}\left(R_{i+1} + R_{i-1} - 2R_i\right) + g_i(t)$$

The Rouse unit size is arbitrary so we can make it very small and:

$$\frac{dR}{dt} = \frac{-k_{spr}}{\xi}\frac{d^2R}{di^2} + g_i(t)$$

With dR/dt = 0 at i = 0 and N

$$\frac{d^2R}{di^2}$$

Reflects the curvature of R in i,
it describes modes of vibration like on a guitar string

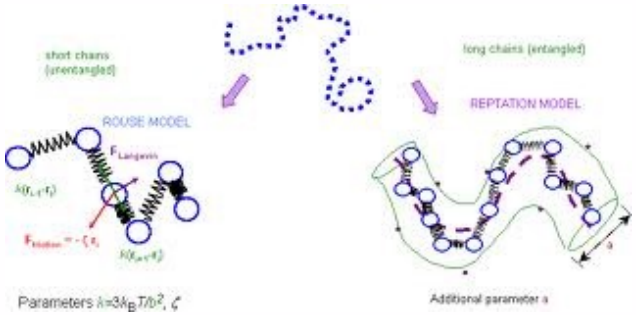

Dilute Solution Chain

Dynamics of the chain

Rouse Motion

$$\frac{d^2R}{di^2}$$ Describes modes of vibration like on a guitar string

For the "p' th" mode (0' th mode is the whole chain (string))

$$k_{spr,p} = \frac{2p^2\pi^2 k_{spr}}{N} = \frac{6\pi^2 kT}{Nb^2}p^2 \qquad \xi_p = 2N\xi \qquad \xi_0 = N\xi$$

$$\tau_p = \frac{\xi_p}{k_{spr,p}} = \frac{2N^2b^2\xi}{3\pi^2p^2kT}$$

Dilute Solution Chain

Dynamics of the chain

Rouse Motion

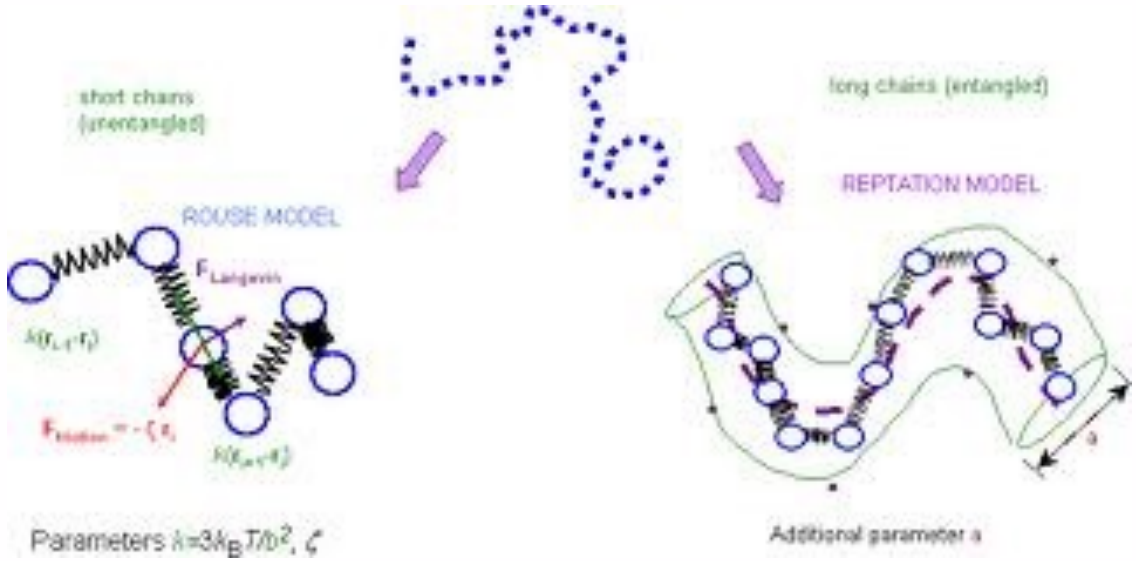

Predicts that the viscosity will follow N which is true for low molecular weights in the melt and for fully draining polymers in solution

Rouse model predicts
Relaxation time follows N^2 (actually follows N^3/df)
Diffusion constant follows 1/N (zeroth order mode is translation of the molecule) (actually follows $N^{-1/df}$)
Both failings are due to hydrodynamic interactions (incomplete draining of coil)

Dilute Solution Chain

Dynamics of the chain

Rouse Motion

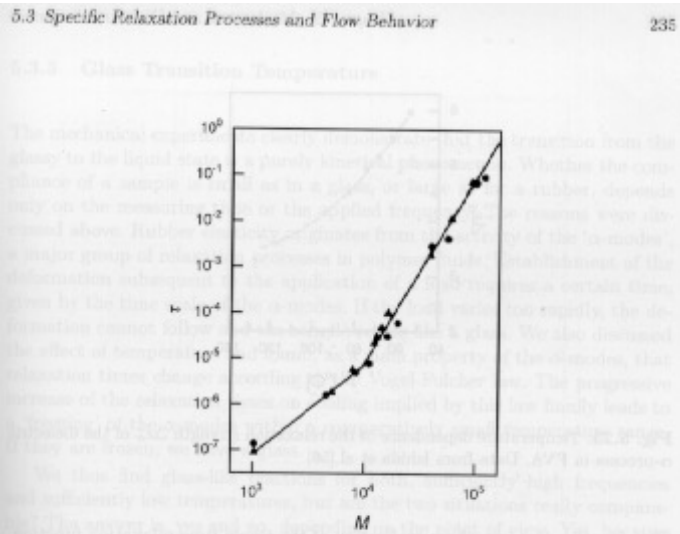

Fig. 5.21. Molecular weight dependence of the relaxation time of the dielectric normal mode in *cis*-PIP. Data from Boese and Kremer [58]

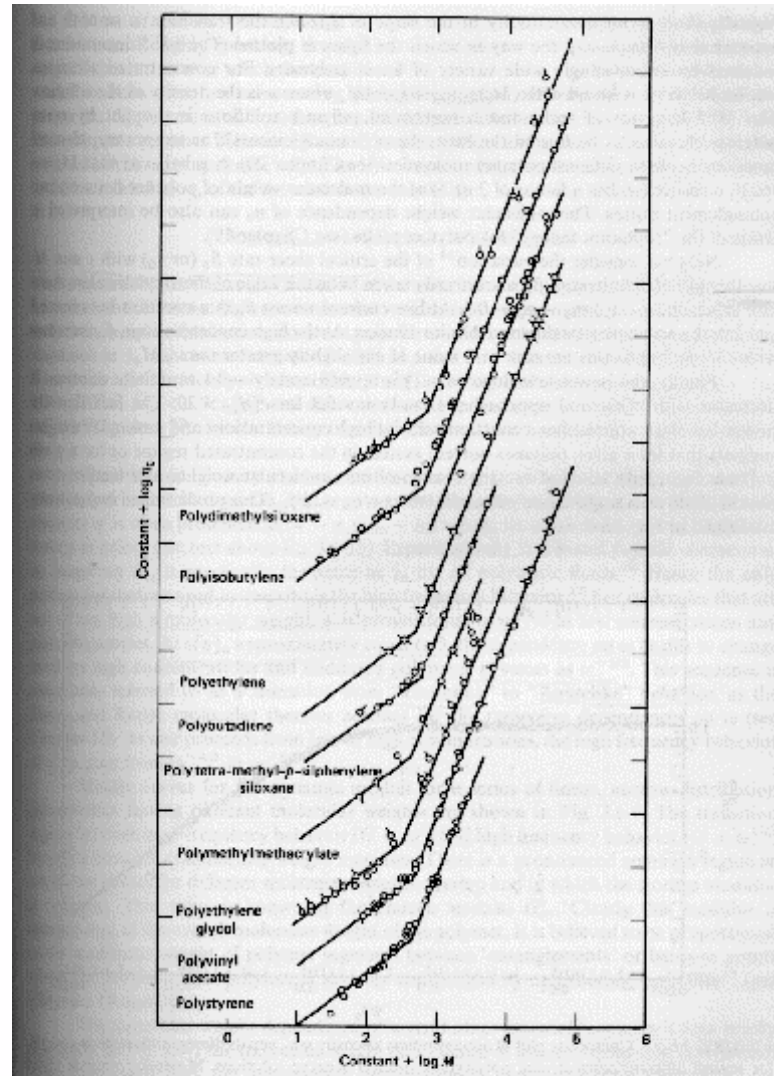

FIGURE 3.6-4. Plots of constant + log η_c vs. constant + log M for nine different polymers. The two constants are different for each of the polymers, and the one appearing in the abscissa is proportional to concentration, which is constant for a given undiluted polymer. For each polymer the slopes of the left and right straight line regions are 1.0 and 3.4, respectively. [G. C. Berry and T. G. Fox, *Adv. Polym. Sci.*, **5**, 261–357 (1968).]

Predicts that the viscosity will follow N which is true for low molecular weights in the melt and for fully draining polymers in solution

Rouse model predicts

Relaxation time follows N^2 (actually follows N^3/df)

Hierarchy of Entangled Melts

Hierarchy of Entangled Melts

Chain dynamics in the melt can be described by a small set of "physically motivated, material-specific paramters"

Tube Diameter d_T
Kuhn Length l_K
Packing Length p

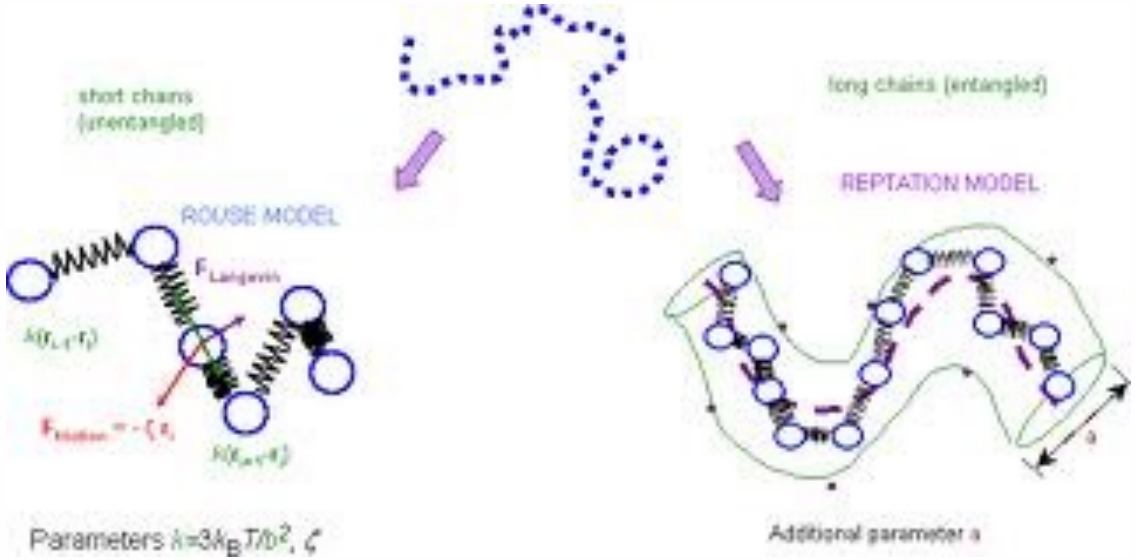

http://www.eng.uc.edu/~gbeaucag/Classes/MorphologyofComplexMaterials/SukumaranScience.pdf

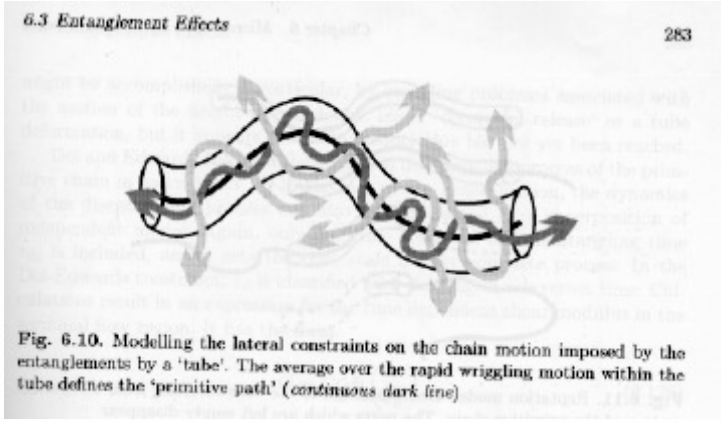

Fig. 6.10. Modelling the lateral constraints on the chain motion imposed by the entanglements by a 'tube'. The average over the rapid wriggling motion within the tube defines the 'primitive path' (*continuous dark line*)

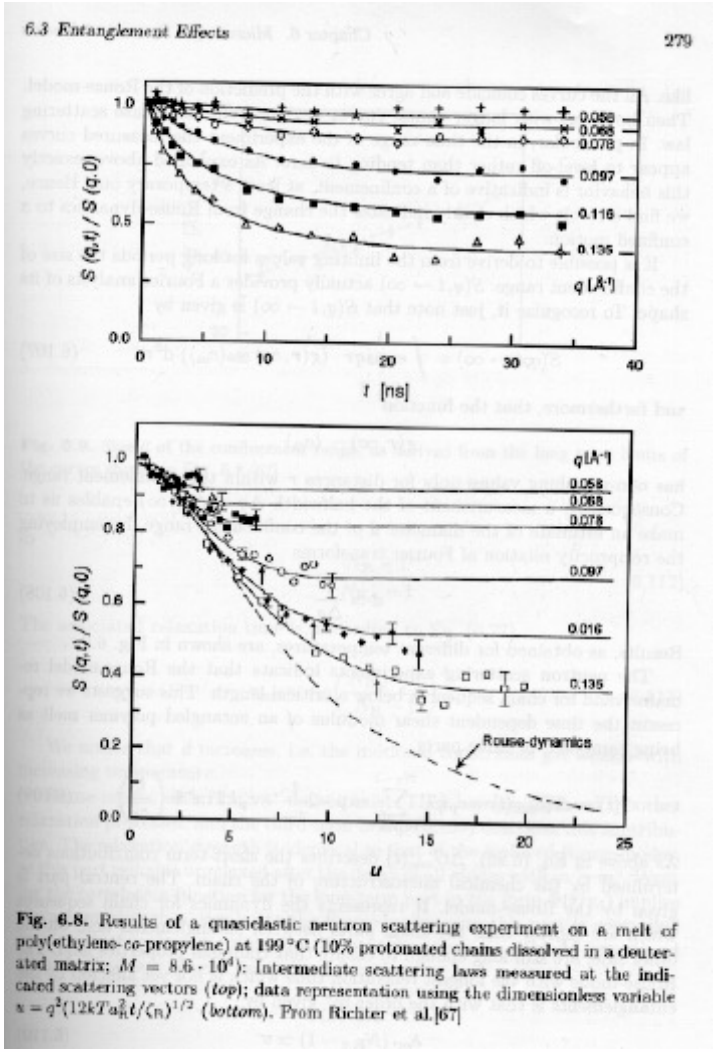

Fig. 6.8. Results of a quasielastic neutron scattering experiment on a melt of poly(ethylene-*co*-propylene) at 199 °C (10% protonated chains dissolved in a deuterated matrix; $M = 8.6 \cdot 10^4$): Intermediate scattering laws measured at the indicated scattering vectors (*top*); data representation using the dimensionless variable $u = q^2(12kTa_R^2t/\zeta_R)^{1/2}$ (*bottom*). From Richter et al.[67]

Quasi-elastic neutron scattering data
demonstrating the existence of the tube

Unconstrained motion => S(q) goes to 0 at very long times

Each curve is for a different q = 1/size

At small size there are less constraints (within the tube)

At large sizes there is substantial constraint (the tube)

By extrapolation to high times
a size for the tube can be obtained
d_T

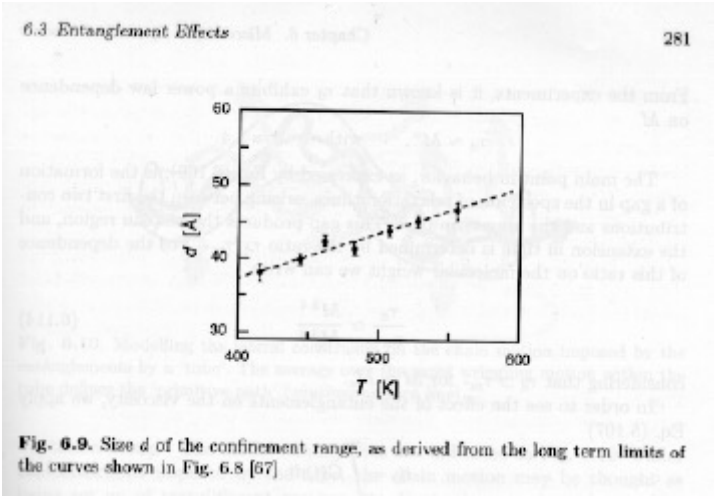

Fig. 6.9. Size d of the confinement range, as derived from the long term limits of the curves shown in Fig. 6.8 [67]

There are two regimes of hierarchy in time dependence
Small-scale unconstrained Rouse behavior
Large-scale tube behavior

We say that the tube follows a "primitive path"
This path can "relax" in time = Tube relaxation or Tube Renewal

Without tube renewal the Reptation model predicts that viscosity follows N^3 (observed is $N^{3.4}$)

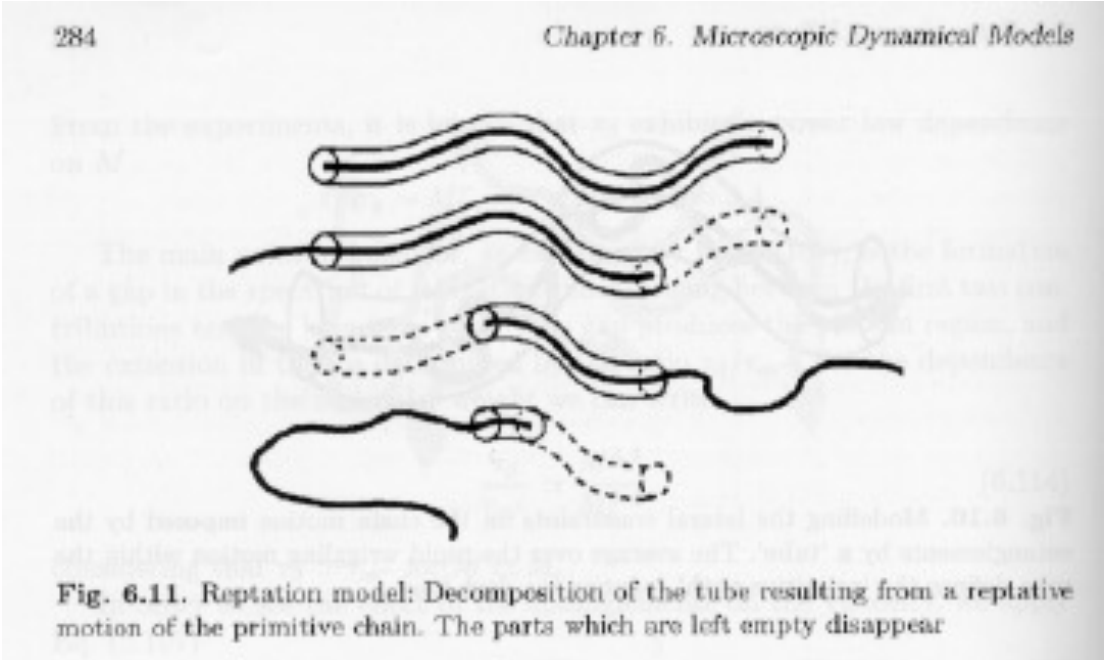

Fig. 6.11. Reptation model: Decomposition of the tube resulting from a reptative motion of the primitive chain. The parts which are left empty disappear

Without tube renewal the Reptation model predicts that viscosity follows N^3 (observed is $N^{3.4}$)

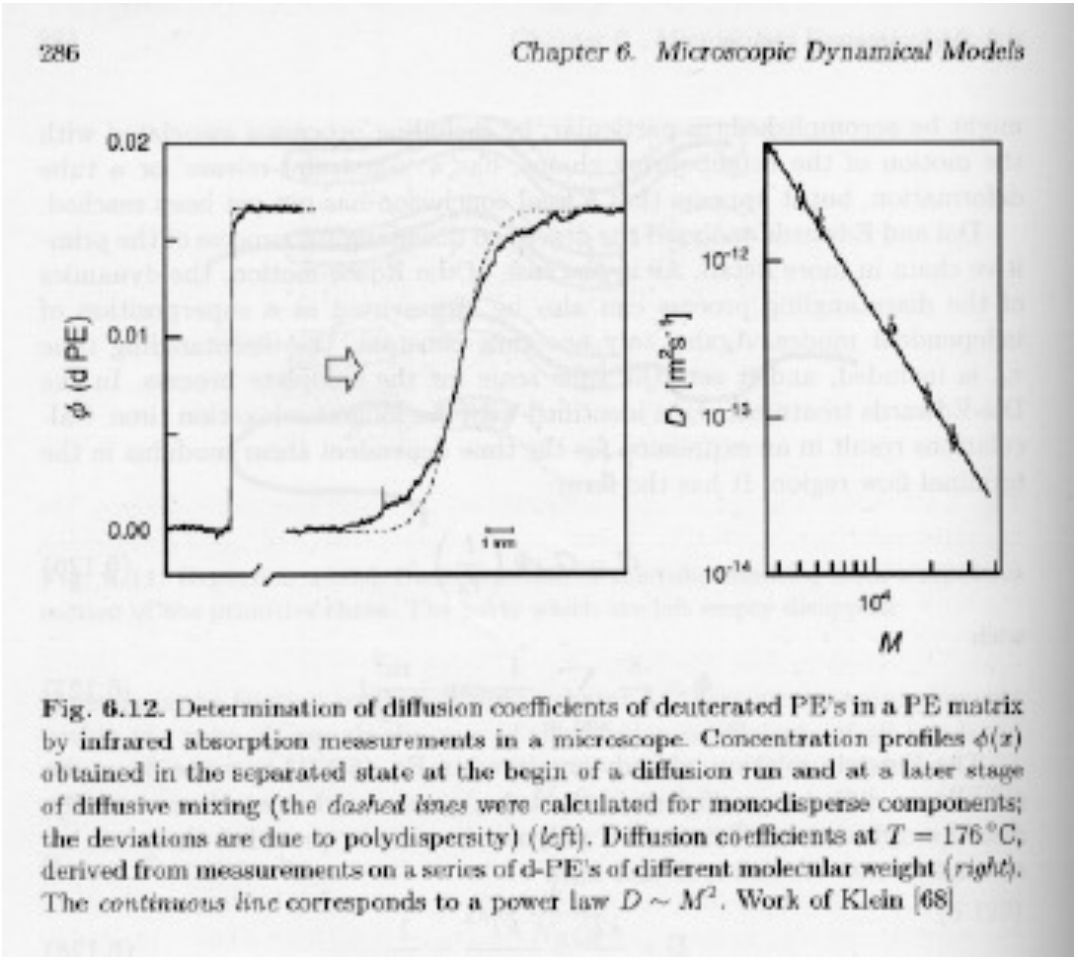

Fig. 6.12. Determination of diffusion coefficients of deuterated PE's in a PE matrix by infrared absorption measurements in a microscope. Concentration profiles $\phi(x)$ obtained in the separated state at the begin of a diffusion run and at a later stage of diffusive mixing (the *dashed lines* were calculated for monodisperse components; the deviations are due to polydispersity) (*left*). Diffusion coefficients at $T = 176\,^{\circ}\mathrm{C}$, derived from measurements on a series of d-PE's of different molecular weight (*right*). The *continuous line* corresponds to a power law $D \sim M^{2}$. Work of Klein [68]

Reptation predicts that the diffusion coefficient will follow N^2 (Experimentally it follows N^2)
Reptation has some experimental verification
Where it is not verified we understand that tube renewal is the main issue.

(Rouse Model predicts D ~ 1/N)

Reptation of DNA in a concentrated solution

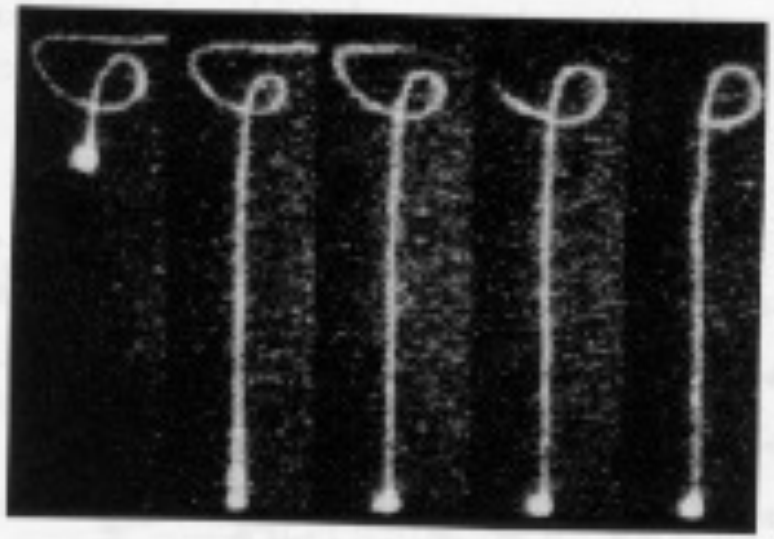

Fig. 6.13. Series of images of a fluorescently stained DNA chain embedded in a concentrated solution of unstained chains: Initial conformation (*left*); partial stretching by a rapid move of the bead at one end (*second from the left*); chain recoil by a reptative motion in the tube (*subsequent pictures to the right*). Reprinted with permission from T.Perkins, D.E.Smith and S.Chu. *Science*, 264:819, 1994. Copyright (1994) American Association for the Advancement of Science

Simulation of the tube

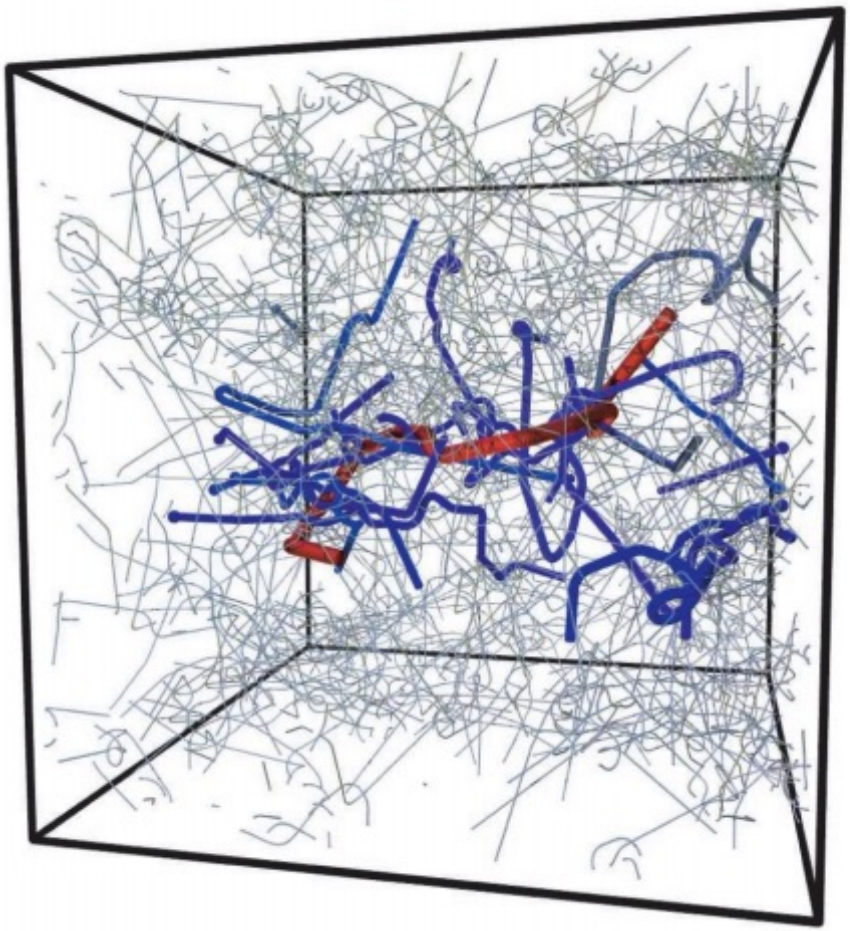

Fig. 3. Result of the primitive-path analysis of a melt of 200 chains of $N + 1 = 350$ beads. We show the primitive path of one chain (red) together with all of those it is entangled with (blue). The primitive paths of all other chains in the system are shown as thin lines.

Simulation of the tube

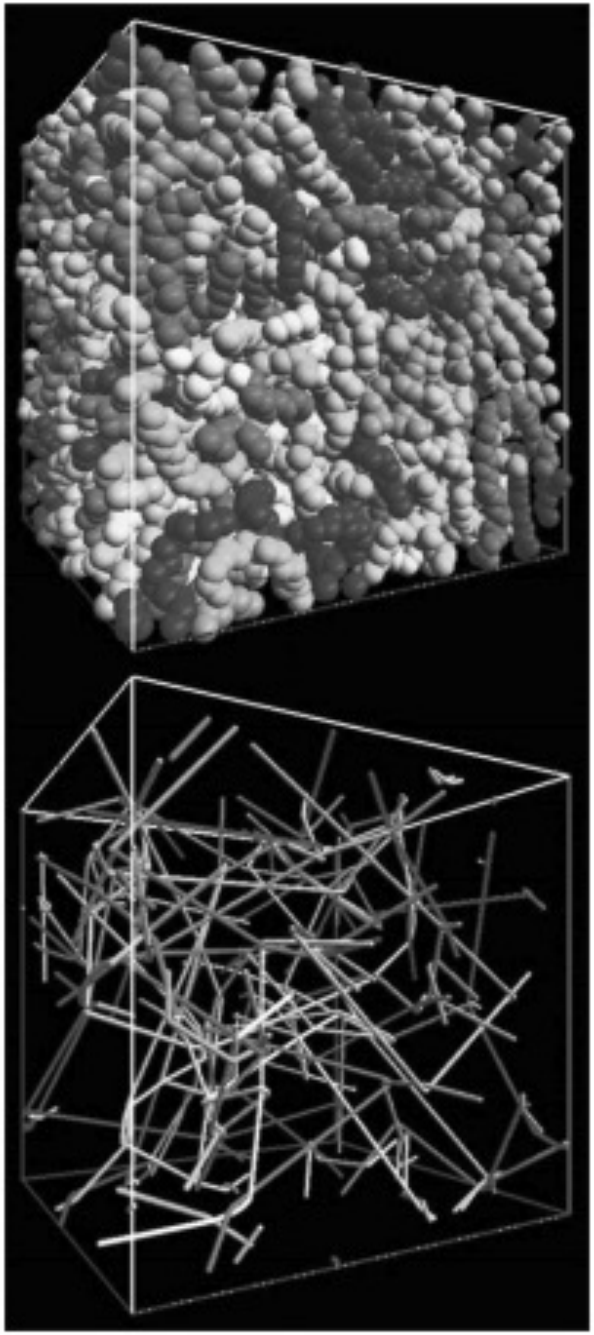

Fig. 3. A representative amorphous polymer sample and the corresponding network of primitive paths.

Plateau Modulus

Not Dependent on N, Depends on T and concentration

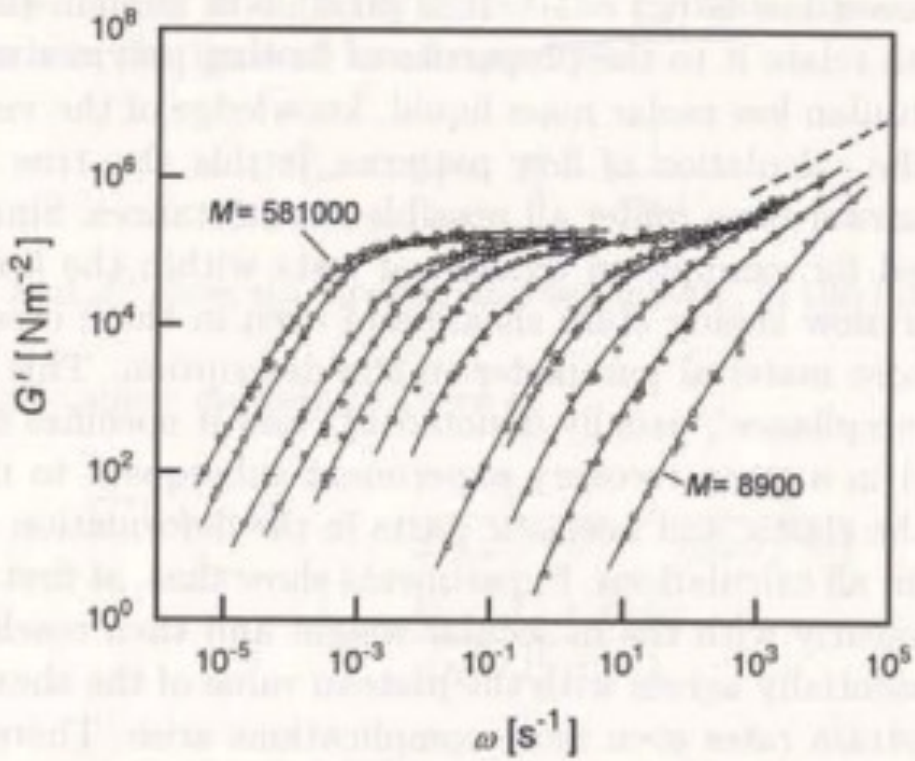

Fig. 5.15. Storage shear moduli measured for a series of fractions of PS with different molecular weights in the range $M = 8.9 \cdot 10^3$ to $M = 5.81 \cdot 10^5$. The *dashed line* in the upper right corner indicates the slope corresponding to the power law Eq. (6.81) derived for the Rouse-model of the glass-transition. Data from Onogi et al.[54]

$$G_0 = \frac{4\rho RT}{5M_e} = \frac{4RT}{5p^3}$$

Kuhn Length- conformations of chains $\langle R^2 \rangle = l_K L$

Packing Length- length were polymers interpenetrate $p = 1/(\rho_{chain} \langle R^2 \rangle)$
where ρ_{chain} is the number density of monomers

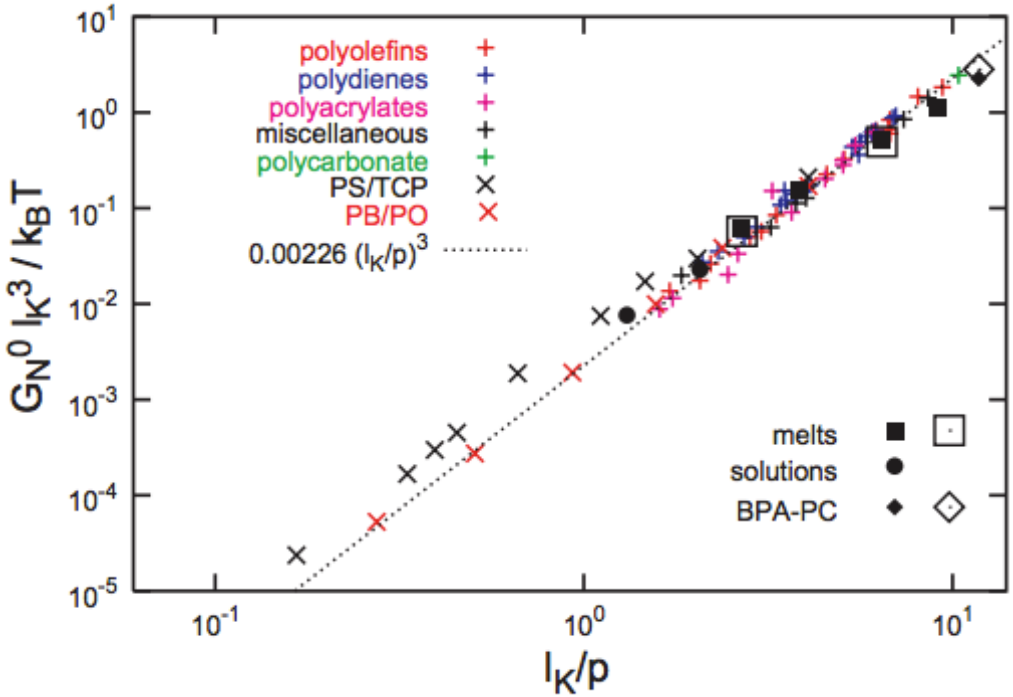

Fig. 2. Dimensionless plateau moduli Gl_K^3/k_BT as a function of the dimensionless ratio l_K/p of Kuhn length l_K and packing length p. The figure contains (i) experimentally measured plateau moduli for polymer melts (*25*) (+; colors mark different groups of polymers as indicated) and semidilute solutions (*26–28*) (×); (ii) plateau moduli inferred from the normal tensions measured in computer simulation of bead-spring melts (*35, 36*) (□) and a semi-atomistic polycarbonate melt (*37*) (◇) under an elongational strain; and (iii) predictions of the tube model Eq. 1 based on the results of our primitive-path analysis for bead-spring melts (■), bead-spring semidilute solutions (●), and the semi-atomistic polycarbonate melt (◆). The line indicates the best fit to the experimental data for polymer melts by Fetters *et al.* (*24*). Errors for all the simulation data are smaller than the symbol size.

this implies that $d_T \sim p$

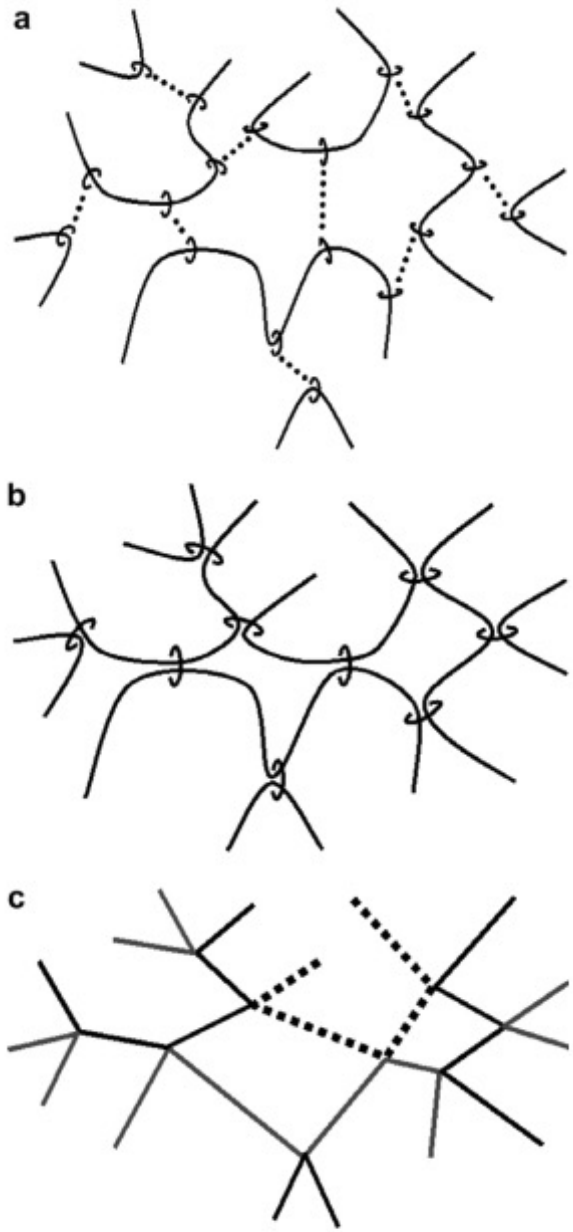

Fig. 1. Schematic representation of dual slip-links. (a) Chains coupled by virtual links. (b) Dual slip-links. (c) Real space representation of the corresponding network of primitive paths.

McLeish/Milner/Read/Larsen Hierarchical Relaxation Model

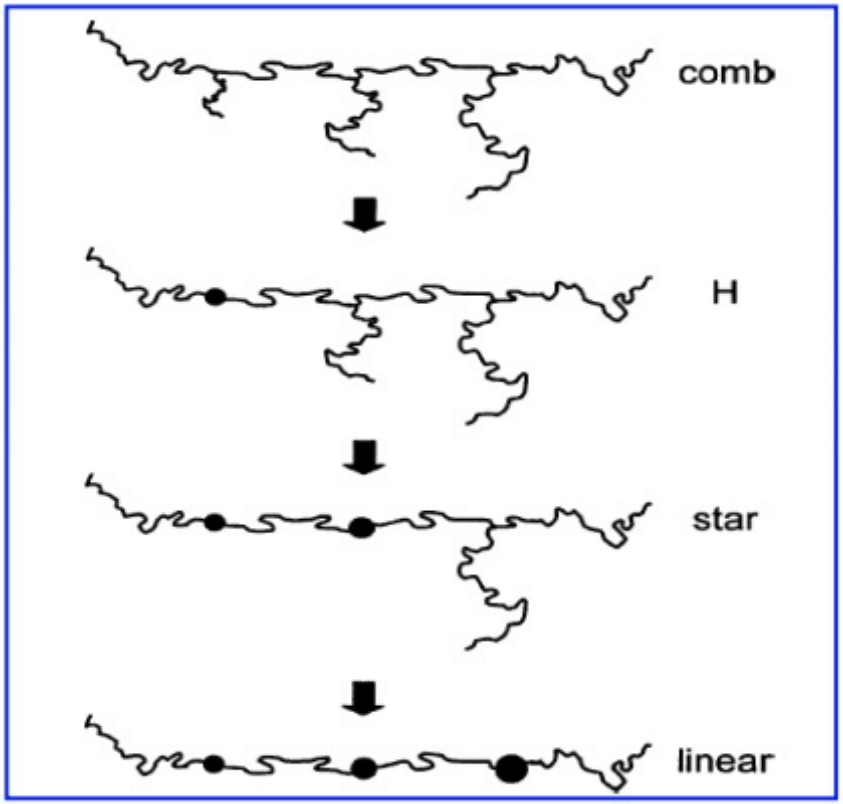

http://www.engin.umich.edu/dept/che/research/larson/downloads/Hierarchical-3.0-manual.pdf

Block Copolymers

http://www.eng.uc.edu/~gbeaucag/Classes/MorphologyofComplexMaterials/BCP%20Section.pdf

Block Copolymers

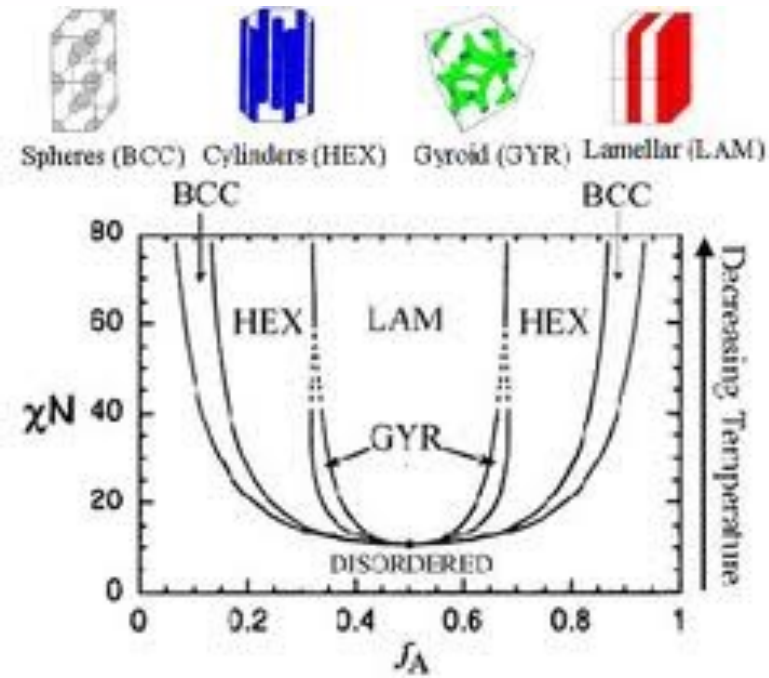

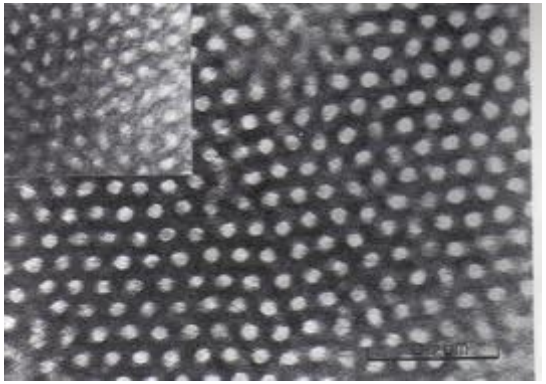

SBR Rubber

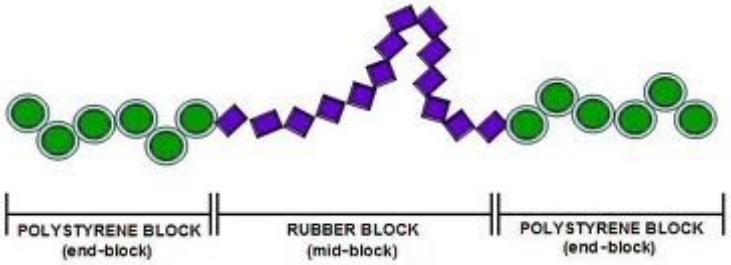

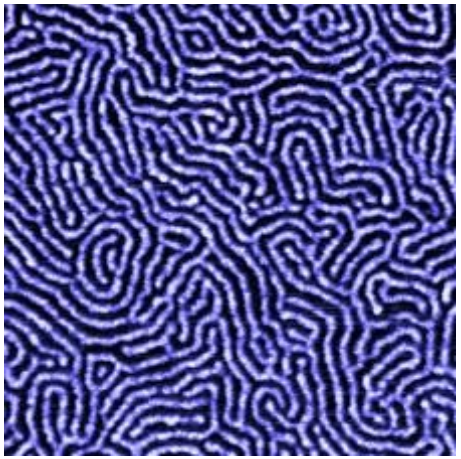

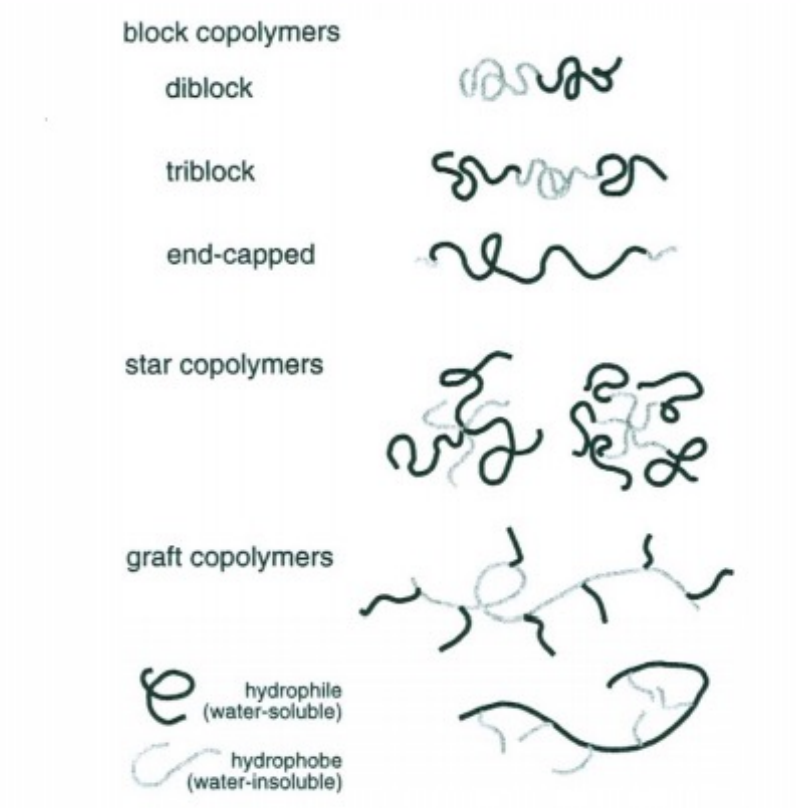

Figure 9. Schematics of block, star, and graft amphiphilic block copolymers.

http://www.eng.uc.edu/~gbeaucag/Classes/MorphologyofComplexMaterials/Amphiphilic.pdf

16

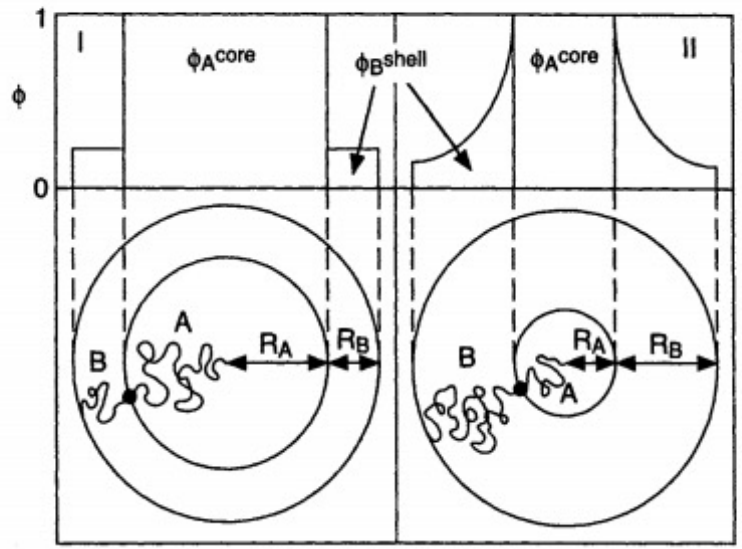

Figure 1. Illustration of model I (left) and II (right) of the AB-diblock copolymer micelle in a selective solvent (lower panel) and the volume fraction profiles of the polymer blocks (upper panel) applied for the large core case ($N_A >> N_B$) and the small core case ($N_A << N_B$), respectively.

http://www.eng.uc.edu/~gbeaucag/Classes/MorphologyofComplexMaterials/BCP%20Modeling.pdf

Hierarchy in BCP's and Micellar Systems

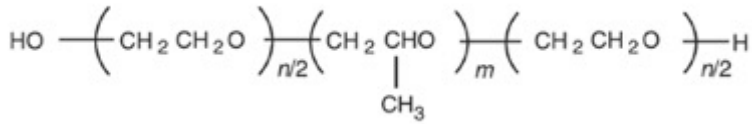

Pluronics (PEO/PPO block copolymers)

We consider primary structure as the block nature of the polymer chain.

This is similar to hydrophobic and hydrophilic interactions in proteins.

These cause a secondary self-organization into rods/spheres/sheets.

A tertiary organizaiton of these secondary structures occurs.

There are some similarities to proteins but BCP's are extremely simple systems by comparison.

What is the size of a Block Copolymer Domain?

Masao Doi, Introduction to Polymer Physics

-For and symmetric A-B block copolymer
-Consider a lamellar structure with Φ = 1/2
-Layer thickness D in a cube of edge length L, surface energy σ
- $F_{surface} \cong 2\sigma \frac{L}{D} L^2$ so larger D means less surface and a lower Free Energy F.
-The polymer chain is stretched as D increases. The free energy of a stretched chain as a function of the extension length D is given by

- $F_{stretch} \cong kT \frac{D^2}{Nb^2} \frac{L^3}{N\upsilon_c}$ where N is the degree of polymerization for A or B,

b is the step length per N unit, vc is the excluded volume for a unit step
So the stretching free energy, F, increases with D^2.

-To minimize the free energies we have $D \cong \left(\frac{\sigma N^2 b^2 \upsilon_c}{kT} \right)^{1/3} \sim N^{2/3}$

Chain Scaling (Long-Range Interactions)

Long-range interactions are interactions of chain units separated by such a great index difference that we have no means to determine if they are from the same chain other than following the chain over great distances to determine the connectivity. That is, Orientation/continuity or polarity and other short range linking properties are completely lost.

Long-range interactions occur over short spatial distances (as do all interactions).

Consider chain scaling with no long-range interactions.

The chain is composed of a series of steps with no orientational relationship to each other.

So <R> = 0

$\langle R^2 \rangle$ has a value:

$$\langle R^2 \rangle = \sum_i \sum_j r_i \bullet r_j = \sum_i r_i \bullet r_i + \sum_i \sum_{j \neq i} r_i \bullet r_j$$

We assume no long range interactions so that the second term can be 0.

$$\langle R^2 \rangle = Nr^2$$